AD-750 724

COMPARATIVE STUDY OF SELECTED ROCK STRESS AND PROPERTY MEASUREMENT INSTRUMENTS

John R. Hoskins

Idaho University

Prepared for:

Advanced Research Projects Agency

June 1972

TECHNICAL REPORT NO. UI-BMR-2

A COMPARATIVE STUDY OF SELECTED ROCK STRESS AND PROPERTY MEASUREMENT INSTRUMENTS

by
C. J. Hall
and
J. R. Hoskins

June 1972

Sponsored by
Advanced Research Projects Agency
ARPA Order No. 1579, Amend. 2
Program Code No. 1F10

Security Classification

Document Control Data R & D
(Security Classification of title, body of abstract and indexing, annotation must be entered when classified)

1. Originating Activity (Corporate Author)
University of Idaho, Bureau of Mining Research, College of Mines, Moscow, Idaho, 83843

2a. Report Security Classification

2b. Group

3. REPORT TITLE

COMPARATIVE STUDY OF SELECTED ROCK STRESS AND PROPERTY MEASUREMENT INSTRUMENTS

4. Descriptive Notes (Type of report and inclusive dates)
Final Technical Report, - April 2, 1971 to June 30, 1972

5. Authors (first name, initial, last name)

John R. Hoskins

c. Report Date	7a. Total No. of Pages	7b. No of Refs
June 1972	250	125

8a. Contract or Grant No.	9a. Originator's Report Number (s)
H0210030	UI-BMR-2
b. Project No. ARPA Order Number 1579, Amend. 2	9b. Other report notes (Any other numbers that may be assigned to this report)
c. Program Code Number 1F10	

10. Distribution Statement

Distribution of this document is unlimited

11. Supplementary Notes	12. Sponsoring Military Activity
	Advanced Research Projects Agency, Washington, D. C.

13. Abstract

This is the Final Technical Report for the reporting period from April 2, 1971 to June 30, 1972.

The report presents information on selected stress and modulus gages designed to measure the deformation of a small hole drilled into rock, and the applied pressure in the case of modulus gages. The gages selected were the USBM Borehole Deformation Gage, the CSIR 'Doorstopper', and the Photoelastic Stressmeter (Glass Plug) to measure stresses; the Goodman Jack, the USBM Cylindrical Pressure Cell, the Menard Pressuremeter and the Borehole Dilatometer (Rocha) to measure rock modulus values. The information was gathered, initially by questionnaire and in greater depth by personal communication, from engineers who have used the instruments in the field.

Information is provided on the use, cost, time, and other factors relating to the selected gages. The information is oriented towards comparative selection of gages to be used in specific applications. Information on problems likely to be encountered in the field is given.

The most pertinent papers describing the instruments, giving the derivation of the equations used to convert deformation measurements to stress or modulus values, and detailing the laboratory and/or field testing to verify these results are given as appendices.

DD FORM 1473
1 Nov 65

Security Classification

Security Classification

14. KEY WORDS	Link A		Link B		Link C	
	Role	Wt.	Role	Wt.	Role	Wt.
Rock	5					
Stress, Modulus, Cost, Performance, Depth	7					
Stress, Modulus, Cost, Performance, Depth	6					
Gages, Gauges	8					
Gages, Gauges	4					
Rocha Dilatometer	1					
Glass Plug	1					
Goodman	1					
CPC	1					
Borehole Deformation Gage (USBM)	1					
Menard Pressure Meter	1					
Doorstopper	1					

Security Classification

ARPA Order Number:	1579, Amed. 2
Program Code Number:	1F10
Contractor:	University of Idaho, Moscow, Idaho 83843
Effective Date of Contract:	April 2, 1971
Contract Expiration Date:	June 30, 1972
Amount of Contract:	$30,067
Contract Number:	H0210030
Principal Investigator:	Dr. J. R. Hoskins
Telephone Number:	(208) 885-6376
Project Scientist or Engineer	Dr. C. J. Hall
Telephone Number:	(208) 885-6376
Title:	Final Report

This research was supported by the Advanced Research Projects Agency of the Department of Defense and was monitored by Bureau of Mines under Contract No. H0210030

Technical Seminar presented by the U. S. Bureau of Mines

On the 25th of July, 1972 a one day seminar was held in the Denver Federal Center entitled "Technology Transfer Seminar: Rock Mechanics Instrumentation for Mine Design" at which full technical and field information was presented by USBM personnel to over one hundred participants from industry and research institutions. The characteristics of the Borehole Deformation Gage, Cylindrical Cell, and other Bureau sponsored instruments were presented. The papers will be published by the USBM (editor Harry R. Nicholls) shortly under the above title.

CONTENTS

TECHNICAL REPORT SUMMARY

This report has been prepared for engineers who wish to determine rock stress or modulus values, and not for research workers. An attempt has been made to assess the amount of assistance the user might expect from the manufacturer or distributor.

The objective of the study is to provide information to engineers on the use, cost, time, and other factors relating to selected rock stress and modulus gages. This information is oriented towards comparative selection of gages to be used in specific applications. Information on problems likely to be encountered in the field is given.

The primary interest is directed towards collections of specific use-data on the U.S. Bureau of Mines Borehole Deformation Gage, the CSIR "Doorstopper," and the Photoelastic Stressmeter (Glass Plug), for in-situ rock stress determination, the Goodman Jack, the U. S. Bureau of Mines CPC, the Menard Pressuremeter, and the Rocha Dilatometer, for in-situ rock modulus determination.

The most pertinent papers describing the instrument, giving the derivation of the equations used to convert deformation measurements to stress or modulus values, and detailing the laboratory and/or field testing to verify these results are given as appendices. In addition, a short history of the field use of each gage is given. Both of these, the appendices and the histories, are included so that engineers do not have to rely on the authors' judgement.

Eight conclusions from the study are listed below.

1. Normally a skilled and experienced engineering crew is required to obtain any value from a rock mechanics investigation, and this crew might well require the assistance of a consultant when starting to use a new gage.
2. Table 1 shows the number of people responding to the questionnaire for each type of gage, and this gives some measure of the field use of gages. Stress gages are used far more widely than modulus gages. The popularity of the Goodman Jack is due to its ease of handling in the field.
3. Table 2 summarizes the merits and limitations of the individual stress gages. It shows that no one gage can be used under all circumstances, and two or three might be necessary on one project.
4. Figure 1 summarizes the range of the modulus gages. There is no generally satisfactory hard rock modulus gage, and laboratory testing must remain the most widely used and useful method of measuring modulus at present.
5. The amount of space and time required to obtain measurements using different gages and methods varies considerable. If development, production, or construction schedules necessitate the driving of separate rooms for engineering purposes, the costs of these investigations in time and money would become very large. In general, the stress and modulus gages considered here require a small amount of space, but tests could take several

shifts to several weeks to complete.

6. The art, science, and tools of rock mechanics are still far from the stage of development needed for good engineering practice. The interpretation of individual results and the formulation of general theories about stress patterns in and around a particular structure is still qualitative more than quantitative.

7. Most operators have found that difficulties in field application and problems with the calculation and interpretation of results are ignored or minimized by most authors.

8. The development of old and new instruments is continuing constantly. It is recommended that this study be repeated in four years or so.

INTRODUCTION

Method - The study was carried out in two sections concurrently. One section was a literature search to provide the history and appendix material, and locate any other useful information available. The list of references at the end of the text was selected and was not intended to be exhaustive. Some earlier major and most minor references have been omitted. The other section was a direct approach to instrument users, initially by form and later by telephone or personal contact. Table 1 shows the number of useful contacts made, classified by instrument.

During the course of the study attempts to evaluate the Griswold Gage were abandoned when it became apparent that the gage was not being commercially produced. One company is developing the gage for its own use.

Background - The earth's crust is in a state of stress, and at any point in the crust this stress is caused by at least two components, the weight of the overlying material and the geological stresses that remain from the forces that caused mountain building. The reactions of the rocks to these stresses can be either elastic, so that they remain in a high state of stress, or plastic, when they flow and reduce the stress level. Usually the rocks are fractured, showing that stresses have exceeded strength in the past.

In general, the forces in the earth's crust are in equilibrium until man made changes upset the balance. These changes may consist of loads placed upon the surface (buildings,dams, lakes) or the removal of forces and constraints within the earth by mining and other excavation work. Under the effect of these changed load systems, the stresses change and the rock or earth deforms, and can even fail. The amount of deformation is important, because it can be used to estimate the stresses present in the rock, or to determine the support that the rock will give to a loaded structure, such as the concrete lining of a penstock, or by using finite element analysis to determine which pillars in an underground structure or which bed or dike members of a geological structure are likely to carry a disproportionate portion of the load.

Increased stress in rock can be beneficial, in that it can change the drilling and blasting characteristics of the rock possibly increasing drilling speed and fragmentation. Failure can also be beneficial in some cases, such as by reducing stress concentrations and improving pillar characteristics so that they do not burst but yield under load. The discing that occurs when diamond drilling highly stressed ground, if applied to a heading driven by a tunneling machine, might well be used to the benefit of the operation.

Around any opening in stressed rock, stress concentrations occur. The pattern and magnitude of the concentrations depends on the shape of the opening. In general, concentrations increase the faster the rate of change of direction of the opening. Thus, they are small in the middle of straight sides, higher around circular openings, and very high at corners. Normal to the axis of a proposed opening in undisturbed ground, the planar stress field may be reduced to two principal stresses, a major and a minor, which are normal to each other. These stresses are either compressive or tensile, with no shear stresses, and they are termed principal because their magnitudes are the maximum tensile and maximum compressive in that plane.

Stress concentrations around an opening produced by an uniaxial stress field are theoretically complex except for the case of circular openings. Stress concentrations for a biaxial field normal to the axis of a circular opening are the resultant of the addition of concentrations from the two uniaxial fields that comprise the biaxial field. Actual conditions may require the more complicated calculations of triaxial stress fields. Thus it is not possible to measure the virgin rock stress field by taking measurements in the immediate wall of the

mine entry, because the stress concentrations factors are not known, and even if they were known, they would be completely distorted by fractures caused by breaking out the rock to make the opening. The stress should be estimated from measurements of deformation made in an opening of circular cross section with no fractures in the wall, at a distance from the mine opening at least equal to the magnitude of the mine opening itself. The simplest solution to this problem is to use a diamond drill hole for measuring the needed data. Neighboring openings such as stopes or rooms add complexity to the problem and should not be ignored.

History - Major efforts to try to determine the values of stresses in rocks in mines, by mathematical analysis, by developing instruments to measure deformation, and by applying strain gages directly to pieces of rock, started about twenty years ago. One of the first really important results of this work was the realization that horizontal stresses were not singularly produced by confining the vertical stress (i.e. affect of Poisson's ratio), and therefore equal to about 20 to 50% of the stress caused by the weight of the overlying rocks, and that in fact in many cases the horizontal stresses exceeded the vertical stress (16) (44). There is also no doubt that the vertical stress is not necessarily equal to the weight per unit area of the overlying rock.

Theortically there is no reason why vertical stresses should not be an order of magnitude greater than the gravity caused stress locally, as long as regionally the mean stress is approximately equal to the gravity caused stress. High vertical stresses have been reported from Canada (16)(44) and Australia (26).

By about 1965 some instruments had been developed to measure deformation, and a very few to measure pressure and deformation. Many other instruments were under development. The measurements of deformation could be converted to estimates of stress by formulas developed mathematically from basic mechanics or from laboratory testing. Instruments to measure deformation are therefore called stress gages. The instruments that measured pressure and deformation could be used to determine how a rock would deform under a load, and these instruments are called modulus gages. It is, of course, impossible to convert deformation measurements to estimates of stress without making some assumptions about the relationship between stress and strain. This means that assumptions have to be made regarding the elastic state of the rock and the value of the rock modulus.

Since 1965 work on many of the instruments has been stopped. Development has been concentrated on improving the performance of a few instruments that showed promise and for which there was sufficient (usually governmental) backing. The major exception to this seems to be the three dimensional instruments, which are still under active development.

From the late 1950's attempts were made to measure stresses at mines and apply the knowledge gained to improving the stability of mine openings and pillars. The amount of applied work has increased steadily, and from about 1965 spread to open pit operations. However, in 1967 Black and Hoek (8) still took industry to task for not employing rock mechanics sufficiently and explained in simple terms the tools that were available.

In order to determine the magnitude of the two principal stresses in a plane, and the direction of the stresses with respect to the horizontal, it is necessary to measure three deformations. Initially this was done by grouting three pins into holes in the side of a drift, to form the corners of an equilateral triangle. The distance between the pins was measured very accurately, and the rock that they were in was then destressed by drilling it free from the main body of rock. The distances between the pins was again measured, and the value of the principal stresses in the plane of the wall rock and their orientation with respect to the pins calculated. The results were of little value, due to the very uneven stress field in the side of the drift.

An improved method used to determine the stresses in the side of a drift is one employing the flat jack (97). Pins grouted into the drift walls are returned to their original position after a stress relief slot is pressurized by a jack. The major advantage of the methods is that no rock modulus values are required, because a measured stress is applied to restore the rock to its original condition. The method is fairly simple, and apart from end effects and axial stresses the pressure exerted by the jack is more or less equal to the average rock stress normal to the slot (74). However, even if there were no mining fractures to complicate the stress pattern, there would still be the complication of the difference in stress concentration with depth into the wall rock, and the fact that this is opposed by a constant flatjack pressure, and the geometrical stress concentration factor itself, which would have to be determined from model studies or finite element analysis. If the rock were anisotropic (the rock properties vary with direction), assumptions of the relative rock properties would have to be made.

The general trend in the design of stress gages has been to those that will measure three or more deformations normal to the axis of a borehole. Some instruments can only react to a decrease in the size of the hole (the instruments cannot be prestressed) and are useful to determine increases in compressive stress with time. These instruments must have a long hole life. Other instruments can measure increases in the diameter of the borehole, and these are used to evaluate absolute stress, by cutting the portion of the borehole in which the instrument is mounted free from the surrounding rock mass. With both types of instrument the direction and magnitude of the absolute principal stresses or change in principal stresses normal to the axis of the borehole is calculated by using the stress strain relationship (modulus values) of the rock. There are many problems associated with the design of the instruments, including robustness, sensitivity to rock deformation, range of deformation measurements, limited creep of the instrument, insensitivity to temperature differences and water, ease of positioning and orienting the instrument, applicability to different rock conditions, life in the hole, distance that the instrument can be placed from the operator, mechanical and technical reliability, the time required for obtaining information and crew size, and the initial cost of the instrument with its components. Leeman (65) produced a major evaluation of rock stress instruments in 1964. Other reviews and investigations (1)(10)(78)(106)(108) are also valuable contributions, as is the report on discussions at the First Congress of the International Society of Rock Mechanics (56). Fairhurst's reviews for long-hole instruments (27)(28) indicate that in this field there are still many difficulties to overcome.

The development of modulus measuring equipment and techniques started, before any major work on rock mechanics, with attempts to measure the deformation modulus of soils and soft and shattered rock near the surface of the earth, for building foundations. Loading tests were performed on prepared exposed surfaces in large static and jacking tests. Borehole instruments were developed to determine the characteristics of the soft material at depth in order to determine excavation and pile driving factors. The concept of jacking tests was then taken underground by the designers of dams as penstocks and power stations were built into excavations of rock. Initially these developments were more or less ignored by the rock mechanics investigators

Mineralized zones, orebodies and mines are explored and evaluated from the material recovered from drill holes. For many reasons, hand specimen of rocks are much more valuable than sludge (or ground up) samples. Thus diamond drilling with core recovery has been a very widely used tool in mining long before rock mechanics investigators to test for strength, modulus, and even stress. Laboratory equipment was developed to

prepare and test sections of small diameter core. When overcoring was used to provide rock stress relief for absolute stress measurements, equipment was quickly developed to use these cores, in the laboratory and in the field. to determine modulus values. The rock mechanics approach to modulus measurements was therefore to use very small specimen, often in the laboratory; soils mechanics to use large specimen in the field.

Rock and soil are not homogeneous, that is their properties vary from one location to another both microscopially and macroscopically. This leads to some confusion regarding the modulus values that are required - maximum, minimum, mean, within certain confidence limits, etc. Deformation modulus values are also a function of stress except in very hard dense competant rock, and measurements should be made over the appropriate stress range. The soils mechanics approach has been to use large samples with necessary low stress levels, because in general their structures are broadly applied at low stress levels. The position in rock mechanics is a little more complex, because modulus values are required for many different purposes. The sample size and method of testing must be selected to give the best value of modulus for the required purpose. Thus, the value of the modulus obtained from the annulus of rock used for absolute stress measurement is the best one to use to calculate the stress values, even if it is not representative of the general body of rock. The present approach is four fold; tests on drill cores; tests in drill holes; tests on the walls of tunnels; and dynamic (sonic) tests. The size of sample tested varies from a few cubic inches to millions of cubic yards, and the numerical values obtained by the different methods on the one rock formation can vary by more than an order of magnitude. Probably the main reason for the difference in values is the amount of cracks and voids in the sample tested. Diamond drill cores that are suitable for testing usually have the minimum amount of cracking, and will therefore produce the maximum value of the deformation modulus. Testing in a diamond drill hole is likely to lead to a lower modulus, because more cracks and voids (nearly all geological phenomena) are likely to be included in the sample. Jacking tests on a tunnel wall are likely to give the lowest values, because the sample includes both geological and mining cracks. Some investigations of comparative methods of measuring modulus are given in (102),(12),(15), and (47).

There are three types of modulus gages for measuring small sample rock properties in situ. These are borehole penetrometers, borehole dilatometers, and borehole jacks. The penetrometers do not appear to have been developed to the point where they can be of practical use. Dilatometers and jacks are further developed both theoretically (mathematically) and as field instruments. Both of these types of instruments are used to attempt to measure Young's modulus or the modulus of deformation in the field, the dilatometers by applying a radial pressure and the jacks a unidirectional pressure, to the inside of a small (-4" diameter) borehole. It is apparent that not nearly as much field work has been done on these instruments as on the stress gages. This presumably is a reflection on the later development of these instruments and also, possibly, the desire on the part of operators to get a measure of rock stress, even if inaccurate, rather than a more accurate estimate of rock properties.

The stress measuring instruments developed so far determine the stress in a plane. The stress field in the rock is three dimensional, and the two planar principal stresses measured might be very different from the three mutually perpendicular principal stresses. Estimates of the primary principal stresses have been made by measuring deformation in three diamond drill holes drilled in different directions from one location. The resolution of the data is simplified through the use of a computer. This method would be satisfactory, apart

from the considerable amount of work required, if it was known that the stress field was homogeneous. In many cases, however, it is likely that the stress field is far from homogeneous, and the concept of an instrument that measures the three dimensional deformation pattern in one small volume of rock becomes attractive. Such instruments are under development, but are not analyzed in this project.

USBM BOREHOLE DEFORMATION GAGE

Introduction - The Borehole Deformation Gage (BDG) is a six component instrument that measures deformations along three diameters in a single plane normal to the axis of a 1½" (EX) diamond drill hole when it is overcored by a 6" thin walled diamond drill bit (5-3/8" core diameter). These measurements can be converted to estimates of the principal stresses in the original rock provided that:

a. There are no cracks or other discontinuities near the instrument to deform the stress concentration pattern.
b. The rock modulae are known correctly, and
c. The stresses parallel to the axis of the borehole are not significant or are known.

The instrument is not suited to measuring stress changes with time at one location, nor has it been used for this purpose, because its hole life is suspect. A full description of the instrument, together with the mathematical development of the equations used to convert deformation measurements to estimates of stress and the laboratory testing to validate the results, is given in Appendix A.

History - The initial instrument produced by the Bureau of Mines was a single component gage, measuring the deformation of one diameter of a borehole on overcoring. Thus the instrument had to be set at three successively deeper positions in the hole and rotated about its axis, in order to determine the biaxial stress field. Some of the initial field work was done in a Louisiana salt dome (Project Cowboy) and was reported very fully by Merrill in 1960 (72). Incidentally, the study showed a superincumbent load, which has since been found to be common in salt formations, which have a high creep rate. In the same year Merrill and Hooker reported work done in a tuff in Nevada (73). In general the computed stresses corresponded with the superincumbent load and confining stresses, as would be expected in this type of rock.

This gage and its calibration was described in RI 5978 (1962) by Obert, Merrill and Morgan (81) and a general report by Obert (79) was used to introduce the instrument to a wider public by publication in Mining Engineering. A report in 1964 (124) described the use of the instrument in granite by private industry. The results in the highly fractured ground fluctuated considerably, with a general tendency to high horizontal stress and lower than gravitational vertical stresses. From this time the amount of literature describing field work increased considerable (11)(16)(59)(74)(75)(90)(107)(122)(123), reporting among other things a comparison with flat jacks and other instruments, improvement in placement tools and the use of the instrument in Canada, where vertical and horizontal stresses in virgin ground of 2,500 and 5,000 psi at a depth of 1,300 feet was reported at Elliot Lake, and in 1968 stresses of the same order at Wawa (44).

In 1966 Suzuki reported his development of a three (or six) component gage in Japan (113). Use of the Bureau of Mines six component gage was reported by Hooker and Johnson (52) in 1967, and in the same year Merrill (71) gave the instrument development report which has been used in Appendix A. From this time

nearly all work was done with the six component gage, and increasingly solutions are being made for the three dimensional stress ellipsoid by computer, based on the work of Panek (86) and Gray and Toews (36). It is of interest that the Bureau of Mines is developing a program for the Hewlett Packard 9100-B desktop computer with the extended memory.

The Bureau of Reclamation has been using the instrument, improving the waterproofing (120) and making other modifications (3), before measuring the stresses in concrete dams. They also developed their own three dimensional computer program (4). Use of the instrument has become almost standard for hydroelectric projects (6)(21)(58). Hooker and Johnson (53) report on rock anisotropy near the surface, which can cause errors in the calculated stress magnitude of 25%, and in orientation of 25 degrees. They found horizontal stresses in quarries along the Appalachia Piedmont of up to 4,500 psi. One remaining problem, reported from Canada (16) and the Coeur d'Alene district of Idaho (14)(18)(19) is the performance of the instrument in fractured ground, or ground that is so highly stressed that it fractures on overcoring. The instrument is being redesigned so that the transducers are at the collar end, to try to reduce the amount of overcore required. However, if the transducer buttons are to be set clear of any end hole stress concentration effects, it is not likely that a large reduction can be made in the length of core required.

Investigation Results - The instrument is not produced commercially,* but may be obtained from the USBM at Denver on loan.* Delays of several weeks could occur.

The engineer in charge of the project should be a graduate engineer, preferably with a masters degree or experience in rock mechanics. He can be trained by Bureau of Mines personnel at Denver in the laboratory there or with a Bureau crew in the field. The latter training could entail a delay of several months, the former only days. The length of time required to cover the field and theoretical training is about two weeks. As with the other instruments, the crew performance will improve with practice, and measurements with a BDG could be attempted after a few hours instruction. This approach is likely to be less efficient than using a longer training period. A new booklet (51) has been published to assist a crew in the field. While it appears to be well written, it will not obviate the necessity for field training. No operators who have used the booklet have been questioned, so that a thorough assessment of its value cannot be made. The engineer in charge of the project could train a technician to operate the instrument in the field in about a week. Should difficulties arise, the USBM at Denver can be approached for verbal advice.*

* A slightly modified gage with different electrical circuit protection is sold by Terrametrics of Golden, Colorado.

* United States Department of the Interior, Bureau of Mines, Building 20, Denver Federal Center, Denver, Colorado, 80225.

An EX hole is drilled to the desired location, using a coring bit. Inspection of the EX core allows an assessment to be made of whether or not the ground is suitable for stress estimations. A 6 inch overcore is started with the EX hole as its center and the BDG is then inserted in the EX hole and oriented at the correct location with the positioning rods. Improved rods over those described in RI 6554 (122) are now available. The instrument cable has to be threaded through the drill and water swivel and attached to the strain indicator. The overcoring is continued, from about 9-inches before the transducers to 9-inches past them, for a total length of 18-inches. In many types of rock a twelve inch core length (6"+6") is adequate. Drill speed and pressure are critical in highly stressed ground, to reduce core breakage to a minimum. Strain gage readings are recorded throughout the drilling, which is stopped when the gages show no further deformation. The instrument is removed and the core annulus broken and pulled. The overcore is quite often tested biaxially for the modulus of deformation at site by portable equipment (29), but may also be tested triaxially (80) in the laboratory. The crew required for the operation is three or four, including a diamond drill runner, an instrument cable handler, and the strain gage reader (or driller, helper, and technician). The maximum distance that the instrument has been placed from the operator is 135 feet, and this might be approaching the limit. Hole inclination is not critical, except that within 10 degrees or so of the horizontal it is difficult to clean the hole, and fine material left under the gage pistons will lead to incorrect measurements. Water in the hole, and even that introduced during the drilling of the annulus, can get into the instrument through one of the "O" rings (piston or cable) and cause an abortive run. The USBR at the Denver Federal Center has put its own waterproofing on the USBM gage, and the Bureau of Mines staff are also working on improving the waterproofing. This sensitivity to water could lead to a short hole life. Changes in the hole diameter of up to ¼", either slowly or quite abruptly, should cause no difficulties. However, because it is necessary to withdraw the instrument from the hole to change the washers in the pistons to preload the transducers correctly, changes in the diameter of the hole slow down the operation considerably. Absolute stress readings can be taken every 12 to 18 inches; that is, a new EX hole for installing the instrument can be started in the bottom of the 6 inch overcore hole.

The amount of time taken for a reading varies with the depth of the hole. For fairly shallow installations, once the drill is set up and the operation started, it might be possible to get two readings per shift. Moving the drill and equipment into the mine and setting it up could take two shifts to two weeks.

The mechanical reliability of the instrument appears to be satisfactory, other than the problem of waterproofing. Damage can be caused by the overcoring annulus breaking off and pulling the cable, which can also be damaged by allowing it to slaken and get twisted by the core barrel. Runs can also be aborted by the pistons extending into cracks, the instrument moving, and the overcore breaking before stress relief is complete (which leads to instrument movement). The greatest single problem is damaging or cutting the cables and connections. In good ground, an 80% success ratio might be achieved. In highly stressed discing ground, the ratio might be less than 5%, and in fact the instrument is not suitable for use under these conditions. (A modified instrument being developed, with the gages near the collar end of the instrument, might make some improvement. However, the gages will still have to be 6 inches inside the EX hole to be in a stable stress concentration area). The range of the instrument might be considered to include any naturally occuring stress provided no discing occurs. The reliability of the results from satisfactory runs would appear to be excellent

(Appendix A) except as the actual three dimensional stress field and rock anisotropy affect the two dimensional deformations. The calculations required to obtain the direction and magnitude of the planar principal stresses are relatively simple (Appendix A). Final data are considered to be an acceptable estimate of total field stress with a reliability of 20% to 100% error in magnitude and 10 to 25% error in direction.

The calculations to obtain the direction and magnitude of the three principal stresses (the three dimensional case) from deformation measurements in three drill holes are extremely complicated and have to be handled by computer. No programs are published, but the USBM at Denver have a program and have also written one for a desk top computer with extended memory.

Costs are difficult to estimate. In good ground, if ten or twelve readings were to be taken at one location, and with a total time of two weeks for the operation including moving the equipment in and out, the cost for drill rental, labor, and bits might amount to $500. per result. Under adverse conditions the figure could be $5,000. per result. In a large scale program, it might be possible to reduce the cost to $200 per result.

CSIR* "DOORSTOPPER"

Introduction - As explained by Leeman (64) the term "Doorstopper" results from the resemblance of the prototype instrument to the red cylinders of rubber used as doorstoppers in South Africa, and not from any scientific connotation. The Doorstopper is a three component instrument, measuring deformations of the end of a standard BX (2-3/8") hole, as the hole is continued with a coring bit. As with the BDG, these measurements may be converted to estimates of field stress provided that there are no cracks or other irregularities at or near the base of the hole; that the rock modulae are known correctly; and that the stresses parallel to the axis of the hole are not significant or are known. The instrument is not suited to measuring stress changes with time, and in fact has a very short hole life (a few hours), depending on the adhesive used to attach it to the rock. A full description of the instrument and the relationship between field stress and deformation (63) are given in Appendix B.

History - The instrument was first described by Leeman in 1964 (60). The report showed the considerable effort had been put into determining stress concentration factors in the bottom of a hole due to stresses in the plane normal to the axis of the hole, in cubes of materials of widely varying E. The stress concentration factors were shown to be constant over the middle 40% of the diameter of the hole, and the gage was designed to be attached to that area of rock. Factors for stress concentration were determined by the laboratory experiments, but these could not be verified theoretically because no mathematical anaylsis was available. The instrument, positioning tools, method of use and one field application were described in detail. Since that time the instrument has been refined and used in many countries, some early work being done by Li (67) in Norway, Van Heerden and Grant (116) in Canada, and in South Africa (56). From 1966 to 1968 several investigators

* South African Council for Scientific and Industrial Research

(Hoskins 55, Bonnechere and Fairhurst 9) began to check Leeman's formula for converting deformation measurements to field stress, and in 1969 Van Heerden (115) established new factors, one of which showed that the axial stress was in fact very significant, and under most circumstances would affect the Doorstopper at the end of the hole considerably more than the BDG further towards the collar. The early Canadian results (116) would tend to confirm this. A finite element analysis by Coates and Yu (17) confirms the importance of the axial stress, and also gives a table of stress concentration factors determined by many investigators.

Stephenson and Murray (110) in Australia developed their own form of Doorstopper, with direct strain gage bonding to the rock and continuous gage readout during overcoring. They got a peaking of the gage reading similar to that observed with the BDG. Extensive tests in South African gold mines by Pallister, Gay and Cook (83) showed these rocks to be stressed by gravitational forces only, as opposed to the very large horizontal and vertical stresses found in a similar environment at Elliot Lake in Canada. Bielenstein and Eisbacker (7) reported on the continuing work at Elliot Lake, where they were using the Bonnechere and Fairhurst stress concentration factors, whereas Leeman (64) preferred the Van Heerden factors. Leeman (64) in 1970 reported the use of gages in coal in South Africa, and measurements of stress in Canada, Sweden, Norway, USA, Italy, Rhodesia, South Africa and Australia. He also reported a cost of $160 (US) per measurement in South Africa, for capital and operating costs. This is presumably the cost for a skilled crew under good conditions with relatively low labor costs. In 1969 and 1970 the Italians reported (13)(69) costs of $250 per installation in excellent papers giving field problems. They compared the BDG with the "Doorstopper" coming out heavily in favor of the latter, but preferred an oversize coring bit.

Investigation Results - The Doorstopper and it's associated equipment is available commercially from South Africa.* The time lag from ordering is one to two months, caused mainly by transportation delays.

The engineer in charge of the project should be a graduate engineer with a masters degree, or considerable industrial experience, in rock mechanics. He could visit some of the engineers who have used the gage on this continent (mainly at the Department of Mines and Technical Surveys, Canada, but possibly at the University of Minnesota or Pennsylvania State University) but could not get any field training under instruction. Once the engineer has become familiar with the field use of the equipment and good practice for the best estimates of field stress (which could take several months) he could train a technician to take measurements in about a week. The technician would require close supervision for a considerable time if field conditions were difficult (eg highly stressed, folded or fractured rocks), and in fact under poor conditions it might well pay to have an engineer on site full time with two or three field crews operating.

A hole of size BX is drilled to the desired location, preferably along the axis of a principal stress. The end of the hole is ground flat and polished with a sequence of special square faced diamond bits. The polished rock face is then thoroughly dried and any water in the rest of the hole removed. A Doorstopper is plugged into the insertion tool, adhesive smeared on the end to be attached to the rock, and inserted into the hole. The

* Corner House Laboratories, Private Bag 1, Emmarentia, Transvaal, S. Africa.

Doorstopper is pushed against the polished rock face with a contact force of about ten pounds, it is oriented with the mercury switch, and held in position until the strain gages show no further movement. This indicates that the glue has set, and the insertion tool and cable are removed from the hole. Drilling is continued with a standard BX coring bit, which fits over the Doorstopper, for about five inches, when the core is broken off and removed with the Doorstopper attached. The Doorstopper is again plugged into the insertion tool and the destressed strain readings taken. The crew for this operation is at least three, two for drilling and an engineer/technician. Some operators prefer a crew of four.

There are a number of precautions that should be taken during these operations. All Doorstoppers should be tested in the laboratory when received, as some have been found to be defective and others have had the strain gage connections reversed. The gages should be taken underground the day before they are to be used to speed up the temperature compensating process (there is a temperature compensating core in the inserting tool). Particular care must be taken to dry the end of the hole and remove any water from the hole itself. The success ratio will not be high in a water bearing porous rock. No holes should be drilled at less than 5 degrees above the horizontal, to ensure good active drainage. Because the strain gages are not connected to the readout box during overcoring, it is not possible to check for inconsistencies, and consequently every apparently successful test must be tested for bonding before the results are accepted. In this connection, one particular set of seventeen successive bond failures in good very hard rock was caused by the rock surface being too smooth. Elimination of the final polishing bit operation overcame the problem.

While the mercury orientation switch is satisfactory in flatter holes, it becomes more difficult to use as the angle of inclination increases, and impossible before the vertical is reached. Under these circumstances a paint mark is put on the Doorstopper and a transit aligned under the hole. The bearing of the paint mark is then marked on the excavation wall, and this is later measured by surveying. The process is probably accurate within 5 to 10 degrees, and the procedure limits the distance at which measurements can be made in steep holes to about 30 feet. The distance in steep holes is also limited by the installing rods, which are hand manipulated rather than using the drill. Placement distances of several hundred feet are possible in near horizontal holes.

The mechanical reliability of the instrument is good, because it is so simple. Success rates of up to 70% are achieved, with the 30% failure rate caused by bond failure. Failures due to rock discontinuities or discing can reduce the success rate considerably. However, results are possible in ground that is too highly stressed or fractured to allow the use of the BDG.

The conversion of strains to stresses appears sound. However, the plane strains that the instrument measures are so sensitive to axial stress that very serious errors could occur if two dimensional solutions are made. For the three dimensional solution, three holes are required, and unless the regional stress field is very homogeneous, the measuring stations should be close together. This implies three drill set-ups and measurements over restricted hole lengths. The solution of the three dimensional case should be based on Panek's work (86) as modified by Gray and Toews (36). Computer programs to solve for field stresses based on these works are in existance (Mining Research Center, Mines Branch, Ottawa) but it is not known if this material is available to the public. Development of a program based on this material by a rock mechanics graduate engineer would probably take several months.

In shallow holes, say within 20 feet of the operator, and where there are no problems (shallow angles, no

ground water, etc.,) it is possible to get two and a half readings per shift. However, Doorstoppers should not be left in position at the bottom of a hole overnight. The placement rate reduces to one per shift at 40 to 50 feet.

The cost of the equipment (including cables, tools, meters etc. but excluding the drilling equipment) is approximately $2,000. The cost per overcoring (not per successful measurement) excluding capital costs and technician and engineer wages, at operations that have continued over two years in Canada, has been estimated at $200. Of this, the Doorstopper cost is about $15. The amount of time spent by the engineer in computing results is about 1/3 to 1/4 of the time spent taking measurements once a computer program has been established. The amount of time spent considering the implication of the results might be considerable. The total cost per successful Doorstopper measurement, for a company undertaking a major rock mechanics, program, might therefore amount to between $500 and $1,000, provided ground conditions were reasonable with reference to water, stress and fractures.

PHOTOELASTIC STRESSMETER

Introduction - The Photoelastic Stressmeter, often referred to as the Glass Plug, is a rigid inclusion instrument ($E = 10 \times 10^6$) for insertion into any size borehole, but in practice the usual size is for an EX (1½") hole. The gage deforms under the action of stresses applied in a plane normal to its axis, and because the glass is birefringent, estimates can be made of the magnitude of the planar principal stresses and their direction. Inspite of its name, it is still a strain instrument.

The instrument is used to measure increases in compressive stress with time, and has a very long hole life. It is not suitable for measuring absolute stress, because neither prestressing nor bonding for tensile loads are satisfactory. A full description of the instrument is given in Appendix C.

History - The Stressmeter was developed in the early 1960's at the University of Sheffield, based on a mathematical analysis developed by Hiramatsu et al in Tokyo and published in 1957 (49). The work at Sheffield consisted of instrument development and laboratory testing (along with other photoelastic gages), and was reported extensively in 1963/65 (94)(95)(92)(93)(92). Some field work was briefly referred to. The early attempts to prestress the instrument with a sliding wedge, to give a unidirectional assessment of field stress on overcoring (50) appear to have been abandoned. Limited field work in the mid 1960's in the United States is reported by Sellers et al (107), and a mathematical analysis of optimum reading positions was developed by Barron in Canada (5) in 1965. Since then little has been reported on the gage except for two articles from Russia (105)(57), but it is still quite widely used in Europe for monitoring stress changes. Its use in the United States is far more limited, although the reasons for this are obscure because it is doubtless a good monitor even when used quite crudely.

Investigation Results - The instrument is produced commercially in England and there is a United States distributor.* There is virtually no delay in delivery. The engineer in charge of the project should preferrably be a graduate, preferrably with some rock mechanics experience. In the past, one week courses were held in England to train engineers and technicians to use the equipment. The minimum training necessary is about half a day spent counting fringes and estimating principal stress magnitudes and directions. Technicians could be

* Terrametrics. 16027 West Fifth Avenue, Golden, Colorado, 80401.

trained to install and read the instrument in half a day. The interpretation of some patterns, and the proper correlation and appreciation of the results being obtained from the field are the province of an engineer. Should problems arise, the U.S. distributor can be approached by telephone or a representative can be hired at commercial rates ($200 per day plus expenses). Company literature provided with the instrument appears very thorough (22)(41) (107), but does not obviate the need for training in photoelastic reading.

A 1½" hole is drilled to the desired depth by diamond (EX) or other machine. It is difficult to drill a sufficiently smooth and even hole in hard rock with a percussive machine, but this is done at some mines. The hole is cleaned and washed with acetone to ensure good bonding, and checked for diameter and length. The allowable diameter variation for one size of gage is 1/8" (from d + 1/8" to d + 1/4," where d is the diameter of the cylinder), but it is possible to obtain gages and insertion tools in incremental sizes if necessary. The Stressmeter is mounted on the insertion tool, the cement mixed and placed in the cup on the instrument, and the instrument installed at the bottom of the hole, the cement being extruded around the edge of the cylinder. No orientation is required. The installing tool is removed immediately and the cement bond inspected for continuity and entrained air bubbles. The crew required for this operation is two or one, with one man required for subsequent readings. There is no necessity for the drill crew nor their machine to be on site during installation, so that drilling and installation are completely independent operations. Since, in general, only one plug will be installed from one drill set up, drilling costs and drill moving, set up and tear down costs are usually a major portion of the total costs. Good mobility in this phase of the operation could reduce costs considerably. The maximum distance the instrument has been placed from the operator is about 30 feet, because at present readings have to be made from outside the hole. This necessitates a telescope for holes deeper than 3 feet. Hole inclination is not critical, except that it is much easier to set the gage above water level, and the success ratio will be much greater. The instrument can be placed and read under clean water, with a good hole life.

The instrument is easy to install and the operation can be completed in an hour or so. It can be placed and operates quite successfully in highly fractured ground, but is not likely to be satisfactory if set across a single fracture in good ground. If the ground is so shattered that the hole tends to close, a 1-3/8" OD pipe may be inserted loosely and butted up against the gage immediately after installation. When installed unsuccessfully the pattern that developes will be unreadable, so that errors cannot be made. However, critical information could be lost over a period of months before it was realized that the gage would give no useful information.

The mechanical reliability of the instrument appears excellent, as is its hole life. The range, however, is very limited. Approximately five fringes can be read, at maybe 500 psi per fringe, to give a total increase in compressive stress of say to 2,500 to 3,000 psi. It is not possible to measure compressive stresses less than those present when the gage was installed.

The instrument is not easy to read accurately, requiring constant practice, and it might be considered a bit of an art. However, it is easy to determine the direction of the planar principal stresses and also major increases in magnitude. The calculations to determine the magnitude of the planar principal stresses are simple, but the instrument will have to be calibrated in the laboratory if the value of the deformation modulus exceeds 2.5 x 10^6 psi (5) or 4 x 10^6 psi (41). Alternatively a calibration factor can be taken from a chart in the distributor's literature (41) if the modulus is determined. No attempt is made to determine changes in the three dimensional stress field, but it has been stated for the Photoelastic Stressmeter (43) and shown for the rigid

brass inclusion (21) that axial stress changes do not affect stress readings normal to this direction.

The initial cost of the equipment, including setting tools, precision viewer and some meters is about $2,500. The individual meters cost about $25 to $45 each, depending on size. The cost per installation might be $100, and the cost to periodically read the meters and calculate and plot the results, very little.

OTHER STRESS GAGES

Griswold Gage - The Griswold Gage is somewhat similar to the BDG, measuring deformation across three diameters of a borehole on overcoring. The deformations measured are in three parallel planes. The instrument was first reported in 1963 (38), and was therefore ahead of the BDG. It has been developed by Cominco and reported on by them (104)(103), but is not available commercially. It would appear to be inferior to the present BDG in that slippage could occur at some measuring contacts when there is high axial ground stress. It requires a smaller hole and overcoring bit, and results by the single user appear acceptable.

Photoelastic Biaxial Gage - The gage is a birefringent plastic patch with a central hole, for attaching to the bottom of a borehole before overcoring. Thus it is the photoelastic equivalent of the "Doorstopper," and was developed in Sheffield at the same time as the Stressmeter (92)(40)(42)(39). It has been used to a limited extent in Norway (45) and Australia. It is available commercially in the United States,* but would not appear to offer any advantages over the "Doorstopper."

CSIR Triaxial Strain Cell - The Triaxial Strain Cell measures nine strains on the surface of a borehole as it is overcored, to give the complete three dimensional state of stress of the rock at one location in a single borehole. The instrument was first referred to by Leeman in 1967 (61), who also gave a full description and equations to determine the stresses in 1968 (62). Non-linear elastic rock characteristics were incorporated into the stress solution in 1969 (66) and a full description of the instrument, tools, and meters was given by Leeman in 1969 (63). Use of the instrument was reported from Norway in 1970 (68). A full mathematical analysis was produced in Canada in 1971 (125)(37). The instrument has been used in Finland and a similar instrument in Australia (89). It is produced commercially in South Africa,* and will probably be used initially by those engineers who have successfully used the "Doorstopper."

USGS* Solid Inclusion Probe - This is a three dimensional instrument with nine strain gages (3 x 3 gage rosettes) mounted on a one inch diameter chrome steel ball. It is not produced commercially, but is fully described in Geological Survey Bulletin 1258-C (76).

Other Gages - There are numerous other hard and soft gages which have been abandoned or superceded, and some still under development. Also many "home-made" models with minor modifications have been successfully used but are not discussed in this report.

*Terrametrics. 16027 West Fifth Avenue, Golden, Colorado, 80401.
*Corner House Laboratories, Private Bag 1, Emmarentia, Transvaal, S. Africa
*United States Geological Survey

OTHER METHODS OF STRESS MEASUREMENT

Flatjacks - Early work on flatjacks was done over twenty years ago both in the United States (Bureau of Reclamation) and in Europe (70). Work has continued on a world wide basis, and the method was used on the Snowy Mountain project in Australia in the late 1950's (2). In 1964 Panek (85) reported replacing the usual extensometer deformation measuring device by hydraulic pressure cells grouted into holes in the rock. In 1966 Hoskins (54) reported extensive laboratory tests, and in the late 1960's Rocha (98)(101) cut the jack slots with a diamond disc, to eliminate grouting. His work, however, was directed at modulus values rather than estimates of stress. As mentioned in the introduction, all these tests are done close to the operator, where field stress values are completely distorted by the presence of the opening itself and mining fractures. It does not appear to be practical to use these measurements to estimate field stresses under normal circumstances.

Hydraulic Fracturing - The pressures required to initiate cracking and propagate the cracks in boreholes theoretically allows the calculation of the maximum and minimum principal stresses. Cracking occurs in the direction normal to the minimum principal stress. The method is still under investigation (28)(27).

Discing - Discing, the breaking of diamond drill core into thin discs as it is being drilled, usually indicates highly stressed ground. It has been observed extensively in the Witwatersrand and Elliot Lake, and makes it impossible to measure stresses by the normal instruments. Obert and Stephenson (77) carried out extensive laboratory tests and came to some conclusions about the relative magnitude of the principal stresses, but as yet there is no way to use this phenomena to estimate the field stresses.

STRESS GAGE SUMMARY

1. Stress changes with time may be measured by a series of absolute stress measurements, using the BDG or "Doorstopper," but the cost of doing this would be at least an order of magnitude greater than by using a Stressmeter. Changes in absolute stress with time could best be obtained by installing Stressmeters, and once these were operating successfully, measuring absolute stress with a suitable gage. The limited range of the Stressmeters might necessitate the installation of two or three gages consecutively, but even this is likely to prove far less expensive than the multiple use of absolute gages.
2. Measurements of absolute stress may be made with the BDG or "Doorstopper" in competent to fractured rock, whether this be elastic or creeps, as long as the immediate response tends to be elastic. In general, as the ground becomes more fractured, the "Doorstopper" will give a greater success ratio than the BDG.
3. In highly stressed ground that tends to disc, the "Doorstopper" is likely to give a greater success ratio than the BDG.
4. As distances from the operator increase past thirty to fifty feet, the cost of using the "Doorstopper" is likely to be considerably less than using the BDG.
5. Use of the "Doorstopper" is likely to lead to use of the CSIR Triaxial Strain Cell when it is fully accepted. This instrument should show considerable cost savings over both the BDG and the "Doorstopper."
6. Under wet conditions, the BDG is likely to give a greater success ratio than the "Doorstopper."
7. If planar principal stresses only are to be evaluated, the axial stress will affect the stresses calculated from the "Doorstopper" deformations far more than the BDG, so that the latter is likely to give more accurate results.

8. The BDG tests a larger sample, which might lead to a better evaluation of the stress field.
9. The relative merits and limitations of the gages are shown in Table 2.
10. The engineer in charge of the project should have a good mathematical background and be familiar with computers.

GOODMAN JACK

Introduction - The Goodman Jack applies a unidirectional pressure to the inside of an NX borehole. The maximum possible pressure is about 10,000 psi, considerably greater than that required for surface or near surface engineering, and covering most of the range of field stresses in rock. The use of two instruments, one for soft and one for hard rock, enables precise (although not necessarily accurate) measurements of E to be made for a wide range of rocks over the pertinent pressure range. A description of the instrument together with the mathematical development and instrument testing is given in Appendix D.

History - In 1968 Goodman, Van and Heuze (34)(35) published the first details of the Goodman Jack. These similar papers gave the mathematical development of the equations used to relate deformation, pressure and deformation modulus, much of which was done by finite element analysis, including the effect of the formation of cracks. The papers gave comparisons of the results produced at three field locations by the Goodman Jack and other instruments, which were inconclusive. No laboratory tests on specimen of known E were reported. The instrument was used by the USBM Spokane Mining Research Laboratory (117)(20)(88) with inconclusive results. In 1970 laboratory work was reported (24) in tests to determine rock strength values, and more field work (46) with comparative but inconclusive modulus determinations. In 1971 a different finite element analysis was used (48) to show that the results might be 30% low due to fractures caused by the Jack. Stowe (112)(111) reported use of the instrument by the Army Corps of Engineers, and in a report to the Corps in 1971 Ohnishi (82) used a formula to give an increased modulus value (k = 1.63 cf 1.25) to allow for cracking. (Values of 1.630 and 1.250 give a highly misleading impression of accuracy). In all this time no valid laboratory work has been reported to show that the instrument actually gives correct values in samples of known modulus.

Preliminary laboratory tests by the U.S. Bureau of Mines Spokane Mining Research Center indicate low results from the Goodman Jack in homogeneous material. The U.S. Army Corps of Engineers, Missouri River Division Laboratory, has also laboratory tested the instrument quite extensively and obtained consistently low results. Reports will be issued shortly by both institutions.

Investigation Results - The instrument is produced commercially, but to date there can be long delays for delivery and repair.*

It is necessary that the engineer in charge of the project should be a graduate engineer, preferrably experienced in rock mechanics theory and practice, geology, and with some knowledge of electronics and hydraulics. The descriptive literature provided with the instrument is sufficient to allow the engineer to

* Slope Indicator Co., 3668 Albion Place N., Seattle, Washington 98103.

assemble, test, and install the instrument, and also to calculate the values of E measured. The instructions could be improved with regard to site preparation, instrument calibration, good practice for best results, and maintenance problems. Thus it is essential that a thoroughly competent engineer be in charge of the first field work. Once he has become proficient with the instrument, he could train a technician to operate the equipment successfully in about a week. Alternatively the manufacturer will provide technical assistance in the field for commercial fees. There should be no major difficulties in transferring control of the operation from one engineer to another.

The instrument (hard or soft rock model) is inserted in an NX (3") borehole attached to the end of BX casing. This allows the instrument to be located and oriented as desired. The crew required for this operation is two on the drill once the equipment can no longer be manhandled (about 20 feet from the collar of the hole), and two on the instrument. It is possible to limit the total crew to three. The maximum distance from the operator that the equipment has been placed is 1,000 feet, (downwards) although it is not suggested that this is the limit. Hole inclination would not appear to be critical, and water pressure within the hole should not cause problems, although little information is available on these points. Changes in hole diameter over long distances can cause delays to measurements, because the instrument might have to be taken out of the hole and adjusted. Changes in diameter over short distances and wall spalling can lead to abortive measurements and the possibility of instrument damage or destruction. The instrument can also be damaged by operating it when it is not concentric with the hole: little information is available on the performance of a centering device to eliminate this problem. The jack cylinders can become fouled by fine shale particles in suspension in water in the hole, so that the instrument has to be withdrawn from the hole and washed off after each cycle. Larger pieces of rock can be stopped from jamming the jack plates open by suitably placed screens. When installing the instrument in deep holes, the build up of fluid pressure in the hoses can lead to opening of the jacks and consequent hanging up on the plates, with subsequent instrument damage or loss. In view of the field difficulties when used in deep holes, and the cost of the (probably uninsurable) instrument, it might be advantageous to hire an experienced technician for two or three days (at a cost of about $500 plus fares) to assist and advise the field crew. It should be noted that the pressure gage reading would probably be low by nearly 10% in the deepest holes. There is no limit to the number of tests that may be made at one position in the hole, nor to the distance between one measuring position and another, provided the ground is not damaged during the tests. No information is available on the length of life of the instrument if left in the hole.

The amount of time to take a set of readings varies with the actual jobs to be done. Assembling the equipment on location and testing might take 40 minutes to a shift; installation and orientation in a shallow hole ten minutes and at depth, 2 hours/100 feet of hole; the loading and unloading at one location ten minutes to an hour per cycle; and removal from the hole a few minutes. Thus it should be possible to complete tests at two positions per day unless there are difficulties due to depth or hole condition. Fractured ground could lead to no results from several weeks work.

The mechanical reliability of the instrument appears to be reasonable, the main trouble being damage to the O ring seals. The limited travel of the jack plates can cause delays due to the need to adjust the

instrument and low pressure results in ground with a low value of E (the maximum travel under full calibration is 0.2"). The calculation required to get a value of E (see Appendix D for derivation) is very simple. The values obtained are about 1/3 to 1/10 of the E values obtained from laboratory tests of diamond drill cores. It has been stated that this is a better estimate of the actual value of the prototype value of E, because it includes the effects of cracks and seams in the body of the rock (35). However, it has also been shown (48) that cracks caused by the operation of the jack could lead to estimates of the value of E 30% lower than the correct value. Two investigators have found that the values of E obtained in the laboratory were much lower than the uniaxial value of the specimen, thus throwing doubt on either the equipment performance or the mathematical and laboratory derivation of the formula.

The instrument costs about $6,000 to purchase, or rents for about 10% of this figure per month. There would occasionally be repairs of $500 or so. The remaining costs consist of:

1. Drilling NX holes, at say $10 to $12 per foot.
2. Labor costs for probably two engineer/technicians, and in addition, for depths greater than 20 feet, one or two drillers.
3. Calculation and data recording (office) charges.
4. Company overheads on the above.
5. On the first deep hole, up to $1,000 for consulting fees and expenses.

In holes more than 20 feet deep at 2 readings per shift the cost per reading could easily approach $100 for a series of several hundred readings.

USBM CYLINDRICAL PRESSURE CELL

Introduction - The Cylindrical Pressure Cell (CPC) applies a radial pressure to the inside of an EX borehole. A full description of the instrument is given in Appendix E. The maximum field pressure applied is about 7,000 psi, so that the range is not quite so large as that of the Goodman Jack, but still covers most field conditions.

History - There appears to be only two papers published on the CPC, the original giving full description of the instrument, the derivation of the equations and the laboratory testing to validate the results in 1964 (84), and in 1970 a report on results obtained in fractured ground (87).

Investigation Results - The cells, tubing, and pressure gage are produced commercially,* and the supplier

* Terrametrics Inc., 16027 West 5th Ave., Golden, Colorado, 80401

could also produce the volume-metering fluid pump and calibration cylinders. Delivery of the presently produced equipment is about three weeks, but longer delays should be expected for the pump unit.

The standard of engineering personnel required on the project is similar to that required for the Goodman Jack. There is no descriptive literature available for the operator in the field other than the original article by Panek (84 and Appendix E), which gives virtually no advice on field use. It is understood that there is a manual in existance at the USBM, Federal Center, Denver, that might be made available to a CPC user. The personnel there would also train operators, but there could be considerable delays. Estimates of the field training necessary vary from two days to two weeks, which is probably realistic. The length of time taken to produce good and quick results, consistent with ground conditions, would also vary widely, depending on the initial training and practical experience of the operator, because the instrument is very difficult to install. Assistance at commercial rates is available from the supplier. Transferring control of the operation from one engineer to another could prove difficult if there is no third party available, skilled in the use of the instrument.

The instrument and calibration cylinders are taken into the mine several hours before they are required, because the instrument is temperature sensitive. (At locations near the bottom of the downcast shaft, and in recently developed or mined areas, there can be large differences between rock and air temperatures, so that this procedure might well be meaningless). At the start of the test the instrument is placed in each of two calibration cylinders and the pressure cycled up and down twice in each, to determine the two calibration constants. The instrument is then placed in an EX (1½") borehole and the pressure cycled twice at the desired location. It is then moved to other locations where values are required, and cycled twice at each. A two man crew is required for this operation, or two crews or two men can be used, one on calibration and the other on rock measurements, to speed the operation. Drilling is also done by a two man crew.

The maximum distance the instrument has been placed from the operator is twenty feet, but it appears that it might be possible to go as far as fifty feet, and one operator has suggested a hundred feet as the maximum distance. Hole inclination presents no problems, except that the flatter holes are more difficult to clean thoroughly. Water presents no problems.

The diameter of the hole is critical. Because the instrument is nearly rigid, the hole must be drilled to + 0.025". The instrument will stick in an undersize hole, and burst in one that is oversize. Spalling of the hole can also lead to jamming or bursting, and incorrect readings. It is generally accepted that the copper sheath will usually only last for one reading, although a highly skilled operator might average two or three readings per sheath. The difficulty in moving the instrument has led one operator to describe the instrument as a stress monitoring meter (for measuring change of stress rather than absolute stress), and a second to be investigating its use to measure absolute stress in high creep materials (salt, etc.).

There is no limit to the number of positions in a hole that the gage may be used, except that in soft rock readings should be at least a foot apart. The life of the instrument, is left undisturbed in a hole, can be several years. Provided there are no difficulties, a crew should be able to complete a calibration and one reading in four hours. If the sheath is then destroyed in moving the instrument in the hole, one reading per day is likely

to be the productivity, otherwise two or three readings might be obtained. Under adverse conditions, or with a diamond drill runner who was not highly skilled, months could be spent for no results. Under ideal conditions, a skilled operator should have a success rate of 75%, with most of the failures arrising from ruptured cells.

The cells should be tested to about 9,000 psi before they are taken into the field, so that mechanical reliability should be very good. It should be planned to resleeve and refill each cell after each attempted test in a proper workshop. Under some conditions, it might be possible to get one reading per cell used; under other conditions, tens of cells might be used per valid result. The calculations to get a value of G (modulus of rigidity, and equal to E/2 (1+v), where v is Poisson's ratio) are relatively simple. If necessary, the USBM can be approached for assistance with the calculations. The results obtained have been compared with standard tests on cores and cylinders by two operators, and have agreed within 10% and 20%. Sonic measurements by a third operator were 50% higher than the CPC results. The laboratory testing of the instrument (see Appendix E) appears to have been very adequate. The instrument is probably reliable for measuring the values of G or E for rocks with an E value of 1×10^6 psi or greater.

The cell and pressure gage complete costs about $145 and the calibration equipment about $500. The cost of a sleeve is about $30, so that with transport and labor charges, the cell cost might be $100 per use. The volume-metering pump would be an extra charge. An approximate estimate of the cost of determining several values of G at one location is from $300 to $2,000 or more per individual value.

MENARD PRESSUREMETER

Introduction - The Menard Pressuremeter applies a radial pressure to the inside of drillholes. Units are made to fit NX (3"), BX (2-3/8"). AX (2") and EX (1½") holes, but the standard instruments provided in the United States are the long and short NX models. A description of the instrument is given in Appendix F. The high pressure model, utilizing a urethane sheath, is designed for pressures up to 1,500 psi, so that the instrument is basically for soils (E 500,000 psi) but will operate up to values of $E = 1 \times 10^6$ psi (soft or fractured rock) with increasing error. At E = 500,000 psi, even when considerable care it taken to prepare the instrument for use, the field value of E measured by the instrument has to be increased by a minimum or 40% because of the softness of the system. This figure can be two or three hundred percent in error if air is left in the liquid system. For $E = 1 \times 10^6$ psi, the minimum correction is about 80%. Under these circumstances the instrument has to be calibrated before and after each set of field readings. It is not known how thoroughly the reproducibility of the instrument has been investigated under these circumstances.

History - Not much literature is available in English on the Menard Pressuremeter because the instrument was developed and has been used mainly in continental Europe. In 1966 Geocel contracted to carry out investigations for the U.S. Army Corps of Engineers, and produced two reports (30)(31), and in 1968 Smith (109) presented a research report on the use of the instrument for full evaluation by the California Highways

Division. The instrument is being used quite widely for sub-surface investigations of soil and shattered rock, but little has been published about this.

Investigation Results - The instrument is manufactured in France and imported into the United States.* Delivery of a used Pressuremeter is two or more weeks, to be replaced by a new model in about six months.

The investigating team should be headed by a graduate engineer with considerable experience in soils mechanics. The field operator need not be an engineer, but should be an experienced practical technician. Because the use of the instrument is quite an art, and because the drilling of the hole can have an appreciable effect on the magnitude of the results, the engineer evaluating the results should be thoroughly acquainted with general soils mechanics field work. Training to interpret the field results might take two days, and two to six days might be required for field training. Considerable literature has been published by the distributor (32)(33), some translated from the French and some prepared by the company, but the use of this alone is likely to cost considerably more than employing the distributor at commercial rates to train the operator's personnel. Ground conditions under which the Pressuremeter is operated are varied, from sands and clays through layered hard and soft material, fractured, fissured, with voids, and with water or dry. Under these circumstances, transferring the control of the operation from one engineer to another, or the field work from one technician to another, is likely to be very expensive either in time or in the value of the results produced after the change over.

The instrument is inserted into an NX hole on the end of an AX rod string. Gas and water pressure are applied simultaneously to membranes inside a cylindrical urethane or rubber sheath. The pressure is held constant for one minute, and changes in the volume of liquid in the meter on surface recorded at the end of 15 seconds, 30 seconds, and 60 seconds. The pressure is then increased to a higher level and the volume measurements repeated. For a full soils analysis program, it is attempted to get well past the pseudo elastic range (where the stress strain curve is linear) into the plastic range, in ten increments of pressure. Whether this range is always necessary depends on the material being tested and the purpose of the test. The drilling, rotary with diamond, tricone or drag bits; auger; or percussive, with a variety of bits; dry or wet, with or without bentonite added to the water, is done by a two man crew. One man is required for the instrument calibration, operation, and recording of results. Usually the full crew of three is required all the time.

The greatest distance that the instrument has been used from the operator is 365 feet, and this is probably getting close to the limit in down holes. It is possible that in horizontal holes, where there is no build up in liquid pressure, greater distances might be reached. Hole inclination probably presents no problems, although only one operator has used the instrument in an up hole, at a distance of 30 feet. (The basic objective of most of the operators of this instrument has been for data on soils, and the instrument has been used in rock only as

* Geocel Inc., P. O. Box 316, 11680 West 44th Avenue, Wheat Ridge, Colo. 80033

it occured in a soils investigation). While water is an added complication in that it changes the properties of the freshly drilled material, it is commonly present. It necessitates instrument readings as soon after the ground is exposed as possible (implying the extension of a hole for each reading, rather than drilling a complete hole and then measuring E at a number of locations) and corrections to the applied pressure.

As with the CPC, the diameter of the drill holes is critical. The magnitude of the problem, however, is different in that the tolerance is greater (drill hole diameters of from 2-7/8" to 3-1/8" are probably satisfactory, depending on the type of ground) but the ground is usually much more difficult to drill accurately. Thus the type of drill used can vary with the ground, as well as the type and size of bit. Poor drilling, a varied diameter of hole, fissured ground, or ground with large voids, can all lead to ruptured sheaths. Poor drilling or caving can cause a hole to be so oversized that no measurement is possible. The instrument can get buried or jammed in a hole, but can always be pulled out, occasionally at the expense of a sheath. In this respect, it is more robust than the Goodman Jack, the limited amount of damage being easily and inexpensively repaired. Sheaths can last from one to twenty five or more readings.

Readings are often taken at three to five foot intervals along a hole. Because the material is often soft, and deforms permanently even in the pseudo-elastic range, it is not normal to take overlapping readings.

Calibrating of the instrument need not be done frequently once the crew is skilled and when operating in low E material. Thus, in general, calibration is not a major time factor on a job. (Even with an unskilled crew, the amount of time spent calibrating is likely to be small compared with the time lost on the field measurements). For a skilled crew, drilling and taking readings alternately over five foot intervals, the optimum performance at depths of less than 100 feet, is one reading per hour. The average is about half that rate, and bad conditions or an unskilled crew might reduce the rate to one per day.

The mechanical reliability of the instrument in the field is good, partly because there are virtually no moving parts, and partly because it its a low pressure instrument. The calculations to obtain E, and determine the range over which it is realistic, are somewhat tedious. There is also no doubt that under some circumstances, such as when the instrument is placed across the boundary between two materials of significantly different E, yield strength, and fracturing, the interpretation of the results could be very difficult and time consuming.

Little work has been done in this country on determining the accuracy of the results produced from the measurements and calculations. One operator says that the results are comparable to triaxial soil tests and blow counts, and that he is now trying to correlate the results with soil plate bearing tests. A second operator has had good agreement in a limited number of tests between the results obtained from a Pressuremeter and a Goodman Jack in soft (E 500,000 psi) shale. This operator also preferred the field qualities of the Pressuremeter, but this might have been influenced by the fact that he was familiar with the Pressuremeter, and also nearly lost the jack, jammed down the hole. It would also seem, from most operators, that for soil and other low E materials, a radial E is preferred to an oriented E. The mathematical derivation of the formula in the appendix is in general agreement with the work done for the CPC. No laboratory testing is reported, although it is understood that the instrument has been used very extensively in Europe.

The cost of the instrument is $5,100 complete with three NX probes (two long and one short) and 165 feet of coaxial tubing. The urethane rock sheath costs $45 and the rubber soil sheath $15. The cost of a skilled technician to operate the instrument or train operators is about $200 per day plus traveling expenses. One consultant charges, $125 per test, the drilling to the client's account. In general, a rough estimate of costs for measurements done by the distribuotr for a client, with drilling costs to the account of the client, are

Soil, from $60 per test

Rock, from $120 per test with the upper iimit probably exceeding $1,000 per test. In general if a limited amount of test work is required (say less than a month), a consultant should be hired to do the work rather than an instrument rented to be operated by personnel unfamiliar with its use and the interpretation of results.

BOREHOLE DILATOMETER

Introduction - The Borehole Dilatometer (BHD) is sometimes called the Rocha Dilatometer after the director of the Laboratorio Nacional de Engenharia Civil (LNEC), where it was designed and is manufactured. There are at present no models in the United States, and anyone wanting to use the instrument would have to import it from Portugal.* The amount of information available in this country on the field use of the instrument is very limited, and there may be many more problems associated with its use than are reported here. In fact, any potential importer of the instrument should be prepared to devote several weeks or even months to field testing the instrument, to overcome both mechanical and data interpretation problems.

The instrument applies a radial pressure to the inside of an NX (3") borehole, but unlike the CPC and Menard instruments, it does not measure the mean increase in radius of the hole (by measuring the volume pumped into the instrument) but four diametral deformations with eight LVDT's, with four pairs at 45 degrees to each other, thus the anisotropy of the rock can be measured. A description of the instrument is given in Appendix G.

History - The instrument was first described in a paper by Rocha et al in 1966 (99). A paper in 1970 by Rocha et al (100) claims that the instrument has been much improved over the 1966 model. Considerable field testing is reported in the latter paper, but as with the Goodman Jack (and Menard Pressuremeter), no laboratory testing in elastic specimen of known modulus. In fact, the field testing seems to have been done in material of low modulus that yields continuously No papers have been found on the Dilatometer by authors other than Rocha.

Investigation Results - The instrument is now in production, after many delays caused by teething

* Laboratorio Nacional de Engenharia Civil, Av. do Brasil, Lisboa 5, Portugal

troubles. The time required to produce and calibrate an instrument is about four months, so that delays in delivery could be anywhere up to that time.

The standard of engineering personnel required on a project employing a BHD is higher than is necessary with other instruments, because the team would be more or less unsupported. The LNEC will give assistance with the interpretation of results, but this is probably of little real value, because the geology of the area and the results would have to be written up and sent to Portugal, and even then there are likely to be language and terminology problems. It is stated that the manual provided with the instrument gives full instructions on use, maintenance, and repair, but there is no copy available in this country to date, and it has not been seen by the author. Under these circumstances, it is apparent that the project leader should have a wide practical, theoretical, and research oriented background.

Holes are drilled ahead of the rock property measurement program. If the ground is fissured, it is cemented in sections of less than ten meters at a time. The holes are then redrilled. This is required to reduce deformation of the sheath, which would lead to incorrect results and bursting of the sheath if not attended to. The placing of cement in limited lengths is done in order to eliminate any effect of grouting, as it is not intended to alter the rock properties, but only to produce a rock surface compatible with the limitations of the instrument sheath. This would tend to suggest that in badly fractured ground, where differential movement is likely to occur between one fragment of rock and another, that the instrument sheath might be damaged and that the readings might be less reliable than those obtained from a volume measuring instrument.

The instrument is positioned and oriented in the hole on the end of steel rods. The rods are scribed, and a removable sight is used for orientation. A crew of two is required to position and operate the instrument in the first twenty to thirty meters of hole. For deeper holes, a larger crew is required. Normally the instrument is placed in the lowest position in the hole, and raised to each new position where readings are required. This ensures that any material that spalls off the sides of the hole during the operating cycle drops clear of the instrument as it is moved.

The instrument has been used up to 100 meters (300 feet) from the operator in a vertical hole, and it is stated that this could be increased to 200 meters. There is more difficulty in placing the instrument in inclined holes, and the maximum horizontal distance might be 50 meters. There is no field experience in placing the instrument in holes inclined above the horizontal. Water is said to present no problems, although the large number of "O" rings used to seal the openings between the interior and exterior of the instrument seems to be a point of weakness, and some unreliability might be expected in this respect. It is normal practice to withdraw the instrument above the water level in a hole (but not out of the hole) if operations are to be suspended overnight before measurements in a hole are completed. This also tends to indicate waterproofing problems.

The instrument measures deformations to the nearest micron (0.001 mm) so that it can be used to measure Young's Modulus up to about 10×10^6 psi. However, since the maximum laboratory pressure that can be applied is about 2,500 psi, and since the field value is probably well below 2,000 psi, it does not cover the range commonly found in stressed rock underground. This means that if the modulus of deformation is a function of stress, then the range of the instrument is limited to measurements in rock occuring within 2,000

feet of the surface. Even here, if the lateral stress is high (and it can well be 10,000 psi within 2,000 feet of the surface) the range of the instrument is exceeded to a considerable extent.

The pressure on the instrument is cycled up and down until three successive curves are superimposed on each other. The instrument may then be rotated 22½ degrees at the same location and the measurements repeated, to get a more detailed plot of the anisotropy at that location. It is not usual to move the instrument less than half a meter vertically, as this would put part of the instrument in virgin hole and part in altered rock. Because clearance between the instrument and the hole is large, the initial positioning of the instrument is quickly accomplished, as is repositioning between measuring locations. Thus in fairly shallow holes, where no problems are encountered, and with an experienced crew, it might take an hour to position the instrument and get the first set of readings, and forty five minutes to reposition the instrument and get each subsequent set of readings. On the other hand, it is possible to lose the instrument in the hole.

The success rate probably averages 60 - 70%, with most failures occuring from neoprene sheath rupture due to fractured or fissured ground or the hole being too large. Replacement of the sheath takes about thrity minutes, and it can be done in the field. It is claimed that the instrument is mechanically reliable.

The instrument is calibrated in a steel tube at LNEC, and should not need recalibration after replacement of a sheath because the LVDT's are connected to steel spheres which are in contact with the side of the hole. The results obtained are always numerically smaller than those from laboratory tests on core from the same location. However, in good competent ground, the dilatometer results are very close (within 10%) to the core results. It should be noted that although considerable mathematical development has been done to prove that cracking caused by the dilatometer has little effect on the value of the modulus computed (Appendix G), no laboratory testing has been carried cut to verify this.

The cost of work done with the dilatometer would be exceptionally high at present, due to both the capital cost of the instrument (around $24,000) and also the limited field experience throughout the world and in this country in particular.

OTHER MODULUS GAGES

There does not appear to be very much activity in developing new modulus gages. Probably the only significant work going on at present is an attempt to produce an instrument like the CPC, but with a more flexible sheath, so that it would be easier to handle in the field.

OTHER METHODS OF MEASURING MODULUS

There are three commonly used methods of determining rock modulus values other than with a gage; the loading of a rock cylinder or annulus, usually obtained from diamond drilling, to determine a value of E for an intact sample of up to several hundred cubic inches; in situ jacking tests, affecting several hundred cubic feet;

and dynamic tests, affecting very large volumes.

Laboratory Tests - The laboratory tests are uniaxial or triaxial on cylindrical specimen, and biaxial or triaxial on annular specimen. The annular specimen usually result from measurements of in situ stress using an overcoring technique. Equipment developed by the USBM for these tests is well documented (29,80), and can be used to apply stresses up to and above those encountered in the field at the test location. The biaxial field instrument, which is being improved to allow faster testing, applies stress in the direction of deformation measurements, but of uniform magnitude rather than the two planar principal stresses that occur in the field. Because the equipment applies stresses of the same magnitude as the original values to the actual rock speciman in which deformation measurements were made, it is likely to give the best values of E for assessing the original field stress. Tests on cylindrical cores are also likely to give the best values of E for the doorstopper tests, although the value of E should be obtained from the confining radial load rather than the axial load, which is not common practice.

Jacking Tests - Jacking tests affect a large volume of rock and are therefore valuable when it it required to assess the modulus of deformation of rock including geological and mining fractures. The stress level applied to the surface of the rock is low (not usually more than 1,000psi), and the value decreases with distance into the rock, so that at depths unaffected by mining, the stress levels are very low. The tests require a considerable amount of room for the equipment, which is normally left in a position for a number of days. The cost is likely to be very high ($50,000 to $200,00). The U. S. Bureau of Reclamation has done more work using this method than any other group, and the present position is well described in an article written by their engineers (119). The method is of most use for major works in a small area near the surface, so that few tests are required and the high cost can be justified by the very large cost of the project.

Dynamic - Dynamic methods appear to give modulus values consistently above jacking tests and usually greater than laboratory static tests (118)(23)(25). However, Timur (114) got dynamic test results less than laboratory static, although considerably greater than the jacking results. There would appear to be more resaerch work required before in situ dynamic methods are reliable; however they offer the greatest potential for economics, speed, accessibility, and versatility.

MODULUS GAGE SUMMARY

1) The four instruments investigated appear to provide the only methods of assessing the geological modulus of deformation, other than large scale jacking tests. This modulus is required directionally for finite element analyses, and is probably the best value to use for many other engineering calculations, including surface and near surface foundation design. Laboratory tests on diamond drill cores from stress relief deformation measurements probably provide the most suitable values of deformation modulus for assessing the field stress values.
2) Of the four instruments investigated, it is recommended that the Rocha Dilatometer should not be considered by investigators until reliable agents are available in this country and that the costs are

reduced to a competitive level.

3) Plate I shows the range covered by the instruments with respect to stress levels and modulus of deformation. The Rocha Dilatometer covers near surface hard rock conditions, the CPC and Goodman Jack cover this range and relatively deep hard rock conditions as well. The Menard Pressuremeter and Rocha Dilatometer are suitable for soft rock, as is the low pressure Goodman Jack. The CPC and high pressure Goodman Jack are not suitable for soft rock measurements.
4) Because there is some doubt about the parameters that the Goodman Jack is measuring results produced by this instrument should be treated with a great deal of caution. The CPC should be used rather than the Goodman Jack whenever possible.
5) It is apparent that there is no really satisfactory hard rock instrument for measuring in situ modulus at a considerable distance from the investigator. The most satisfactory method must still be laboratory testing of diamond drill cores.

REFERENCES

1. Abel, John F., Jr. Evaluation of Stress Instrumentation for Project Payette, Special Projects Branch, Technical Letter, Special Reports - 22, U. S. Dept. of Int/Bureau of Mines, Federal Center, Denver, June 11, 1968.

2. Alexander, L. G. Field and Laboratory Tests in Rock Mechanics, Conf Proc 3rd Austral, New Zealand, Con on Soil Mech, Found Engng pp 161-68, 1958.

3. Austin, W. G. Field and Laboratory Tests for "Safety of Dams" Investigation at Salt River Project, Arizona, U. S. Dept. of Int/Bureau of Reclamation, REC-OCE-70-7, February 1970.

4. _____. Development of a Stress Relief Method with a Three-directional Borehole Deformation Gage, REC-OCE-70-10, March 1970.

5. Barron, K. Glass Insert Stressmeters, Canada Dept. of Mines and Techn Surveys, Mines Branch Reports, October 1964.

6. Benson, R. P., T. W. Kierans, and O. T. Sigvaldason. In Situ and Induced Stresses at the Churchill Falls Underground Powerhouse, Labrador, the 2nd Congress of the International Society of Rock Mechanics, Belgrade, Yugoslavia, September 1970.

7. Bielenstein, H. U., and G. H. Eisbacher. In-Situ Stress Determinations and Tectonic Fabric at Elliot Lake, Ontario, Proc 6th Canadian Rock Mech Symp, Montreal, 1970.

8. Black, R. A. L., and E. Hoek. Status of Rock Mechanics as Applied to Mining, 9th Symp on Rock Mechanics, Colorado School of Mines, 1967.

9. Bonnechere, Francois. A Comparative Field Study of Rock Stress Determination Techniques, M.SC Thesis, Univ Minnesota, 1967.

10. Bonnechere, F., and C. Fairhurst. Determination of the Regional Stress Field from 'Doorstopper' Measurements, Jl S Afr Inst Min Metall, Vol. 68, No. 12, July 1968.

11. Buchbinder, G. G., E. Nyland, and J. E. Blanchard. Measurement of Stress in Boreholes, Geological Survey of Canada, Paper 66-13, Drilling for Scientific Purposes.

12. Cannaday, Francis X. Modulus of Elasticity of a Rock Determined by Four Different Methods, U. S. Dept. of Int/Bureau of Mines, RI 6355, 1964.

13. Capozza, F., S. Martinetti, and R. Ribacchi. Results of State-of-Stress Measurements in Rock Masses by Means of Borehole Devices, Int Symp on the Determination of Stresses in Rock Masses, Lisbon, 1969.

14. Chan, Samuel S. M., and Thomas O. Meyer. Overcoring Stress Relief Experience in the Belt Rocks, 9th Symp. on Eng Geology and Soils Eng, Boise, Idaho, April 5-7, 1971.

15. Clark, G. B. Deformation Moduli of Rocks, Testing Techn for Rock Mech, ASTM STP402, Am Soc Testing Mats, p 133, 1966.

16. Coates, D. F., and F. Grant. Stress Measurements at Elliot Lake, The Canadian Mining and Metallurgical Society Bulletin, Vol. 69, No. 649, pp 182-192, 1966.

17. Coates, D. F., and Y. S. Yu. A Note on the Stress Concentrations at the End of a Cylindrical Hole, Int J Rock Mech Min Sci, Vol. 7, No. 6, p 583-588, 1970.

18. Conway, John P. Suggestions for Improvement of the Overcore Method, Internal Report, U. S. Dept. of Int/Bureau of Mines, Spokane Mining Research Center.

19. _____ . Progress Report on Crescent Mine Overcoring Studies, Support Load Prediction Project, Internal Report, U. S. Dept. of Int/Bureau of Mines, Spokane Mining Research Center, January 10, 1968 - April 15, 1968.

20. _____ . Goodman Jacking Tests, Internal Report, U. S. Dept. of Int/Bureau of Mines, Spokane Mining Research Center, 1969.

21. Copen, Merlin D., and George B. Wallace. Determination of In-Situ Stresses in Concrete Dams, Journal of the Power Division, Proceedings of the American Society of Civil Engineers, March 1971.

22. Dhir, R. K., and I. Hawkes. The Measurement of Stress Change in Concrete Using the Biaxial Photoelastic Stressmeter, Conf on Experimental Methods of Investigating Stress and Strain in Structures, Prague, 1965.

23. Dodd, Jerry S. A Technical Presentation of Morrow Point Underground Powerplant Rock Mechanics Investigations, U. S. Dept. of Int/Bureau of Reclamation, March 1967.

24. Drozd, Karel, Richard E. Goodman, Francois E. Heuze, and Tran K. Van On the Problem of Borehole Strength Testing, Proc of the 2nd Cong of the International Soc for Rock Mechanics, Beograd, Vol. II, pp 325-333, September 1970.

25. Dvorak, Arnost. Seismic and Static Modulus of Rock Masses, Proceedings of the 2nd Congress of the International Society for Rock Mechanics Beograd, Vol. I, pp 313-317, 1970.

26. Dyson, L. A. A Rock Mechanics Survey and Its Use in an Underground Stability Analysis at Kambalda, W. A., Proc 1st Australia-New Zealand Con Geomechanics, Melbourne, Vol. 1, pp 67-72, August, 1971.

27. Fairhurst, C. Borehole Methods of Stress Determination, Int Symp on Rock Mechanics, Madrid, October 1968.

28. Fairhurst Charles. Methods of Determining In-Situ Rock Stresses at Great Depths, Tech Report No. 1-68, School of Mineral and Metallurgical Engineering, University of Minnesota, February 1968.

29. Fitzpatrick, John. Biaxial Device for Determining the Modulus of Elasticity of Stress-Relief Cores, U. S. Dept. of Int/Bureau of Mines, R1 6128, 1962.

30. Geocel, Inc. Report of Pressure Meter Investigation, Pre Gondola - 1, U. S. Army Corps of Engineers, Nuclear Cratering Group.

31. _____. Pressuremetric Investigation after Blasting, Pre-Gondola Project, U. S. Army Corps of Engineers, Nuclear Cratering Group.

32. _____. The Geocel Pressuremeter, Interpretation of a Pressuremeter Test, Golden Colorado.

33. _____. Menard Pressuremeter, Equipment Operation, Data Interpretation.

34. Goodman, Richard E., Tran K. Van, and Francois E. Heuze. The Measurement of Rock Deformability in Boreholes on Earth, Adaptability to a Lunar Exploration Program, NASA Contractor Report, NASA CR-61202, February 1968.

35. Goodman, Richard E., Tran K. Van, and Francois E. Heuze. The Measurement of Rock Deformability in Boreholes, 10th Symp on Rock Mechanics, University of Texas, Austin, May 1968.

36. Gray, W. M., and N. A. Toews. Analysis of Accuracy in the Determination of the Ground-Stress Tensor by Means of Borehole Devices. Proceedings 9th Symp on Rock Mechanics, Colorado School of Mines, Golden, Colorado.

37. _____. Optimization of the Design and Use of the CSIR Triaxial Strain Cell for Stress Determination, Canada Dept. of Eng, Mines & Resources, Mining Research Center, Internal Report MR 71/94-LD, September 1971.

38. Griswold, George E. How to Measure Rock Pressures, New Tools, and Proved Techniques Aid Mine Design, E&MJ, Vol. 164, No. 10, pp 90-95, 1963.

39. Hawkes, I. Theory of Photoelastic Biaxial Strain Gage, Int J Rock Mech and Min Sci, Vol. 5, No. 1, pp 57-63, January 1968.

40. Hawkes, I., and S. Moxon. The Measurements of In-Situ Rock Stress Using the Photoelastic Biaxial Gage with the Core Relief Technique, Int J Rock Mech and Min Sci, Vol. 2, No. 4, 1965.

41. Hawkes, Ivor. Instruction Manual, Photoelastic Stressmeter, Terrametrics.

42. Hawkes, Ivor. Theory of Photoelastic Biaxial Gage and Its Applications In Rock Stress Measurements, Strain, Vol. 3, No. 3, pp 36-43, July 1967.

43. _____. Personal Communication.

44. Hedley, D. G. F., G. Zahary, H. W. Soderlund, and D. F. Coates. Underground Measurements in a Steeply Dipping Orebody, 5th Canadian Rock Mechanics Symp, Toronto, pp 105-125, December 1968.

45. Heltzen, A. M., S. Moxon, and R. Schach. Support Considerations for a Railway Tunnel in Norway, Preceedings of the International Symp for Large Permanent Underground Openings, Oslo, September 1969.

46. Heuze, F. E. Sources of Errors in Rock Mechanics Field Measurements and Related Solutions, Int J Rock Mech Min Sci, Vol. 8, pp 297-310, 1971.

47. Heuze, Francois E., and Richard E. Goodman. Mechanical Properties and In-Situ Behavior of the Chino Linestone, Crestmore Mine, Riverside, California, 9th Symp on Rock Mech, Colorado School of Mines, 1967.

48. Heuze, Francois E., Richard E. Goodman, and Ann Bornstein. Numerical Analysis of Deformability Tests in Jointed Rock – "Joint Perturbation" and "No Tension" Finite Element Solutions, Rock Mechanics, Vol. 3, No. 1, 1971.

49. Hiramatsu Y., Y. Niwa, and Y. Oka. Measurement of Stress in Field by Application of Photoelasticity, Tech Rep, Kyoto University, No. 37, 1957.

50. Hobbs, N. B., and D. A. Clarke. Residual Stress Measurements by the Drillhole Prestressed Meter and the Rigid Brass Plug, Proceedings of the First Congress of the International Society of Rock Mechanics, Lisbon, Vol. II, 1966.

51. Hooker, Verne E., and David L. Bickel. Overcoring Equipment and Techniques, U. S. Dept. of the Int/Bureau of Mines, Progress Report DMRC 10002.

52. Hooker, Verne E., and Charles F. Johnson. In-Situ Stresses Along the Appalachian Piedmont, 4th Canadian Symp on Rock Mechanics, Ottawa, March 1967.

53. _____. Near-Surface Horizontal Stresses Including the Effects of Rock Anistropy, U. S. Dept. of Int6Bureau of Mines, RI 7224, February 1969.

54. Hoskins, E. R. An Investigation of the Flatjack Method of Measuring Rock Stress, Int J Rock Mech and Min Sci, Vol. 3, No. 4, pp 249-264, 1966.

55. Hoskins, E. R. An Investigation of Strain Rosette Relief Methods of Measuring Rock Stress, Int J Rock Mech and Min Sci, Vol. 4, No. 2, pp 155-164, 1967.

56. International Society of Rock Mechanics. Residual Stresses in Rock Masses, Proc 1st Cong, Vol. 3, pp 311-383, 1966.

57. Ivanova, N. V. Errors in Measurements of Mechanical Stresses by Optical Sensors, Soviet Mining Science, No. 3, pp 33-335, May-June, 1970.

58. Kruse, George H. Powerplant Chamber Under Oroville Dam, A. S. C. E., National Water Resources Engineering Meeting, Underground Chambers, Phoenix, Arizona, January 11-15, 1971.

59. _____ _____. Static Stress Determinations At Oroville Underground Powerhouse, Rock Mechanics Report, No. RM-4, State Water Facilities, Oroville Division, State of California, December 1963.

60. Leeman, E. R. Absolute Rock Stress Measurements Using a Borehole Treparning Stress-Relieving Technique, Conf 6th Symp on Rock Mech Univ of Missouri at Rolla, 1964.

61. _____. The Borehole Deformation Type of Rock Stress Measuring Instrument, Int J of Rock Mech and Min Sci, Vol. 4, No. 1, pp 23-44, 1967.

62. Leeman, E. R. Determination of the Complete State of Stress in Rock in a Single Borehole, Laboratory and Underground Measurements, Int J of Rock Mech and Min Sci, Vol. 5, No. 1, pp 31-56, 1968.

63. _____. The 'Doorstopper' and Triaxial Rock Stress Measuring Instruments Developed by the C. S. I. R., J of the So African Institute of Mining and Metallurgy, Vol. 69, No. 7, pp 305-339, February 1969.

64. _____. Experience Throughout the World with the CSIR Doorstopper Rock Stress Measuring Equipment, Proc 2nd Cong Int Soc for Rock Mech, Beograd, September 1970.

65. _____. The Measurement of Stress in Rock, Journal of the South African Institute of Mining and Metallurgy, Vol. 65, No. 2, September 1964, Vol. 65, No. 4, November 1964.

66. Leeman, E. R., and H. G. Denkhaus. Determination of Stress in Rock with Linear or Non-Linear Elastic Characteristics, Rock Mechanics, Vol. 1, No. 4, pp 198-206, December 1969.

67. Li, Bjorn. Improving Limestone Pillars by Presplitting, Institutt for Gruveteknikk, NTH, 7000 Trondheim, Norway.

68. _____ . Natural Stress-Values Obtained in Different Parts of the Fennoscanidan Rock Masses, Proc 2nd Cong of the Int Soc for Rock Mech, Belgrade, 1970.

69. Martinetti, S., and R. Ribacchi. Lessons Drawn from Field Experience in Rock Stress Measurements, II Congress of the International Society for Rcok Mechanics, Belgrade, 1970.

70. Mayer, A., P. Habib, and R. Marchand. Underground Pressure Testing, Conf Internationale sur les pressions de terrains et le soutenement dans les chantiers d'exploitation, Liege, du 24 au 28, April, 1951.

71. Merrill, R. H. Three-Component Borehole Deformation Gage for Determining the Stress in Rock, U. S. Bureau of Mines, R. I. 7015, August 1967.

72. Merrill, Robert H. Static Stress Determination in Salt Site Cowboy, U. S. Bureau of Mines, Applied Physics Research Laboratory, College Park, Maryland, July 29, 1960.

73. Merrill, Robert H., and Verne E. Hooker. Static Stress Determinations and Crushed Zone Measurements Site Hobo, U. S. Dept. of the Int/Bureau of Mines, Applied Physics Research Laboratory, College Park, Maryland, July 1960.

74. Merrill, Robert H., James V. Williamson, David M. Ropchan, and George H. Druse. Stress Determinations by Flatjack and Borehole-Deformation Methods, U. S. Dept. of Int/Bureau of Mines, RI 6400, 1964.

75. Morgan, Thomas A., William G. Fischer, and William J. Sturgis. Distribution of Stress in the Westvaco Trona Mine, Westvaco, Wyoming, U. S. Dept. of Int/Bureau of Mines, RI 6675, 1965.

76. Nichols, Thomas C., John F. Abel Jr., and Fitzhugh T. Lee. A Solid-Inclusion Borehole Probe to Determine Three-Dimensional Stress Changes at a Point in a Rock Mass, U. S. Dept. of Int/ Geological Survey Bulletin 1258-C, 1968.

77. Obert, L., and D. E. Stephenson. Stress Conditions Under Which Core Discing Occurs, AIME Transations, Vol. 232, pp 227-232, September 1965.

78. Obert, Leonard. Determination of Stress in Rock--a State-of-the-Art Report, ASTM Special Tech Publication, No. 429, 1966.

79. Obert, Leonard. In-Situ Determination of Stress in Rock, Mining Engineer, Vol. 14, No. 8, pp 51-58, August 1962.

80. Obert, Leonard. Triaxial Method for Determining the Elastic Constants of Stress Relief Cores, U. S. Dept. of Int/Bureau of Mines, RI 6490, 1964.

81. Obert, Leonard, Robert H. Merrill, and Thomas A. Morgan. Borehole Deformation Gage for Determining the Stress in Mine Rock, U. S. Bureau of Mines, RI 5978, 1962.

82. Ohnishi, Y., F. E. Heuze, and R. E. Goodman. Borehole Jack Deformability Measurements, and Strength Testing of Selected Rocks from the Auburn Dam Site, Report to U. S. Army Corps of Engineers, Missouri River Division, Omaha, Nebraska, September 1971.

83. Pallister, G. F., N. C. Gay, and N. G. W. Cook. Measurements of the Virgin State of Stress in Rock at Depth, Proc of the 2nd Cong of the Int Soc for Rock Mech, Beograd, Vol. 1, pp 25-28, 1970.

84. Panek, L. A., Edward E. Hornsey, and Robert L. Lappi. Determination of the Modulus of Rigidity of Rock by Expanding a Cylindrical Pressure Cell in a Drill Hole, Conf 6th Symp Rock Mech Univ Missouri at Rolla, pp 427-448, October 1964.

85. Panek, L. A., and J. A. Stock. Development of a Rock Stress Monitoring Station Based on the Flat Slot Method of Measuring Existing Rock Stress, U. S. Dept. of Int/Bureau of Mines, RI 6537, 1964.

86. Panek, Louis A. A Calculation of the Average Ground Stress Components from Measurements of the Diametral Deformation of a Drill Hole, U. S. Dept. of Int/Bureau of Mines, RI 6732, 1966.

87. _____. Effect of Rock Fracturing on the Modulus, as Determined by Borehole Dilation Tests, Proc of the 2nd Cong of the Int Soc for Rock Mech, Beograd, 1970.

88. Pettibone, Howard C., and Galen G. Waddell. Stability of an Underground Room in Frozen Gravel, U. S. Dept. of Int/Bureau of Mines, Spokane Mining Research Center.

89. Radmanovick, M., and R. G. Friday. Rock Stress Measurement by a Borehole Strain Gage Technique, Australian Institute of Mining and Metallurgy, Proc, pp 19-25, 1968.

90. Rausch, D. O., A. Soderberg, and S. J. Hubbard. Progress in Slope Stability Research, Highway Research Record No. 17, Wash. DC, pp 43-52, 1963.

91. Roberts, A. Photoelastic Glass Insertion Stressmeter, The Engineer, London, Vol. 220, pp 165-171, July 30, 1965.

92. _____. Progress in the Application of Photoelastic Techniques to Rock Mechanics, Proc of the 6th Symp on Rock Mech, The Univ of Missouri at Rolla, Missouri, October 1964.

93. Roberts, A., I. Hawkes, and F. T. Williams. Some Field Applications of the Photoelastic Stressmeter, Int J of Rock Mech and Min Sci, Vol. 2, No. 2, pp 93-103, 1965.

94. Roberts, A., Hawkes, F. T. Williams, and R. K. Dhir. A Laboratory Study of the Photoelastic Stressmeter, Int J of Rocl Mech and Min Sci, Vol. 1, No. 3, May 1964.

95. Roberts, A., I Hawkes, F. T. Williams, and S. A. F. Murrell. The Determination of the Strength of Rock In Situ, 8th Int Cong on Large Dams, Edinburgh, Great Britain, Vol. 1, May 4-8, 1964.

96. Rocha, M. BHD-Borehole Dilatometer, Tests and Equipment, No. TE 9, Laboratorio Nacional de Engenharia Civil, Lisboa.

97. Rocha, Manual. New Techniques for the Determination of the Deformability and State of Stress in Rock Masses, Proc of the Int Symp on Rock Mech, Madrid, 1968.

98. Rocha, Manuel, and Jorge Neves Da Silva. A New Method for the Determination of Deformability in Rock Masses, Proc of the 2nd Cong of the Int Soc for Rock Mech, Beograd, Vol. 1, September 21-26, 1970.

99. Rocha, Manuel, Antonio Da Silveira, Nuno Grossmann, and Emilio De Oliveira. Determination of the Deformability of Rock Masses Along Boreholes, Memoria No. 339, Ministerio Das Obras Publicas, Laboratorio Nacional De Engenharia Civil, Lisboa, 1969.

100. Rocha, Manuel, Antonio Da Silveira, F. Peres Rodrigues, Arnaldo Silverio, and Armando Ferreira. Characterization of the Deformability of Rock Masses by Dilatometer Tests, Laboratorio Nacional de Engenharia Civil, Lisboa, 1970.

101. Rocha, Manuel, Joao J. Baptista Lopes, and Jorge Neves Da Silva. A New Technique for Applying the Method of the Flat-Jack in the Determination of Stresses Inside Rock Masses, Memoria No. 324, Ministerio Das Obras Publicas, Lanoratorio Nacional De Engenharia Civil, Lisboa, 1969.

102. Ropchan, David M. Evaluation of In-Situ Test Methods for Determining The Mechanical Properties of Rock, Mech of Rock Deformation, Colorado School of Mines, March 15, 1967.

103. Royea, M. J. Rock Stress Measurement at the Sullivan Mine, 5th Canadian Symp on Rock Mech, Univ of Toronto, December 1968.

104. Royea, M. J., and K. G. Davies. Rock Mechanics Applied to Extraction of Pillars at Sullivan Mine, Canadian Institute of Mining and Metallurgy Bulletin, Vol. 61, No. 678, pp 1185-1194, October 1968.

105. Sashurin, A. D., N. P. Vlokh, and A. V. Zubkov. Optical Gages for Measuring Stresses in Rocks, 4R Min Sci, Vol. 1, No. 3, pp 222-227, 1967.

106. Sellers, J. B. Rock Mechanics Instrumentation for Salt Mining, Northern Ohio Geol Soc, Cleveland, Ohio, Vol. 2, pp 236-248, 1970.

107. Sellers, J. B., G. R. Haworth, and P. G. Zambas. Rock Mechanics Research on Oil Shale Mining, Colorado School of Mines Research Foundation.

108. Singhal, R. K. Rock Stress Measurement, Mining Magazine, Vol. 123, No. 6, December 1970.

109. Smith, Travis W. Embankment Testing with the Menard Pressuremeter a sub project of movement within large fills, State of California, Dept. of Public Works, Division of Highways, Material and Research Dept., Report No. M&R 632509-2, May 1968.

110. Stephenson, B. R., and K. J. Murray. Application of the Strain Rosete Relief Method to Measure Principal Stresses Throughout a Mine, Int J Rock Mech and Min Sci, Vol. 7, pp 1-22, January 1970.

111. Stowe, R. L. Results of In-Situ Modulus of Deformation Test, Cannelton Lock and Dam, U. S. Army Engineer Waterways Experiment Station, Vicksburg, Mississippi, Misc. Paper C-71-4, May 1971.

112. Stowe, Richard L. Comparison of In-Situ and Laboratory Test Results on Granite, Society of Petroleum Engineers of AIME, Paper No. SPE 3217.

113. Suzuki, Ko. Fundamental Study on the Rockstress Measurement by Borehole Deformation Method, 1st Cong Int Soc Rock Mech, Lisbon, 1966.

114. Timur, A. E. A Study on Correlation of Dynamic and Static Elasticity Modulus Determined by In-Situ and Laboratory Tests, Proc of the 2nd Cong of the Int Soc for Rock Mech, Vol. 1, pp 543-565, Beograd, 1970.

115. Van Heerden, W. L. Stress Concentration Factors for the Flat Borehole End for Use in Rock Stress Measurements, Engineering Geology, Vol. 3, pp 307-323, 1969.

116. Van Heerden, W. L., and F. Grant. A Comparison of Two Methods for Measuring Stress in Rock, Int J Rock Mech Min Sci, Vol. 4, No. 4, 1967.

117. Waddell, Galen G., and Eugene H. Skinner. Progress Report Summary, Crescebt Mine, Study of Initial Deformation of a Tunnel Heading in Relation to Ultimate Stress and Strain as a Possible Means for Predicting Support Load Requirements, June 1, 1968 - June 30, 1969. U. S. Dept. of Int/Bureau of Mines, Spokane Mining Research Center.

118. Waldorf, W. A., J. A. Veltrop, and J. J. Curtis. Foundation Modulus Tests for Karadj Arch Dam, Journal of the Soil Mechanics and Foundation Division, Proc of the American Soc of Civil Engineers, Vol. 89, pp 91-126, July 1963.

119. Wallace, G. B., E. J. Slebir, and F. A. Anderson. In-Situ Methods for Determining Deformation Modulus used by the Bureau of Reclamation, American Society for Testing and Materials, Special Tech Publication 477, 1970.

120. Wallace, George B., Edward J. Slebir, and Fred A. Anderson. Foundation Testing for Auburn Dam, 11th Symp on Rock Mech, Univ of California, June 16-19, 1969.

121. Wilson, A. H. A Laboratory Investigation of a High Modulus Borehole Plug Gage for the Measurement of Rock Stress, Conf 4th Symp Rock Mech, Pennsylvania State Univ, April 1961.

122. Wisecarver, David W A Device for Placing a Borehole Deformation Gage in a Horizontal Hole, U. S. Dept. of Int/Bureau of Mines, RI 6544, 1964.

123. Wisecarver, David W., S. Jackson Hubbard, Robert H. Merrill, and Donald O. Rausch. Investigation of In-Situ Rock Stresses, Ruth Mining District, Nevada, with Emphasis on Slope Design Problems in Open-Pit Mines, U. S. Dept. of Int/Bureau of Mines, RI 6541, 1964.

124. Wright, F. H. In-Situ Stress in Granite, Project Shoal, VUF-2600, Lucius Pitkin, Inc., May 1965.

125 Yu, Y. S., and W. M. Gray. Strain Equations for the C. S. I. R. Triaxial Strain Cell, Canada Dept. of Energy, Mines and Resources, Mining Research Center, Internal Report MR 71/41-LD, May 1971.

Table 1

RESPONSE TO QUESTIONNAIRE

Name of Instrument	Number of Replies			Number Followed Up	Other Contacts
	Total	From United States/ Canada	Possibly Connected with Instrument Development or Distribution		
USBM BDG	20	19/0	3	10	3
CSIR Doorstopper	12	1/4	2	3	1
Stressmeter	6	2/0	3	2	2
Goodman Jack	9	9/0	4	8	1
USBM CPC	5	5/0	2	4	0
Menard Pressuremeter	2	2/0	1	1	1
Rocha Dilatometer	1	0/0	1	1	1

Table 2

RATING OF INSTRUMENTS FOR MEASURING ABSOLUTE STRESS

Item		Gage		
		BDG	D	PS
Performance in:	competent rock	G	G	N x
	fractured rock	P	F	N
	very fractured rock (plastic behavior)	N	N	P to G
	plastic rock (immediate response elastic)	G	G	G*
	discing rock (very highly stressed)	N	P	N
	wet conditions	F	P	-*
'Maximum' distance from operator (feet)		50	200	25
Response to axial stress		Small	Large	None

BDG	Borehole Deformation Gage
D	CSIR "Doorstopper"
PS	Photoelastic Stressmeter
G	Good
F	Fair
P	Poor
N	No results likely
*	Results will take months to develop
+	Not affected by clean water

x This table assesses the instruments as absolute stress gages and does not reflect their validity to measure stress changes.

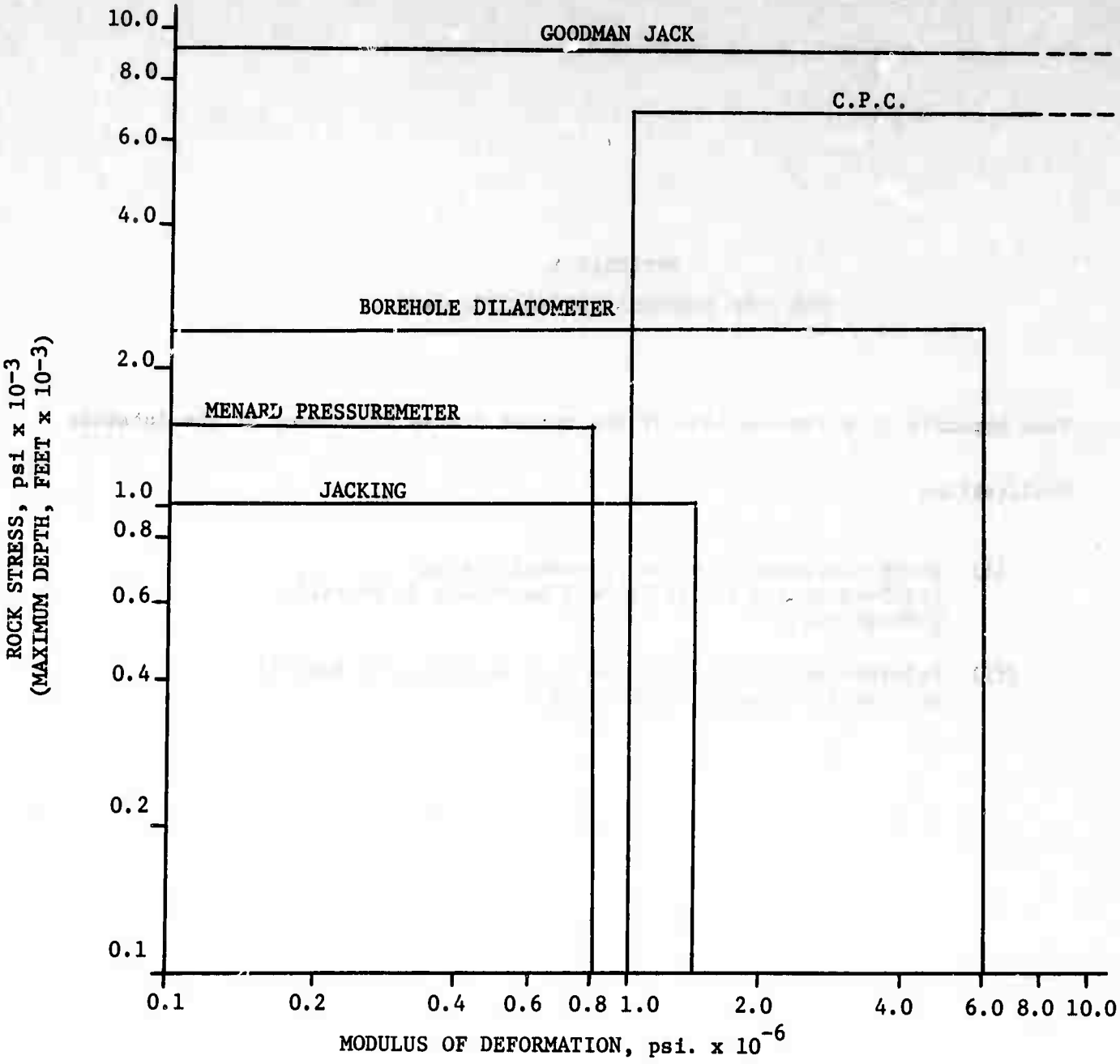

FIGURE 1
RANGE OF MODULUS GAGES

The vertical scale represents the stress one would expect to measure in the rock in thousands of pounds per square inch (which is approximately the same as depth underground in thousands of feet). The horizontal scale is the in-situ deformation modulus of the rock in millions of pounds per square inch. The plot indicates the range of reliability of each instrument with regard to stress (vertical) and modulus (horizontal). For example, if your expected stress including stress concentrations were 9,000 psi or less, the Goodman Jack could be used in any rock type with the appropriate modifications recommended by the manufacturer.

APPENDIX A

THE USBM BOREHOLE DEFORMATION GAGE

This Appendix is a reproduction of the United States Department of the Interior Publications

(i) Three-Component Borehole Deformation Gage for Determining Stress in Rock by Robert H. Merrill, USBM-RI 7015

(ii) Deformation of a Borehole in Rock by Robert H. Merrill and Jon R. Peterson, USBM-RI 5881.

THREE-COMPONENT BOREHOLE DEFORMATION GAGE FOR DETERMINING THE STRESS IN ROCK

by

Robert H. Merrill[1]

ABSTRACT

This Bureau of Mines report summarizes the design and tests of a gage that will simultaneously measure the deformation of a borehole along three diameters 60 degrees apart; the measurements are in a single plane normal to the axis of the borehole. The inherent errors in measurement are considered together with the problems associated with the use of the gage in the relatively severe environments in and around mine openings. These problems were treated in the design and tests of the gage and the results establish that the gage can be used to satisfactorily determine estimates of the stresses in rock.

INTRODUCTION

In previous investigations the Bureau of Mines developed and tested the relationships between the deformation of a borehole and the stress in rock, the procedure and equipment for determining stress in rock in situ, and made a number of stress determinations in various rock types around various mine openings (2, 3, 4, 6).[2] These investigations were made with gages that sensed the borehole deformation (change in diameter) along one diameter. Because the deformations along three diameters are needed to determine the magnitude and direction of the stresses (2), interpolation was necessary between measurements taken along different diameters at different depths in the borehole.

The single-component gage proved to be satisfactory in rocks from which solid, intact cores could be drilled, and where the depth at which measurements were repeated (along a specific diameter) did not exceed 18 to 24 inches. However, in rocks that are difficult to core, or where changes in deformation along a specific diameter could not be repeated within 24 inches, the interpolation cast much doubt upon the accuracy of the stress determinations. Consequently, a deformation gage was developed that is capable of simultaneously sensing the deformation of a borehole along three different

---

[1]Research physicist, Denver Mining Research Center, Bureau of Mines, Denver, Colo.

[2]Underlined numbers in parentheses refer to items in the list of references at the end of this report.

diameters. The general considerations used in selecting the design and specifications for the gage, the general features of gages used in the laboratory and field tests, and the tests performed to compare the resolution and accuracy of the three-compartment gage with the single-component gage are described briefly in the sections that follow.

GENERAL CONSIDERATIONS

To satisfy the requirements for stress determinations for most mine rocks, the borehole gage should meet the following specifications:

1. The gage must be rugged enough to withstand the conditions generally encountered in surface or underground mines such as corrosion, moisture, rough handling.

2. The gage should be used in a borehole that is EX size (about 1.5 inches) or larger,[3] so that the borehole has a diameter which is large compared with the grain size in the rock, yet small enough to be efficiently drilled and overcored.

3. To detect a stress of about 50 psi in a rock with an elastic modulus of 6×10^6 psi, the sensitivity should be sufficient to resolve a change in borehole diameter of about 35 microinches; for a modulus of 3×10^6 psi, the sensitivity should be about 70 microinches (see equation 2, reference (2)).

4. To detect a stress change of 20,000 psi for a rock with a modulus of 6×10^6 psi, the range of any specific measurement should be about 0.015 inch. To avoid damage to the sensing elements or transducers within the gage, to allow for variations in the diameter of a borehole, and to be useable in slightly larger or smaller boreholes, the transducers in the gage should have a tolerance of about 0.040 inch without external adjustment, and a tolerance of 0.150 inch with external adjustment.

5. For gages to be used for measurements in rock, the drift must be small compared to the change in diameter created by changes in stress. Because overcoring stress relief usually requires 5 to 10 minutes, the drift should be less than 10 microinches per hour.

6. The errors created by placement of the gage in the hole, the tangential deformation, and the longitudinal displacement of the hole should be less than 10 percent of the true borehole deformation.

---

[3] The larger boreholes provide information over larger areas of influence and give a desirable borehole diameter to grain-size ratio; on the other hand, the size of the drilling equipment, drill bits, and drilling costs, increase with hole size. Also, the hole size can become too large compared with the size of the opening from which the holes are drilled and overcored. Because a 1.5- to 3-inch-diameter borehole is very small compared to the size of most mine openings, any standard diamond-drill size between the EX and NC sizes could be used. The EX-size hole was selected for this gage to reduce the costs imposed by larger drilling equipment.

Because the above specifications are dependent, to some degree, upon one another, the above specifications and other requirements are considered collectively. Perhaps the most critical consideration is the problem created by the errors that are inherent in any measurement of borehole deformation. Suppose that the gage will be used for borehole-deformation, stress-relief measurement. For this use, the gage must accurately respond to the borehole deformations which are a result of stress relief from overcoring. To illustrate, the borehole-deformation, stress-relief technique is based in part on the assumption that the applied stresses in a rock are removed when the rock is cored; further, the stress so relieved is presumed to be equal to the stress when the rock was in its precoring environment. The changes in displacement in the overcored rock are dependent upon both the stress environment and the elastic properties of the rock. If the core is taken from rock very near the edge of an opening, the rock is subject principally to a biaxial-stress field parallel to the surface of the opening; if the core is taken from rock at a distance from the opening, the components are probably triaxial. Whether or not the rock is subject to biaxial or triaxial stress, the stress components are not necessarily equal in magnitude. Consequently, the displacements of a borehole near the surface of an opening are primarily normal to the axis of the borehole; the displacements of a borehole at depth from an opening are both normal and parallel to the axis of the borehole (fig. 1).

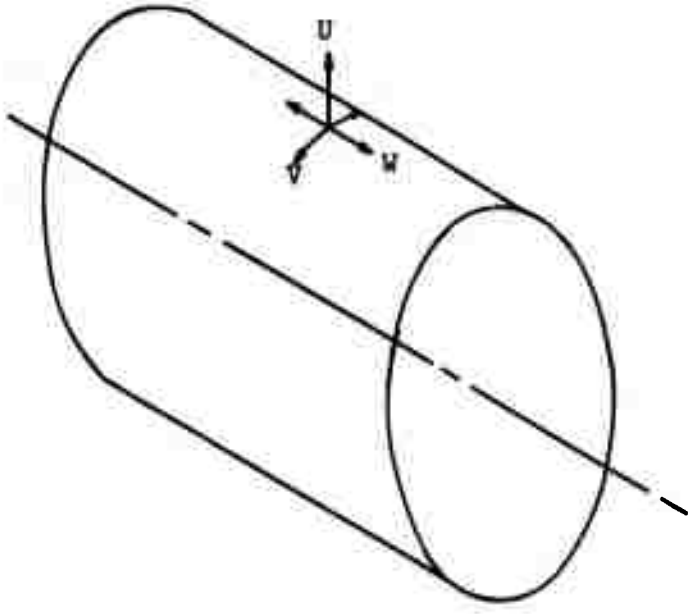

U RADIAL DISPLACEMENT
V TANGENTIAL DISPLACEMENT
W LONGITUDINAL DISPLACEMENT

FIGURE 1 - Components of Displacement Near the Edge of a Hole in Rock

The components of borehole displacement normal to the axis of the hole were considered in the development of the relationships between the tangential and the radial displacement of the borehole and the applied stresses (2). Although these relationships are for changes in displacement around a circular hole in a thin plate subject to conditions of plane stress or plane strain, tests have shown that these relationships can be used to relate the stresses in rock to the deformations of boreholes in the rock (2). For the conditions of plane stress, the radial and tangential displacements, u and v, at the edge of the borehole are related to the applied orthogonal biaxial stresses S and T by

$$u = \frac{a}{E} [\ (S + T) + 2(S - T) \cos 2\theta\ ], \quad (1)$$

$$v = -\frac{2a}{E} [\ (S - T) \sin 2\theta\ ], \quad (2)$$

where:

a = radius of the borehole,

E = modulus of elasticity,

S,T = applied stresses,

θ = angle from the algebraically larger applied stress (S), to the point where u or v is considered (fig. 2).

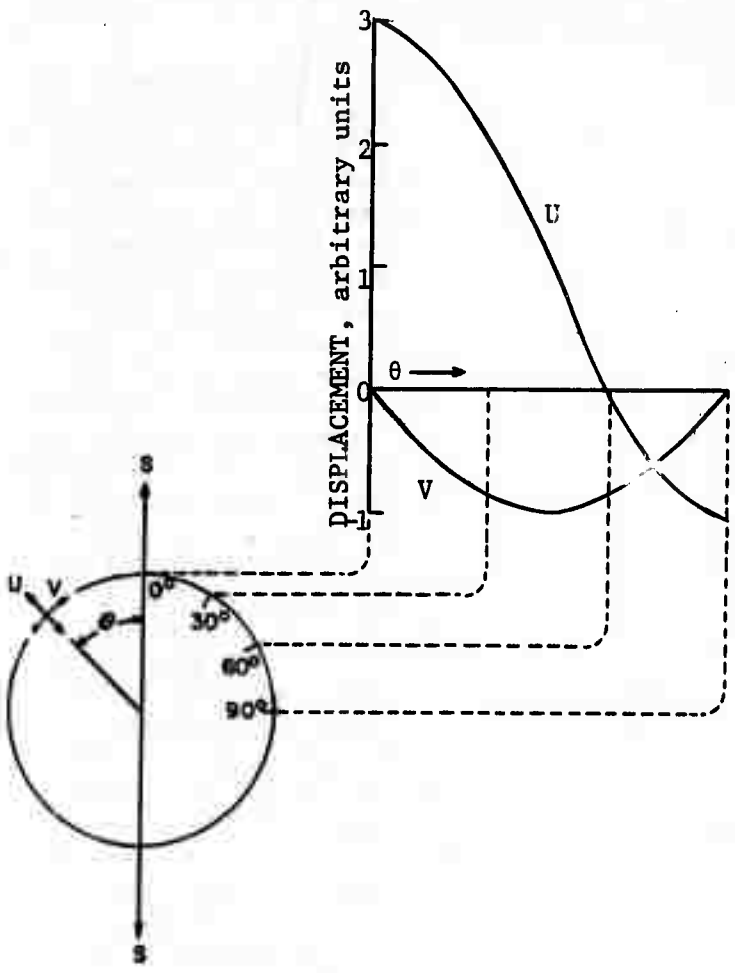

FIGURE 2 - Relative Tangential Displacement and Borehole Deformation at the Edge of a Borehole.

For conditions of plane strain, radial and tangential displacements are given by equations 1 and 2 multiplied by $(1 - \nu^2)$, where ν is Poisson's ratio.

The change in diameter of a borehole is twice the radial displacement; therefore, the change in diameter of the borehole, U (borehole deformation), is obtained by letting $U = 2u$ and the borehole diameter, $d = 2a$; then equation (1) is rewritten as (2):

$$U = \frac{d}{E}[\ (S+T) + 2(S-T) \cos 2\theta\ ]. \quad (3)$$

The borehole deformation is measured by borehole gages in both laboratory and field measurement (2), (3), (6). However, the borehole also deforms tangentially (equation 2); consequently, the optimum borehole gage should not be significantly influenced by the tangential displacement.

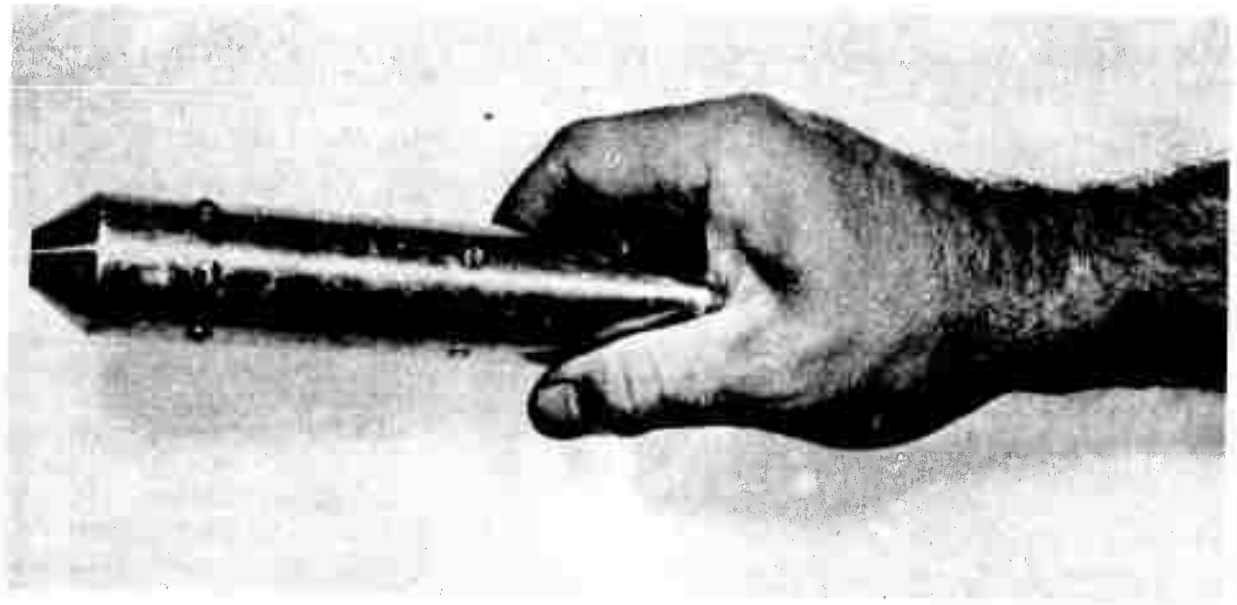

FIGURE 3 - Photograph of Gage Used for Laboratory Tests

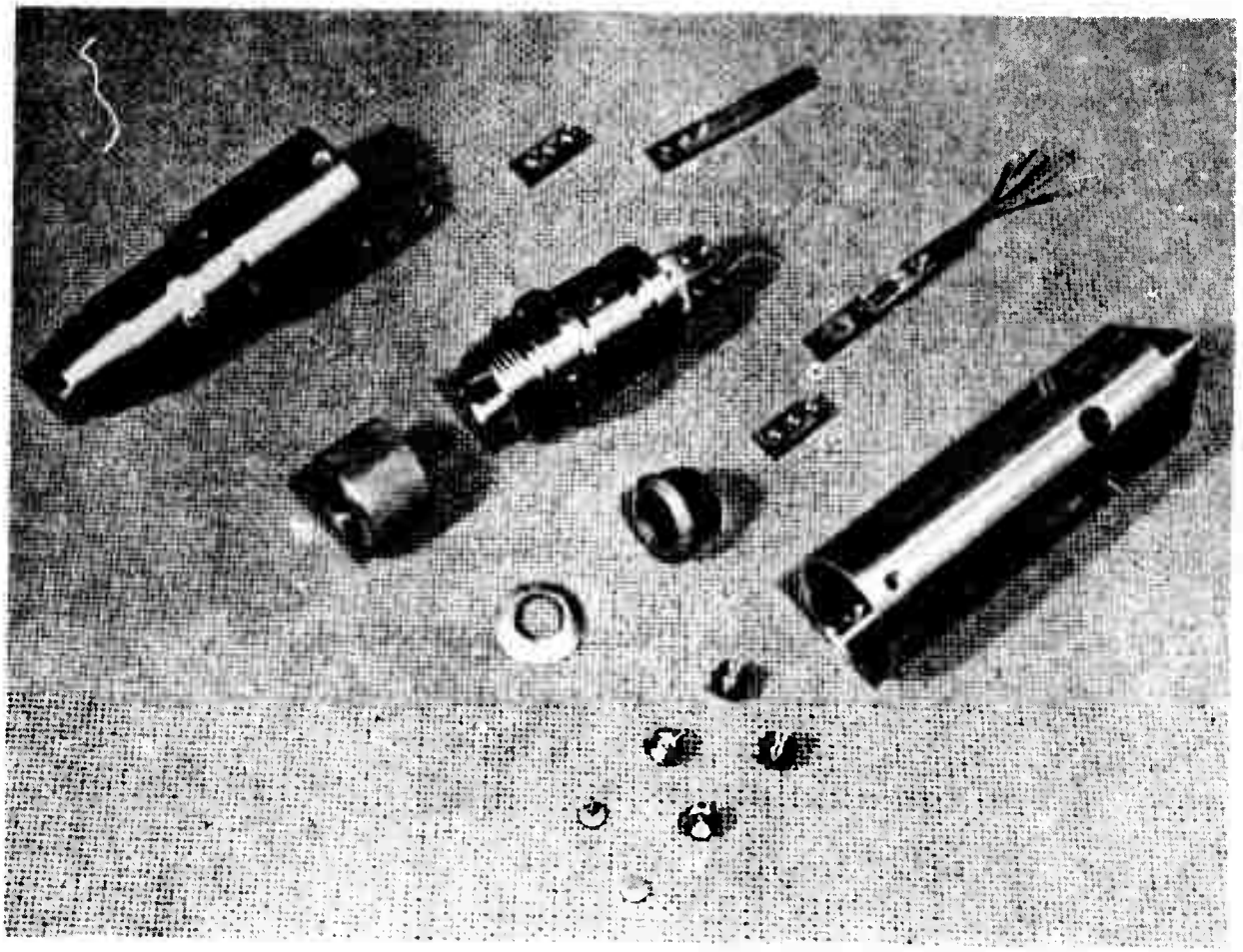

FIGURE 4 - Photograph of Parts for Gages for Field Measurements

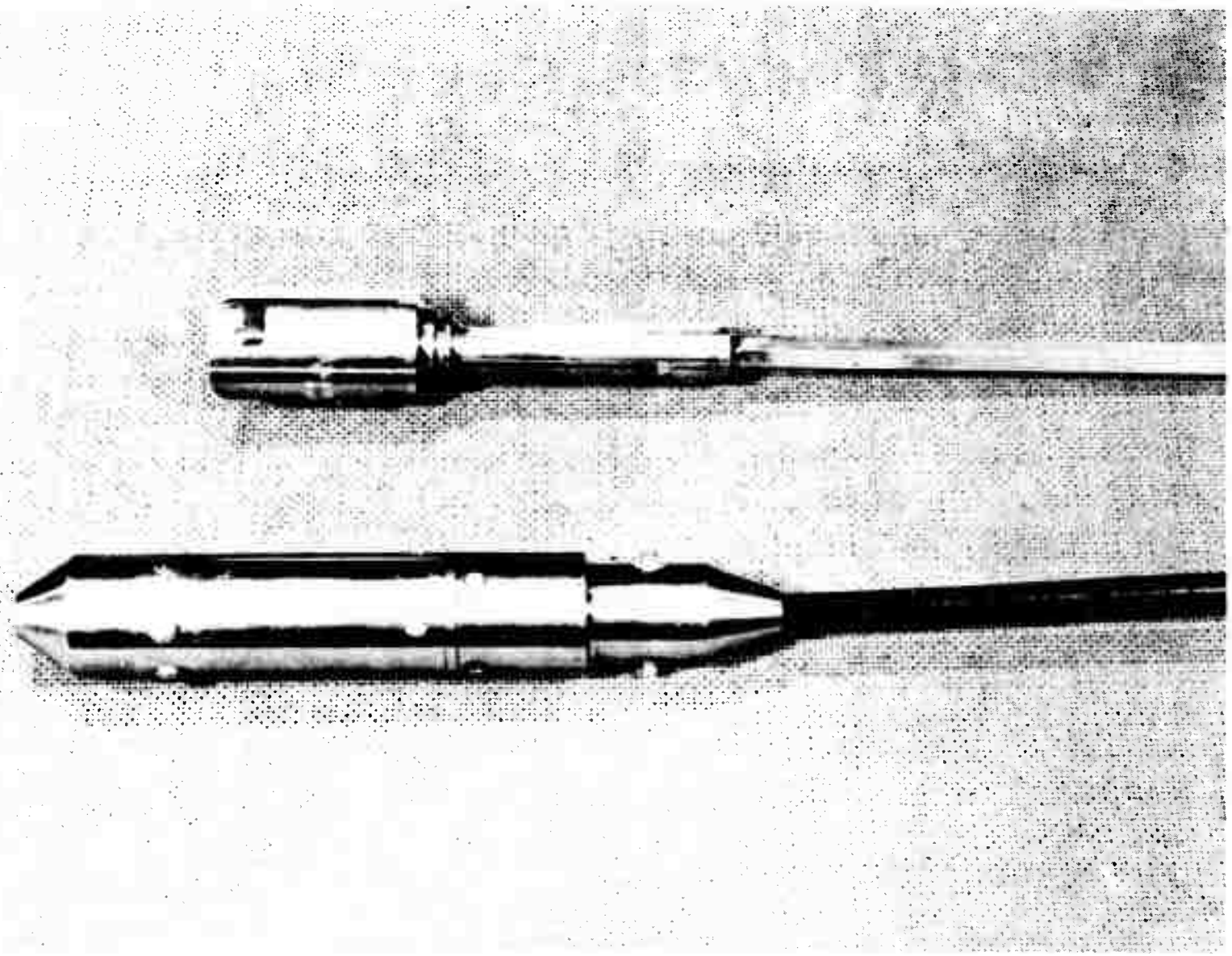

FIGURE 5. - Photograph of Assembled Gage Used for Field Measurements.

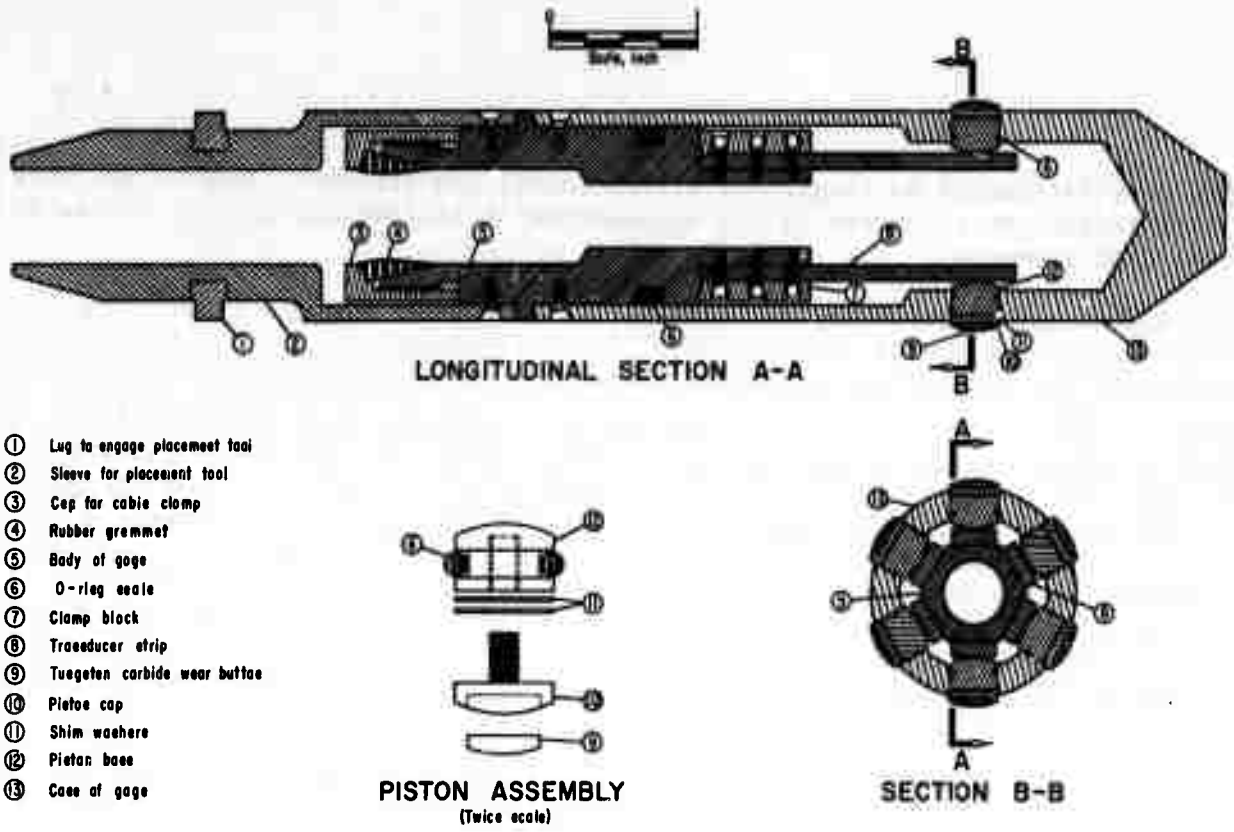

FIGURE 6 - Drawing of Principal Parts of the Three-Component Gage Used for Field Measurements

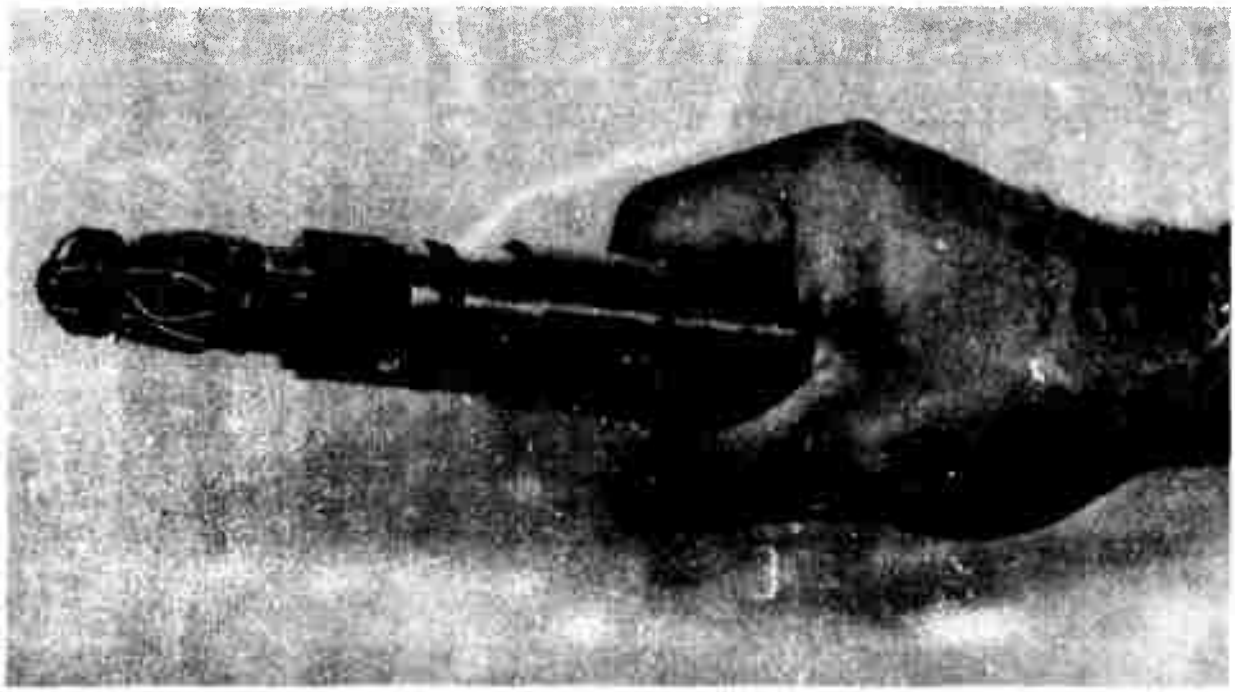

FIGURE 7 - Photograph of Transducers in Gage Used for Laboratory Tests

If a gage were influenced by tangential displacement, the influence must be accounted for by calibration, or corrected by the mathematical relationships between stress and tangential displacement.

The tangential displacements increase as the difference between S and T increases and as the angle θ approaches 45° (equation 2). For example, if S = T, the tangential displacement of the hole is zero; when T = 0 and θ = 45°, the tangential displacement is equal to $-\frac{2aS}{E}$. For a rock with a modulus of elasticity equal to 6 x 10^6 psi, with a borehole diameter of 1.5 inches (approximately EX size), and with a uniaxial stress of 6,000 psi, the tangential displacement would be 1,500 microinches. The change in borehole deformation at the same point (θ = 45°) is also equal to 1,500 microinches (equation 3). The borehole deformations and tangential displacements at other angles were computed for applied stresses of S = 1 and T = 0, and these computations are summarized graphically in figure 2. If the hole is at depth from an opening, the core and hole are also subjected to longitudinal displacements (fig. 1). The equations relating changes in longitudinal strain and borehole deformation are given in another report (5).

As longitudinal displacements may occur during overcoring, the contacts to measure borehole deformation should be along a single circumference, or there should be decoupling between contacts that are not on a circumference. To illustrate, consider a condition where the contacts are not on a circumference, where the components of the gage are about 1 inch apart, and where the space between the contacts are not decoupled; that is, the contacts that sense the borehole changes at the 0° orientation are 1 inch from the contacts at 60° and are 2 inches from the contacts at 120°, and there is a solid case of metal between the contacts. During overcoring, the core of rock moves parallel to the axis of the borehole. Because the rock moves and the contacts cannot move, the gage contacts must slip at the point where the contact touches the rock. Although the magnitude of this possible error is unknown, the effects of the error can be eliminated by placing the contacts along a single circumference. Also, for identical reasons, any centering device (located at a point other than the location of the contacts) should exert less force on the hole than the force of the contacts. Otherwise, the centering device will remain fixed and the contacts will move or slip. The latter condition applies to any borehole deformation gage with any number of contacts.

DESIGN OF THE GAGE FOR LABORATORY AND FIELD TESTS

To satisfy a part of the requirements for ruggedness and resistance to corrosion, the primary components of the gages are made from stainless steel (figs. 3, 4, 5). Waterproofing is achieved by O-ring seals located both on the contacts and where the case joins the body of the gage. The cable is sealed with a tapered rubber bushing. Abrasion of the tips of the contacts is reduced by disks of tungsten carbide (figs. 4, 5, and 6).

Because the transducer in the single component deformation gage met all the requirements for ruggedness, sensitivity, range, and drift, a similar strain-displacement transducer was used in the three-component gage (fig. 7).[4]

The transducers shown in the photographs in figures 4 and 7 are heat-treated, beryllium-copper strips mounted as cantilevers. Electric resistance strain gages are bounded to the strip at points near the clamps. The strips are 2-1/16 inches long, five-sixteenth of an inch wide (at the clamped end), and 0.1 inch thick. The cantilever strip is tapered so that one strip will not affect another strip during large deflections (fig. 7). The strain gages are one-eighth by one-eighth inch foil elements embedded in bakelite. Epoxy resin cements were used to bond the gages to the cantilever strip, and the accepted practices were followed to prepare the metal strip for the gage application (sandblasting and etching), to apply the clamping forces (about 100 pounds), and to polymerize the cement (160° F for 4 to 6 hours). After assembly, the distance between the cantilever clamp and the point where the contact strikes the transducer is 1-1/8 inches.

The arrangement of the transducers is shown in figures 6 and 7. A strain gage is bonded on top and bottom of the cantilever, and the two opposing transducers (along one diameter) constitute a single component in the gage. To maximize the sensitivity and minimize temperature effects, the four gages in a component are connected in a four-arm-bridge circuit. To assure that the deflection of one or both of the transducers represents the change in diameter of the borehole, care was exercised to construct each transducer (within a component) as nearly identical as possible. If the transducers have the same deflection-strain ratio, (which is called the calibration constant), the deflection of one or both of the strips will produce the same indicated strain per unit deflection. To exclude interference between different circuits, a separate four-wire system is used for each four-arm bridge. Therefore, each component has four leads connected to a strain gage indicator. All leads are carried to the indicator through a shielded cable with a neoprene jacket. The average outside diameter of the cable is nine-sixteenth inch (fig. 5).

CALIBRATION

The transducers were calibrated for the approximate deflection-strain ratio before the laboratory gage was assembled. A calibration jig was used for these tests (fig. 8). After calibrating, the same jig was used to determine the drift in the indicated strain when the cantilever was under constant deflection. The transducers were cycled over 50 times before these tests began. Transducers were accepted if the drift was less than 10 microinches per hour. Several transducers had drifts less than 4 microinches per hour.

---

[4]A device that allowed for longitudinal displacement and that used different types of transducers was considered in the design of the gage; although the device provided the desired decoupling between the contacts, it did not meet the specifications for ruggedness. Further, the other transducers did not satisfy the requirements for low drift; consequently, the decision was made to place all contacts along one circumference and to use the cantilever strip transducer.

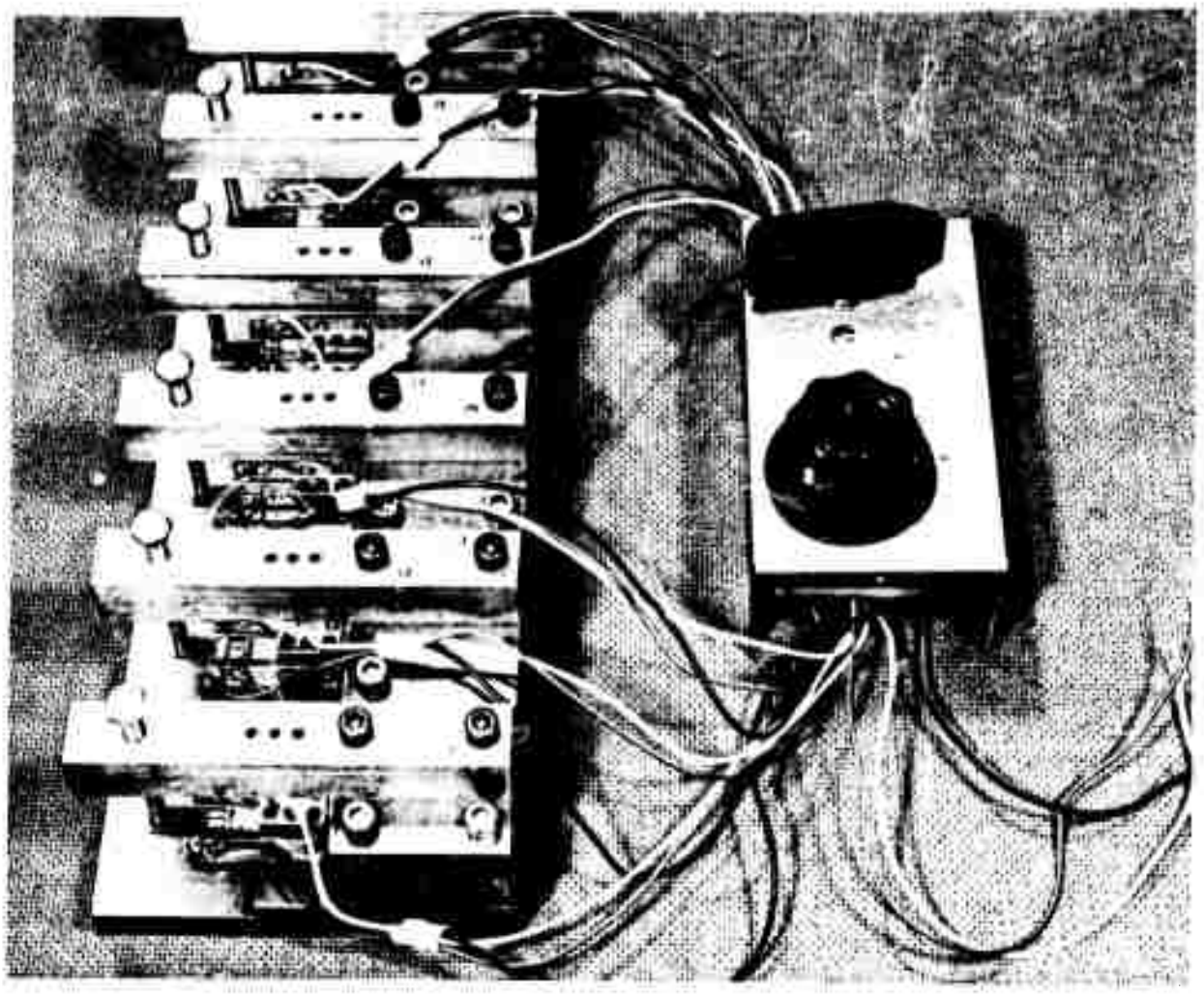

FIGURE 8 - Calibration Jig Used to Obtain Approximate Calibration and Time Stability of Transducers.

Eight transducers were calibrated, of which six closely matched pairs of transducers were selected for each component of the gage. The calibration constant[5] ranged from 6.17 to 6.40 and the constants for the pairs of transducers selected for each component were as follows:

Component 1, 6.17 and 6.23,

Component 2, 6.37 and 6.40, and

Component 3, 6.20 and 6.21.

[5]Microinches deflection per unit indicated microstrain

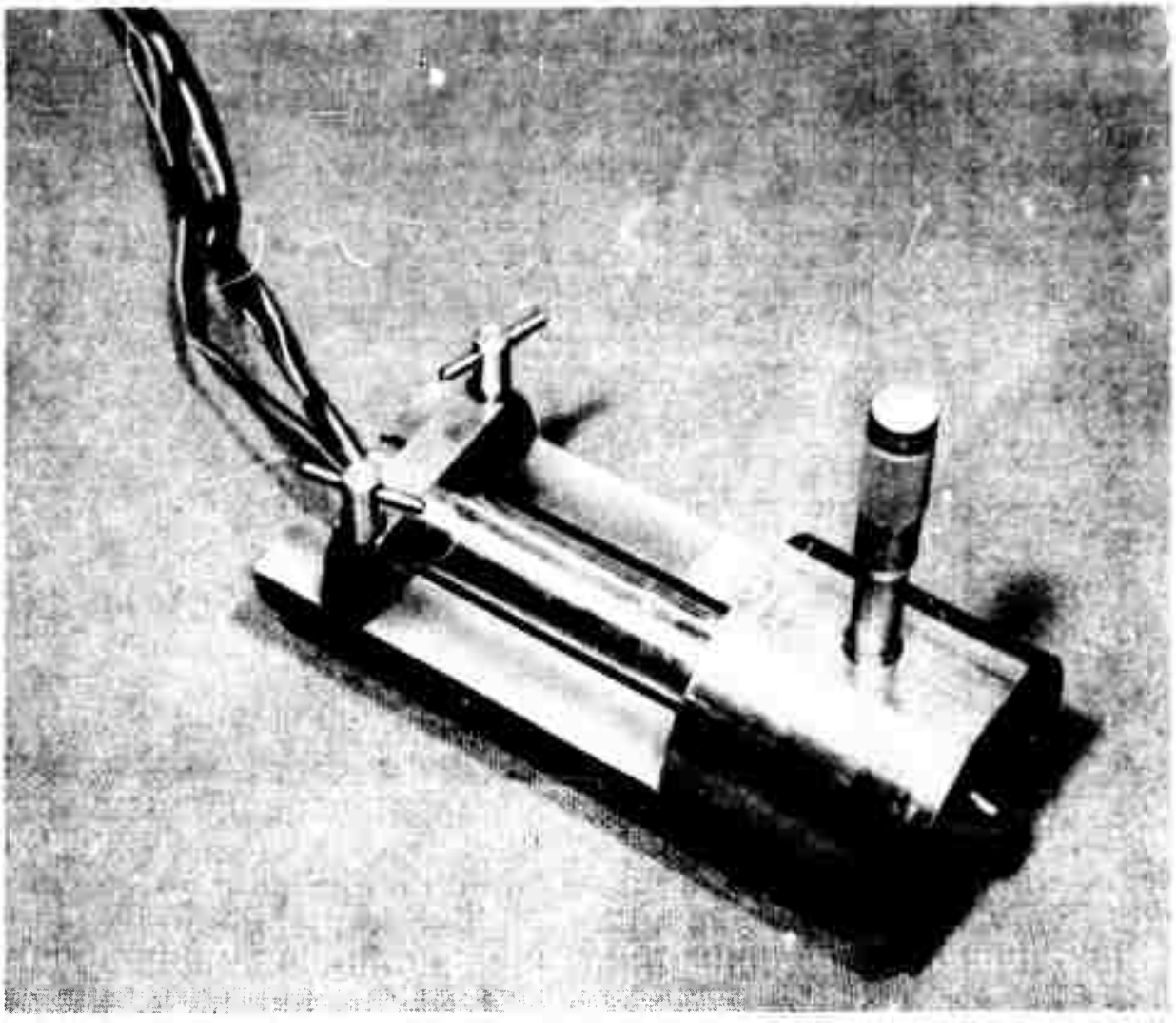

FIGURE 9 - Jig Used to Calibrate Individual Transducers and Components in the Three-Component Borehole Gage.

After assembly, the pairs of transducers in each component were more accurately calibrated in the unit shown in figure 9. These calibrations were, for component 1, 6.19 $\pm$ .02, and for component 2, 6.46 $\pm$ .02, and for component 3, 6.25 $\pm$ .02, where the confidence interval of the strain-deflection slope (calibration curve) is constant for each transducer.

The change in diameter across any component can be sensed by either one or both of the transducers. Therefore, the total response of the gages is determined, to a great extent, by the response of each transducer or the combination of both transducers within a specific component. To determine this response, the deformation versus strain was calibrated with (1) each transducer individually measuring the change in deformation and (2) the change in deformation being applied across both transducers. The calibration device shown in figure 9 was used for these tests and each deformation-strain test was repeated 10 times. The average of the results is summarized in table 1

where the change in deformation (20,000 microinches) is the difference in deformation between 10,000 and 30,000 microinches. The corresponding change in indicated strain is the difference in strain measured at these deformations. These magnitudes were selected because the single component gage is normally preset between 10,000 and 30,000 microinches when used in boreholes in rock.

TABLE 1 - Changes in indicated strain versus the changes in deformation applied to individual transducers and to both transducers in a component

Transducer	Change in deformation, microinches	Change in indicated strain, microstrain
1.	20,000	3,291
2.	20,000	3,211
1 and 2.	20,000	3,284
3.	20,000	3,141
4.	20,000	3,126
3 and 4.	20,000	3,097
5.	20,000	3,226
6.	20,000	3,221
5 and 6.	20,000	3,198

The difference between the indicated strain, for a deformation change of 20,000 microinches, is less than 2.2 percent whether recorded from a single transducer or from the combination of two transducers within a component. Also, from one deformation-strain test to another, the indicated strain seldom differed more than 0.5 percent from the average of the strains from all the tests; consequently, the reproducibility and the small differences noted in table 1 are considered to be insignificant when compared with errors that could originate from other sources discussed in the section of this report which follows. Therefore, the gage could be calibrated by deforming both transducers simultaneously in a calibrator as shown in the photograph in figure 10.

Typical calibration curves of transducers are shown graphically in figure 11. These curves were plotted from data collected at room temperature (76° F) in a laboratory oven (106° F) and in a refrigerator (46° F). The important features of these curves are that the curves are linear and have the same slope at each of the three temperatures. Although no attempt was made to determine why the deformation-indicated strain values are slightly different for each gage, it is presumed that these differences are caused more by the expansion of the metal parts in the gage and in the calibration unit rather than by inherent differences in the transducers.

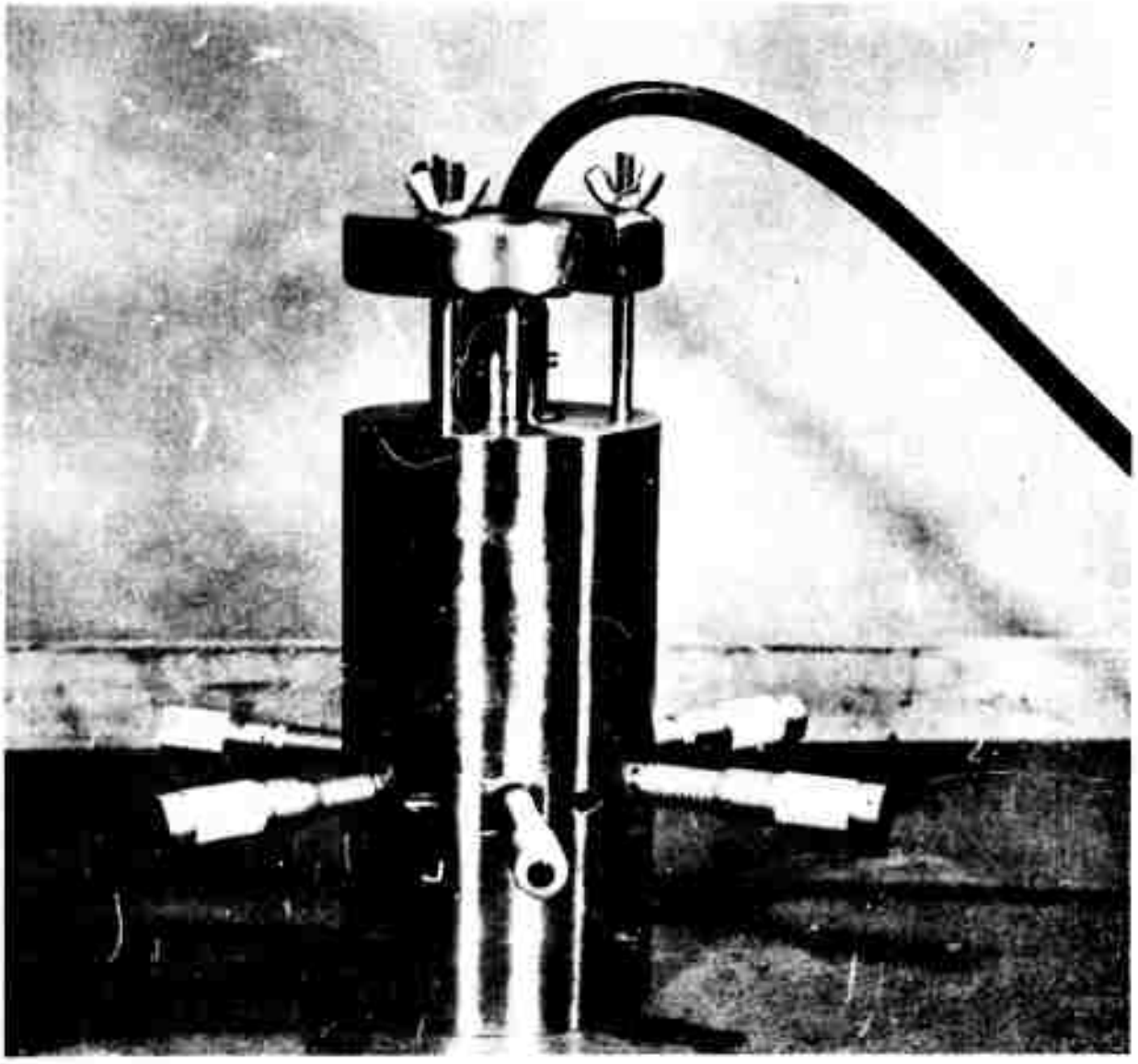

FIGURE 10 - Calibration Device for Simultaneous Calibration of the Three Components

TESTS OF THE GAGE

The accuracy of the stress determinations using borehole deformation techniques is governed by factors that are both independent and dependent upon the gage. Some of the more important independent factors are the degree of isotropy or inelasticity of the rock, the ratio of the grain-size of the rock to the diameter of the borehole, and the magnitude of the stress field.[6] Some of the dependent factors include the resolution, stability, reproducibility, range, and sensitivity of the gage. A number

[6]For example, a high stress could cause inelastic deformation of the hole or could break the core during the overcoring; a small stress, in a rock with a high modulus of elasticity, results in deformations that could be small enough to be within the resolution of the gage.

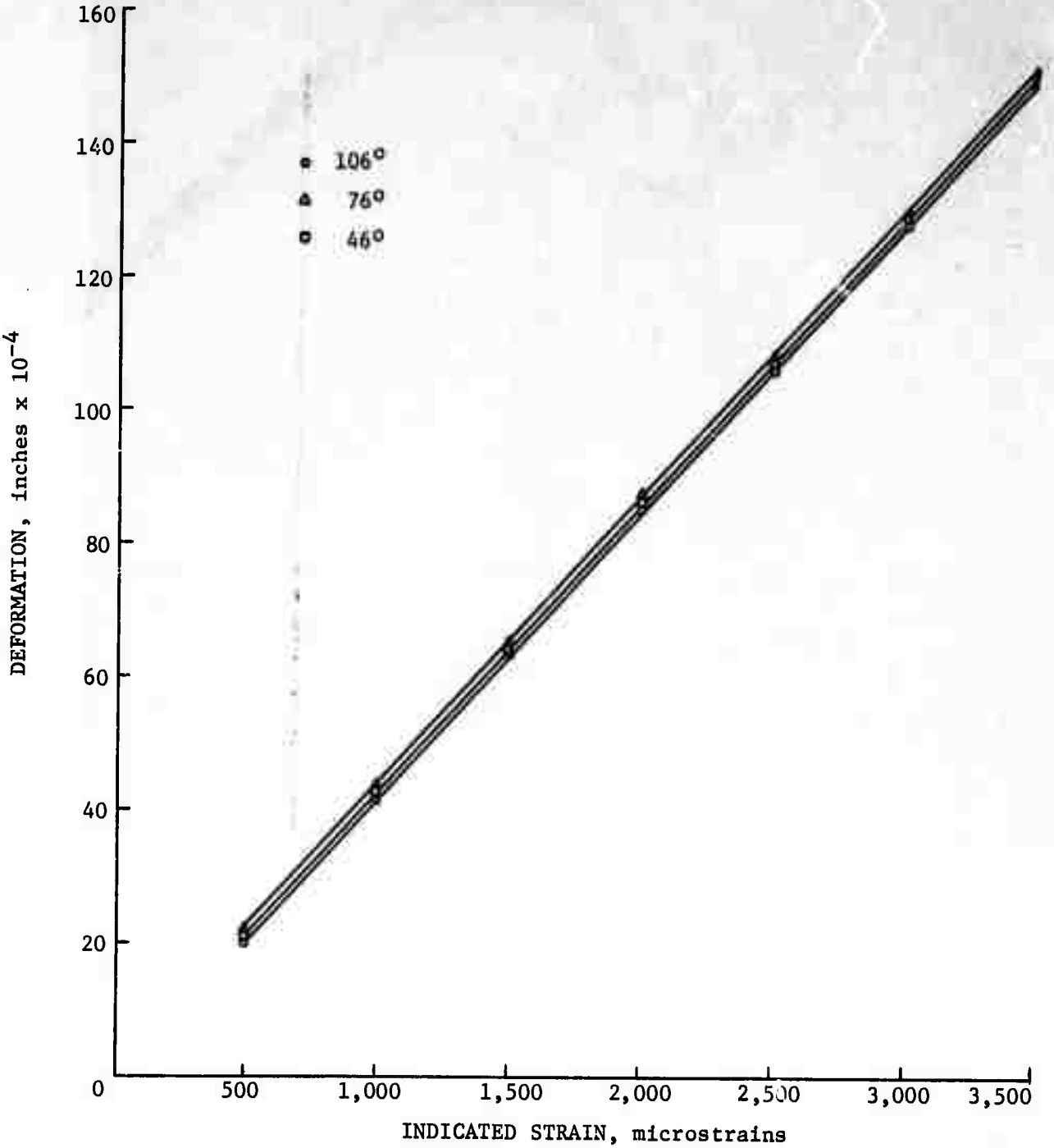

FIGURE 11 - Calibration Curves at Temperatures of 46, 76, and 106° F

of investigations were made to obtain estimates of most of the dependent factors. The investigations included tests to (1) determine whether the procedure used to place the gage affected the deformation measurements, (2) measure the response of the three-component gage in metal and rock specimens that have different elastic properties, (3) measure the response of the single component borehole deformation gage and an air gage in the same specimens and compare the results with (2) above, (4) determine the deformation when the preset transducer displacement is different for each component, and (5) determine the in situ rock stress around mine openings.

The specimens of metal and rock were formed into "models" in an effort to approximate or simulate the condition for a hole in an infinite plate or a hole in media where each of the three dimensions is infinite. Because past investigations had shown that the conditions were approximated by a model in which the outside dimensions were large compared with the diameter of the 1.5-inch borehole in the center, the models were constructed with dimensions as noted in table 2 (2). Also given in table 2 are the results of tests for the modulus of elasticity of the specimens as determined from stress-strain relationships obtained from special tests on some of the specimens.[7] A photograph of some of the models is shown in figure 12. The model materials were selected to have large differences in the elastic modulus and, hence, differences in the deformations per unit applied stress (equation 1). Further, model 4 (sandstone) was selected to test the gage in a rock which has a different modulus in different directions.

TABLE 2 - Model dimensions, materials, and modulus of elasticity of specimens used to test the gage

Model	Material	Dimensions, inches			Longitudinal modulus of elasticity, psi x 10^6	Lateral modulus of elasticity, psi x 10^6
		Height	Width	Thickness		
1	Steel	8	6	1	30	30
2	Brass	8	6	1	14	14
3	Magnesium	8	6	1	6.5	6.5
4	Sandstone[1]	12	6	6	1.0	0.62
5	Limestone[2]	12	6	6	4.7	4.7
6	Aluminum[3]	-	(4)	-	10.8	10.8
7	Steel[3]	-	(4)	-	30	30
8	Limestone[2 3]	-	(4)	-	5.1	5.1

[1]Thinly bedded (1/4 inch between beds), grain size about 1 to 2 mm; bedding parallel to major axis of the model.

[2]Very indistinctly bedded, grain size less than 1 mm; bedding normal to the major axis of the model.

[3]Length, 10 inches; hole diameter, 1.5 inches; outer diameter, 5-5/8 inches.

[4]Cylindrical.

To establish whether or not the method of placement of the gage would contribute to errors in measurement, a series of experiments were performed in which the gage was placed in the hole as follows: In the first set of measurements, the gage was placed

[7]These moduli of the rock models were computed from stress-strain measurements obtained from laboratory tests. The moduli of the metal models are typical handbook values.

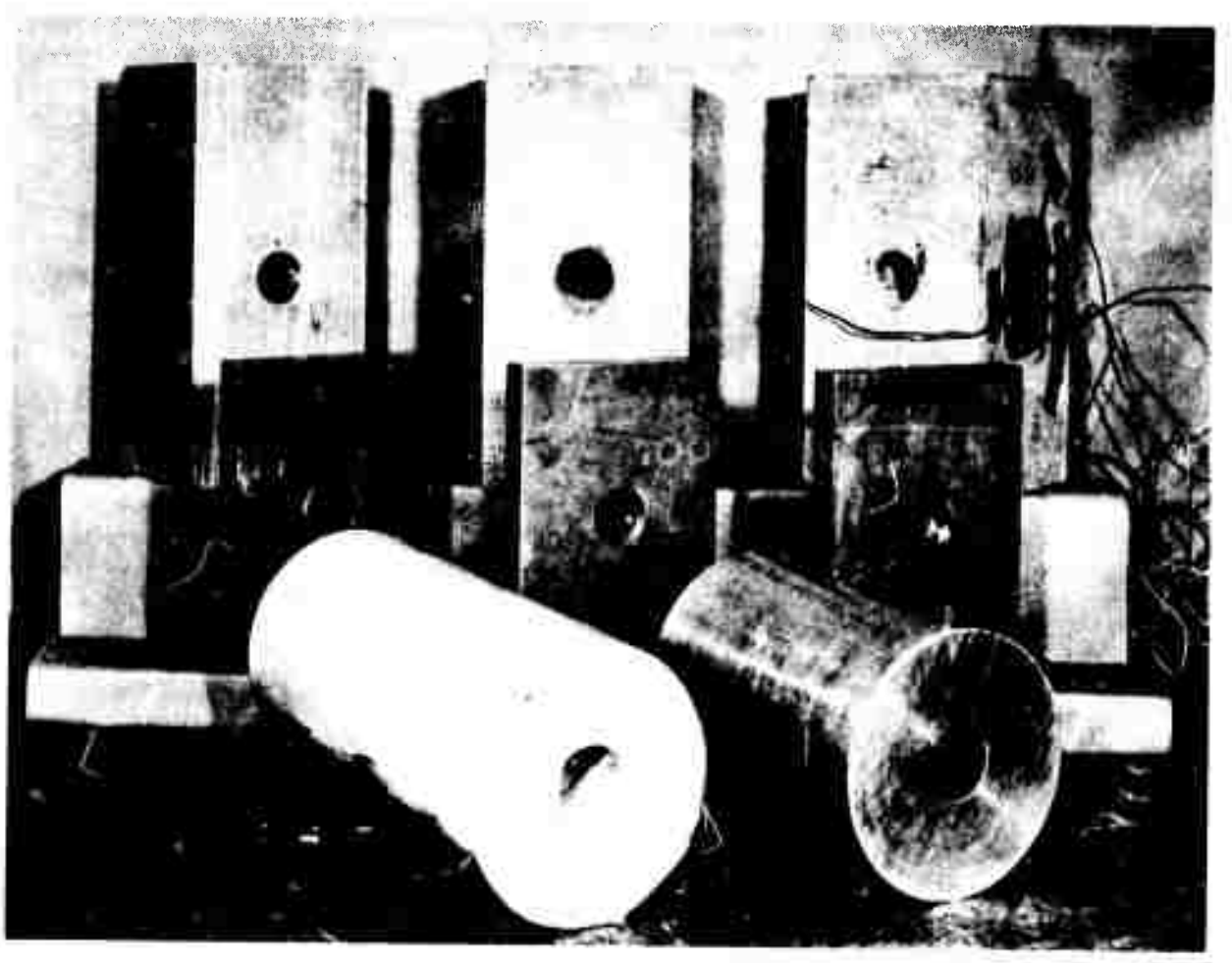

FIGURE 12 - Photograph of Models Used in Laboratory Tests

in the hole in the steel plate, and borehole deformations were measured as the plate was longitudinally loaded (parallel to the major axis) to 15,000 psi and back to zero. The gage was rotated 60 degrees clockwise and measurements were repeated. This procedure was repeated until the measurements were reproduced 10 times, that is, deformations were measured along the three diameters over 10 separate cycles. This procedure was also repeated for placements in which the gage was rotated counterclockwise. Lastly, the gage was inserted in the hole, perhaps with one component at 0 degrees (parallel to the applied stress) and deformations measured over the same pressure cycle; the gage was removed and returned to the hole so that different components of the gage were randomly located along different diameters 60 degrees apart. These measurements were repeated 20 times.

To determine the differences between deformation measured individually along the specific diameters (with a single component gage) and concurrently along three diameters (with the three-component gage), the following procedures and tests were performed: Lines were scribed in 15-degree increments from a reference line parallel to the major axis of the block; hence, the lines were at 15, 30, 45, 60, 75, and 90 degrees. First a single component air gage was located in the hole in the steel plate, oriented so that the component was parallel to the major dimension of the plate, that is, along the 0-degree line. Changes in borehole diameter were measured over three separate cycles as the applied stress was increased to 15,000 psi and reduced to zero. This procedure was repeated with the gage component parallel to the other lines at 15-degree intervals from the reference line. The air gage used in this test was identical to the device used in the earlier investigations regarding borehole measurement (2). Next, a lateral load, equal to one-third the maximum longitudinal load, was applied to the model, and the borehole deformations were measured as the longitudinal load was increased and decreased over the same range. The hydraulic device used to apply the lateral load is also similar to the equipment used in preceding investigations (2). This procedure was then repeated but the deformations were measured with a single component borehole deformation gage, and the procedure was again repeated using the three-component gage. Similar procedures and gages were used for the tests with the brass and magnesium plates, with the three rock prisms, and with the cylindrical models of metal and rock. The applied stresses used on each model are summarized in table 3. The stresses on models 6, 7, and 8 were biaxially applied (hydrostatic stress perpendicular to the major axis of the model) with the cylindrical loading device shown in figure 13. The features of the device and the procedure are described in a previous report (1). A photograph of the steel plate subject to vertical and horizontal applied stresses is shown in figure 14. The loading devices, x-y plotters and the universal press used for the uniaxial and biaxial tests are shown in figure 15.

TABLE 3 - Stresses applied to models

Model	Material	Longitudinal stress, psi	Lateral stress, psi
1	Steel	15,000	5,000
2	Brass	6,000	2,000
3	Magnesium	3,000	1,000
4	Sandstone	300	100
5	Limestone	1,500	2,000
6	Aluminum	2,000	5,000
7	Steel	5,000	5,000
8	Limestone	500	500

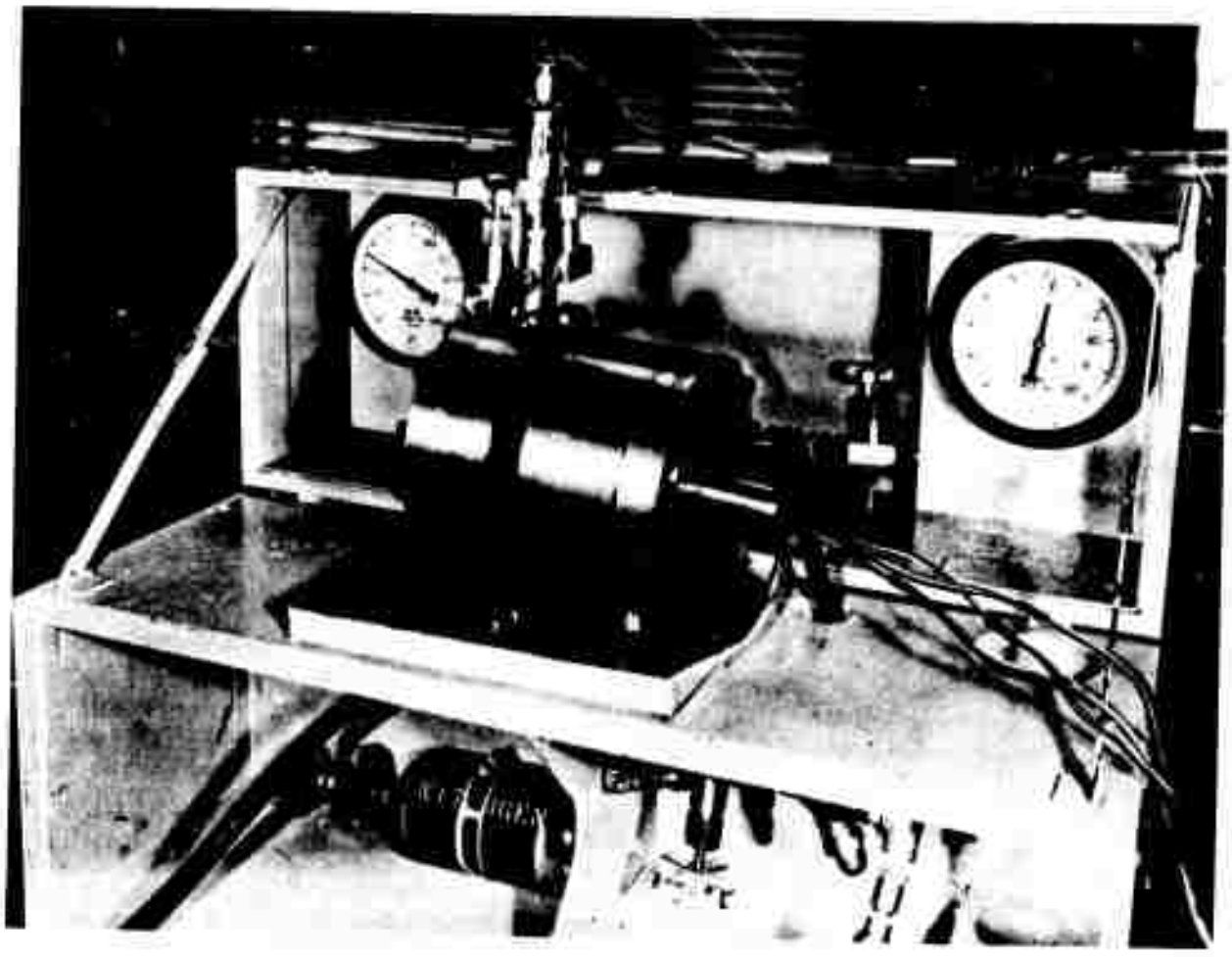

FIGURE 13 - Photograph of Cylindrical Model in the Cylindrical Loading Device

To determine the possible errors created by different contact force[8] on each component, the following series of tests were performed in the steel plate: The contacts in the gage were adjusted with shims so that each component was deformed about 20,000 microinches when placed in the hole in the steel plate. The gage was oriented with the component as 0, 60, and 120 degrees, and the pressure cycled from 0 to 15,000 psi and back to zero. The gage was then rotated 15 degrees clockwise and the pressure cycle repeated. This test was repeated with the gage rotated 30, 45, 60, 75, and 90 degrees from the original position. Following this series of tests, the contacts were adjusted so that the initial deformations were 5,000, 10,000, and 15,000 microinches; 5,000, 15,000, and 30,000 microinches; and 10,000, 20,000 and 30,000 microinches; and the different orientations and pressure cycles were repeated for each combination of preset deformation.

[8]The contact force is defined as the present force on the cantilever (6). Because the force-deformation curve is linear within the specified range of the cantilever strip, the units of deformation are reasonable estimates of the force. The equations relating the deformation of the cantilever to strain and force are described in more detail in (6).

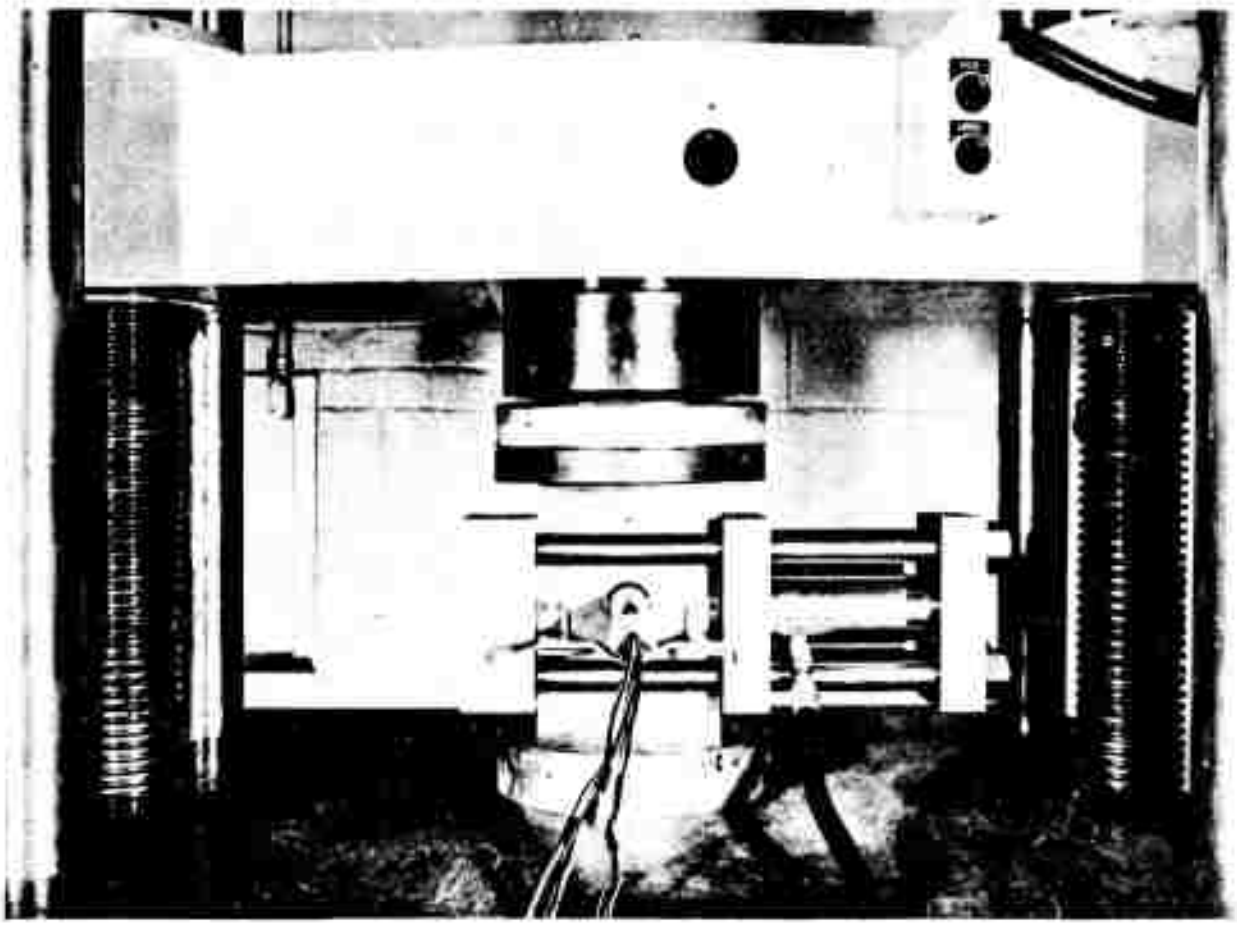

FIGURE 14 - Photograph of the Steel Plate in the Horizontal and Vertical Loading Devices

To quickly evaluate the computed stresses from data taken with the single- and three-component gages, the gages were located in models 1, 2, and 3 at orientations that represent three, 60-degree rosettes. The rosettes were 0, 60 and 120 degrees; 30, 90 and 150 degrees; and 45, 105 and 165 degrees. The models were uniaxially cycled to 15,000, 6,000 and 3,000 psi, respectively, and deformations were recorded over three cycles.

To determine the deformations with the three-component gage in mine rock and to make comparisons with similar determinations with a single component gage, stress-relief overcoring techniques were used in the porphyry rocks in the west wall of the Kimbley Pit near Ely, Nev., and in the Climax Molybdenum Mine, Climax, Colo. These sites were selected because the rock does not core exceptionally well, the modulus of the rock changes from point to point, there was no active mining near the sites, and borehole deformations were difficult to obtain with the single component gage. These sites presumably represent a more severe condition than would sites where the rock can be easily cored and the modulus of the rock is the same from point to point.

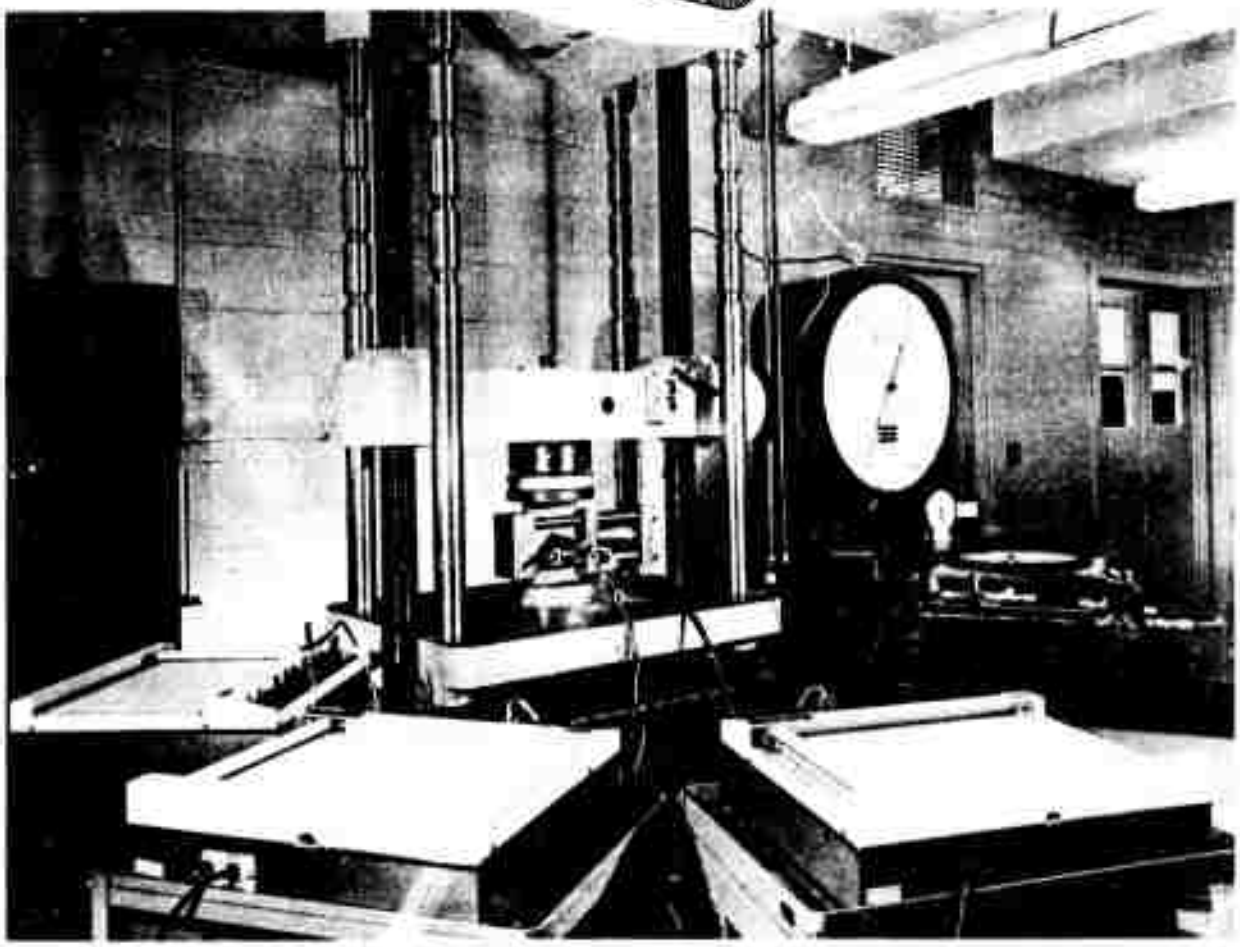

FIGURE 15 - Photograph of the Loading Device, Model, and the Recorders

The overcoring stress reliefs in the pit were made at a location about 2 feet north of and parallel to an overcoring hole in which stress reliefs were unsuccessfully attempted using a single component gage. The test sites in the Climax mine were in dead-end drifts in a newly developed area. At this site the stress reliefs with the field model of the three-component gage were made in a borehole parallel to and 18 inches from the borehole used for the stress reliefs with the single component gage.

Procedures similar to those used for the single component gage were used in these tests (3, 4). Briefly, the gage was placed in an EX-size hole with the components oriented at angles of 30, 90, and 150 degrees from the right-hand horizontal; the gage was overcored until relief was indicated by the measurements; the gage was moved forward about 6 inches and overcored for stress relief. The deformations from all three components were measured concurrent with the overcoring. Several attempts were unsuccessful because the core broke before relief was complete. In these cases, the gage was moved 4 to 6 inches beyond the depth of the overcore and stress relief repeated.

DATA

The data obtained from the deformation measurements with the air gage and the single component gage were reproducible to a value governed primarily by the operator's ability to interpolate a scale division. For example, the divisions of the air gage are 50 microinches and the reading can be easily estimated (by any operator) to 10 microinches. The divisions on the strain indicator are 10 microinches, and the reading can be easily estimated to 2 microinches. Because the calibration factor (the deformation-strain ratio) is about 6.5 (microinches deformation per unit microstrain), the optimum resolution for each device is about the same and is about 10 to 13 microinches; because the operator could always obtain reproducibility within 20 microinches of the average of three or more readings, this value is used as the estimated resolution of the gage. Because the single component gage is simpler and easier to use for borehole measurement, the single component gage was accepted as a standard. Several spot checks were made between these gages during the measurements to assure that the single component gage was an acceptable standard. These spot checks were always made at the 0-degree orientation to reduce the possible errors that could develop by inaccurate placement of the gage.[9]

The deformation data from the tests to determine the error created by the method of gage placement were reduced as follows: The deformation measured at the maximum pressure in each of the 10 cycles was recorded by rows, and the rows were identified by the angles at which the deformations were measured. For example, for the first cycle on the tests where the gage was inserted and rotated clockwise to the appropriate angle, the deformation at 0 degree was 2,325 microinches; the deformation at 60 degrees was 55 microinches; and the deformation at 120 degrees was 1,580 microinches. For the second cycle, the deformations were 2,338, 67, and 1,603 microinches for 0, 60, and 120 degrees, respectively. An identical listing of data was used when the components of the gage were set at other angles; for example, at 30, 90 and 150 degrees and at 45, 105, and 165 degrees, etc. Further, the same listing was followed for the data from the tests where the gage was inserted and rotated counterclockwise and where the gage was randomly placed in the hole. Because these data are obviously very voluminous and are almost identical to data obtained from tests of the gage with different, preset contact pressures, only the data obtained from the latter tests is included and presented in the following section of this report.

---

[9]The relationship between the deformation and uniaxial applied stresses is $U = \frac{Sd}{E}(1+2\cos 2\theta)$; see equation 3. Because the slope of the curve changes very slowly as θ approaches zero, small errors in orientation create negligible difference in the measurement of deformation whether the gage is oriented at precisely 0 degree or at some angle close to 0 degree. On the other hand, the relationship has an inflection point at 45 degrees and the slope changes rapidly; consequently, small errors in the angle of gage placement near 45 degrees could result in relatively large differences in measured deformation.

The last 7 of the 10 pressure cycles produced deformations that were less than 20 microinches apart. The difference between the deformations recorded during each of the first three pressure cycles on the models were slightly higher but always within 50 microinches of the average of the three readings. To illustrate, the deformations at 0 degree and 15,000 psi in the steel model were 2,325, 2,338, and 2,340 for cycles 1, 2, and 3; the deformation at 0 degree and 6,000 psi in the brass model were 1,925, 1,876, and 1,908 for cycles 1, 2, and 3, respectively. In terms of percent, the readings were within $\pm$ 2.5 percent of the average of the deformations (at angles less than 30 degrees. In most instances, the reproducibility is within the estimated resolution of the single component gage and is less than 1 percent of the total deformation.

In the tests to determine the agreement between the deformations measured with the single- and three-component gages, the best cycle-to-cycle reproducibility was obtained from the cylindrical models subjected to equal biaxial pressure (hereinafter called hydrostatic pressure) and the deformations were always less than 20 microinches from the average; the worst reproducibility was obtained at the 45- and 60-degree gage orientations when the magnesium plate (model 3) was subject to uniaxially applied stress; in most cases the reproducibility was within 30 microinches, but there were a few cases where the reproducibility was between 40 and 50 microinches. The worst reproducibility is expected for the latter case because (1) errors could be caused by tangential displacement and (2) the percentage difference between readings becomes greater because the absolute magnitude of the deformation is closer to zero (see equations (2) and (3)). Because the absolute magnitude of those data are always reproducible within 50 microinches and usually reproducible within 20 microinches of the average of three measurements, the data are averaged and summarized graphically in figures 15, 17, and 18 (for the tests on the metal models 1, 2, 3, and 7) and in figures 19 and 20 (for the tests on rock models 4, 5, and 8). Also included on these graphs are the plots of deformations computed using equation (3) and the elastic modulus of the model material. Because this curve is used only for purposes of comparison, the simplified theory for a hole in an infinite plate was used to compute these curves.

Although the graphs in figures 16 and 20 are of data obtained at the maximum applied stress on each model, continuous plots (on x-y recorders) were obtained of the deformation versus stress. The stress-deformation curves from the metal models were reproducible within the resolution of the equipment after the first stress deformation cycle. The stress-deformation data from the rock models were not as reproducible as the data from the metal models. The stress-deformation curves from the sandstone model (No. 4) showed considerable hysteresis on the first cycle, and the hysteresis became less as the number of stress-deformation cycles increased. The hysteresis curve was practically closed on the third cycle.

The data from the tests to evaluate the differences in deformation measured when the contact pressures are at different preset values are voluminous. The data from the tests when component 1 was at 0, 15, 30, 45, 60, 75, and 90 degrees are summarized in tables 4 through 10, respectively. The data obtained when components 2 and 3 were placed at these angles are very similar to the data from component 1, and therefore for brevity these data are omitted from this report. Because these tests were performed with the field model of the borehole gage as uniaxial stresses from 0 to 15,000 psi were applied to model 1 (steel plate), comparisons can be made with these data and the data from the tests with the laboratory gage. For example, the average deformation obtained with the laboratory gage oriented at 0 degree in the steel model (at 15,000 psi) is 2,350 microinches (see fig. 16). The deformation obtained with the field gage is the average of readings 1, 2, and 3 given in table 4. These comparisons are summarized in table 11 where the readings from the field gage (tables 4 through 10) have been averaged.

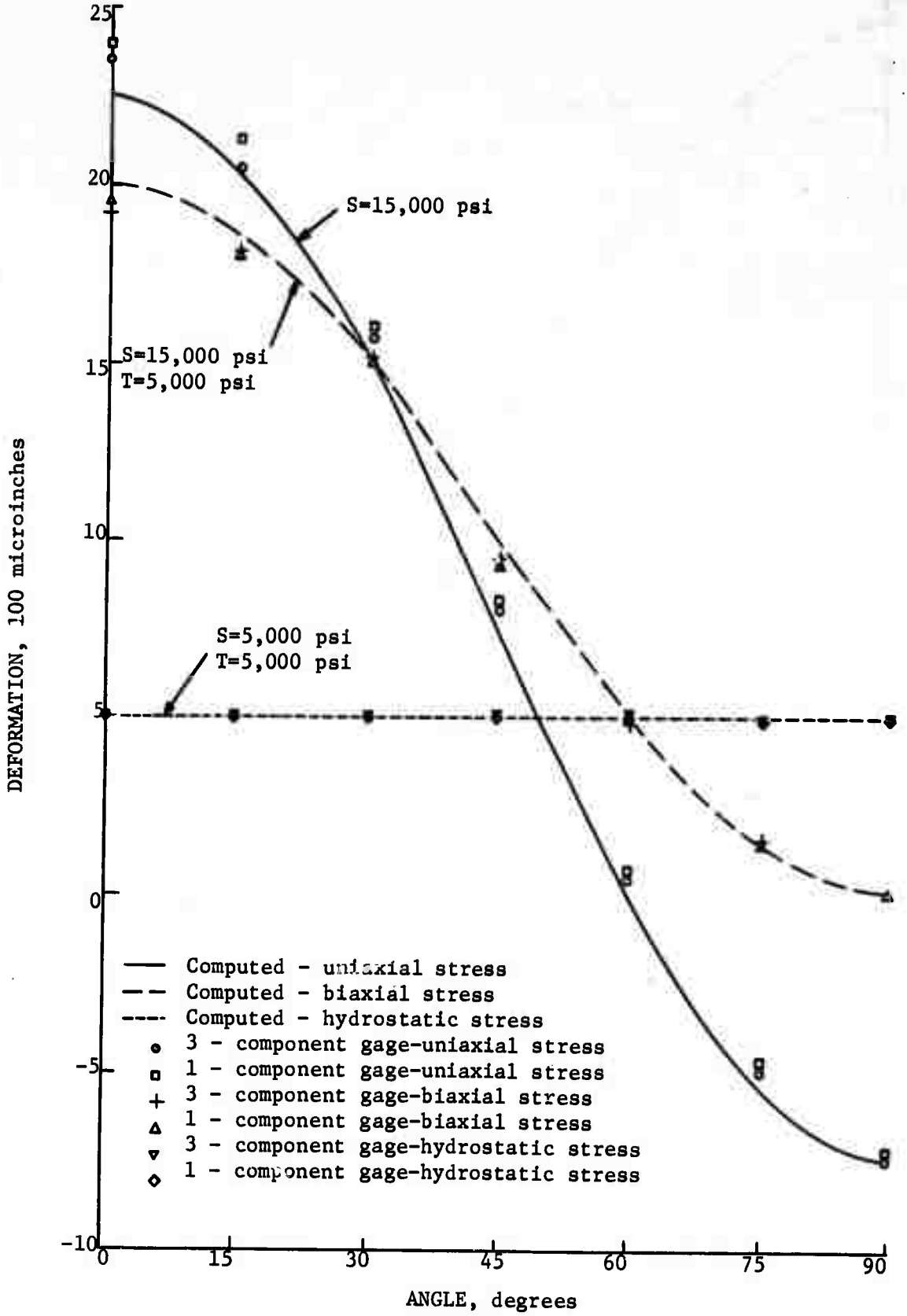

FIGURE 16 - Deformation Versus Angle-Steel Model

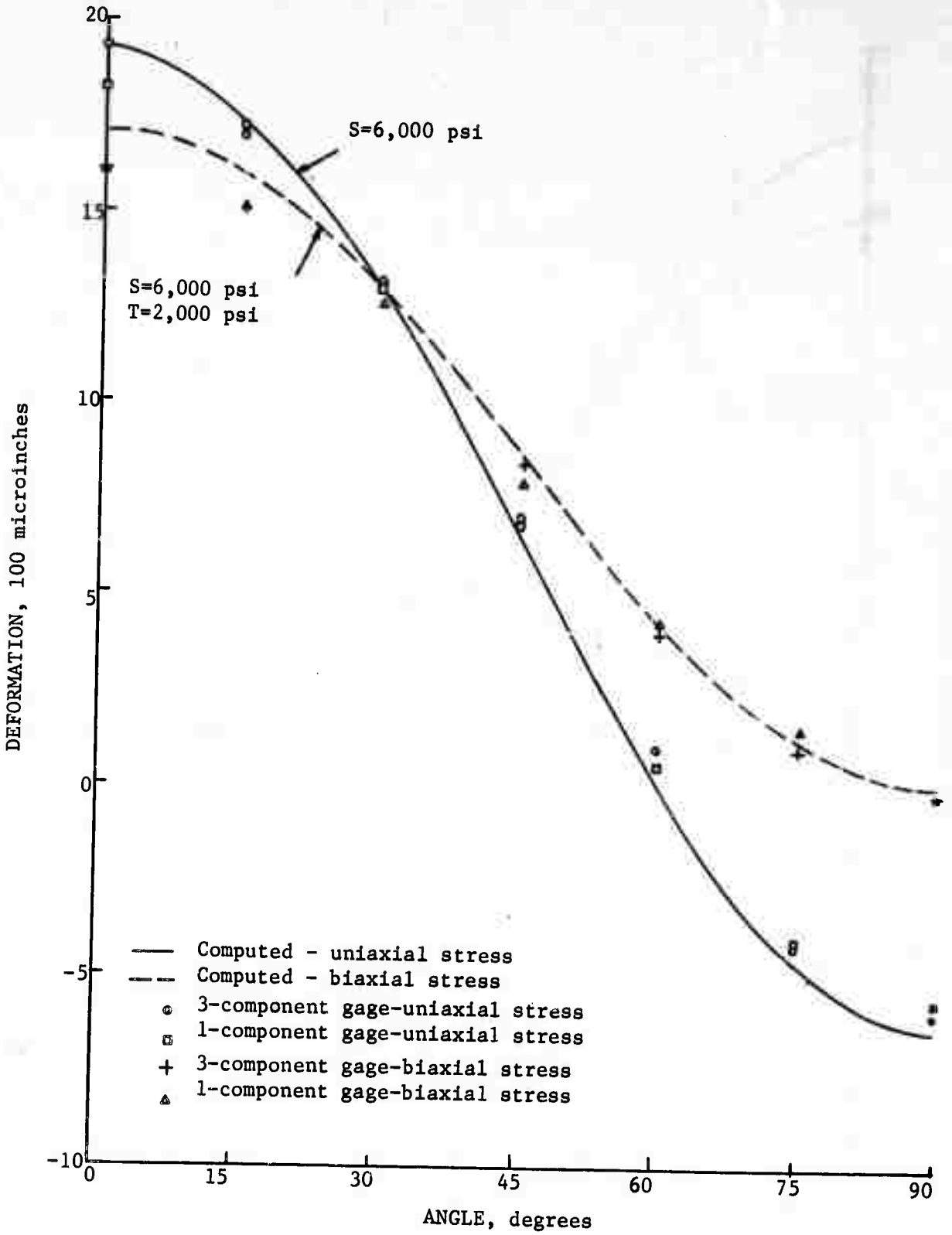

FIGURE 17 - Deformation Versus Angle-Brass Model

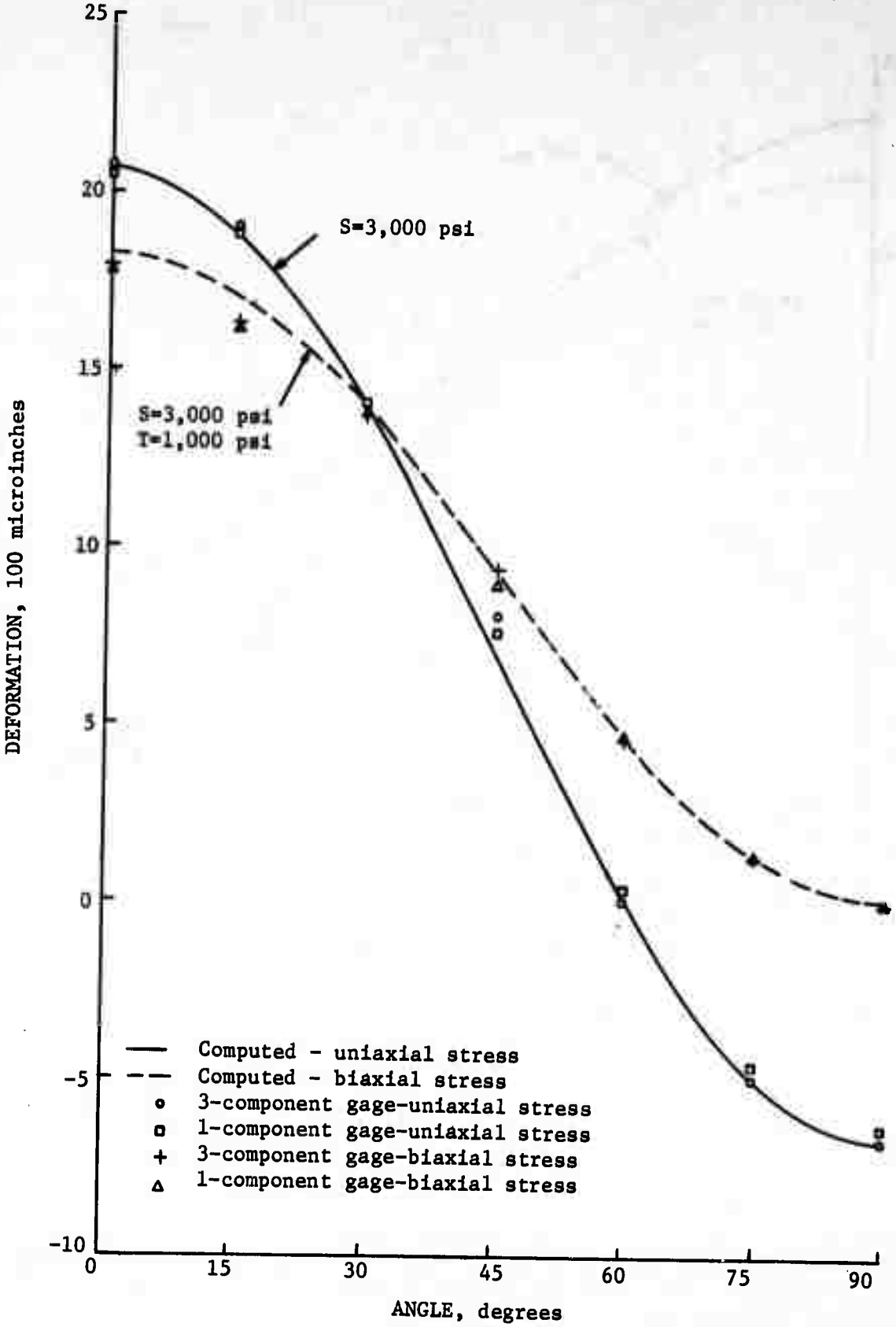

FIGURE 18 - Deformation Versus Angle-Magnesium Model

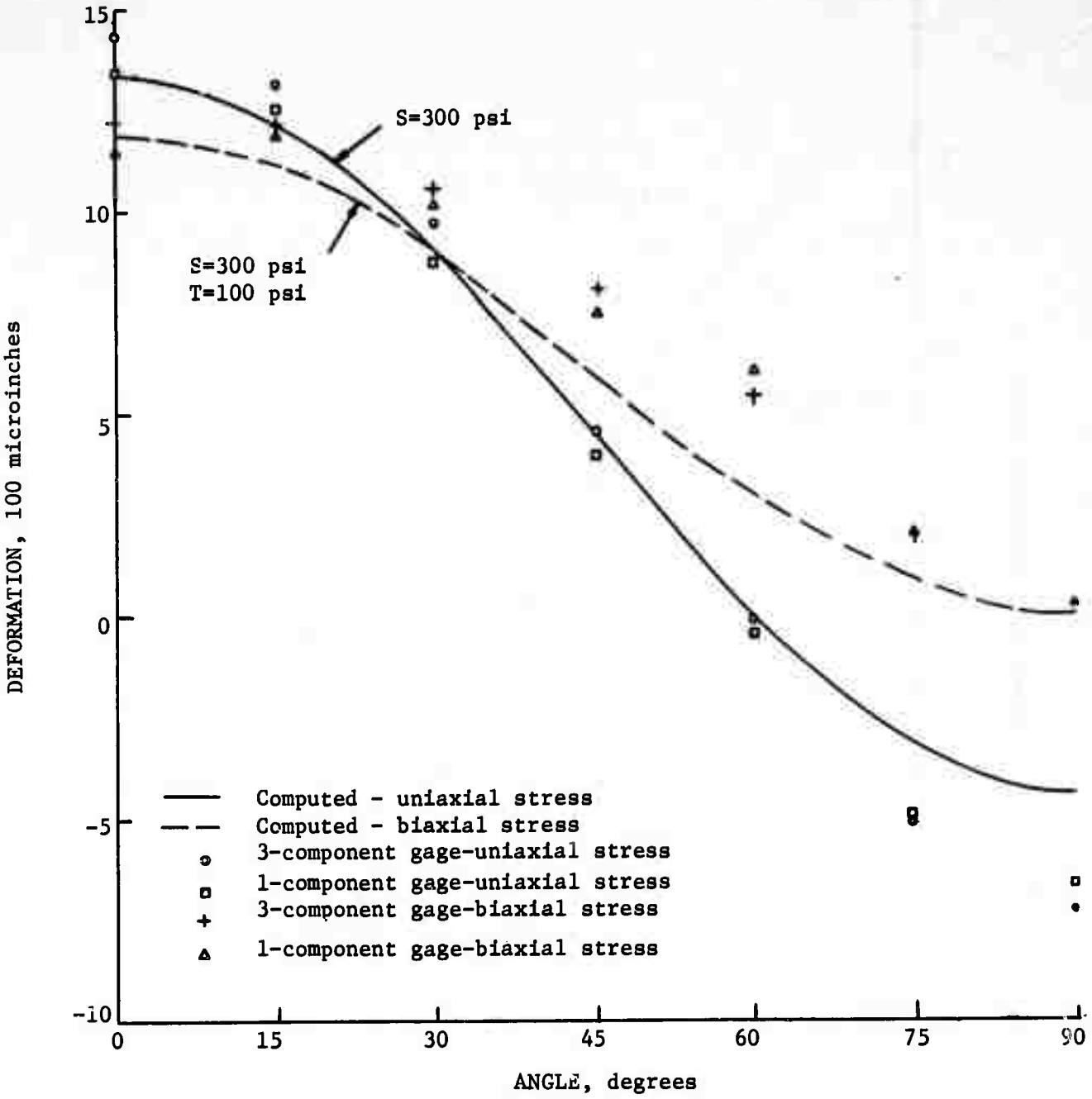

FIGURE 19 - Deformation Versus Angle-Sandstone Model

Table 12 is a summary of average deformations made both with the single-component and the three-component, field gage at orientations of 0, 30, 45, 60, 90, 105, 120, 150, and 165 degrees. The pressures applied to models 1, 2, and 3 were 15,000, 6,000, and 3,000 psi, respectively.

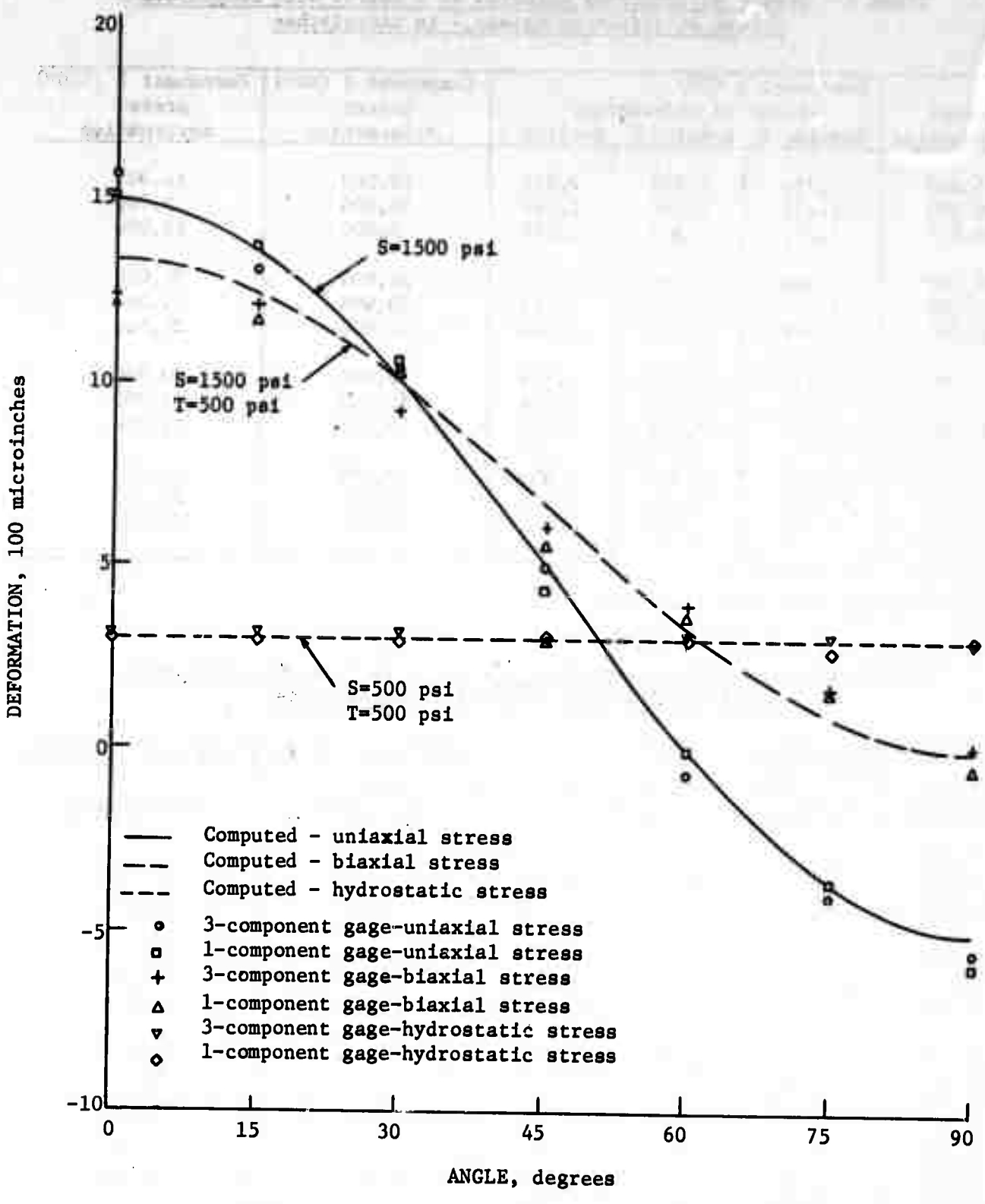

FIGURE 20 - Deformation Versus Angle-Limestone Model

TABLE 4 - Preset deformations measured at 0 degree with components preset at different values,[1] in microinches

Preset deformation	Component 1 (0°) Change in deformation Reading 1	Reading 2	Reading 3	Component 2 (60°) preset deformation	Component 3 (120°) preset deformation
5,000	2,320	2,300	2,341	10,000	15,000
10,000	2,237	2,260	2,244	15,000	5,000
20,000	2,296	2,308	2,318	5,000	10,000
10,000	2,338	2,356	2,342	20,000	30,000
20,000	2,243	2,302	2,283	30,000	10,000
30,000	2,291	2,301	2,325	10,000	20,000
5,000	2,333	2,344	2,325	15,000	30,000
15,000	2,274	2,274	2,294	30,000	5,000
30,000	2,325	2,356	2,341	5,000	15,000
20,000	2,316	2,332	2,305	20,000	20,000
20,000	2,307	2,285	2,313	20,000	20,000
20,000	2,358	2,326	2,342	20,000	20,000

[1]Model 1 loaded from 0 to 15,000 psi.

TABLE 5 - Preset deformations measured at 15 degrees with components preset at different values,[1] in microinches

Preset deformation	Component 1 (15°) Change in deformation Reading 1	Reading 2	Reading 3	Component 2 (75°) preset deformation	Component 3 (135°) preset deformation
5,000	2,132	2,088	2,130	10,000	15,000
10,000	2,034	2,050	2,034	15,000	5,000
15,000	2,082	2,105	2,114	5,000	10,000
10,000	2,073	2,029	2,014	20,000	3,000
20,000	2,064	2,074	2,096	30,000	10,000
30,000	2,044	2,037	2,056	10,000	20,000
5,000	2,043	2,043	2,025	15,000	30,000
15,000	2,073	2,114	2,094	30,000	5,000
30,000	2,025	2,056	2,041	5,000	15,000
20,000	2,116	2,132	2,105	20,000	20,000
20,000	2,107	2,085	2,113	20,000	20,000
20,000	2,058	2,026	2,093	20,000	20,000

[1]Model 1 loaded from 0 to 15,000 psi.

TABLE 6 - Preset deformations measured at 30 degrees with components preset at different values,[1] in microinches

Preset deformation	Component 1 (30°) Change in deformation Reading 1	Reading 2	Reading 3	Component 2 (90°) preset deformation	Component 3 (150°) preset deformation
5,000	1,527	1,527	1,518	10,000	15,000
10,000	1,556	1,573	1,556	15,000	5,000
20,000	1,599	1,600	1,628	5,000	10,000
10,000	1,588	1,610	1,617	20,000	30,000
20,000	1,553	1,546	1,572	30,000	10,000
30,000	1,601	1,590	1,619	10,000	20,000
5,000	1,576	1,564	1,566	15,000	30,000
15,000	1,523	1,520	1,549	30,000	5,000
30,000	1,578	1,562	1,582	5,000	15,000
20,000	1,569	1,557	1,544	20,000	20,000
20,000	1,587	1,543	1,516	20,000	20,000
20,000	1,585	1,533	1,586	20,000	20,000

[1]Model 1 loaded from 0 to 15,000 psi.

TABLE 7 - Preset deformations measured at 45 degrees with components preset at different values,[1] in microinches

Preset deformation	Component 1 (45°) Change in deformation Reading 1	Reading 2	Reading 3	Component 2 (105°) preset deformation	Component 3 (165°) preset deformation
5,000	804	804	866	10,000	15,000
10,000	866	831	888	15,000	5,000
15,000	1,052	1,068	993	5,000	10,000
10,000	868	898	895	20,000	30,000
20,000	763	768	810	30,000	10,000
30,000	872	879	910	10,000	20,000
5,000	875	859	842	15,000	30,000
15,000	844	885	916	30,000	5,000
30,000	742	773	744	5,000	15,000
20,000	771	794	783	20,000	20,000
20,000	879	863	863	20,000	20,000
20,000	838	854	818	20,000	20,000

[1]Model 1 loaded from 0 to 15,000 psi.

TABLE 8 - Preset deformations measured at 60 degrees with components preset at different values,[1] in microinches

Preset deformation	Component 1 (60°) Change in deformation Reading 1	Reading 2	Reading 3	Component 2 (120°) preset deformation	Component 3 (180°) preset deformation
5,000	53	88	65	10,000	15,000
10,000	63	27	44	15,000	5,000
15,000	19	23	65	5,000	10,000
10,000	94	67	58	20,000	30,000
20,000	44	39	44	30,000	10,000
30,000	23	23	50	10,000	20,000
5,000	50	50	23	15,000	30,000
15,000	78	88	71	30,000	5,000
30,000	27	34	41	5,000	15,000
20,000	0	6	6	20,000	20,000
20,000	66	78	100	20,000	20,000
20,000	23	50	50	20,000	20,000

[1]Model 1 loaded from 0 to 15,000 psi.

TABLE 9 - Preset deformations measured at 75 degrees with components preset at different values,[1] in microinches

Preset deformation	Component 1 (75°) Change in deformation Reading 1	Reading 2	Reading 3	Component 2 (135°) preset deformation	Component 3 (195°) preset deformation
5,000	-403	-355	-448	10,000	15,000
10,000	-535	-521	-552	15,000	5,000
15,000	-497	-452	-491	5,000	10,000
10,000	-462	-429	-431	20,000	30,000
20,000	-459	-435	-461	30,000	10,000
30,000	-516	-506	-524	10,000	20,000
5,000	-339	-382	-419	15,000	30,000
15,000	-497	-497	-536	30,000	5,000
30,000	-487	-426	-436	5,000	15,000
20,000	-483	-486	-477	20,000	20,000
20,000	-509	-500	-490	20,000	20,000
20,000	-524	-530	-510	20,000	20,000

[1]Model 1 loaded from 0 to 15,000 psi.

TABLE 10 - Preset deformations measured at 90 degrees with components preset at different values,[1] in microinches

Preset deformation	Component 1 (90°) Change in deformation Reading 1	Reading 2	Reading 3	Component 2 (150°) preset deformation	Component 3 (210°) preset deformation
5,000	-680	-661	-701	10,000	15,000
10,000	-660	-668	-664	15,000	5,000
15,000	-670	-672	-678	5,000	10,000
10,000	-696	-704	-704	20,000	30,000
20,000	-653	-721	-691	30,000	10,000
30,000	-678	-714	-685	10,000	20,000
5,000	-660	-727	-690	15,000	30,000
15,000	-631	-648	-717	30,000	5,000
30,000	-690	-690	-730	5,000	15,000
20,000	-685	-720	-736	20,000	20,000
20,000	-669	-680	-680	20,000	20,000
20,000	-728	-717	-711	20,000	20,000

[1]Model 1 loaded from 0 to 15,000 psi.

TABLE 11 - Summary of data from tests on the steel model, using the laboratory and field gages

Stress, psi	Angle, degrees	Deformation, microinches Laboratory gage	Field gage
15,000	0	2,350	2,310
15,000	15	2,050	2,072
15,000	30	1,565	1,567
15,000	45	805	855
15,000	60	52	48
15,000	75	-497	-472
15,000	90	-743	-690

TABLE 12 - Summary of deformations measured in models 1, 2, and 3 with the single-component (1-C) and the three-component (3-C) field gage

Model	Material	Gage	Deformation, microinches 0°	30°	45°	60°	90°	105°	120°	150°	165°
1	Steel	1-C	2,475	1,754	883	142	-717	-528	131	1,576	2,160
		3-C	2,395	1,690	888	83	-744	-465	67	1,605	2,100
2	Brass	1-C	1,961	1,349	746	52	-643	-518	41	1,261	1,680
		3-C	1,870	1,310	691	100	-568	-396	45	1,265	1,725
3	Magnesium	1-C	2,310	1,585	747	84	-813	-651	205	1,695	2,185
		3-C	2,025	1,405	745	46	-626	-430	61	1,422	1,885

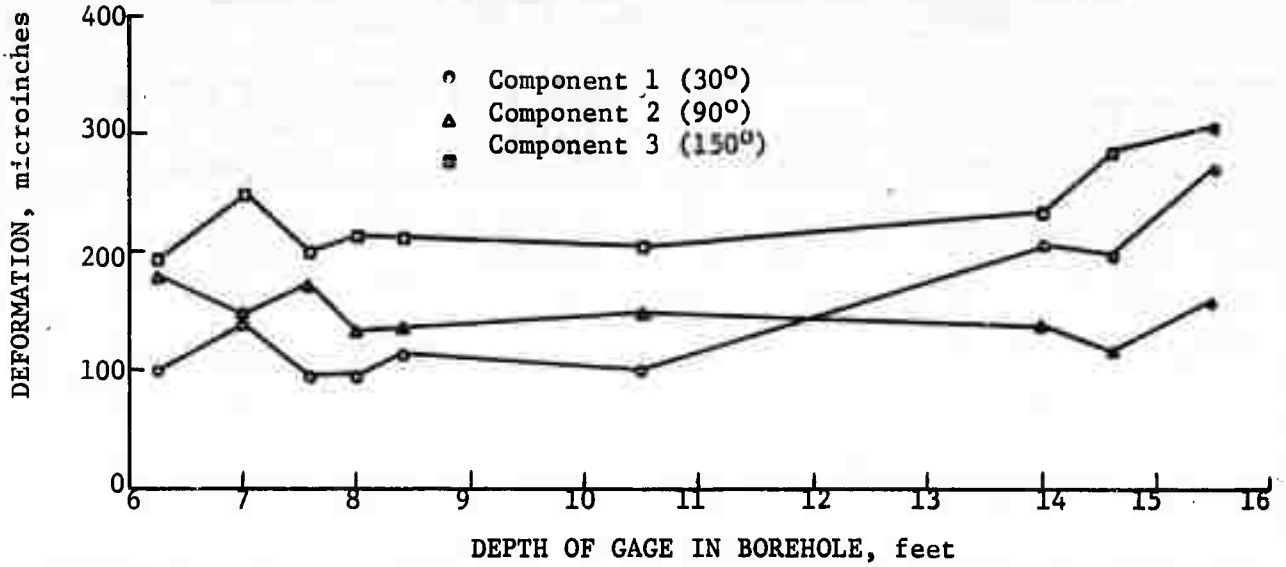

FIGURE 21 - Borehole Deformation Versus Distance From the Edge of an Open Pit, Three-Component Gage.

The data from field tests of the gage in quartz monzonite rocks near open pits and underground openings are presented by plots in figures 21 and 22. Data obtained from the single component gage in a hole parallel to the hole used for the three-component gage are given graphically in figure 23. In these plots, the orientation of the components are at 30, 90, and 150 degrees from the right-hand horizontal.

RESULTS AND CONCLUSIONS

As stated previously, the objective of this investigation was to develop a rugged, three-component borehole gage that would have a range, sensitivity, and accuracy approximately equivalent to the single component gage. Following a survey of various transducers, components, and design features that would meet the specifications for range and sensitivity, a gage was designed that would also meet the specifications to withstand rugged environments.

The component-to-component errors created by longitudinal borehole displacements were obviated by the design, but the possible component-to-component errors created by tangential displacement could not be economically eliminated by the design and still meet the requirements of ruggedness. Consequently, the larger part of the data from this study was collected in an effort to determine inaccuracies caused by tangential displacement in the borehole and adaptability of the gage to the rugged environment associated with mining and stress-relief overcoring.

A routine analysis of variance was performed using the data from the tests to determine errors from gage placement. This analysis established that the measurements were not significantly different (at the 2.5-percent confidence level) whether or not the gage was rotated to the proper angles of component orientation or randomly placed at the proper angles.

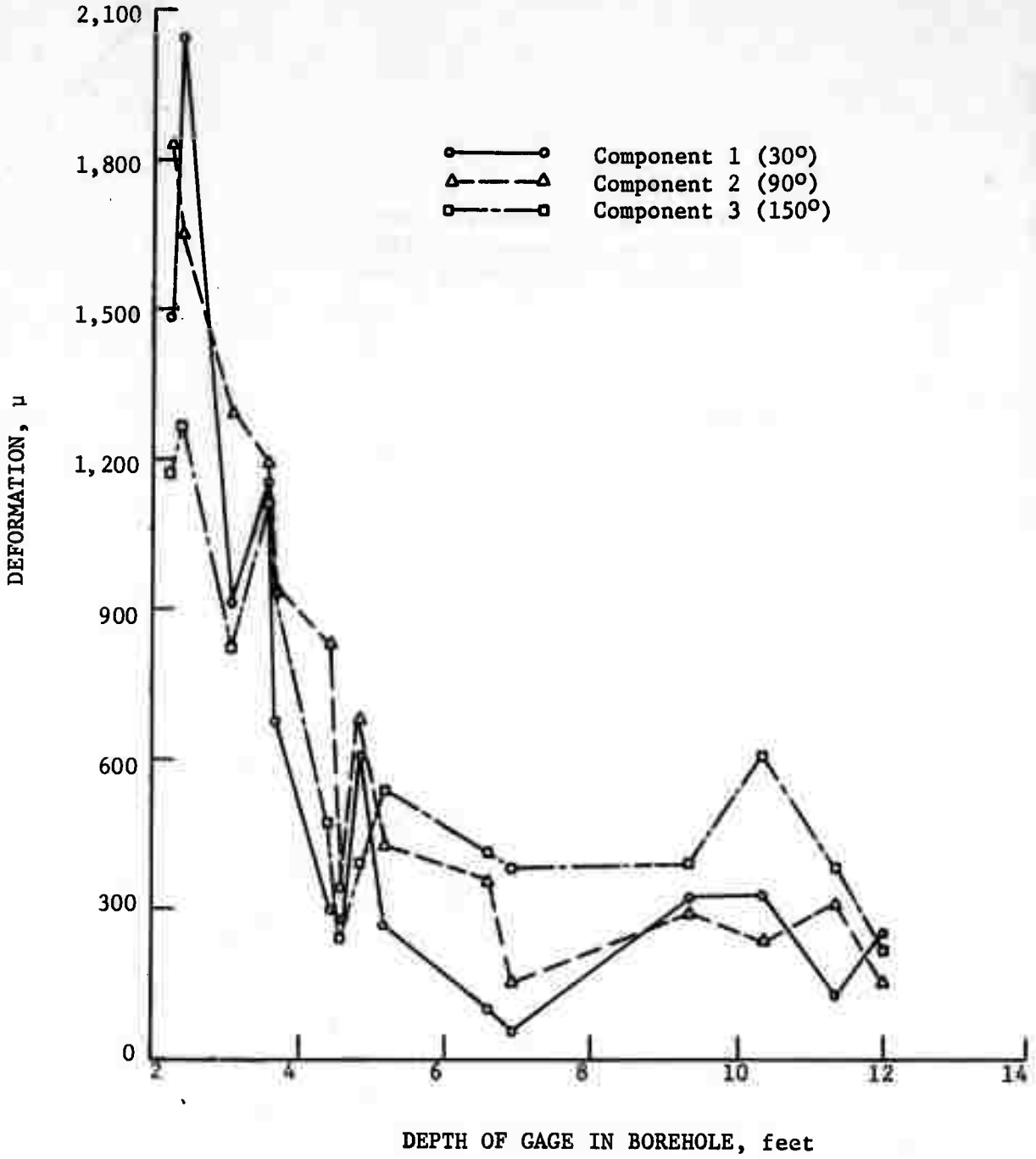

FIGURE 22 - Borehole Deformation Versus Distance From the Edge of an Underground Opening, Three-Component Gage.

The laboratory tests made to compare the response of the three-component and single-component gages in identical models and under identical conditions disclosed small differences that may be caused by tangential displacement. Examination of the data summarized in figures 16 through 20 establishes that, on the average, the difference between borehole deformations measured with the two gages was greatest when the models were loaded uniaxially and was least when the models were loaded hydrostatically.

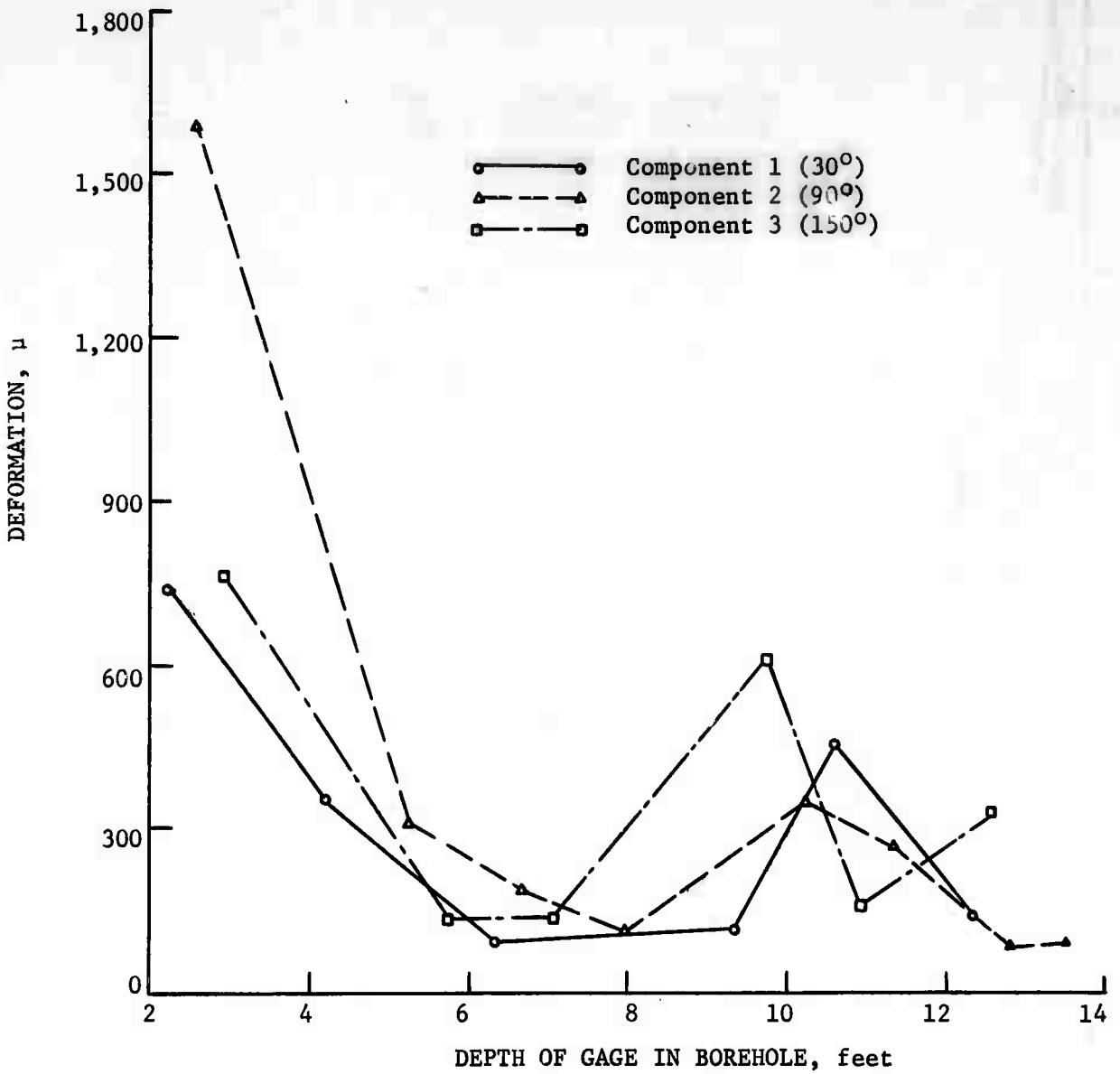

FIGURE 23 - Borehole Deformation Versus Distance From the Edge of an Underground Opening, Single-Component Gage.

Also, the difference between deformations under biaxial loads were, on the average, less than the difference from the uniaxially loaded models and greater than the difference from the hydrostatically loaded models. Because the tangential displacements decreased as the ratio of the applied stresses approached unity and the decrease is consistent with the decreases predicted from calculations using equation 2, the differences are presumed to be caused by tangential displacement of the hole.

Of importance is the fact that the average absolute difference (that is, the magnitude of the measurement of the three-component gage minus the measurement of the single component gage, or vice versa) of most of the deformations was less than 50 microinches (figs. 16 through 20). Further, the largest absolute differences were measured in the sandstone model, a material known to anisotropic (table 2). Equally important is the fact that these differences were not associated with any particular angle.

If the average differences were considered as an error in measurement, and this error were substituted for the deformation, U, at 0 degrees, the computed stress (uniaxial loads, T = 0) would be about 20 psi for a modulus of 1 x 10^6 psi; 60 psi for a modulus of 3 x 10^6 psi; and 200 psi for a modulus of 10 x 10^6 psi. Obviously, the magnitude of the estimated error would be much less from similar calculations using data from the biaxially and hydrostatically loaded specimens. Because the errors are small compared with stress magnitudes normally measured in mines and most stresses in mine rock measured to date are biaxial or hydrostatic (4) for most if not all practical applications, the differences in measurement of deformation with the single component and three-component gage are small enough to be ignored.

Inspection of the data from the tests to determine the differences in measured deformation when the three components were at various preset values (tables 4 through 10) discloses evidence that the differences are not large enough to significantly affect the accuracy of the measurement. To verify this observation, a routine analysis of variance was made and the differences were not significant at the 95-percent confidence level.

The deformations measured when the single- and three-component gages were used at nine different angles can be compared with the data obtained at six different angles. For example, the data taken at five of the nine positions in the steel plate (see table 12), can be compared with the data at the same positions presented in figure 16. These five positions are 0, 30, 45, 60, and 90 degrees. Note that, in both groups of data, the deformations measured with the single-component gage are usually slightly larger than deformations measured with the three-component gage. A similar result is noted in both the brass and magnesium models (see table 12 and figs. 17 and 18). The deformations presented in table 12 can also be used to compute the applied stresses on the models. To make these calculations, the handbook values of the modulus of elasticity of the steel, brass, and magnesium models were used in the equations for the 60-degree deformation rosette (2). These computations are summarized in table 13. The applied stresses on the models were uniaxial and equal to 15,000, 6,000, and 3,000 psi. Therefore, if the models were infinitely large, thin plates and if all the test conditions and measurements were exact, the computed maximum stresses, S, for model 1 should have been 15,000 psi; the minimum stress, T, and the angle, θ, should have been zero. Similarly, the computed maximum stresses in models 2 and 3 should be 6,000 and 3,000 psi, respectively, and the minimum stresses and angle should be zero. Although the conditions of the test could not be exact, the computed maximum stresses are not greatly different from the applied stresses (see table 14). A more noteworthy result is that the standard deviation of the stresses calculated from three-component borehole deformation data are less than the deviations computed from the calculated stresses from single-component data. The computed angles from the three-component gage data are all zero except one and no standard deviations are required because the quality of the results can be noted by inspection (see table 14).

The computed stresses and angles from three-component gage data are more nearly equal to the value of the applied stresses and have a smaller standard deviation. The reason for this result is unknown; however, it is probably due to the fact that the rosette angles (three angles, 60 degrees apart) are "fixed" in the three-component gage. When using the single-component gage, the gage must be placed at all of the three rosette angles and the three-component gage needs to be set only at one. Any error in gage placement with the single-component gage would be reflected in both the computed stresses and angles. Errors in gage placement with the three-component gage would appear only in the computed angles.

TABLE 13 - Computed stresses from data taken with the single-component (1-C) and three-component (3-C borehole gages in models 1, 2, and 3

Model	Rosette angles, degrees	S, psi		T, psi		θ, degrees	
		1-C	3-C	1-C	3-C	1-C	3-C
1	0-60-120	15,823	15,134	1,275	701	0	0
1	30-90-150	15,554	15,361	704	510	3	0
1	45-105-165	15,075	15,262	574	436	1	1
2	0-60-120	6,303	6,056	222	236	0	0
2	30-90-150	6,220	6,135	28	242	1	0
2	45-105-165	6,066	6,127	-2	286	3	0
3	0-60-120	3,442	2,962	312	116	1	0
3	30-90-150	3,866	3,061	10	117	1	0
3	45-105-165	3,027	3,005	268	112	0	0

TABLE 14 - Applied and computed stresses from data taken with the single-component (1-C) and three-component (3-C) gages

Model	Gage	Maximum stress, psi		SD[1]	Minimum stress, psi		SD[1]
		Applied	Computed average		Applied	Computed average	
1	1-C	15,000	15,484	279	0	851	372
1	3-C	15,000	15,252	113	0	582	145
2	1-C	6,000	6,196	120	0	142	180
2	3-C	6,000	6,106	43	0	255	27
3	1-C	3,000	3,445	420	0	197	163
3	3-C	3,000	3,009	50	0	115	3

[1]Standard deviations (SD) are listed for the computed stresses.

The data and results obtained with the three-component gage in model 3 (magnesium plate) are particularly significant in that the modulus of elasticity of magnesium (about 6.5 x 10^6 psi) is more closely equal to the modulus of rocks. The differences in the applied and computed stresses for this model were very small and the standard deviations were only 50 psi and 3 psi on the maximum and minimum stresses, respectively.

Because of closely spaced jointing and alterations in the rock, much difficulty was experienced in the overcoring, stress relief measurements in open pits. To illustrate, only one borehole deformation measurement was obtained between the depths of 8.5 and 14 feet in rock near an open pit (fig. 21). Also, because of blasting

fractures and weathering in near surface rock, stress reliefs could not be made between the surface of the pit and the depth of 6.25 feet. A similar difficulty was experienced when the same location was stress-relieved using the single component gage. In fact, the distances between the various stress reliefs were so large that the data from the single component gage could not be accurately interpolated. To illustrate, in the previous investigation, a stress relief was obtained at the orientation of 30 degrees and a depth of about 8 feet. Because it is necessary to rotate the single component gage to obtain the required three deformations (3, 4), the next relief was at a gage orientation of 90 degrees and a depth of about 10.5 feet, and the third relief was at a depth of 14 feet and an orientation of 150 degrees; therefore, the hole depth was almost 15 feet before a second relief could be obtained at an orientation of 30 degrees. Consequently, the depths between the measurements at 30-degree orientations were far too great for reasonable interpolation of the data. In the tests with the three-component gage, readings were obtained at all three angles at the depths of 8.5, 10.5, and 14 feet, which not only gives three times the data but also removes the requirement for the interpolation of data.

The stress relief measurements around openings in the Climax Molybdenum mine were in a more favorable rock for stress relief measurements. As noted in graphs of the data (figs. 22 and 23), stress reliefs were obtained on an average of about 1.5 reliefs per foot of hole. Consequently, deformations at a particular orientation of the single component gage were usually repeated within 1.5 to 2 feet. Under these circumstances, interpolation of the data would not materially affect the accuracy of stress determinations made from the deformation data. Also, the inspection of the data from the two gages (figs. 22 and 23) shows that, on the average, the deformations from each gage are in good agreement.

In conclusion, the results of the laboratory and field tests of the three-component borehole gage indicate that the instrument will measure borehole deformation with sufficient accuracy to obtain engineering estimates of the stress in mine rock. A primary advantage of the gage is the ability to reproduce deformations at a specific angle at much shorter intervals in the hole; possible errors created by tangential displacement of the hole are the primary disadvantage. However, this disadvantage is not significant in most stress investigations because the type and magnitude of the stress fields around mine openings is such that the possible errors in the measurements are small enough to be ignored. Another primary advantage is the fact that the components are fixed at angles 60 degrees apart. Because these angles are fixed, there can be no error in the calculation of the stress caused by errors in the placement of the gage with respect to some known direction; however, any error in gage placement would be reflected in the calculations for the angles of the stresses with respect to the known direction. Therefore, in field or laboratory measurement particular care should be taken to orient the gage toward a known direction.

REFERENCES

1. Fitzpatrick, John. Biaxial Device for Determining the Modulus of Elasticity of Stress Relief Cores. BuMines Rept. of Inv. 6128, 1962, 13 pp.

2. Merrill, Robert H., and Jon R. Peterson. Deformation of a Borehole in Rock. BuMines Rept. of Inv. 5881, 1961, 32 pp.

3. Merrill, Robert H. In Situ Determination of Stress by Relief Techniques. Proc. Internat. Conf. on State of Stress in the Earth's Crust, American Elsevier Publishing Co., New York, 1964, pp. 343-378.

4. Obert, Leonard. In Situ Determination of Stress in Rock. Min. Eng., v. 14, No. 8, August 1962, pp. 51-58.

5. _____. Triaxial Method for Determining the Elastic Constants of Stress Relief Cores. BuMines Rept. of Inv. 6490, 1964, 22 pp.

6. Obert, Leonard, Robert H. Merrill, and Thomas A. Morgan. Borehole Deformation Gage for Determining the Stress in Mine Rock. BuMines Rept. of Inv. 5978, 1962, 1[illegible] pp.

DEFORMATION OF A BOREHOLE IN ROCK[1]

by

Robert H. Merrill[2] and Jon R. Peterson[3]

SUMMARY

Measurement of the deformation of a borehole in rock subjected to a change in applied stress can be used to calculate the magnitude and direction of the applied stress, provided a satisfactory deformation-applied stress relationship exists.

In this investigation by the Bureau of Mines the deformation of a borehole in a rock model subjected to a known applied stress was compared with the theoretical deformation of a hole in an elastic, isotropic plate and was found to be in good agreement. Hence, this relationship can be used to calculate the applied stress on a borehole from borehole deformation measurements.

INTRODUCTION

This report describes the first phase of an investigation the purpose of which is to determine the direction and magnitude of the stress in rock surrounding an underground opening. The basis for the method considered in this investigation is as follows: (1) The deformation of a borehole in rock depends upon the direction and magnitude of the applied stress; (2) the relationship between the deformation of a hole in an infinite, isotropic, elastic plate and the applied stress is known from theory, and (3) if it can be shown that the deformation of a borehole in rock and a hole in a plate are essentially the same, the stress in rock can be calculated from borehole deformation measurements, using the applied stress-deformation relationship.

The purpose of this phase of the investigation was to study, in rock models, the deformation of a borehole as a function of the applied stress and to compare the results with those calculated from stress-deformation theory. This report presents (1) the theory for the deformation of a hole in an infinite, isotropic, elastic plate subject to a uniaxial or biaxial stress field and under the condition of plane stress or plane strain, (2) the results of borehole deformation measurements in rock models, and (3) a comparison of the stress applied to the model with that calculated from the

---

[1]Work on manuscript completed January 1961.

[2]Physicist, Denver Mining Research Center, Bureau of Mines, Denver, Colo.

[3]Former Bureau of Mines physicist; now with U. S. Geological Survey, Washington, D. C.

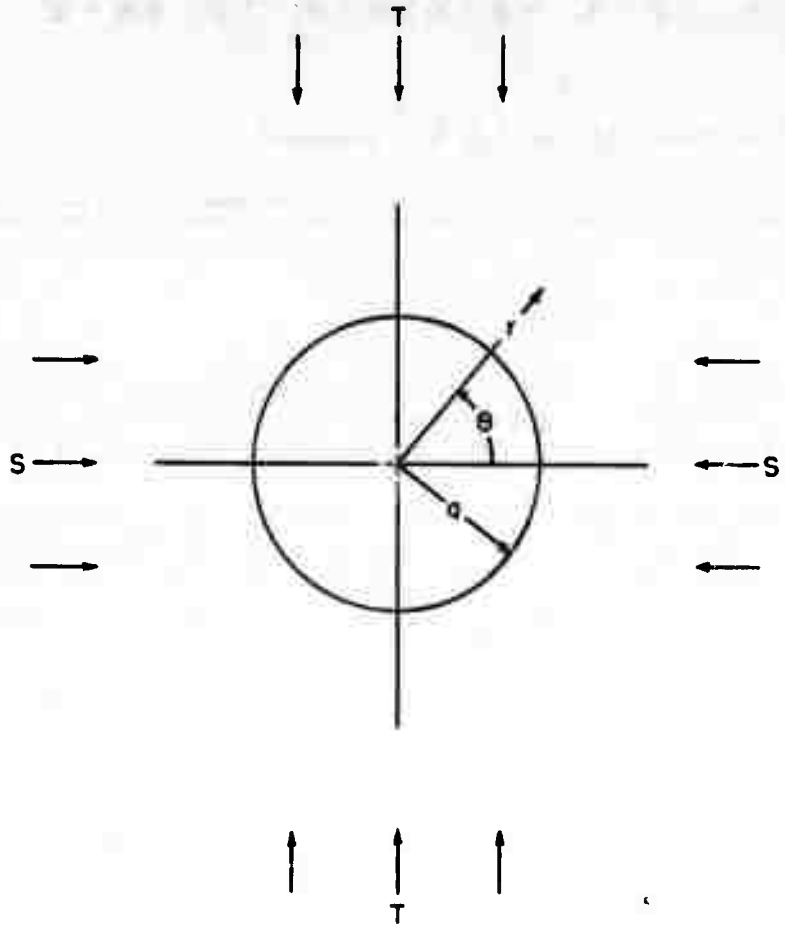

FIGURE 1 - Cross Section of Hole in Plate

In a report covering the second phase of this investigation, a borehloe deformation gage is described together with the results of measurements in mine rock.

THEORY

The derivations for the deformation of a hole in a plate (for the conditions for plane stress and plane strain) subjected to uniaxial and biaxial stress fields[4] are presented in appendix I, part A. The more important equations and special cases are as follows:[5] [6]

The deformation of the hole in a uniaxial stress field (T=0) and in plane stress is given by (see fig. 1)

$$U = \frac{dS}{E}(1+2\cos 2\theta), \qquad (1)$$

where

U = deformation of hole (change in length of a diameter),
a = radius of hole,
d = diameter of hole = 2a.
S,T = perpendicularly applied stress (for a uniaxial stress field T = 0),
θ = angle (counterclockwise) from S to r (see fig. 1 and appendix I, part A), and
E = modulus of elasticity.

---

[4]In this investigation compressive stresses are positive, and tensile stresses are negative.

[5]Some of these equations have been published by Hast and Isaacson without derivation(3 4).

[6]Underlined numbers in parentheses refer to items in the bibliography at the end of this report.

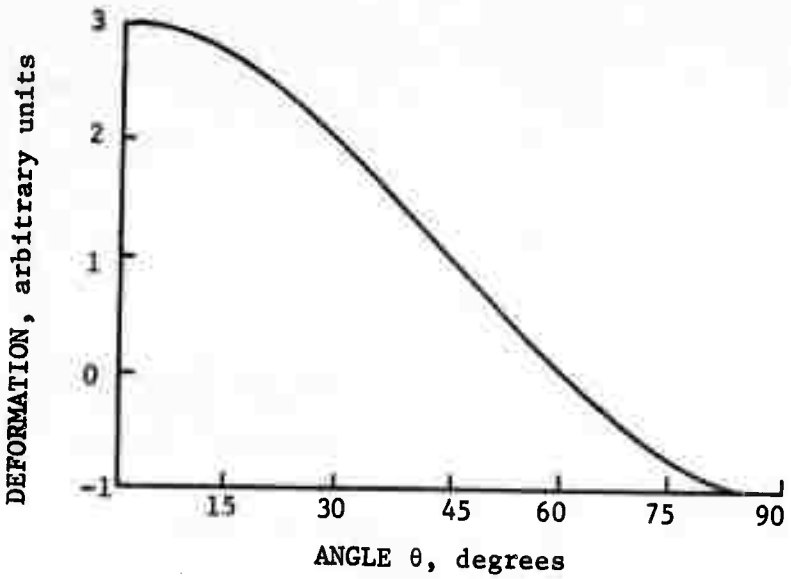

FIGURE 2 - Borehole Deformation Versus Angle θ.

When θ = 0, the deformation is in the direction of the applied uniaxial stress, and equation 1 reduces to

$$U = \frac{3dS}{E} . \qquad (2)$$

When θ = 90°, the deformation is

$$U = -\frac{dS}{E} , \qquad (3)$$

and the minus sign signifies that as the stress increases, the hole (at that point) is expanding.

The deformation versus the angle θ for one quadrant of the hole (θ = 0° to θ = 90°) is plotted in figure 2.

For a uniaxial stress field and plane strain, the deformation is related to the stress by (see appendix I, part A, case 2)

$$U = \frac{dS}{E} (1 - \nu^2) (1 + 2 \cos 2\theta), \qquad (4)$$

where ν = Poisson's ratio.

When θ = 0°,

$$U = \frac{3dS}{E} (1 - \nu^2). \qquad (5)$$

When θ = 90°,

$$U = - \frac{dS}{E} (1 - \nu^2). \qquad (6)$$

Equations (1) and (4) for the cases of plane stress and plane strain differ only by the quantity $(1-\nu^2)$. When Poisson's ratio is between 0.25 and 0.3 (which is the case for most rocks), the difference between the deformation for the cases of plane stress and plane strain is bout 6 to 10 percent.

For a biaxial stress field and plane stress, the deformation is related to the biaxial stresses S and T by (see fig. 1 and appendix I, part A, case 3)

$$U = \frac{d}{E}\,[(S+T) + 2(S-T)\cos 2\theta] \tag{7}$$

When $\theta = 0$,

$$U = \frac{d}{E}\,(3S-T), \tag{8}$$

and when $\theta = 90^{o}$,

$$U = \frac{d}{E}\,(3T-S). \tag{9}$$

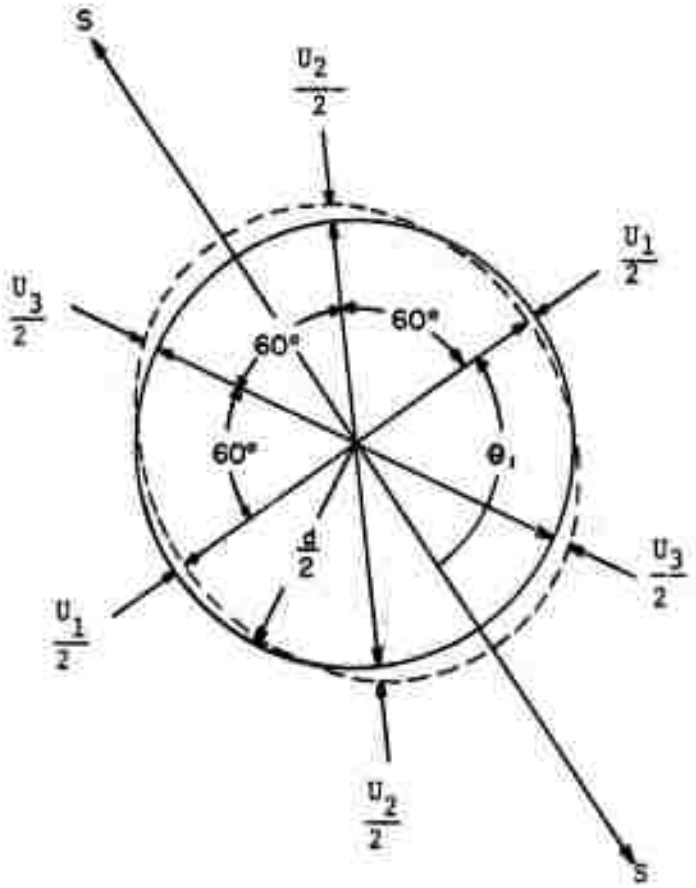

FIGURE 3 - Cross Section for a 60-Degree-Deformation Rosette.

For the case of plane strain, the deformation is (see appendix I, part A, case 4)

$$U = \frac{d(1-\nu^2)}{E}\,[(S+T) + 2(S-T)\cos 2\theta]. \tag{10}$$

If the deformation is measured across three different diameters and the modulus of elasticity and Poisson's ratio are known, the magnitude and direction of the stresses S and T can be computed. (Derivation of the equations is given in appendix I, part B, case 1.) If the measured deformations are 60° apart (that is, a 60° rosette) the relationships are (see fig. 3)

$$S + T = \frac{E}{3d(1-\nu^2)}\,(U_1+U_2+U_3) \tag{11}$$

and

$$S - T = \frac{\sqrt{2}E}{6d(1-2\nu^2)}\,[(U_1-U_2)^2 + (U_2-U_3)^2 + (U_1-U_3)^2]^{1/2}. \tag{12}$$

The angle between S and the direction in which the deformation U_1 is measured is

$$\tan 2\theta_1 = \frac{-\sqrt{3}\,(U_2-U_3)}{2U_1-U_2-U_3}, \tag{13}$$

where

U_1, U_2, U_3 = deformation across diameters 60° apart,
S, T = stresses,
and θ_1 = the angle from S to U_1 measured counterclockwise.

Where the measured deformations are 45° apart, S and T are related to deformations by (see appendix II, part B, case 2)

$$S + T = \frac{E(U_1+U_3)}{2d(1-\nu^2)} \tag{14}$$

and

$$S - T = \frac{E[(U_1-U_2)^2 + (U_2-U_3)^2]^{1/2}}{2d\sqrt{2}\,(1-\nu^2)} \tag{15}$$

and the angle between S and the direction in which the deformation U_1 is measured is

$$-\tan 2\theta_1 = \frac{2U_2-U_1-U_3}{U_1-U_3}. \tag{16}$$

The conditions for plane stress are satisfied in the rosette equations when the tern $(1-\nu^2)$ is equal to 1. For plane stress and a 60° deformation rosette, S and T are given by

$$S + T = \frac{E}{3d}\,(U_1+U_2+U_3) \tag{17}$$

$$S - T = \frac{\sqrt{2}\,E}{6d}\,[(U_1-U_2)^2 + (U_2-U_3)^2 + (U_1-U_3)^2]^{1/2}, \tag{18}$$

and θ_1 is obtained from equation (13).

For a 45-degree-deformation rosette in plane stress, S and T are given by

$$S + T = \frac{E(U_1+U_3)}{2d} \tag{19}$$

and

$$S - T = \frac{E[(U_1-U_2)^2 + (U_2-U_3)^2]^{1/2}}{2d\sqrt{2}}, \tag{20}$$

and θ_1 is obtained from equation (16).

The angle θ_1 could have two values 90° apart. The correct angle can be determined by using the following rules:

For a 60° rosette (angular measurements positive in the counterclockwise direction and all angles measured from S to U_1):

1. If $U_2 > U_3$, θ_1 lies between + 90° and + 180° or 0° and -90°.

2. If $U_2 < U_3$, θ_1 lies between 0° and + 90°.

3. If $U_2 = U_3$, and if

   a. $U_1 > U_2 = U_3$, $\theta_1 = 0°$;

   b. $U_1 < U_2 = U_3$, $\theta_1 = \pm 90°$.

For a 45° rosette:

1. If $U_2 > \frac{U_1 + U_3}{2}$, θ_1 lies between + 90° and + 180° or 0° and - 90°.

2. If $U_2 > \frac{U_1 + U_3}{2}$, θ_1 lies between 0° and + 90°.

3. If $U_2 = \frac{U_1 + U_3}{2}$, and if

   a. $U_1 > U_3$, $\theta_1 = 0°$;

   b. $U_1 < U_3$, $\theta_1 = 90°$.

These rules are similar to rules used for strain rosette calculations (5). In instances where some doubt exists concerning the correct angle, the direction can be easily checked by graphical methods (see reference (5) for examples of graphical analyses).

MODEL STUDIES

To determine the agreement between the deformation of a borehole in rock and a hole in a plate, two models were prepared from each of three materials, Indiana limestone, Georgia marble, and hydrostone (a high-strength gypsum cement). These materials were known to have significantly different elastic properties and grain size (see table 1 and fig. 4).

TABLE 1 - Physical properties of materials used for models

Material	Grain size	Modulus of elasticity (x 10^6 p.s.i.)		Elastic behavior (shape of stress-strain curve)
		Longitudinal	Lateral	
Hydrostone	Microscopic	2.6	2.2	Linear.
Indiana limestone	0.1 to 1.0 mm.	5.1	5.0	Do.
Georgia marble	1 to 5 mm.	7.0	8.0	Curved.[1]

[1]The slope gradually increased (see fig. 4).

The models were ground to a finished size of 5x5x 10 inches, and the opposite surfaces were parallel to within 0.002 inch. A 1-inch-diameter hole was drilled through each model at the center of a 5- by 10-inch surface (see fig. 5). The diameter of the hole was large compared to the grain size of the model material. The model was sufficiently large so that the deformation of the 1-inch-diameter hole was not significantly affected by the model dimensions.[7] The 5- by 5-inch end dimensions were chosen so that a stress of 4,800 pounds per square inch could be applied by a compression machine having a capacity of 120,000 pounds. The models were made 10 inches long to accommodate the apparatus for applying lateral loads and to reduce the error caused by friction between the model and the bearing heads of the compression machine.

Photographs of the model and test equipment are shown in figures 6 and 7. The longitudinal load was applied by the compression machine on the 5- by 5- inch ends. The lateral load was applied by a specially constructed hydraulic press, the maximum capacity of which was 30,000 pounds, or 1,200 pounds per square inch on a bearing area of 25 square inches. The press was calibrated in the compression machine and was accurage to within ± 125 pounds at maximum load.

[7]If the surfaces of the model are 2-1/2 radii from the center of the hole, the effect of the surface on the stress distribution around the hole is less than 10 percent. (2 4).

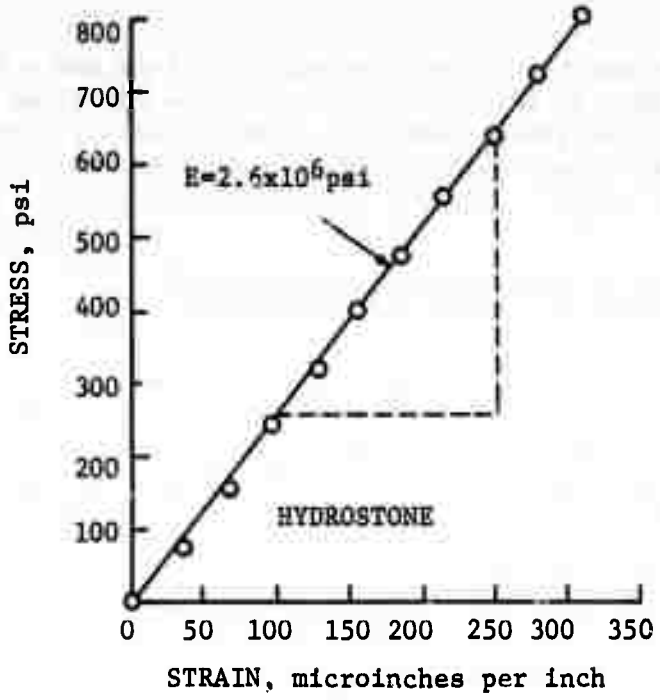

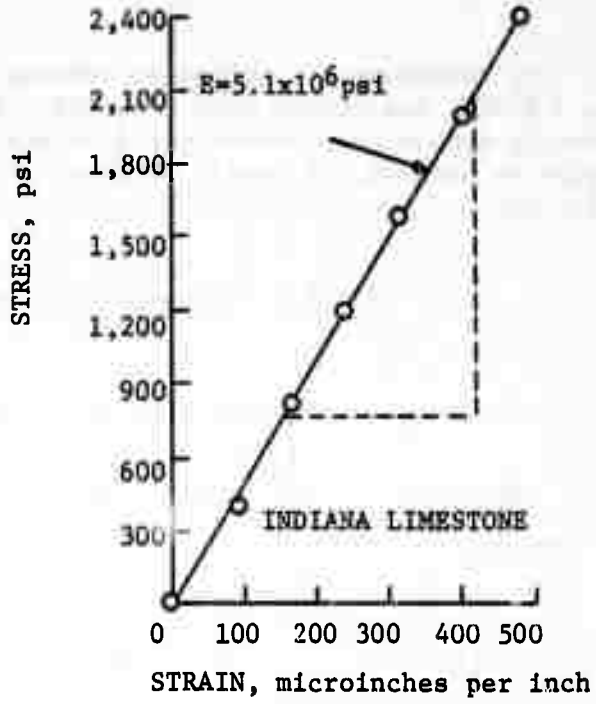

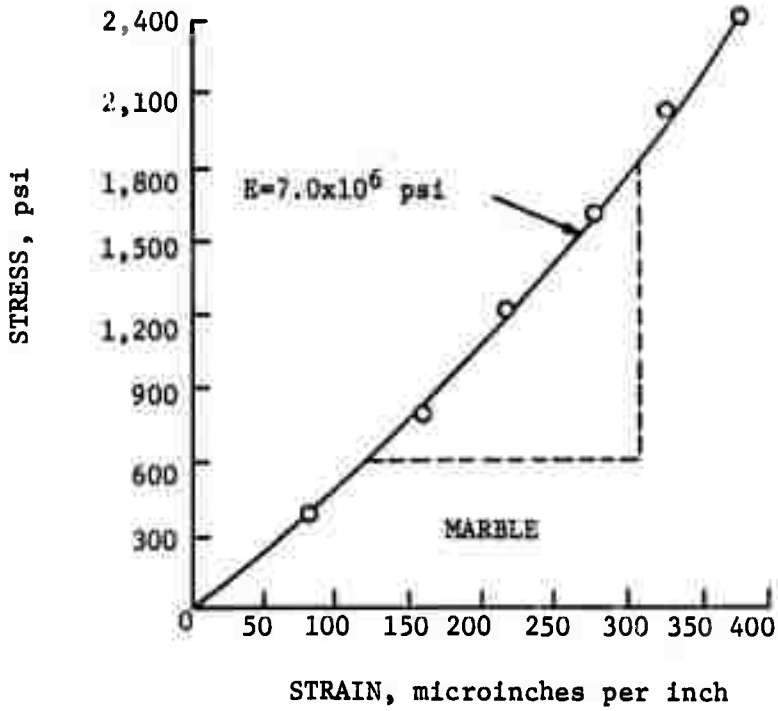

FIGURE 4 - Stress-Strain Curves for Hydrostone, Indiana Limestone, and Georgia Marble

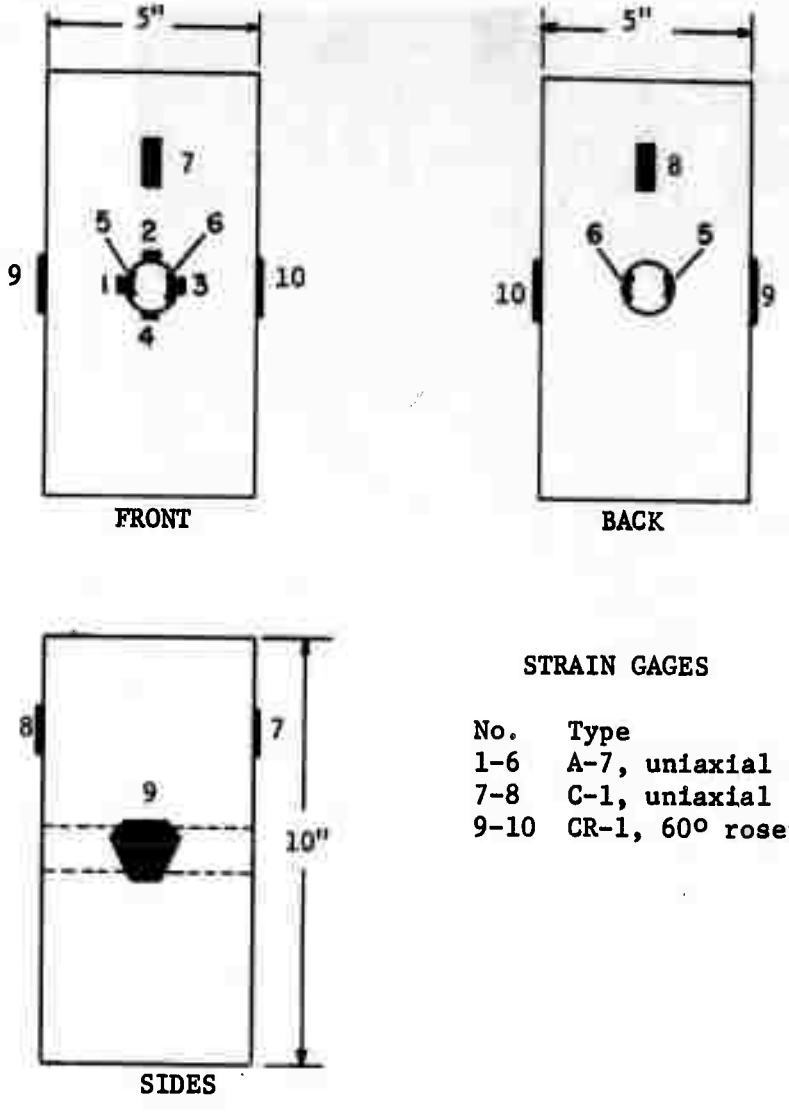

STRAIN GAGES

No.	Type
1-6	A-7, uniaxial
7-8	C-1, uniaxial
9-10	CR-1, 60° rosette

FIGURE 5 - Model Showing Position of Strain Gages.

The borehole deformations were measured with a precision air gage, which has a sensitivity of 10 microinches over a range of 0.003 inch (see fig. 7). This type of gage offers no resistance to the borehole deformation (1).

To determine if the load applied to the model was uniform over the cross section of the model, several resistance-type strain gages were bonded to the exterior surfaces of the model and in the borehole (see fig. 5). The gages were connected to a strain-gage bridge through a strain-gage switching and balancing unit (see fig. 6). The estimated accuracy of the strain measurements was 10 microinches per inch.

To obtain an estimate of the bearing strength of the models, one model of each material was loaded to failure or to the limit of the compression machine. The limestone and marble models did not fail at the maximum load (4,800 pounds per square inch) that could be applied, whereas the hydrostone model failed at an applied compressive stress of 1,600 pounds per square inch. No further use was made of these models. The second model of each material was used for the tests of deformation versus applied stress. The maximum stress applied to these models was limited to one-half the stress applied to the first model, 800 pounds per square inch for hydrostone and 2,400 pounds per square inch for limestone and marble.

The hydrostone model was longitudinally loaded (vertically) in increments of 80 pounds per square inch up to the maximum load (800 pounds per square inch) and was unloaded in the same increments to 0 pounds per square inch. Borehole diameters and strains were measured at each increment of increasing or decreasing stress. These tests were made for air-gage orientations of 0, 30, 45, 60, 90, 120, 135, and 150 degrees (from the horizontal). These angles are denoted as $\phi = 0$, $\phi = 30$, and so forth (see figs. 8-14). Next, the model was loaded laterally (on its side) over the same load range,

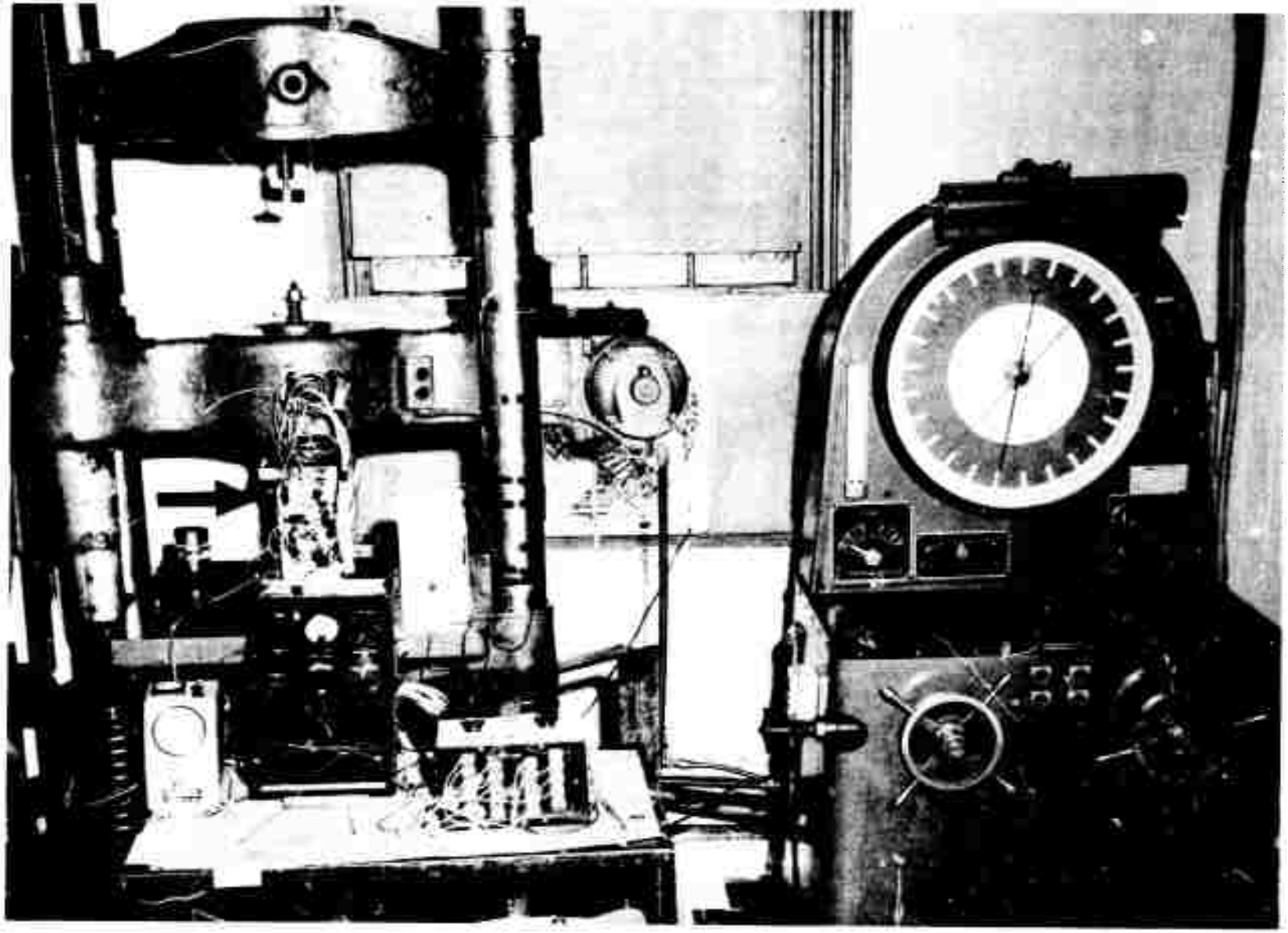

FIGURE 6. - Apparatus Used for Uniaxial Tests. (Arrow points to specimen under examination.)

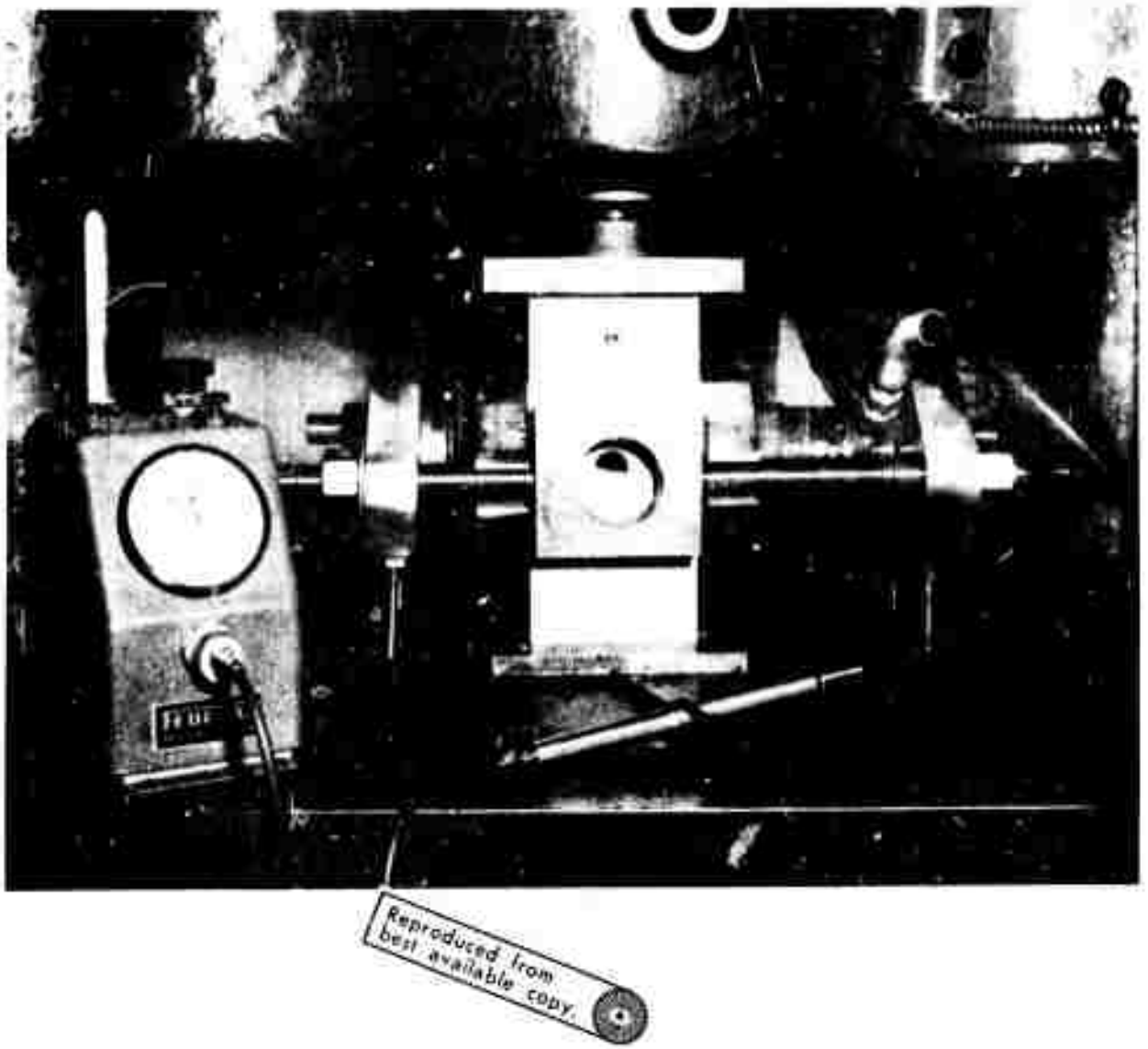

FIGURE 7 - Apparatus Used for Biaxial Tests

in the same increments, and for air-gage orientations of 0 and 90 degrees. Strain gages 9 and 10 were removed for these tests (see fig. 5). For the biaxial tests the models were longitudinally loaded in the same increments as used in the uniaxial tests and were at a constant lateral load (side stress) of 6,000 pounds, that is, 240 pounds per square inch.

The same procedure was used on the limestone and marble models except that the longitudinal stresses were applied in increments of 400 pounds per square inch up to the maximum load (2,400 pounds per square inch), and the lateral stress was 1,000 pounds per square inch.

The data from the uniaxial and biaxial tests on hydrostone models were averaged and are presented by graph in figures 8 and 9; data from limestone and marble models are presented in figures 10 to 13. Usually, the borehole-deformation measurements were reproducible within ± 2.5 percent. Samples of the data taken over a complete cycle from a uniaxial test for each of the models are presented by graph in figure 14 to demonstrate this reproducibility.

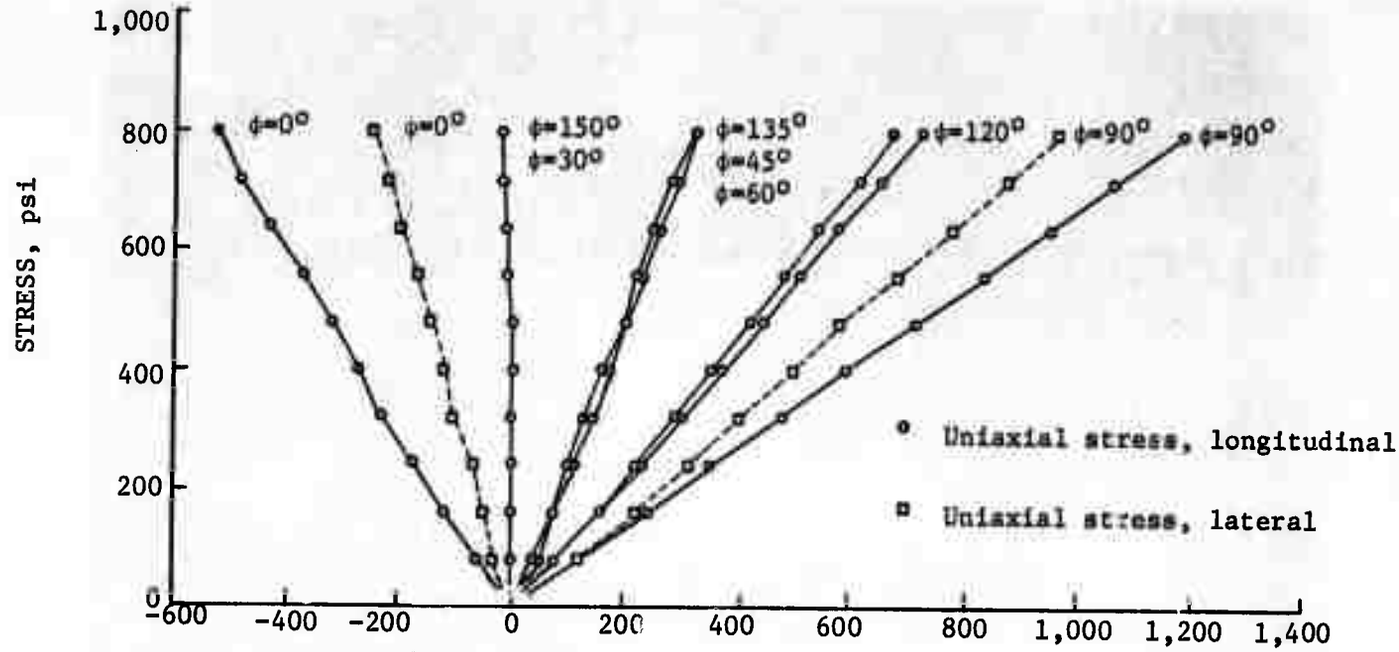

FIGURE 8 Hydrostone-Deformation Versus Uniaxial Stress

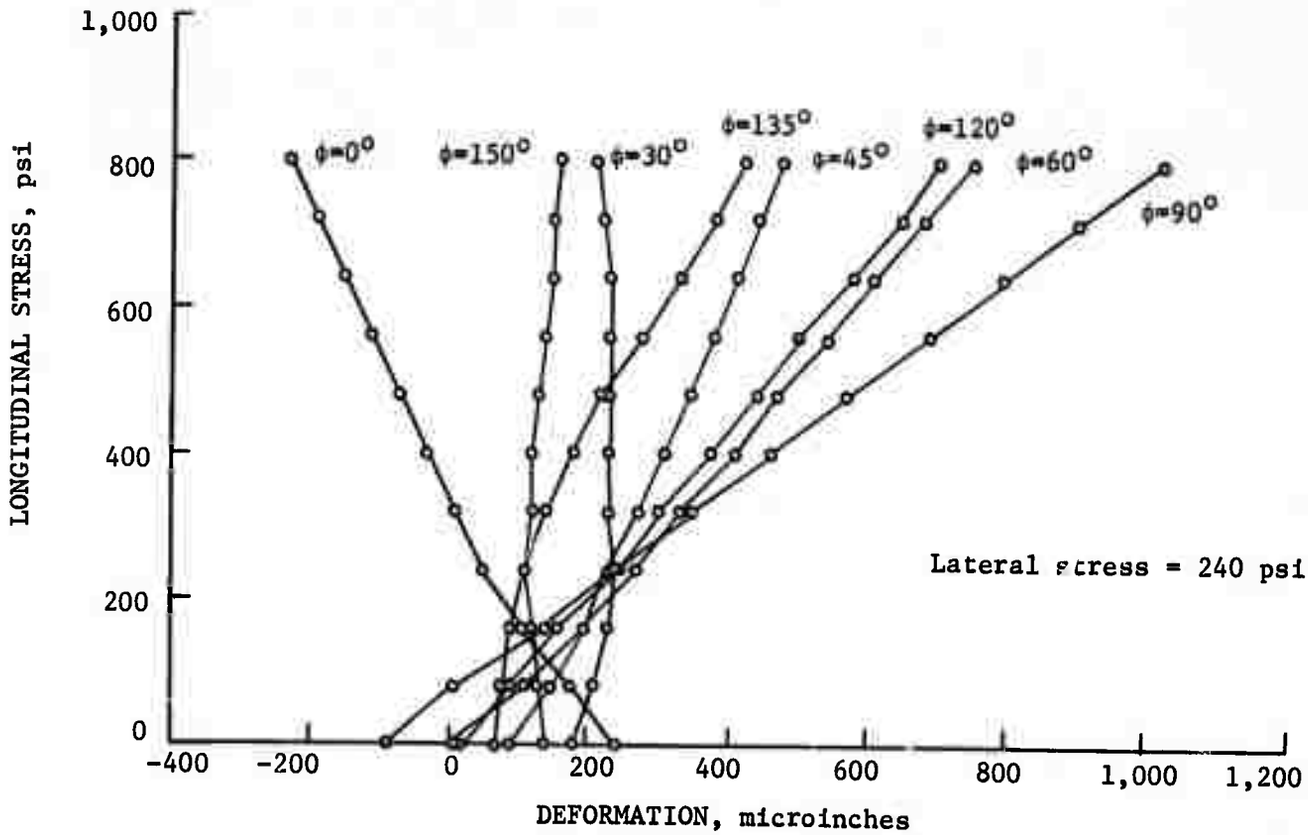

FIGURE 9 Hydrostone-Deformation Versus Biaxial Stress

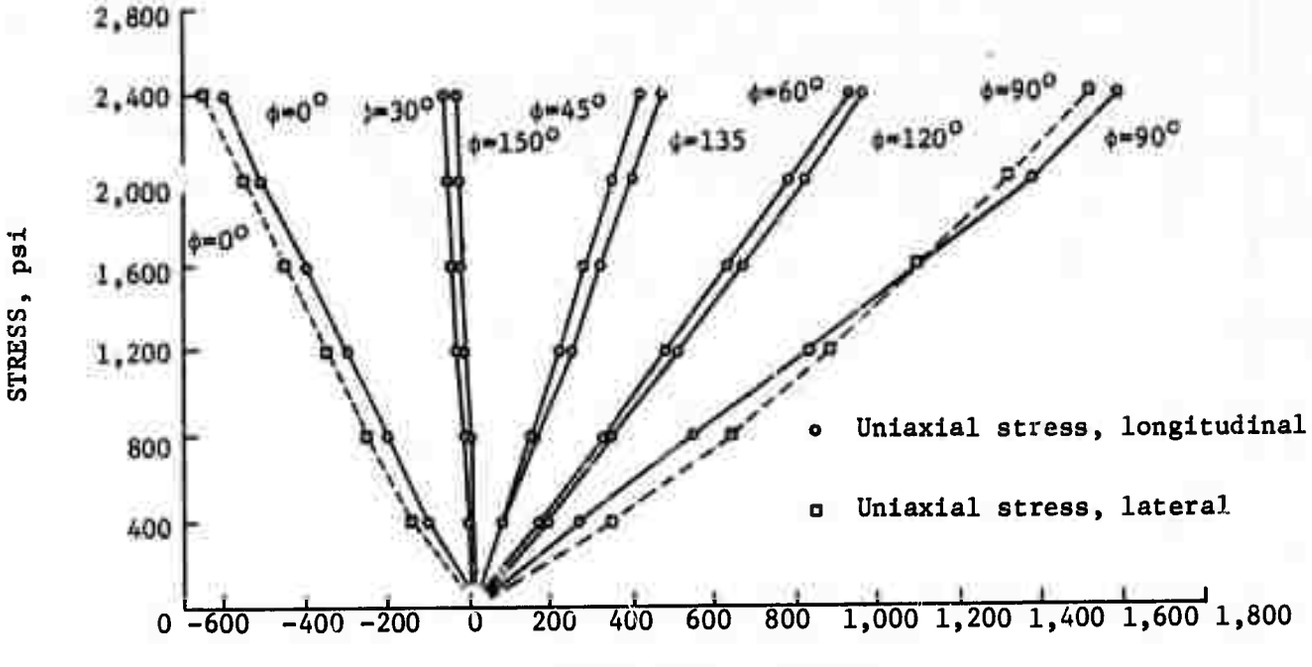

FIGURE 10 - Limestone-Deformation Versus Uniaxial Stress

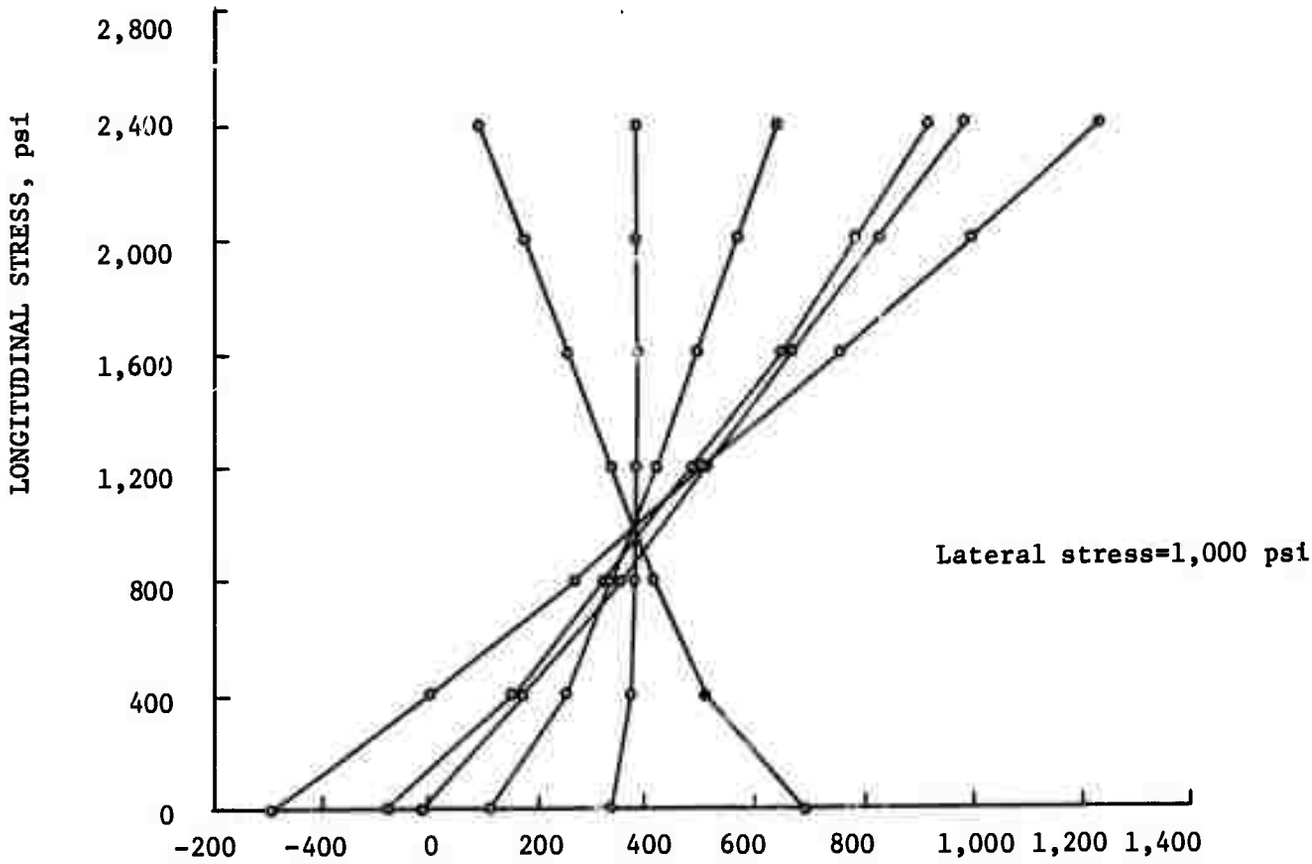

FIGURE 11 - Limestone-Deformation Versus Biaxial Stress

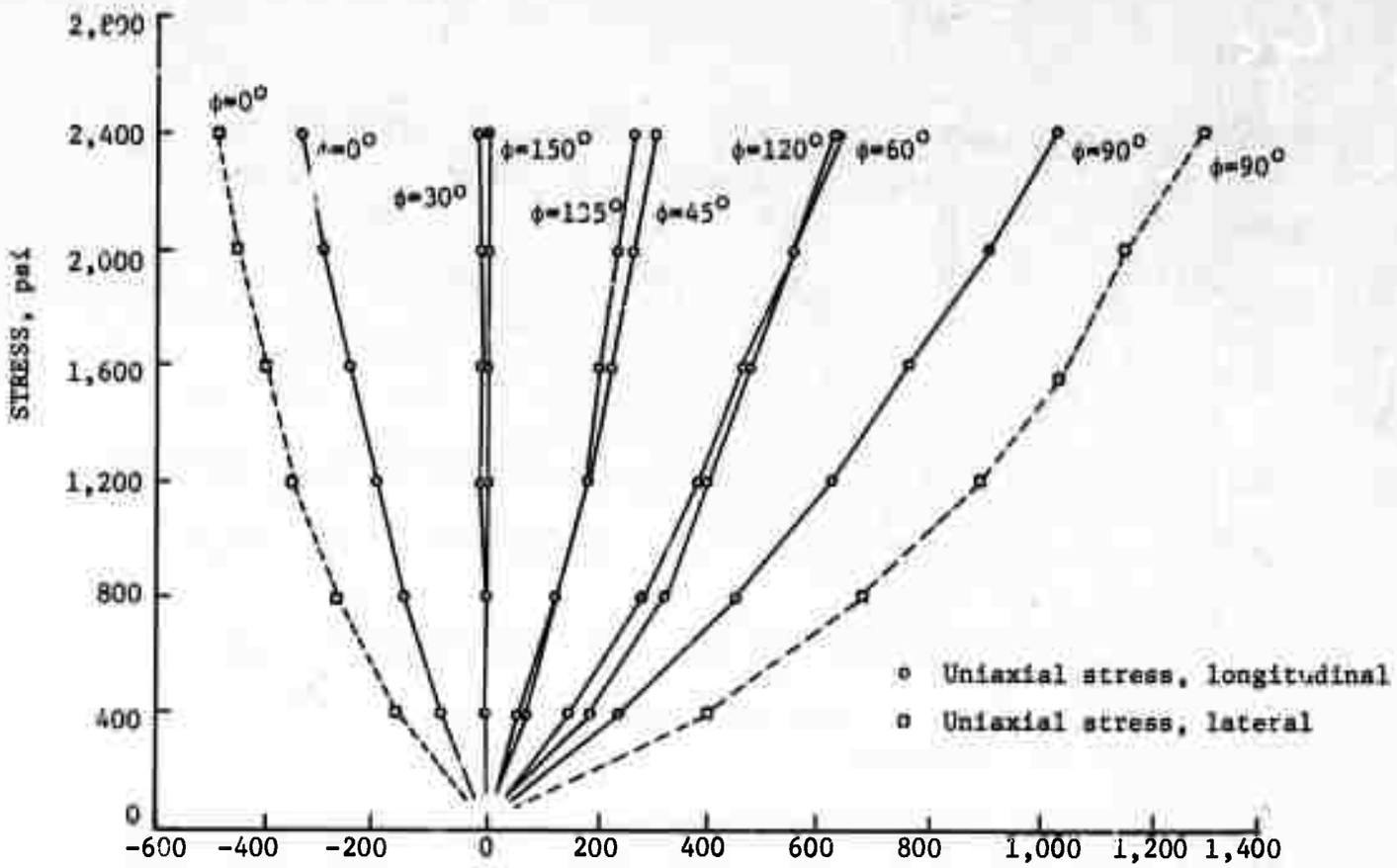

FIGURE 12 - Marble-Deformation Versus Uniaxial Stress

The strain-gage measurements taken from opposite surfaces of the model and borehole showed that in all cases the model was loaded uniformly. Representative samples of these data are given in table 2.

TABLE 2 - Samples of data showing symmetry of stress distribution in the model

Model	Gage No.	Gage position	Maximum applied stress (p.s.i.)	Strain (μ in./in.)
Hydrostone	5	Inside hole (left)	800	900
Do	6	Inside hole (right)	800	905
Limestone	7	Front	2,400	400
Do	8	Back	2,400	420
Marble	9	Side (left)[1]	2,400	342
Do	10	Side (right)[1]	2,400	359

[1]Vertical component of rosette gage.

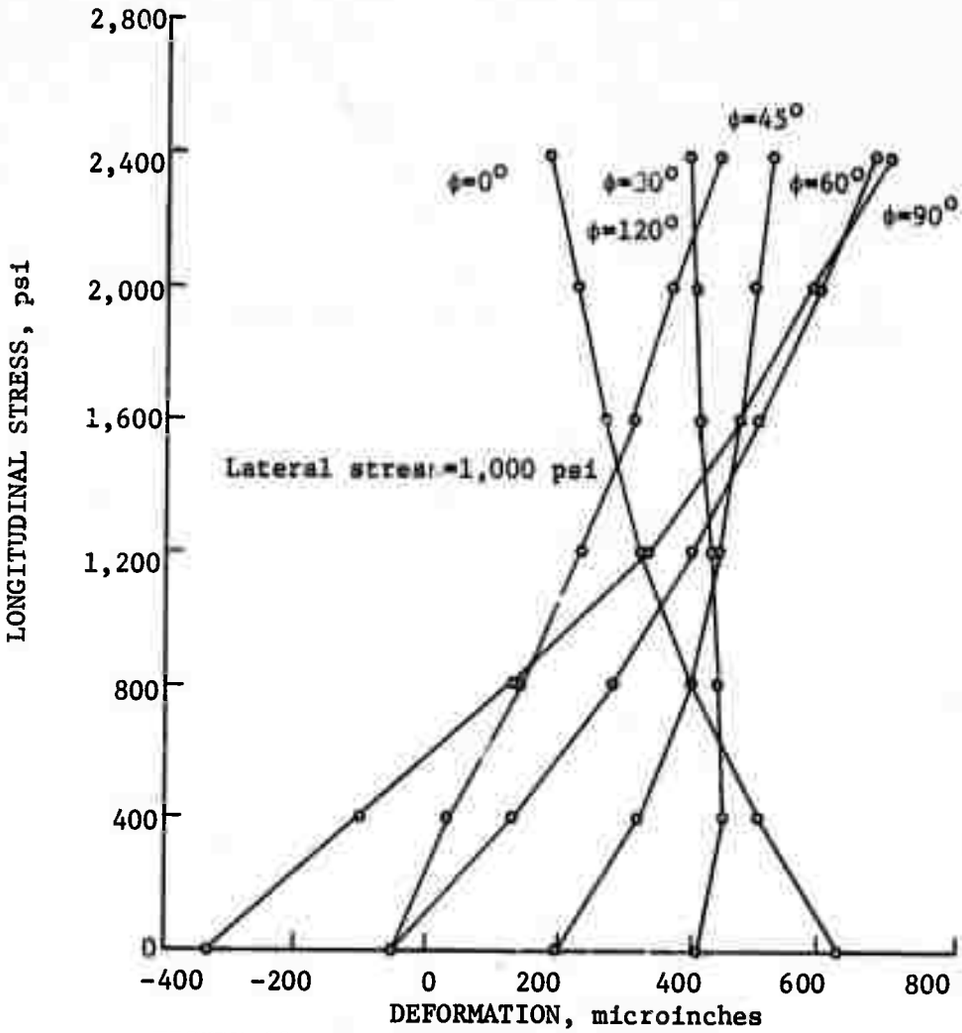

FIGURE 13 - Marble-Deformation Versus Biaxial Stress

RESULTS AND CONCLUSIONS

The data in figure 14 show that for the three model materials, the loading and unloading curves were essentially the same and that when the stress was removed, the deformation returned to zero. Therefore, it can be concluded that the models were not loaded past the elastic limit.

The stress-deformation plots for hydrostone and limestone shown in figures 8 through 13 were linear, whereas the plots for marble were curved (with an increasing slope). This finding is in agreement with the stress-strain measurements made in the physical property tests (see fig. 4).

The deformation measurements at 0 and 90 degrees (with respect to the horizontal) made on the hydrostone and marble models (loaded first longitudinally and then laterally; see figs. 8 and 12) indicate that these materials are anisotropic. The largest percentage difference in deformation was measured for hydrostone at a gage orientation of 0 degrees and at applied stresses greater than 200 pounds per square inch. Also, in the physical property tests on hydrostone, the modulus of elasticity in the longitudinal direction was 18 percent greater than in the lateral direction (see table 1). For marble, the modulus in the lateral direction was 14 percent greater than in the longitudinal direction. Hence, physical property tests also show these materials to be anisotropic. Both the models and the physical property tests on limestone showed this rock to be essentially isotropic (see table 1 and fig. 10).

The agreement between the deformation calculated from theory (equations 1 through 10) and the deformation measured in the models is shown graphically as a function of the

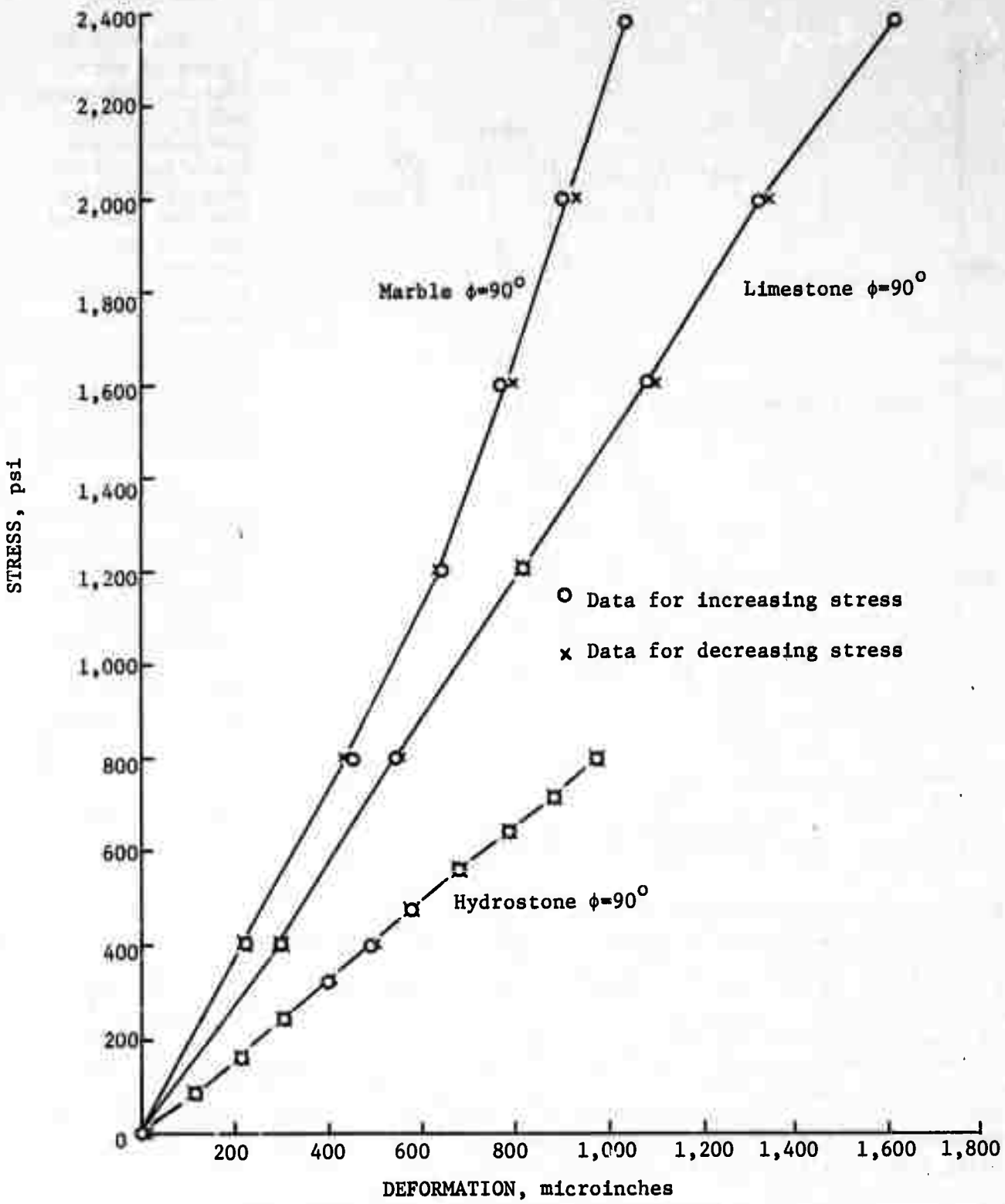

FIGURE 14 - Representative Data for Deformation Versus Uniaxial Stress for Hydrostone, Limestone, and Marble.

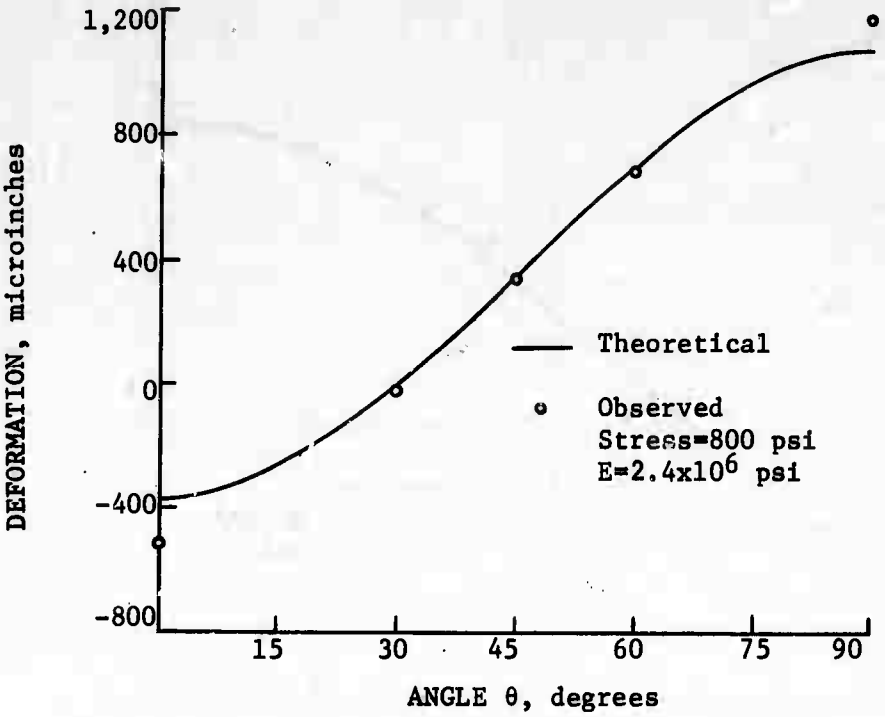

FIGURE 15 - Hydrostone-Deformation Versus Angle, Uniaxial Stress

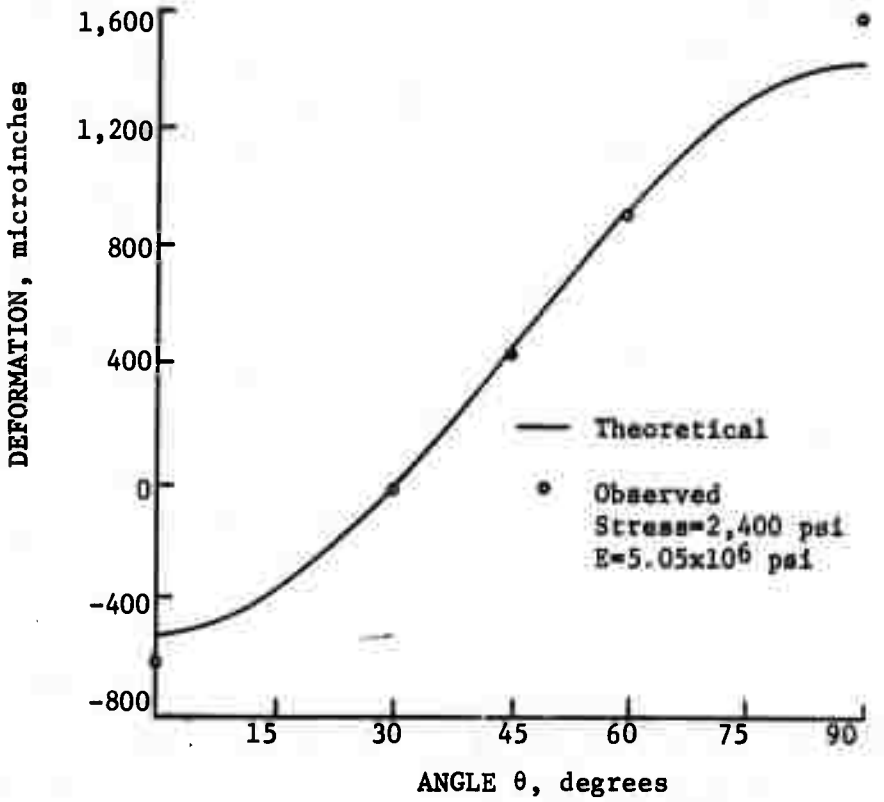

FIGURE 16 - Limestone-Deformation Versus Angle, Uniaxial Stress

angle in figures 15 through 20. These comparisons are presented for both an applied uniaxial and biaxial stress. The measured deformations plotted in these graphs are from data taken at the maximum stress applied to the models. To obtain the calculated value, the horizontal and vertical moduli of elasticity presented in table 1 were averaged and substituted in equations (1) and (7). The modulus of elasticity of the materials can also be computed by substituting the applied stress and measured deformation into equations (1) or (7) and solving for E. These moduli are (uniaxial loading, gage orientation of 90 degrees) 2.2 x 10^6 pounds per square inch for hydrostone, 5.0 x 10^6 for limestone, and 7.7 x 10^6 for marble. The moduli are within 10 percent of those determined from the physical property tests (see table 1).

For longitudinal loading and for a uniaxial stress, the agreement between measured and calculated deformation was best for angles between 30 and 60 degrees, and was poorest for angles of 0 or 90 degrees (see figs. 15-17). In particular, the best agreement for all gage orientations was for marble, and the poorest for materials was for hydrostone at a gage orientation of 0 degrees.

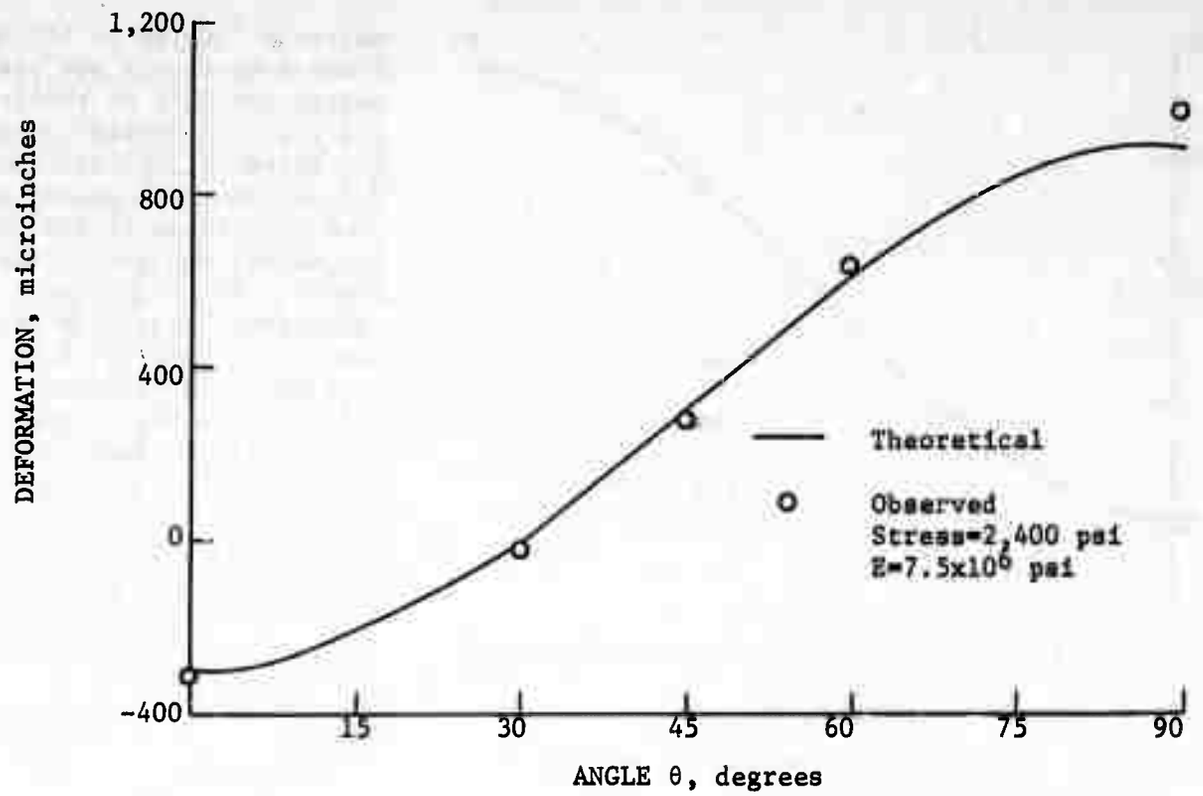

FIGURE 17 - Marble-Deformation Versus Angle, Uniaxial Stress

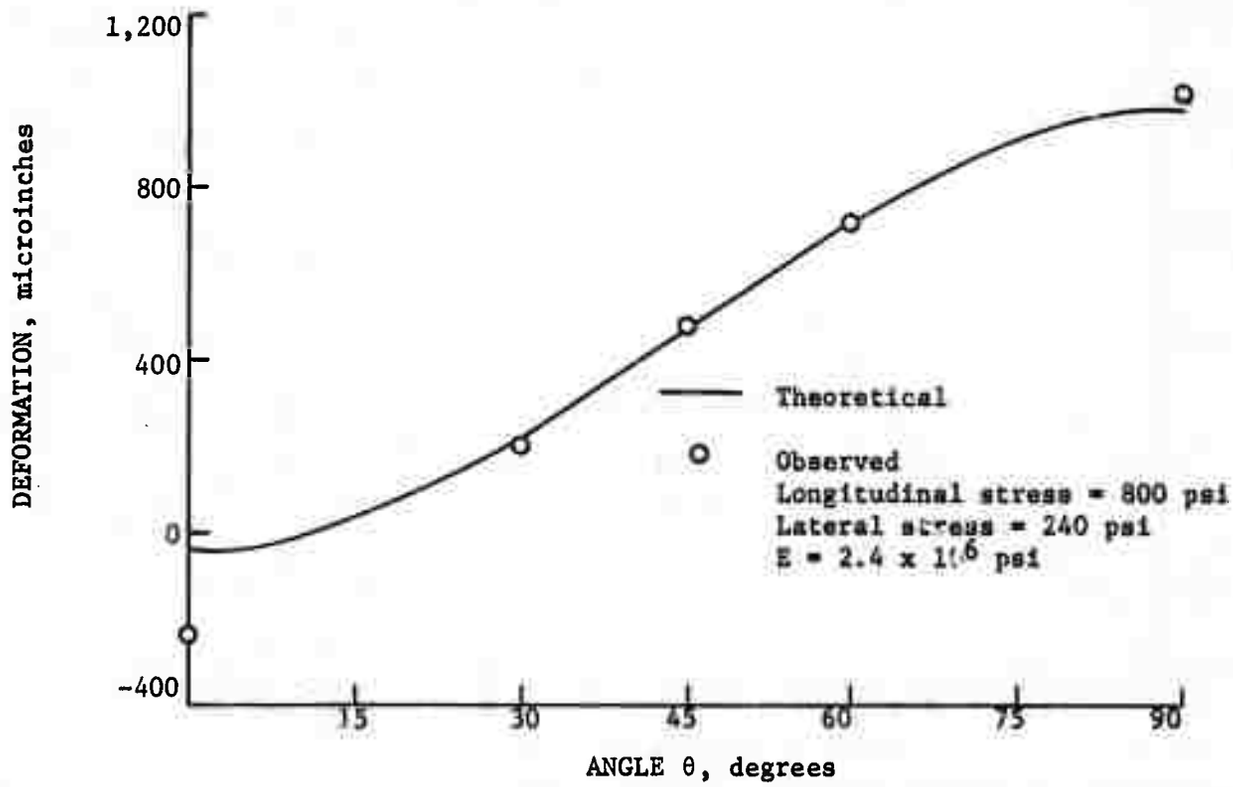

FIGURE 18 - Hydrostone-Deformation Versus Angle, Biaxial Stress

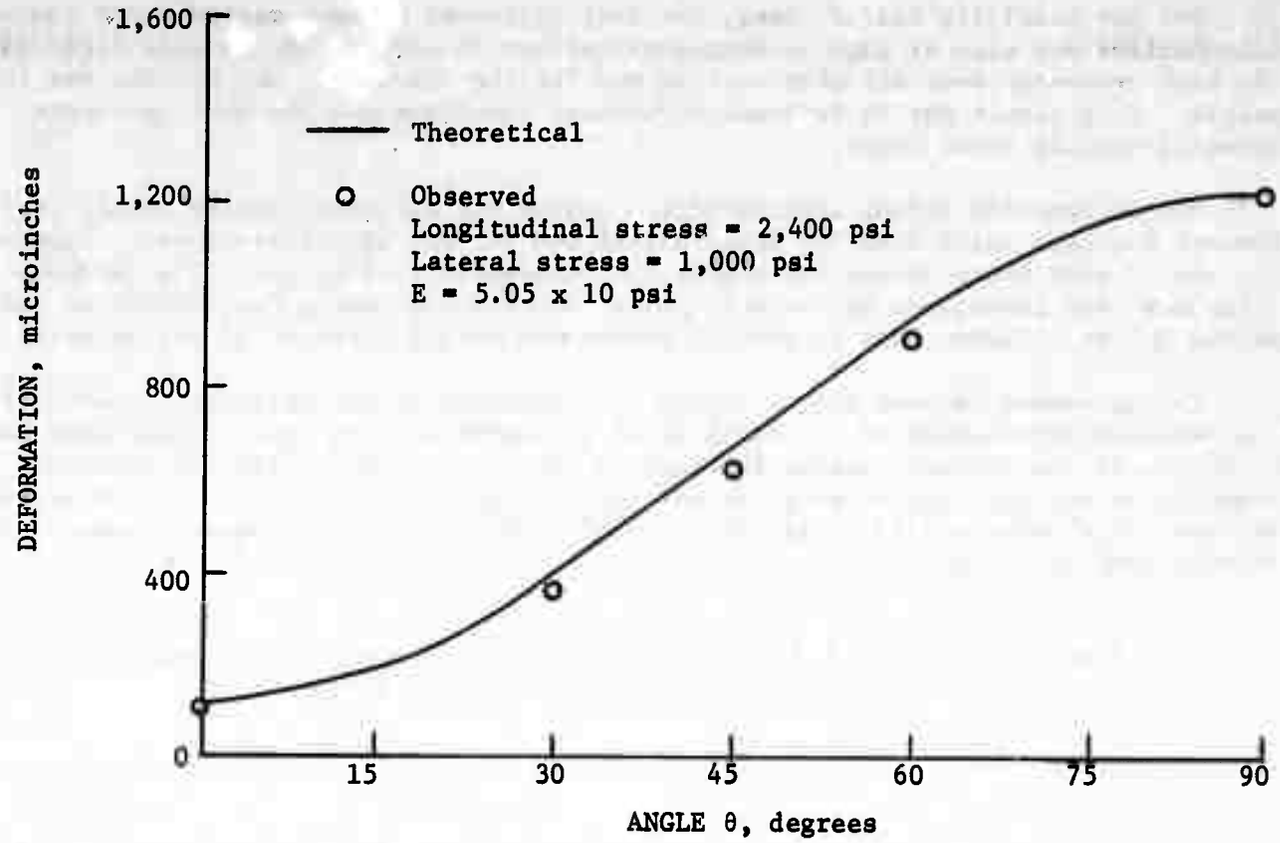

FIGURE 19 - Limestone-Deformation Versus Angle, Biaxial Stress

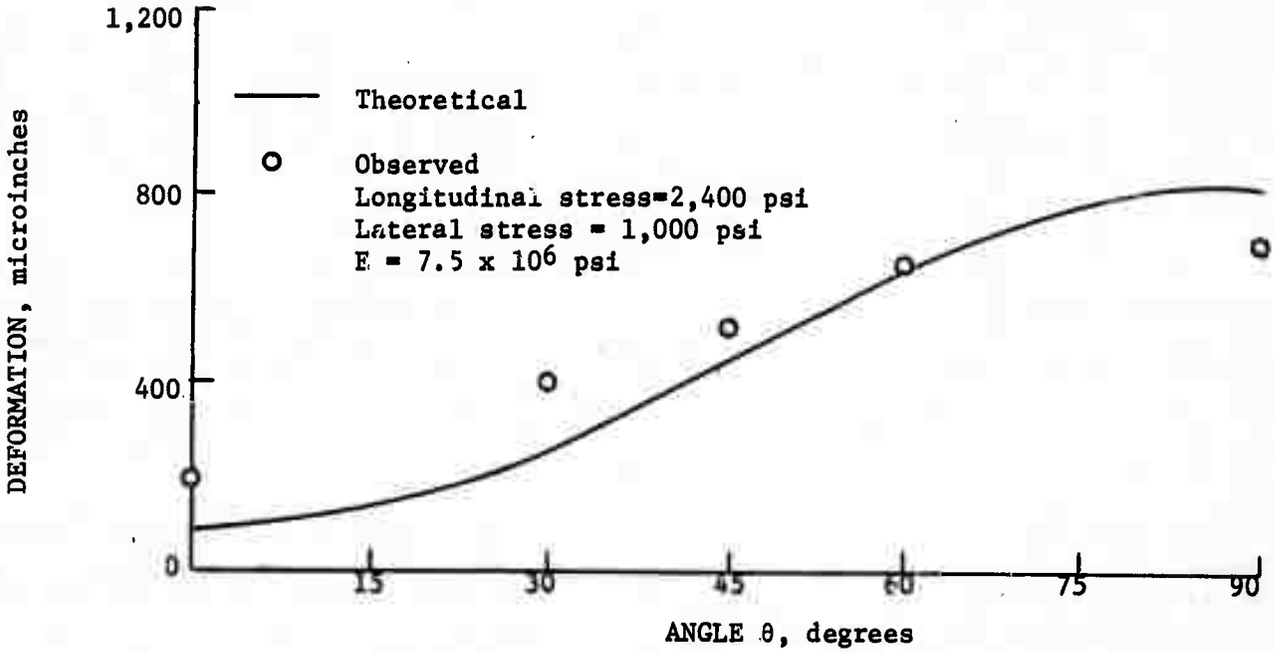

FIGURE 20 - Marble-Deformation Versus Angle, Biaxial Stress

For the biaxially loaded cases, the best agreement between measured and computed deformations was also at gage orientations between 30 and 60 degrees (see figs. 18-20). The best agreement over all orientations was for the limestone; the poorest was for marble. This result was to be expected because limestone was the most isotropic material used in these tests.

The deformation versus applied-stress curves for different angles should pass through a common point when the longitudinal and lateral stress are equal. Figures 9, 11, and 13 show these curves for hydrostone, limestone, and marble. The curves for limestone pass through an approximate point, whereas the curves for hydrostone and marble do not. Again, this is another indication of the isotropy of the material.

The agreement between the magnitude and direction of the stresses computed from the measured deformation of the borehole in the model and the applied magnitude and direction of the applied biaxial stresses is shown in table 3. The deformations measured at maximum applied longitudinal stress (see figs. 9, 11, and 13) were substituted into equations (13) and (16) through (20) to calculate these stresses. The calculations are presented in appendix II.

TABLE 3 - Comparison of the magnitude and direction of the computed stresses and the applied biaxial stress

Rock type	Rosette	Longitudinal stress (p.s.i.)		Lateral stress (p.s.i.)		Angle α (degrees)[1]	
		Calculated	Applied	Calculated	Applied	Calculated	Applied
Hydrostone	45-degree	808	800	177	240	-89	$\pm$90
Do	60-degree	817	800	203	240	91	90
Limestone	45-degree	2,340	2,400	920	1,000	88	90
Do	60-degree	2,355	2,400	935	1,000	88	90
Marble	45-degree	2,200	2,400	1,180	1,000	99	90
Do	60-degree	2,215	2,400	1,125	1,000	-76	90

[1]The definition of the angle α is given in appendix II.

The best agreement between the calculated stresses and the applied stresses was for limestone, using the 60-degree-rosette equations. The poorest agreement was for marble and hydrostone, using the 45-degree-rosette equations. The best agreement between the direction of the larger computed and applied stresses (longitudinal) was for limestone and hydrostone; the poorest agreement was for marble. Again, it was concluded that the difference between the magnitude and direction of the computed and applied stresses was due to the anisotropy of the hydrostone and marble.

In this report all calculations were made on the basis of plane stress, owing to the conditions imposed by the test. In application, when the purpose is to measure the stress in rock media, particularly at depth, calculations made in plane strain may fit the test conditions better than plane stress, a factor that should be considered in further experiments. However, the difference between the magnitude of stresses computed on the basis of plane strain or plane stress would not exceed 10 percent for most rocks.

BIBLIOGRAPHY

1. BEHAR, M. F. The Handbook of Measurement and Control. The Instruments Publishing Company, Inc., Pittsburgh, Pa., 1951, pp. 41, 237.

2. GOODIER, J. N. Concentration of Stress Around Spheroidal and Cylindrical Inclusion and Flaws. Trans. ASME, 55 A-39, 1933, pp. 39-44.

3. HAST, NILS. Bertrycksmatningar I Gruvor-Del I (The Measurement of Rock Pressure in Mines, Part I, The Method), Foredrag, Den 25 Mag. 1957, pp. 1-27.

4. ISAACSON, E. DE ST. Q., Rock Pressure in Mines. Mining Publications, Ltd., Salisbury House, London, 1958, pp. 209.

5. MURRAY, M. M., AND STEIN, P. K. Strain Gage Techniques. University of California at Los Angeles, Los Angeles, Calif., 1959, pp. 587-645.

6. TIMOSHENKO, S. Theory of Elasticity. McGraw Hill Book Co., Inc., New York, N. Y., 1934, pp. 1-134.

APPENDIX I[8]

The equations for the deformation of holes in an infinite plate that is perfectly elastic, homogeneous, and isotropic are presented in part A of this appendix. The cases for uniaxial and biaxial stress fields in plane stress and plane strain are considered.

The equations relating the principal stresses in a medium to the deformation of a hole as measured along three diameters 45 or 60 degrees apart are derived in part B of this appendix. These equations are called the 45- and 60-degree-deformation-rosette equations.

The symbols used in part A are as follows (see fig. 1):

e_r = radial strain

e_θ = tangential strain

$\lambda_{r\theta}$ = shearing strain

σ_r = radial stress

σ_θ = tangential stress

$\tau_{r\theta}$ = shearing stress

θ = angle measured counterclockwise from S to r

u = radial displacement

v = tangential displacement

E = Young's modulus

ν = Poisson's ratio

a = radius of hole

d = diameter of hole

r = radial distance

S, T = perpendicularly applied stresses

U = deformation (change in length of a diameter) of the hole

---

[8]Wilbur I. Duvall, physicist, Applied Physics Research Laboratory Bureau of Mines, College Park, Md. has derived a part of the equations presented in this appendix.

Part A, Case 1 - Deformation of a hole in a plate subjected to a unidirectional stress field under the condition of plane stress

To obtain the deformation of a hole in a plate under plane stress, the Kirsch equations (6) for the stress distributions around a hole are substituted in Hooke's law equations for plane stress and integrated.

The relationships for the strain components and displacements in polar coordinates are

$$e_r = \frac{\delta u}{\delta r} , \tag{1}$$

and

$$e_\theta = \frac{u}{r} + \frac{\delta v}{r\delta\theta} , \tag{2}$$

$$\lambda_{r\theta} = \frac{\delta u}{r\delta\theta} + \frac{\delta v}{\delta r} - \frac{v}{r} . \tag{3}$$

Hooke's law equations for plane stress are

$$e_r = \frac{1}{E} (\sigma_r - \nu\sigma_\theta), \tag{4}$$

$$e_\theta = \frac{1}{E} (\sigma_\theta - \nu\sigma_r), \tag{5}$$

and

$$\lambda_{r\theta} = \frac{2(1+\nu)}{E} \tau_{r\theta}. \tag{6}$$

The Kirsch equations for the stress distributions around a circular hole (unidirectional stress field, T = 0) are

$$\sigma_r = \frac{S}{2} (1 - \frac{a^2}{r^2}) + \frac{S}{2} (1 - \frac{4a^2}{r^2} + \frac{3a^4}{r^4}) \cos 2\theta, \tag{7}$$

$$\sigma_\theta = \frac{S}{2} (1 + \frac{a^2}{r^2}) - \frac{S}{2} (1 + \frac{3a^4}{r^4}) \cos 2\theta, \tag{8}$$

and

$$\tau_{r\theta} = - \frac{S}{2} (1 + \frac{2a^2}{r^2} - \frac{3a^4}{r^4}) \sin 2\theta. \tag{9}$$

Combining equations (1) and (4), (2) and (5), (3) and (6) yields

$$\frac{\delta u}{\delta r} = \frac{1}{E} (\sigma_r - \nu\sigma_\theta), \tag{10}$$

$$\frac{u}{r} + \frac{\delta v}{r\delta\theta} = \frac{1}{E} (\sigma_\theta - \nu\sigma_r), \tag{11}$$

and

$$\frac{\delta u}{r\delta\theta} + \frac{\delta v}{\delta r} - \frac{v}{r} = \frac{2(1+\nu)}{E} \tau_{r\theta}. \tag{12}$$

Substituting equations (7) and (8) into (10) gives

$$\frac{\delta u}{\delta r} = \frac{1}{E} \left[\frac{S}{2} \left(1-\frac{a^2}{r^2}\right) + \frac{S}{2} \left(1-\frac{4a^2}{r^2} + \frac{3a^4}{r^4}\right) \cos 2\theta\right]$$

$$- \frac{\nu}{E} \left[\frac{S}{2} \left(1 + \frac{a^2}{r^2}\right) - \frac{S}{2} \left(1 + \frac{3a^4}{r^4}\right) \cos 2\theta\right]. \tag{13}$$

Integrating equation 13 gives

$$u = \frac{1}{E} \left[\frac{S}{2} \left(r + \frac{a^2}{r}\right) + \frac{S}{2} \left(r + \frac{4a^2}{r} - \frac{a^4}{r^3}\right) \cos 2\theta\right]$$

$$- \frac{\nu}{E} \left[\frac{S}{2} \left(r - \frac{a^2}{r}\right) - \frac{S}{2} \left(r - \frac{a^4}{r^3}\right) \cos 2\theta\right] + g_1 (\theta), \tag{14}$$

where $g_1 (\theta)$ is an arbitrary function of θ only.

Substituting equations (7), (8), and (14) into equation (11) and combining terms gives

$$\frac{\delta v}{\delta\theta} = \frac{1}{E} \left[- \frac{S}{2} \left(2r + \frac{4a^2}{r} + \frac{2a^4}{r^3}\right) \cos 2\theta \right]$$

$$- \frac{\nu}{E} \left[\frac{S}{2} \left(2r - \frac{4a^2}{r} + \frac{2a^4}{r^3}\right) \cos 2\theta \right] - g_1 (\theta). \tag{15}$$

Integrating equation (15) gives

$$v = \frac{1}{E}\left[- \frac{S}{2}\left(r + \frac{2a^2}{r} + \frac{a^4}{r^3}\right) \sin 2\theta \right]$$

$$- \frac{\nu}{E}\left[\frac{S}{2}\left(r - \frac{2a^2}{r} + \frac{a^4}{r^3}\right) \sin 2\theta \right] - \int g_1(\theta)\, d\theta + g_2(r) \qquad (15)$$

where $g_2(r)$ is a function of r only.

Differentiating equation (14) with respect to θ, gives

$$\frac{\delta u}{\delta \theta} = \frac{1}{E}\left[- S\left(r + \frac{4a^2}{r} - \frac{a^4}{r^3}\right) \sin 2\theta \right] - \frac{\nu S}{E}\left(r - \frac{a^4}{r^3}\right) \sin 2\theta + \frac{\delta g_1(\theta)}{\delta \theta} . \qquad (17)$$

Differentiating equation (16) with respect to r gives

$$\frac{\delta v}{\delta r} = \frac{1}{E}\left[- \frac{S}{2}\left(1 - \frac{2a^2}{r^2} - \frac{3a^4}{r^4}\right) \sin 2\theta\right]$$

$$- \frac{\nu}{E}\left[\frac{S}{2}\left(1 + \frac{2a^2}{r^2} - \frac{3a^4}{r^4}\right) \sin 2\theta \right] + \frac{\delta g_2(r)}{\delta r} . \qquad (18)$$

Substituting equations (9), (16), (17), and (18) into equation (12) and collecting terms gives

$$\frac{\delta g_1(\theta)}{\delta \theta} + \frac{r \delta g_2(r)}{\delta r} + \int g_1(\theta)\, d\theta - g_2(r) = 0. \qquad (19)$$

Since $g_1(\theta)$ is a function of θ only, and $g_2(r)$ is a function of r only, the terms containing θ and the terms containing r must be equal to zero; thus

$$\frac{r\, dg_2(r)}{dr} - g_2(r) = 0, \qquad (20)$$

$$\frac{d^2 g_1(\theta)}{d\theta^2} + g_1(\theta) = 0, \qquad (21)$$

where total derivatives are used because g_2 is a function of r only, and g_1 is a function of θ only. Integrating equation (20) gives

$$g_2(r) = Cr. \tag{22}$$

Integrating equation (21) gives

$$g_1(\theta) = A \sin \theta + B \cos \theta. \tag{23}$$

As there can be no tangential displacements on either the x or y axis, the boundary conditions are

$v = 0$ when $\theta = 0$ for all values of r;

$v = 0$ when $\theta = \frac{\pi}{2}$ for all values of r.

Substituting equations (22) and (23) and the boundary condition into equation (16) gives

$$A = 0, \; B = 0, \; C = 0.$$

Because the constants in equations (22) and (23) are zero, the arbitrary functions $g_1(\theta)$ and $g_2(r)$ are zero; thus, the displacements u and v, from equations (14) and (16), are

$$u = \frac{1}{E}\left[\frac{S}{2}\left(r + \frac{a^2}{r}\right) + \frac{S}{2}\left(r + \frac{4a^2}{r} - \frac{a^4}{r^3}\right)\cos 2\theta\right]$$

$$- \frac{\nu}{E}\left[\frac{S}{2}\left(r - \frac{a^2}{r}\right) - \frac{S}{2}\left(r - \frac{a^4}{r^3}\right)\cos 2\theta\right], \tag{24}$$

and

$$v = -\frac{1}{E}\left[\frac{S}{2}\left(r + \frac{2a^2}{r} + \frac{a^4}{r^3}\right)\sin 2\theta\right] - \frac{\nu}{E}\left[\frac{S}{2}\left(r - \frac{2a^2}{r} + \frac{a^4}{r^3}\right)\sin 2\theta\right]. \tag{25}$$

Equation (24) and (25) describe radial and tangential displacements anywhere in the medium. To obtain the change in any diameter, U, of the hole (deformation), substitute $r = a = \frac{d}{2}$ into equation (24); thus

$$U = \frac{Sd}{E}(1 + 2\cos 2\theta). \tag{26}$$

Part A, Case 2 - Deformation of a hole in a plate subjected to a unidirectional stress under the condition of plane strain

To obtain the deformation of a hole in a plate in plane strain the Kirsch equations (equations (7), (8), and (9) are substituted in the Hooke's law equations for plane strain which are

$$e_r = \frac{1}{E} [(1 - \nu^2) \sigma_r - \nu (1 + \nu) \sigma_\theta], \tag{27}$$

$$e_\theta = \frac{1}{E} [(1 - \nu^2) \sigma_\theta - \nu (1 + \nu) \sigma_r], \tag{28}$$

and

$$\lambda_{r\theta} = \frac{2 (1 + \nu)}{E} \tau_{r\theta}. \tag{29}$$

Equations (1), (2), (3), (7), (8), and (9) are valid under conditions of both plane stress or plane strain. Hooke's law equations for plane strain differ from the plane stress equations only by the terms $(1 - \nu^2)$ and $(1 + \nu)$. Therefore, the method of solution and the boundary conditions are valid for both cases, and the radial and tangential displacements anywhere in the medium are

$$u = \frac{1 - \nu^2}{E} [\frac{S}{2} (r + \frac{a^2}{r}) + \frac{S}{2} (r + \frac{4a^2}{r} - \frac{a^4}{r^3}) \cos 2\theta]$$

$$- \frac{\nu (1 + \nu)}{E} [\frac{S}{2} (r - \frac{a^2}{r}) - \frac{S}{2} (r - \frac{a^4}{r^3}) \cos 2\theta], \tag{30}$$

and

$$v = - \frac{1 - \nu^2}{E} [\frac{S}{2} (r + \frac{2a^2}{r} + \frac{a^4}{r^3}) \sin 2\theta]$$

$$- \frac{\nu (1 + \nu)}{E} [\frac{S}{2} (r - \frac{2a^2}{r} + \frac{a^4}{r^3}) \sin 2\theta]. \tag{31}$$

To obtain U, $r = a = \frac{d}{2}$ is substituted into equation (30); thus

$$U = \frac{Sd}{E} (1 - \nu^2) (1 + 2 \cos 2\theta). \tag{32}$$

Part A, Case 3 - Deformation of a hole in a plate subjected to a biaxial stress field and for the condition of plane stress

The equations for the stress distribution around a hole are obtained by superposition, and equations (7), (8), and (9) become

$$\sigma_r = \frac{S+T}{2}\left(1 - \frac{a^2}{r^2}\right) + \frac{S-T}{2}\left(1 - \frac{4a^2}{r^2} + \frac{3a^4}{r^4}\right)\cos 2\theta, \tag{33}$$

$$\sigma_\theta = \frac{S+T}{2}\left(1 + \frac{a^2}{r^2}\right) - \frac{S-T}{2}\left(1 + \frac{3a^4}{r^4}\right)\cos 2\theta, \tag{34}$$

$$\tau_{r\theta} = -\frac{S-T}{2}\left(1 + \frac{2a^2}{r^2} - \frac{3a^4}{r^4}\right)\sin 2\theta. \tag{35}$$

The solution for the displacements is obtained by the same method as used for Case 1; the displacements are

$$u = \frac{1}{E}\left[\frac{S+T}{2}\left(r + \frac{a^2}{r}\right) + \frac{S-T}{2}\left(r + \frac{4a^2}{r} - \frac{a^4}{r^3}\right)\cos 2\theta\right]$$

$$- \frac{\nu}{E}\left[\frac{S+T}{2}\left(r - \frac{a^2}{r}\right) - \frac{S-T}{2}\left(r - \frac{a^4}{r^3}\right)\cos 2\theta\right], \tag{36}$$

and

$$v = -\frac{1}{E}\left[\frac{S-T}{2}\left(r + \frac{2a^2}{r} + \frac{a^4}{r^3}\right)\sin 2\theta\right]$$

$$- \frac{\nu}{E}\left[\frac{S-T}{2}\left(r - \frac{2a^2}{r} + \frac{a^4}{r^3}\right)\sin 2\theta\right]. \tag{37}$$

To obtain the deformation of the hole, $r = a = \frac{d}{2}$ is substituted in equation (36); thus

$$U = \frac{d}{E}\left[(S+T) + 2(S-T)\cos 2\theta\right]. \tag{38}$$

Part A, Case 4 - Deformation of a hole in a plate subjected to biaxial stress and for the conditions for plane strain

The equations for the stress distributions around a hole in a plate subjected to a biaxial stress field, (equations (33), (34), and (35) are substituted in equations (27), (28), and (29). Then, the procedures outlined under Case 1 are followed to obtain

$$U = \frac{(1-\nu^2)\,d}{E}\left[(S+T) + 2(S-T)\cos 2\theta\right]. \tag{39}$$

Part B, Case 1 - The 60-degree-deformation-rosette equations for a biaxial stress field and plane stress

The equations for the deformation of a hole in a plate in biaxial stress fields are used to relate the stresses in the plate to the deformations measured across three diameters of the hole.

The symbols for Part A are the same in Part B; the following symbols are also used (see fig. 3):

U_1 = deformation measured across a diameter in the hole

U_2 = deformation at angle 60 degrees from U_1

U_3 = deformation at angle 120 degrees from U_1

θ_1 = angle measured counterclockwise from S to the direction of U_1

A, B, K = constants

The equation for the deformation of a hole in a plate in a biaxial stress field is (see equation (38))

$$U = \frac{d}{E} [(S + T) + 2 (S - T) \cos 2\theta].$$

If we let $K = \frac{d}{E}$, $A = S + T$, and $B = S - T$, equation (38) becomes

$$U = KA + 2KB \cos 2\theta. \tag{40}$$

To obtain U_1, U_2, and U_3,

$$U_1 = KA + 2KB \cos 2\theta_1, \tag{41}$$

$$U_2 = KA + 2KB \cos 2\theta_2, \tag{42}$$

and

$$U_3 = KA + 2KB \cos 2\theta_3. \tag{43}$$

For a 60-degree rosette, $\theta_2 = \theta_1 + 60^\circ$ and $\theta_3 = \theta_1 + 120^\circ$; equations (41), (42), and (43) become

$$U_1 = KA + 2KB \cos 2\theta_1, \tag{44}$$

$$U_2 = KA + 2KB \cos 2 (\theta_1 + 60^\circ), \tag{45}$$

and

$$U_3 = KA + 2KB \cos 2 (\theta_1 + 120^\circ). \tag{46}$$

The cosine of the sum of the angles in equations (45) and (46) is

$$\cos 2\theta_1 + 120^\circ = - \frac{1}{2} \cos 2\theta_1 - \frac{\sqrt{3}}{2} \sin 2\theta_1 \tag{47}$$

and

$$\cos 2\theta_1 + 240^\circ = - \frac{1}{2} \cos 2\theta_1 + \frac{\sqrt{3}}{2} \sin 2\theta_1. \tag{48}$$

Substituting equations (47) and (48) in equations (45) and (46) and solving for A and B gives

$$A = \frac{U_1 + U_2 + U_3}{3K}$$

and

$$B = \frac{\sqrt{2}}{6K} \left[(U_1 - U_2)^2 + (U_2 - U_3)^2 + (U_1 - U_3)^2 \right]^{1/2}. \quad (50)$$

Substituting equations (47) and (48) in equations (44), (45), and (46) and solving for θ_1 gives

$$\tan 2\theta_1 = - \frac{\sqrt{3} (U_2 - U_3)}{2U_1 - U_2 - U_3} . \quad (51)$$

Because A = S + T and B = S - T, the sum and difference of the stresses are

$$S + T = \frac{E}{3d} (U_1 + U_2 + U_3), \quad (52)$$

and

$$S - T = \frac{\sqrt{2}E}{6d} \left[(U_1 - U_2)^2 + (U_2 - U_3)^2 + (U_1 - U_3)^2 \right]^{1/2}. \quad (53)$$

Hence, the stresses in the medium can be obtained from a measurement of U_1, U_2, and U_3. The angle between the stresses and the angle at which U_1 is measured are obtained from equation (51).

The conditions for plane strain can be obtained by dividing equations (52) and (53) by the term $(1 - \nu^2)$.

Part B, Case 2 - The 45-degree-deformation-rosette equations

The solution for the 45-degree-deformation rosette is obtained by the same steps as were used for the solution of the 60-degree-deformation rosette. The solutions for the sum and difference of the stresses are

$$S + T = \frac{E}{2d} (U_1 + U_3), \quad (54)$$

and

$$S - T = \frac{E}{2\sqrt{2}\, d} \left[(U_1 - U_2)^2 + (U_2 - U_3)^2 \right]^{1/2}, \quad (55)$$

and the tangent of twice the angle between the stress S and the deformation U_1 is

$$\tan 2\theta_1 = - \frac{2U_2 - U_1 - U_3}{U_1 - U_3} . \quad (56)$$

Again, for plane strain, equations (54) and (55) can be used by dividing by the term $(1 - \nu^2)$.

APPENDIX II

Example No. 1 - Hydrostone, 60-degree-deformation rosette:

U_1 = 210 μin.

U_2 = 1,020 μin.

U_3 = 160 μin.

$E = 2.2 \times 10^6$ p.s.i.

d = 1.0 in.

From equation (17)

$$S + T = \frac{2.2 \times 10^6}{3 \times 1.0} \quad (210 + 1{,}020 + 160)\ 10^{-6} = 1{,}020 \text{ p.s.i.}$$

From equation (18)

$$S - T = \frac{\sqrt{2} \times 2.2 \times 10^6}{6 \times 1.0} \left[(810)^2 + (860)^2 + (50)^2 \right]^{1/2} \times 10^{-6} = 614 \text{ p.s.i.}$$

S = 817 p.s.i. (applied stress = 800 p.s.i.)

T = 203 p.s.i. (applied stress = 240 p.s.i.).

The direction of S with respect to U_1 is given by equation 13.

$$\text{Tan } 2\theta_1 = \frac{-\sqrt{3}\ (1{,}020 - 160)}{2 \times 210 - (1{,}020 + 160)} = 1.96$$

$$2\theta_1 = 63^\circ \text{ or } 243^\circ$$

$$\theta_1 = 121^\circ \text{ (see rule for a 60-degree rosette, p.88).}$$

The direction of U_1 was 30° counterclockwise from the horizontal. If α is the angle between S and the horizontal measured counterclockwise from S, then $\alpha = \theta_1 - 30^\circ$; thus

$$\alpha = 121^\circ - 30^\circ = 91^\circ \text{ (angle of applied stress = 90°).}$$

Example No. 2 - Hydrostone, 45-degree-deformation rosette:

U_1 = 475 μin.

U_2 = 1,020 μin.

U_3 = 420 μin.

E = 2.2 x 10^6 p.s.i.

d = 1.0 in.

From equations (19) and (20), respectively,

$$S + T = \frac{2.2 \times 10^6}{2 \times 1.0} \quad (475 + 420)\ 10^{-6} = 985 \text{ p.s.i.}$$

$$S - T = \frac{2.2 \times 10^6}{2 \times \sqrt{2} \times 1.0} \left[(545)^2 + (600)^2 \right]^{1/2} \times 10^{-6} = 630 \text{ p.s.i.}$$

S = 808 p.s.i. (applied stress = 800 p.s.i.)

T = 177 p.s.i. (applied stress = 240 p.s.i.).

The direction of S with respect to U_1 is given by equation (16).

$$\text{Tan } 2\theta_1 = - \frac{2 \times 1{,}020 - (475 + 420)}{(475 - 420)} = - 20.8$$

$$2\theta_1 = - 87^\circ \text{ or } + 93^\circ$$

$$\theta_1 = - 44^\circ \text{ (see rule 1 for a 45-degree rosette, p.88).}$$

The direction of U_1 was 45° counterclockwise from the horizontal. If α is the angle between S and the horizontal measured counterclockwise from S, then $\alpha = \theta_1 - 45^\circ$; thus

$$\alpha = - 44^\circ - 45^\circ = - 89^\circ \text{ (angle of applied stress } = \pm 90^\circ).$$

Example No. 3 - Limestone, 60-degree-deformation rosette:

U_1 = 85 μin.

U_2 = 910 μin.

U_3 = 974 μin.

E = 5.0 x 10^6 p.s.i.

d = 1.0 in.

From equations (17), (18), and (13), respectively,

$$S + T = \frac{5.0 \times 10^6}{3 \times 1.0} (85 + 910 + 974) \times 10^{-6} = 3,280 \text{ p.s.i.}$$

$$S - T = \frac{\sqrt{2} \times 5.0 \times 10^6}{6 \times 1.0} \left[(-825)^2 + (-64)^2 + (889)^2 \right]^{1/2} \times 10^{-6}$$

$$= 1,430 \text{ p.s.i.}$$

$$S = 2,355 \text{ p.s.i. (applied stress = 2,400 p.s.i.)}$$

$$T = 925 \text{ p.s.i. (applied stress = 1,000 p.s.i.)}$$

$$\tan 2\theta_1 = \frac{-\sqrt{3}(910 - 974)}{2 \times 85 - (910 + 974)} = -0.065$$

$$2\theta_1 = -4^\circ \text{ or } 176^\circ$$

$$\theta_1 = 88^\circ \text{ (see rule 2 for a 60-degree rosette, p.88).}$$

The direction of U_1 was 0° from the horizontal. If α is the angle between S and the horizontal measured counterclockwise from S, then $\alpha = \theta_1$; thus

$$\alpha = 88^\circ \text{ (angle of applied stress = 90°).}$$

Example No. 4 - Limestone, 45-degree-deformation rosette:

$U_1 = 85$ μin.

$U_2 = 630$ μin.

$U_3 = 1,220$ μin.

$E = 5.0 \times 10^6$ p.s.i.

$d = 1.0$ in.

From equations (14), (15), and (16), respectively,

$$S + T = \frac{5.0 \times 10^6}{2 \times 1.0} (85 + 1,220) \times 10^{-6} = 3,260 \text{ p.s.i.}$$

$$S - T = \frac{5.0 \times 10^6}{2 \times \sqrt{2} \times 1.0} \left[(-545)^2 + (-590)^2 \right]^{1/2} \times 10^{-6} = 1,420 \text{ p.s.i.}$$

$$S = 2,340 \text{ p.s.i. (applied stress = 2,400 p.s.i.)}$$

$$T = 920 \text{ p.s.i. (applied stress = 1,000 p.s.i.)}$$

$$\tan 2\theta_1 = \frac{2 \times 630 - (85 + 1{,}220)}{85 - 1{,}220} = -0.04$$

$$2\theta_1 = -2^\circ \text{ or } 178^\circ$$

$$\theta_1 = 88^\circ \text{ (see rule 2 for a } 45^\circ \text{ rosette, p.88).}$$

The direction of U_1 was 0° from the horizontal. If α is the angle between S and the horizontal measured counterclockwise from S, then $\alpha = \theta_1$; thus

$$\alpha = 88^\circ \text{ (angle of applied stress = } 90^\circ)$$

Example No. 5 - Marble, 60-degree-deformation rosette:

$U_1 = 675$ μin.

$U_2 = 440$ μin.

$U_3 = 185$ μin.

$E = 7.7 \times 10^6$ p.s.i.

$d = 1.0$ in.

From equations (17), (18), and (13), respectively,

$$S + T = \frac{7.7 \times 10^6}{3 \times 1.0} (675 + 440 + 185) \times 10^{-6} = 3{,}340 \text{ p.s.i.}$$

$$S - T = \frac{\sqrt{2} \times 7.7 \times 10^6}{6 \times 1.0} \left[(235)^2 + (255)^2 + (-490)^2 \right]^{1/2} \times 10^{-6}$$

$$= 1{,}090 \text{ p.s.i.}$$

$S = 2{,}215$ p.s.i. (applied stress = 2,400 p.s.i.)

$T = 1{,}125$ p.s.i. (applied stress = 1,000 p.s.i.)

$$\text{Tan } 2\theta_1 = \frac{-\sqrt{3}(440 - 185)}{2 \times 675 - (440 + 185)} = -0.61$$

$$2\theta_1 = -31.4^\circ \text{ or } 148.6^\circ$$

$$\theta_1 = -16^\circ \text{ (see rule 1 for a 60-degree rosette, p.88).}$$

The direction of U_1 was 60° from the horizontal measured in the counterclockwise direction. If α is the angle between S and the horizontal, measured counterclockwise from S, then $\alpha = \theta_1 - 60^\circ$; thus

$$\alpha = (-16^\circ) - 60^\circ = -75^\circ \text{ (angle of applied stress = } \pm 90^\circ).$$

Example No. 6 - Marble, 45-degree-deformation rosette:

$U_1 = 185$ μin.

$U_2 = 520$ μin.

$U_3 = 695$ μin.

$E = 7.7 \times 10^6$ p.s.i.

$d = 1.0$ in.

From equations (14), (15), and (16), respectively,

$$S + T = \frac{7.7 \times 10^6}{2 \times 1.0} (185 + 695) \times 10^{-6} = 3{,}385 \text{ p.s.i.}$$

$$S - T = \frac{7.7 \times 10^6}{2\sqrt{2} \times 1.0} [\,(-335)^2 + (-175)^2\,]^{1/2} \times 10^{-6} = 1{,}022 \text{ p.s.i.}$$

$S = 2{,}200$ p.s.i. (applied stress = 2,400 p.s.i.)

$T = 1{,}180$ p.s.i. (applied stress = 1,000 p.s.i.)

$$\tan 2\theta_1 = -\frac{2 \times 520 - (185 + 695)}{185 - 695} = 0.314$$

$2\theta_1 = 17.4^\circ$ or 197.4°

$\theta_1 = 99^\circ$ (see rule 1 for a 45-degree rosette, p. 88).

The direction of U_1 was 0° from the horizontal. If α is the angle between S and the horizontal measured counterclockwise from S, then $\alpha = \theta_1$; thus

$\alpha = 99^\circ$ (angle of applied stress = 90°).

APPENDIX B

THE CSIR 'DOORSTOPPER'

This appendix is abstracted from The "Doorstopper" and Triaxial Rock Stress Measuring Instruments Developed by the C.S.I.R., by E. R. Leeman and published in the Journal of the South African Institute of Mining and Metallurgy, Vol. 69, No. 7, February 1969, pp 305-339, with the permission of the Institute. It may not be reproduced, in whole or in part, without the permission of the Institute.

THE DOORSTOPPER STRAIN CELL

It should perhaps first be explained that the name 'doorstopper' was given to these strain cells because of their resemblance in colour, shape and size in the early days to the red rubber cylindrical blocks used as doorstops in most homes. The name therefore possesses no scientific connotation whatever!

The principle underlying the 'doorstopper' method of determining the stress in rock

A borehole is drilled into the rock to the depth at which it is desired to measure the stress. Strain gauges are glued on the flattened end of the borehole. The depth of the borehole is then extended using the coring crown used to drill the borehole to the original depth. This is in effect an overcoring or trepanning operation which relieves the stresses present on the flattened end of the borehole and results in change of strain which are measured by means of the strain gauges. The strain readings are multiplied by the elastic constants of the rock and the stresses which were present on the end of the borehole before overcoring are obtained. If the relationship between the stresses present on the flattened end of a borehole and those in the surrounding rock is known, the stress in the surrounding rock (which it is desired to measure) may be calculated.

The relationship between the stresses on the flattened end of a borehole and those in the surrounding rock

The stress at a point in the rock can be represented by the system of stresses σx, σy, σz, τxy, τyz and τzx illustrated in Fig. 1(a). If a borehole be drilled as shown in Fig. 1(b) in the Z direction of the co-ordinate system used to specify the directions of the six stress components the stresses on the flattened end of the borehole will be as shown in Fig. 1(c). The stresses therefore which will be measured by strain gauges glued on the flattened end of the borehole will be $\sigma'x$, $\sigma'y$ and $\tau'xy$. To obtain the stresses σx, σy, etc. in the surrounding rock from the stresses measured on the end of the borehole the relationship between them must be known.

No theoretical relationship has yet been derived. Laboratory measurements, however, on loaded prisms and cylinders of steel, rock and araldite by Bonnechere[11, 12] and Van Heerden[13] using electrical resistance strain gauges and photoelasticity to determine the stress distributions on the flat end of boreholes drilled into the specimens have thrown light on the subject. The object of their investigation was to determine the effect of the stress components, σx, σy, σz, τxy, τyz and τzx in the rock upon the stress components $\sigma'x$, $\sigma'y$ and $\tau'xy$ acting upon the end of the borehole.

They wrote $\sigma'x$, $\sigma'y$ and $\tau'xy$ as follows:

$$\sigma'x = a\,\sigma x + b\,\sigma y + c\,\sigma z$$

$$\sigma'y = a\,\sigma y + b\,\sigma x + c\,\sigma z$$

$$\tau'xy = d\,\tau xy$$

and found the following values, for a, b, c, and d

	Bonnechere	Van Heerden
a	1.25	1.25
b	0	-0.064
c	-0.75 (0.5 + ν)	-0.75 (0.645 + ν)
d	1.25	--

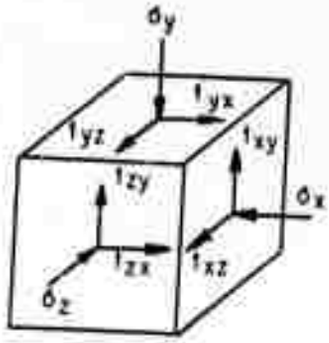

(a) CO-ORDINATE SYSTEM OF THE STRESS AT A POINT IN THE ROCK MASS

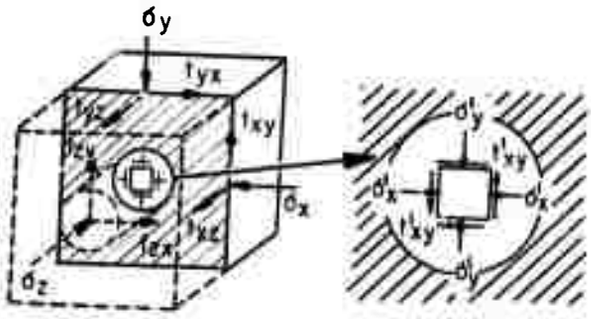

(b) STRESSES ON THE FLATTENED END OF A BOREHOLE

(c) ENLARGEMENT OF THE FLATTENED END OF A BOREHOLE

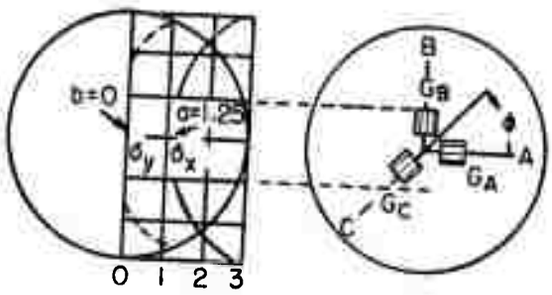

$\frac{\sigma^1 x}{\sigma x}, \frac{\sigma^1 y}{\sigma y}$ $\phi_A=0$; $\phi_B=90^\circ$; $\phi_C=225^\circ$

(d) DISTRIBUTION OF STRESSES ON THE END OF THE BOREHOLE (ACC. VAN HEERDEN)

(e) CONFIGURATION OF STRAIN GAUGES GLUED ON THE END OF THE BOREHOLE

Fig. 1 The Stresses on the Flattened End of a Borehole

Other investigators have obtained other values, particularly for a but it is believed that the above values are the most reliable available. The author is inclined to accept the value of c obtained by Van Heerden since it is the result of several measurements.

It should be mentioned that the value of a = 1.53 obtained by, amongst others, the author, resulted from using cubes instead of prisms in the laboratory tests. The necessary conditions of uniform stress cannot be and were not achieved in the cubes and caused the higher erroneous value of a to be obtained.

The value of d gives the effect of τxy upon strain readings from strain gauges glued on the end of the borehole. Since τxy has the same effect as two normal stresses, of equal magnitude and opposite sign, acting at right angles to each other and at 45 degrees to τxy, the value of d = 1.25, the same as a would seen to follow.

The shear components τyz and τzx would appear to have no effect on the stresses in the XY plane. Since they have the effect of only rotating this plane around the X and Y axes respectively strain gauges glued on it should not be influenced by them.

The value of b = -0.064 is small and may be neglected. Hence we can write

$$\sigma'x = 1.25\ \sigma x - 0.75(0.645 + \nu)\ \sigma z \qquad (1)$$

$$\sigma'y = 1.25\ \sigma y - 0.75(0.645 + \nu)\ \sigma z \qquad (2)$$

$$\tau'xy = 1.25\ \tau xy \qquad (3)$$

The distribution of $\frac{\sigma'x}{\sigma x}$ and $\frac{\sigma'y}{\sigma y}$ over the end surface of the borehole, obtained photoelastically, is shown in Fig. 1(d). As will be seen from this figure $\frac{\sigma'x}{\sigma x}$ and $\frac{\sigma'y}{\sigma y}$ are constant over approximately the middle third of the end of the borehole having the values of a = 1.25 and b = 0 (approx.). Strain measurements should therefore be made in this area.

The determination of the stresses from doorstopper strain readings.

(a) Measurements in one borehole only

Since only three strain measurements are made with a doorstopper during any single overcoring operation it is not possible to obtain any more information than the magnitudes and directions of the principal stresses acting on the end of the borehole before overcoring (and thence of course the stresses in the surrounding rock as indicated previously).

Thus if measurements are to be made in only one borehole, it should be drilled parallel to one of the minor principal stresses. The end of the borehole then becomes the principal plane in which the major and the other minor principal stress act.

If as shown in Fig. 1(b) the borehole is drilled in a direction parallel to the σz principal stress, the stresses $\sigma'x$, $\sigma'y$ and $\tau'xy$ (see Fig. 1(c)) will be measured by a doorstopper glued on the end of the borehole.

If the configuration of the gauges in the rosette is as shown in Fig. 1(e), and they are glued on the end of the borehole so that the A and B directions are parallel to the X and Y directions respectively, then the normal stresses $\sigma'_A = \sigma'x$ and $\sigma'_B = \sigma'y$ and $\tau'_{AB} = \tau'xy$ are given by (see Appendix)

$$\sigma'A = \sigma'x = \frac{E}{2}\left\{\frac{e_A + e_B}{1 - \nu} + \frac{e_A - e_B}{1 + \nu}\right\} \tag{4}$$

$$\sigma'B = \sigma'y = \frac{E}{2}\left\{\frac{e_A + e_B}{1 - \nu} - \frac{e_A - e_B}{1 + \nu}\right\} \tag{5}$$

$$\tau'AB = \tau'xy = \frac{E}{2}\left\{\frac{2e_C - (e_A + e_B)}{1 + \nu}\right\} \tag{6}$$

where E and ν are the Young's modulus and Poisson's ratio of the rock and e_A, e_B, and e_C are the strains measured in the A, B, and C directions respectively.

If $\tau'xy = 0$, then $\sigma'x$ and $\sigma'y$ are the principal stresses and the directions of the gauges A and B are parallel with the principal directions.

If $\tau'xy \neq 0$, then $\sigma'x$ and $\sigma'y$ are not the principal stresses which are then given by

$$\sigma'_{1,2} = \frac{E}{2}\frac{1}{\{(1 - \nu)\ (e_A + e_B) \pm \frac{1}{(1 + \nu)}\sqrt{\{2e_C - (e_A + e_B)\}^2 + (e_A - e_B)^2}\}} \tag{7}$$

and their directions by

$$\tan \phi'_{1,2} = \frac{2(e_{1,2} - e_A)}{2e_C - (e_A + e_B)} \tag{8}$$

where ϕ' is measured anti-clockwise from the OA direction as shown in Fig. 1(e).

The stress in the surrounding rock σx, σy and τxy are then given by substitution in equations (1), (2) and (3).

(b) Measurements in three boreholes

As will be seen from equations (4), (5) and (6) the normal components of stress σ'_A and σ'_B and shear stress component τ'_{AB} on the end of any borehole are easily obtained from the doorstopper strain readings e_A, e_B, and e_C.

If measurements are made in three boreholes inclined at any angle to one another, it is necessary to resolve the components σ'_A, σ'_B, and τ'_{AB} measured in each borehole in three arbitrarily chosen orthogonal directions in order to bring them into relationship with each other.

The stress at any point in a body can be defined by six independent stress components σx, σy, σz, τxy, τyz, and τzx with respect to any arbitrarily chosen co-ordinate system represented by three axes OX, OY, and OZ as shown in Fig. 2.

The normal component of stress σ acting on any plane PQR has the direction cosines l, m, and n and is given by

$$\sigma = l^2\sigma x + m^2\sigma y + n^2\sigma z + 2lm\tau xy + 2mn\tau yz + 2nl\tau zx \tag{9}$$

The tangential component of stress τ^I acting in the l^I, m^I, n^I direction will be given by

$$\tau^I = ll^I\ \sigma x + mm^I\sigma y + nn^I\sigma z + (mn^I + m^I n)\ \tau yz + (nl^I + n^I l)\ \tau zx + (lm^I + l^I m)\ \tau xy \tag{10}$$

A similar expression will be given for τ^{II} acting on the l^{II}, m^{II}, n^{II} direction.

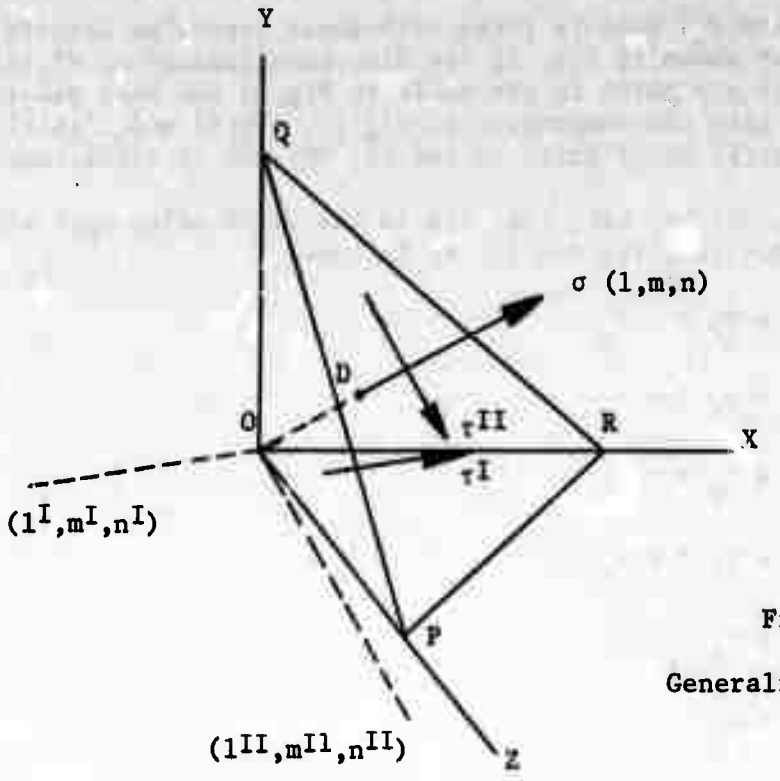

Figure 2

Generalised co-ordinate system

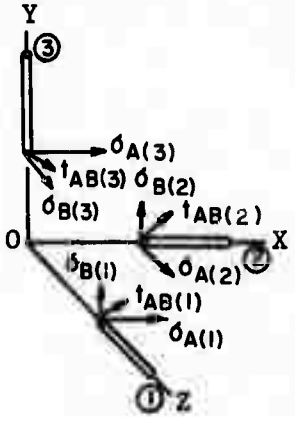

Figure 3 A

Normal stress components in three boreholes drilled in the OX, OY, and OZ directions

Thus if measurements are made in three orthogonal boreholes drilled in the OX, OY, and OZ directions as shown in Fig. 3, the direction cosines of $\sigma'_{A}(i)$, $\sigma'_{B}(i)$, and $\tau'_{AB}(i)$ in each borehole are given in the table in Fig. 3 and when substituted in equations (9) and (10) give the components of $\sigma'_{A}(i)$, $\sigma'_{B}(i)$ and $\tau'_{AB}(i)$ namely $\sigma'_{Z}(i)$ $\sigma'y(i)$ and $\tau'xy(i)$, $\tau'yz(i)$ and $\tau'zx(i)$ in the OX, OY, and OZ directions.

The components σx, σy, σz, τxy, τyz, τzx in the surrounding rock will be found by substitution in equations (1), (2), and (3) as follows:

$$\sigma'_{A(1)} = \sigma'_{x(1)} = a\,\sigma_x + c\,\sigma_z \qquad (11)^*$$

$$\sigma'_{A(3)} = \sigma'_{x(3)} = a\,\sigma_x + c\,\sigma_y \qquad (12)^*$$

$$\sigma'_{B(1)} = \sigma'_{y(1)} = a\,\sigma_y + c\,\sigma_z \qquad (13)^*$$

$$\sigma'_{B(2)} = \sigma'_{y(2)} = a\,\sigma_y + c\,\sigma_x \qquad (14)^*$$

$$\sigma'_{A(2)} = \sigma'_{z(2)} = a\,\sigma_z + c\,\sigma_x \qquad (15)^*$$

$$\sigma'_{B(3)} = \sigma'_{z(3)} = a\,\sigma_z + c\,\sigma_y \qquad (16)^*$$

and $$\tau'_{AB(1)} = \tau'_{xy(1)} = a\,\tau_{xy} \qquad (17)$$

$$\tau'_{AB(2)} = \tau'_{yz(2)} = a\,\tau_{yz} \qquad (18)$$

$$\tau'_{AB(3)} = \tau'_{zx(3)} = a\,\tau_{zx} \qquad (19)$$

If measurements are made in three coplanar boreholes (a configuration usually more suited to underground circumstances) a similar procedure to the above is followed.

Thus, if as shown in Fig. 4 the three boreholes 1, 2, and 3 are drilled parallel to and at angles of δ_2 and δ_3 respectively to the OZ axis, the direction cosines of each stress component and their components in the three directions are as shown in the table in Fig. 4.

The components σ_x, σ_y, σ_z, τ_{xy}, τ_{yz} and τ_{zx} in the surrounding rock will be found by substitution in equations (1), (2), and (3) as before (see corresponding equations for three orthogonal boreholes - (11) to (19)).

---

*Only three of these six equations are required to obtain σ_x, σ_y and σ_z, e.g. $\sigma'_{X(1)}$, $\sigma'_{Y(1)}$ and $\sigma'_{Z(2)}$. If, however, all six are measured, a useful check on the results is obtained.

BOREHOLE No.	MEASURED STRESS	DIRECTION COSINES			SUBSTITUTING THE DIRECTION COSINES IN EQUATIONS (9) and (10)
		1	m	n	
1	$\sigma^1A(1)$	1	0	0	$\sigma^1A(1) = \sigma^1X(1)$
	$\sigma^1B(1)$	0	1	0	$\sigma^1B(1) = \sigma^1Y(1)$
	$\tau^1AB(1)$	1,0	0,1	0,0	$\tau^1AB(1) = \tau^1XY(1)$
2	$\sigma^1A(2)$	0	0	1	$\sigma^1A(2) = \sigma^1Z(2)$
	$\sigma^1B(2)$	0	$\frac{1}{\sqrt{2}}$	$\frac{1}{\sqrt{2}}$	$\sigma^1B(2) = \sigma^1Y(2)$
	$\tau^1AB(2)$	0,0	$0\frac{1}{\sqrt{2}}$	$0\frac{1}{\sqrt{2}}$	$\tau^1AB(2) = \tau^1YZ(2)$
3	$\sigma^1A(3)$	0	0	1	$\sigma^1A(2) = \sigma^1X(3)$
	$\sigma^1B(3)$	$\frac{1}{\sqrt{2}}$	0	$\frac{1}{\sqrt{2}}$	$\sigma^1B(3) = \sigma^1Z(3)$
	$\tau^1AB(3)$	$1,\frac{1}{\sqrt{2}}$	0,0	$0,\frac{1}{\sqrt{2}}$	$\tau^1AB(3) = \tau^1ZX(3)$

Fig.3B Normal Stress Components in Three Boreholes Drilled in the OX, OY, and OZ Directions

STRESS COMPONENT	DIRECTION COSINES 1	m	n	SUBSTITUTING THE DIRECTION COSINES IN EQUATIONS (9) AND (10)
$\sigma^1A(1)$	1	0	0	$\sigma^1A(1)=\sigma^1X(1)$
$\sigma^1B(1)$	0	1	0	$\sigma^1B(1)=\sigma^1Y(1)$
$\tau^1AB(1)$	1,0	0,1	0,0	$\tau^1AB(1)=\tau^1XY(1)$
$\sigma^1A(2)$	$\cos\delta_2$	0	$\sin\delta_2$	$\sigma^1A(2)=\sigma^1X(2)\cos^2\delta_2+\sigma^1Z(2)\sin^2\delta_2+2\tau^1ZX(2)\sin\delta_2\cos\delta_2$
$\sigma^1B(2)$	0	1	0	$\sigma^1B(2)=\sigma^1Y(2)$
$\tau^1AB(2)$	$\cos\delta_2$,0	0,1	$\sin\delta_2$,0	$\tau^1AB(2)=\tau^1YZ(2)\ \sin\delta_2+\tau^1XY(2)\ \cos\delta_2$
$\sigma^1A(3)$	$\cos\delta_3$	0	$\sin\delta_3$	$\sigma^1A(3)=\sigma^1X(3)\cos^2\delta_3+\sigma^1Z(3)\ \sin^2\delta_3+2\tau^1ZX(3)\sin\delta_3\ \cos\delta_3$
$\sigma^1B(3)$	0	1	0	$\sigma^1B(3)=\sigma^1Y(3)$
$\tau^1AB(3)$	$\cos\delta_3$,0	0,1	$\sin\delta_3$,0	$\tau^1AB(3)=\tau^1YZ(3)\ \sin\delta_3+\tau^1XY(3)\ \cos\delta_3$

Fig.4B Normal Stress Components in Three Boreholes Drilled in the XZ Plane at δ_1^o, δ_2^o, and δ_3^o to the OZ Ordinate

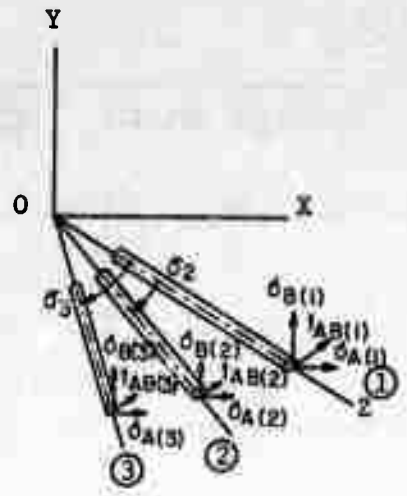

FIGURE 4 A

Normal stress components in three boreholes drilled in the XZ plane at δ_1^o, δ_2^o and δ_3^o to the OZ ordinate

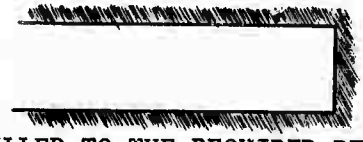

(a) BS BOREHOLE DRILLED TO THE REQUIRED DEPTH AND END FLATTENED AND POLISHED WITH DIAMOND TOOLS.

(b) STRAIN CELL BONDED ON TO END OF BOREHOLE AND STRAIN READINGS RECORDED.

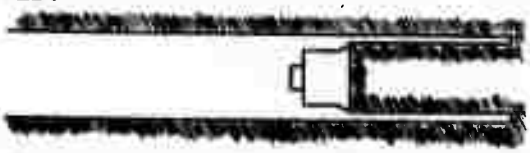

(c) BOREHOLE EXTENDED WITH BX DIAMOND CORING CROWN THEREBY STRESS RELIEVING THE CORE.

(d) BX CORE, WITH STRAIN CELL ATTACHED, REMOVED AND STRAIN READINGS TAKEN.

Fig. 5 The Overcoring Technique Using a Doorstopper

Similar procedures are followed for boreholes drilled at any angles to one another.

The three principal stresses in the rock (σ_i =) σ_1, σ_2 and σ_3 are the three roots of the well known equation:

$$\sigma_i^3 - \sigma_i^2 (\sigma_x + \sigma_y + \sigma_z) + \sigma_i (\sigma_x \sigma_y + \sigma_y \sigma_z + \sigma_z \sigma_x - \tau_{xy}^2 - \tau_{yz}^2 - \tau_{zx}^2) - (\sigma_x \sigma_y \sigma_z - \sigma_x \tau_{yz}^2 - \sigma_y \tau_{xy}^2 + \sigma_z \tau_{xy}^2 + 2\tau_{xy} \tau_{yz} \tau_{zx}) = 0 \quad (20)$$

This can be written in the forms

$$\sigma_i^3 + B\sigma_i^2 + C\sigma_i + D = 0 \quad (21)$$

and

$$W_i^3 + \alpha W_i + \beta = 0 \quad (22)$$

where

$$\sigma_i = W_i - \frac{B}{3}$$

$$\alpha = 1/3 (3C - B^2)$$

$$\beta = \frac{1}{27} \left(2B^3 - 9BC + 27D\right)$$

Equation (22) has real roots W_1, W_2, and W_3 if

$$\frac{\beta^2}{4} + \frac{\alpha^3}{27} < 0$$

and have the values

$$W_1 = 2 \times \sqrt{-\frac{\alpha}{3}} \cdot \cos \frac{\phi}{3}$$

$$W_2 = 2 \times \sqrt{-\frac{\alpha}{3}} \cdot \cos \left(\frac{\phi}{2} + 120^o\right)$$

$$W_3 = 2 \times \sqrt{-\frac{\alpha}{3}} \cdot \cos \left(\frac{\phi}{3} + 240^o\right)$$

where $\phi = \cos^{-1} \left\{ \frac{-\beta/2}{\sqrt{-\frac{\alpha^3}{27}}} \right\}$

Thus it is possible to determine W_1, W_2, and W_3 and hence σ_1, σ_2, and σ_3.

The direction cosines l_i, m_i, n_i of each principal stress $\sigma_i = \sigma_1$, σ_2, σ_3 are found by substitution in equation (9) written as

$$\sigma_i = l_i^2 \sigma_x + m_i^2 \sigma_y + n_i^2 \sigma_z + 2l_i m_i \tau_{xy}, 2m_i n_i \tau_{yz} + 2n_i l_i \tau_{zx}$$

The overcoring technique used with doorstoppers

The overcoring technique used is represented diagrammatically in Fig. 5.

A standard BX diamond coring crown is used to drill the borehole (approximately 2 3/8 in. diameter) to the depth in the rock at which it is desired to determine the stress as shown in Fig. 5(a). The end of the borehole is ground flat and smooth with specially prepared square faced and flat faced diamond impregnated bits, photographs of which are shown in Fig. 6.

The direction in which the borehole is drilled should be parallel to one of the minor principal stresses as indicated in a previous paragraph if measurements in only one borehole are to be made. If measurements are being made in three boreholes to determine the complete state of stress then the directions in which the boreholes are drilled is governed by the considerations outlined in the previous paragraph.

Having cleaned and dried the end of the borehole, a doorstopper is glued on to it and strain gauge readings taken when the glue has hardened. The installing tool is then removed leaving the doorstopper stuck on the end of the hole as shown in Fig. 5(b).

Using the same BX coring crown as was used to drill the borehole, the length of the borehole is extended as shown in Fig. 5(c) - thereby relieving the stresses on the end of the borehole. The core is broken off the end of the hole as shown in Fig. 5(d) with the doorstopper still attached to it and the strain relieved readings taken from the doorstopper strain gauges.

The stresses present on the end of the borehole before overcoring may then be calculated from the change in strain readings as indicated in the previous paragraph.

Description of the doorstopper strain cell equipment

As will be seen from the diagrammatic sketch of one of the strain cells ('doorstopper') in Fig. 7, a rectangular strain gauge rosette (consisting of three strain gauges measuring in the 0 degree (horizontal) 45 degree and 90 degree (vertical) directions) is moulded into a rubber casting which fills a plastic shell. Four gold plated connector pins are moulded in the plastic shell, as shown in Fig. 7, in such a way that when they are plugged into the inserting tool (described later) they effect electrical contact between the strain gauges and the strain indicating instrument. The connections to the pins are shown in the lower illustration in Fig. 7.

The presence of a keyway in the plug section of the plastic shell, ensures that the 'doorstopper' can be plugged into the installing tool with only one possible orientation.

The diameter of the 'doorstopper' was chosen so that it can be used in a standard BX diamond drilled borehole which is approximately 2 3/8 in. in diameter.

When a 'doorstopper' is installed on the end of a BX borehole, changes in strain on the surface of the rock resulting from the overcoring operation are transmitted to the strain indicating instrument via the strain gauges which are glued on the rock. The rubber and plastic shell serve to protect the strain gauges from damage and from water during the overcoring operation. Normally, sufficient glue would be used to ensure that the base of the plastic shell is also glued to the rock surface.

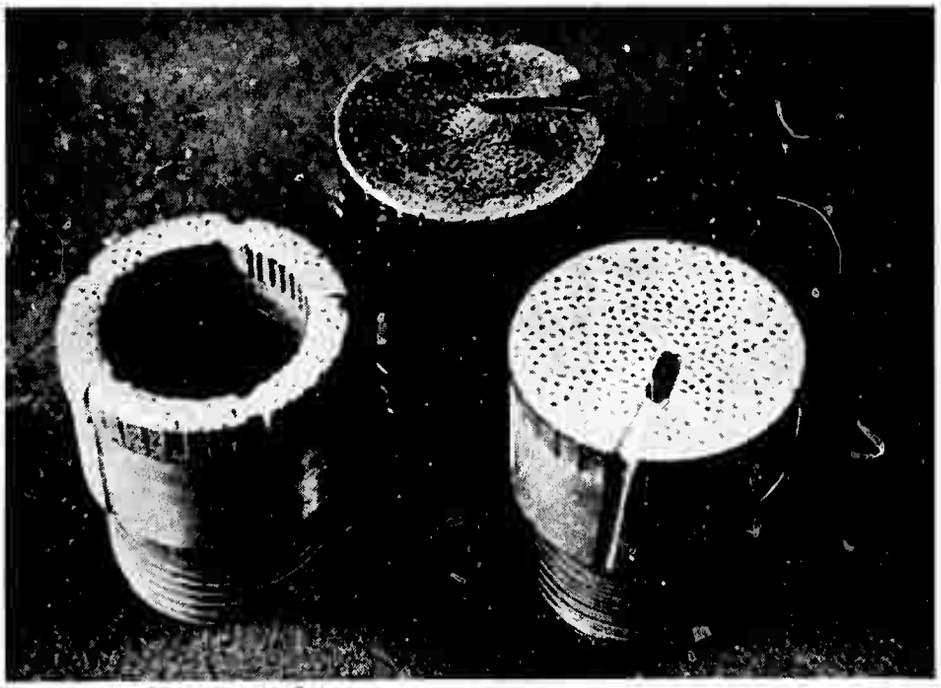

Fig. 6. The diamond bits used for drilling the BX borehole and preparing the end of the borehole.

Fig. 8 A doorstopper (left) showing the rosette strain and gauge and and (right) glued to a short lenght of core.

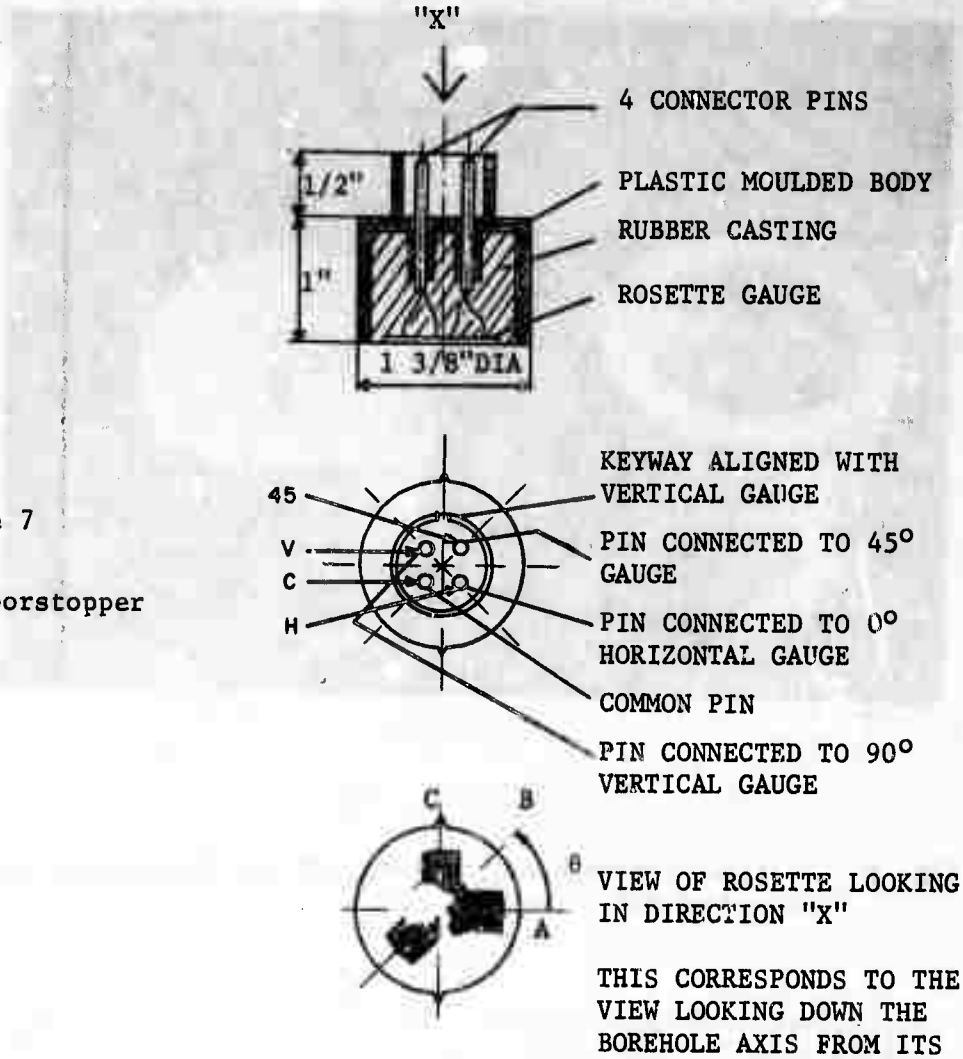

Figure 7

Details of a doorstopper

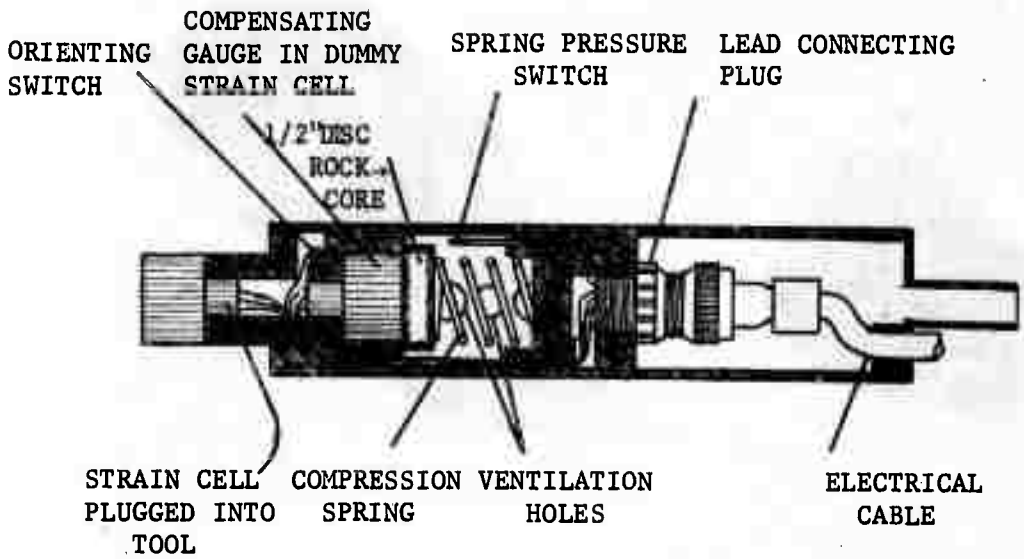

Fig. 9 Doorstopper Strain Cell Installing Tool

A photograph of doorstoppers is given in Fig. 8, one showing the strain gauge rosette, the other glued to a short length of core.

A cross sectional drawing of the installing tool used to glue a doorstopper on the end of the borehole is given in Fig. 9 and a photograph in Fig. 10. As will be seen in Fig. 9, the 'doorstopper' and compensating gauge plug into a piston unit which slides against a compression spring inside a simple brass tubular unit. An orienting mercury switch is also housed in the piston unit to enable the doorstopper to be accurately oriented. The electric lead cable is connected to the instrument through an eight-channel plug. Ventilation holes, visible also in the photograph in Fig. 10, are machined in the tubular body of the tool to ensure that the temperature of the disc of rock on which the dummy gauge is glued reaches the same temperature as that upon which the measuring 'doorstopper' is attached as quickly as possible.

The compensating dummy gauge consists of a 'doorstopper' glued to a 1/2 in. length of BX core of the rock in which the stresses are to be measured. In fact, this is prepared initially by gluing a 'doorstopper' upon the end of the borehole in which the stresses are to be measured, overcoring and cutting off a 1/2 in. length from the core at the end on which the 'doorstopper' is glued. This 'doorstopper' is very easily plugged into the inner plug of the piston unit and acts as a termperature compensating dummy gauge.

When the installing tool with a 'doorstopper' plugged into it is pushed up to the end of the hole by means of specially designed installing rods, and pushed against the end of the borehole, the piston unit is forced into the tubular body of the tool against the compression spring until the spring pressure switch, shown in Fig. 9, closes. A lamp lights up in the control box to which the installing tool is connected and indicates that the desired load of approximately 10 lb is being applied to the 'doorstopper'. This must be maintained until the glue has hardened. The installing tool can then be removed from the borehole leaving the doorstopper glued to the end of the borehole.

A photograph of the control box is shown in Fig. 11. This houses the electrical lead, the installing tool, spare doorstoppers, the strain indicator and control panel. On the control panel are two lamps, one connected to the mercury orienting switch and the other to the spring pressure switches in the installing tool. A three-way switch is provided to enable readings from each of the three strain gauges in the doorstopper rosette to be made in turn.

Glues and rock drying agents used

Any of the commerically available strain gauge cements may be used to glue the doorstoppers to the rock. Araldite strain gauge cement has been found very reliable. Its setting time is, however, rather long. The setting time should on the other hand not be so short that the doorstopper cannot be installed before the glue has wholly or partly set.

In coal, Philips strain gauge cement No. P.R. 9244/04, a quick setting cement, has been successfully used.

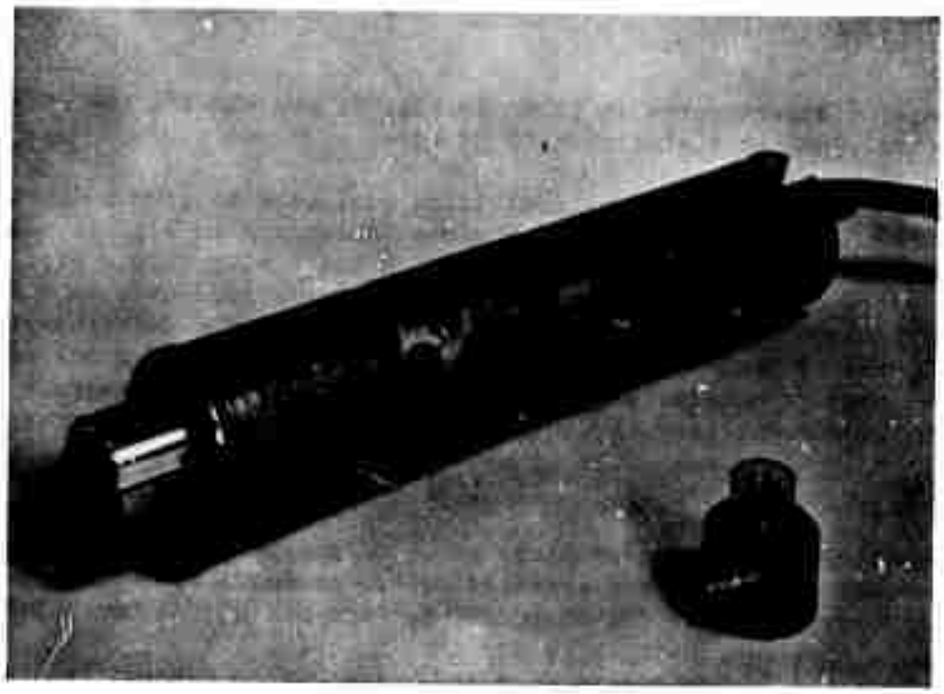

Fig. 10. The doorstopper installing tool showing a doorstopper in the foreground.

Fig. 11. The control box/carrying case for the doorstopper equipment.

The use of a water dispellant has also been proved very beneficial in producing reliable and consistent gluing on of the doorstoppers. In this connection a 10 percent mixture in pure alcohol of Union Carbide Silane Coupling Agent No. A 1120 has been found to be very effective[15]. This enables doorstoppers, and triaxial cells for that matter to be used in wet rock.

The doorstopper borehole assimulator

The determination of the stresses from the doorstopper strain measurements described in a previous paragraph requires a knowledge of the elastic moduli of the rock. Due to the variations in these properties, depending upon the locality and the reliability of the laboratory methods used to determine them, serious errors can be introduced in the calculated stress results.

In order to overcome this difficulty a so-called 'borehole assimulator' was designed in which the stress relieved core to which the doorstopper is glued, is loaded in such a way as to restore the stresses which existed in it before the core was overcored. Two radial loads at right angles are applied to the core hydraulically and the oil pressures required to restore the doorstopper strain readings to their values before overcoring are a measure of the original stresses on the end of the borehole.

It can be shown[16, 17] that if a cylindrical core is loaded biaxially under the pressures p and q, each uniformly distributed over a quarter of its circumference as shown in Fig. 12 the radial, tangential and shear stresses at the centre are given by

$$\sigma_r = 1/2 \left[(p + q) + \frac{4}{\pi} (p - q) \cos 2\theta\right]$$

$$\sigma_\theta = 1/2 \left[(p + q) - \frac{4}{\pi} (p - q) \cos 2\theta\right]$$

$$\tau_{r\theta} = \frac{2}{\pi} (p - q) \sin 2\theta$$

The radial strains for $\theta = 0^o$, 45^o, and 90^o are given by Hooke's Law for plane stress as follows:

$$e_{ro^o} = \frac{1}{2E} \left[(1 - \nu) (p + q) + \frac{4}{\pi} (1 + \nu) (p - q)\right]$$

$$e_{r45^o} = \frac{1 - \nu}{2E} (p + q)$$

$$e_{r90^o} = \frac{1}{2E} \left[(1 - \nu) (p + q) - \frac{4}{\pi} (1 + \nu) (p - q)\right]$$

Fig. 12-A cylindrical core subjected to hydraulic pressures p and q over four equal segments

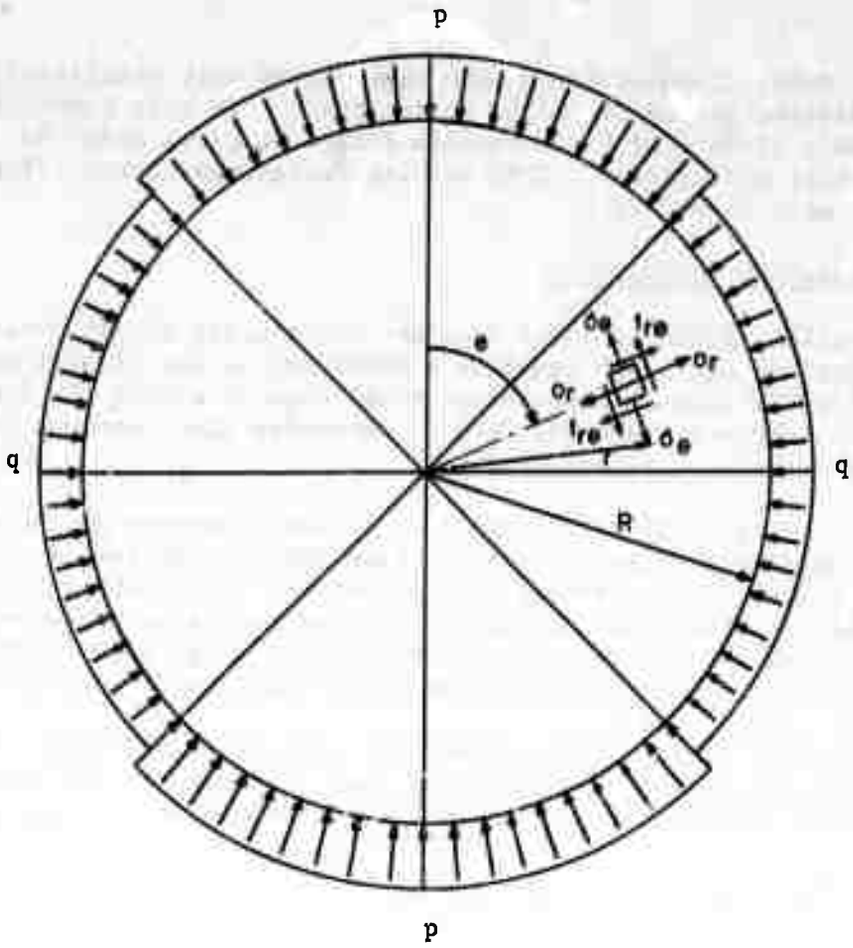

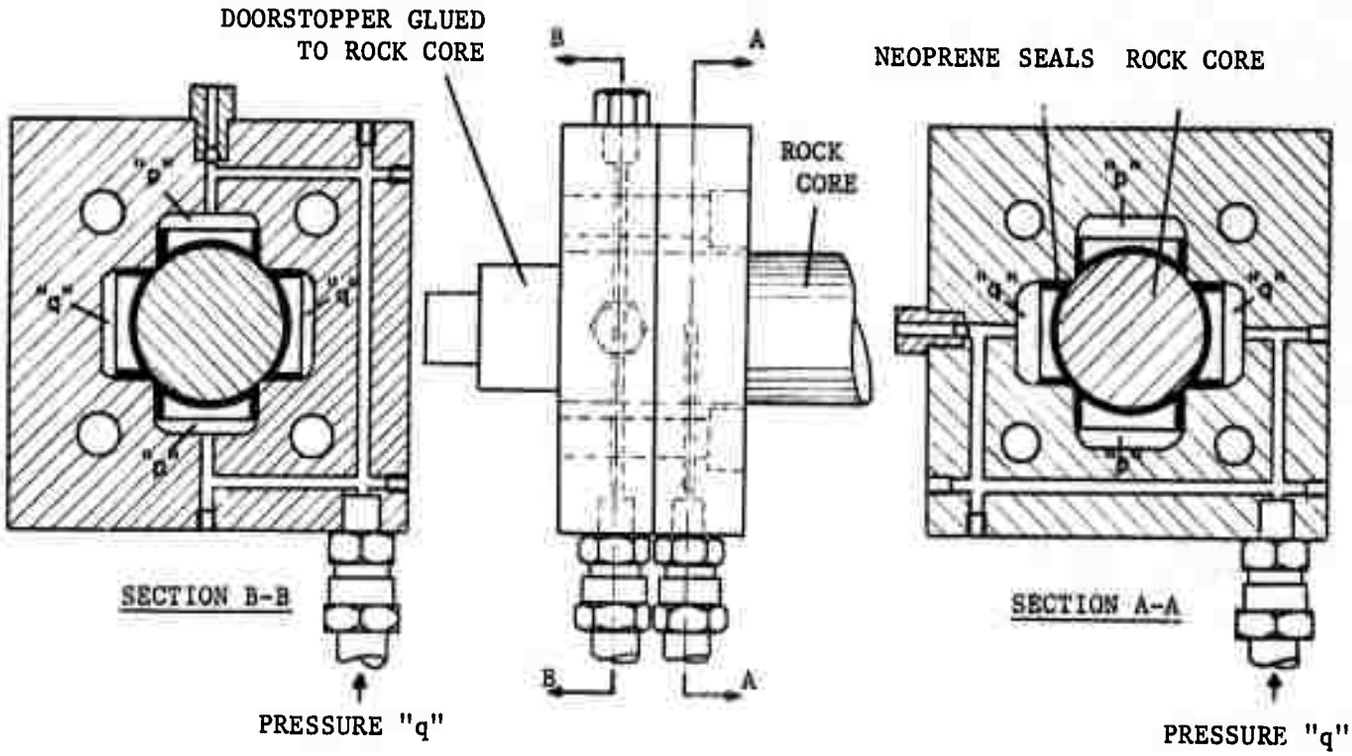

Fig. 13 The Hydraulic Assimulator

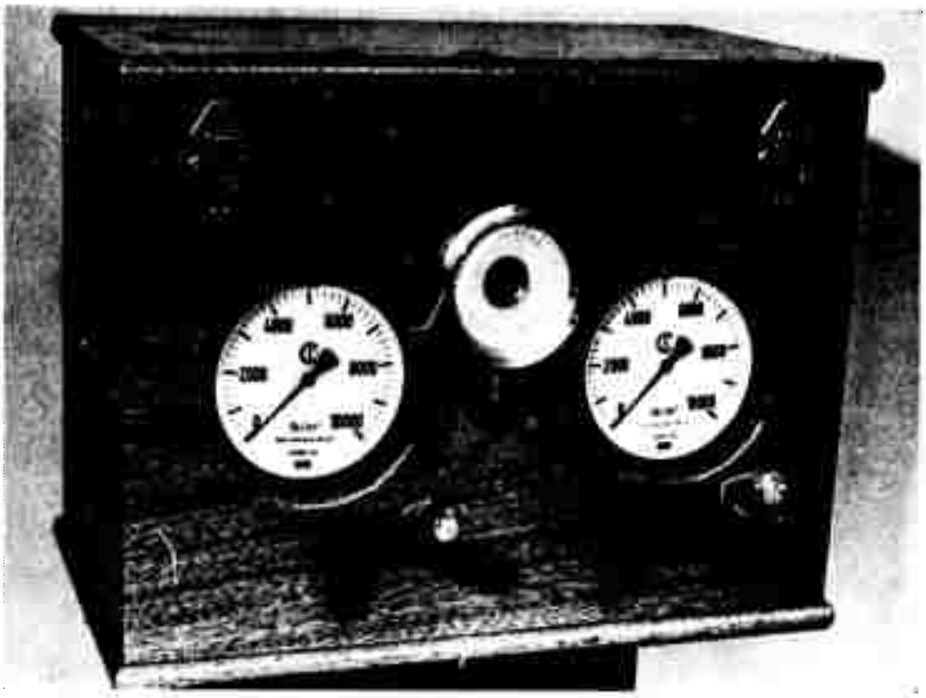

Fig. 14. An assimulator built into a suitable carrying case.

The components of stress on the end of a borehole in a uniform stress field with principal stresses P and Q are given by

$$\sigma'_r = \frac{1.25}{2} \left[(P + Q) + (P - Q) \cos 2\theta\right]$$

$$\sigma'_\theta = \frac{1.25}{2} \left[(P + Q) - (P - Q)\right] \cos 2\theta$$

$$\tau'_{r\theta} = \frac{1.25}{2} (P - Q) \sin 2\theta$$

where the value of 1.25 is the factor a referred to on page 121.

The radial strains for $\theta = 0^o$, 45^o, and 90^o are given by Hooke's Law for plane stress as follows:

$$e'_{ro^o} = \frac{1.25}{2E} \left[(1 - \nu) (P + Q) + (1 + \nu) (P - Q)\right]$$

$$e'_{r45^o} = \frac{1.25}{2E} (P + Q)$$

$$e'_{r90^o} = \frac{1.25}{2E} \left[(1 - \nu) (P + Q) - (1 + \nu) (P - Q)\right]$$

Thus for the state of stress in the core in the assimulator to be identical to that at the end of the borehole:

$$e_{ro^o} = e'_{ro^o}$$

$$e_{r45^o} = e'_{r45^o}$$

$$e_{r90^o} = e'_{90^o}$$

Solving for P and Q in terms of p and q we obtain

$$P = \frac{1}{2.50} \left[\left(1 + \frac{4}{\pi}\right) p + \left(1 - \frac{4}{\pi}\right) p\right] \quad (23)$$

$$Q = \frac{1}{2.50} \left[\left(1 - \frac{4}{\pi}\right) p + \left(1 + \frac{4}{\pi}\right) q\right] \quad (24)$$

Thus by applying the hydraulic pressures p and q on the rock core to restore the strain, the original principal stresses P and Q in the rock can be obtained, without requiring any knowledge of the properties of the rock.

A diagrammatic sketch of an assimulator* is given in Fig. 13 and a photograph in Fig. 14. As can be seen in Fig. 13, the pressures p and q are applied around the circumference of the rock core via the neoprene seals which fit snugly around it. In Fig. 14 the assimulator is shown assembled in a carrying case. Pressure pump handles, pressure gauges and protractor for orienting the core can be clearly seen in the photograph.

The assimulator is used as follows: Having obtained the three strain readings after overcoring, the directions of the principal stresses represented by θ are determined from equation (8).

The core with the doorstopper glued to it is inserted in the assimulator and oriented at angle θ. The hydraulic pressures p and q to be applied to the core will then act in the same directions, relative to the gauges on the core, as the principal stresses P and Q before overcoring. The pressures p and q required to restore the strain readings to those before overcoring are obtained and substituted in equations (23) and (24) to obtain P and Q.

The accuracy of doorstopper stress measurements

Van Heerden[15] has carried out tests to determine the accuracy of doorstopper stress measurements in coal which could be no means be described as the classical material from the point of view of homogenity, isotropy and continuity assumed in elastic theory. In these tests large 3 ft x 3 ft x 6 ft high coal specimens were cut in situ in coal pillars underground and known uniaxial compressive stresses were applied to them by means of hydraulic jacks. The stresses in the pillars were measured by means of doorstoppers installed in them and this enabled a comparison to be made between applied and measured stresses.

The results obtained are included in Table I from which it can be seen that the vertical stresses σ_1 obtained by using the assimulator agreed remarkably well with the applied stresses. The horizontal stresses σ_2 were zero and very small stresses were measured.

On the other hand the stresses obtained by calculation using the elastic moduli determined in compression tests on small cylindrical specimens in an underground laboratory (to eliminate influences of temperature and humidity changes) in most instances did not give very good results (see Table I). It must therefore be emphasized that for materials such as coal reliable results cannot be expected, if they are calculated by multiplying the strain readings by the elastic constants obtained on small laboratory specimens, and that the assimulator should be used to obtain the stresses in such materials. It is in fact recommended that the assimulator be used in stress measurements even in hard homogeneous rock in spite of the fact that reliable results using the elastic constants can be expected in such rock.

---

*For reasons of accuracy two versions of the assimulator have been developed, one for low strength rock such as coal, and one for high strength rock such as quartzite.

TABLE I

COMPARISON OF RESULTS OBTAINED IN COAL USING THE ASSIMULATOR AND BY CALCULATION BASED UPON ELASTIC CONSTANTS OBTAINED IN THE LABORATORY.

Relief of strain during overcoring of doorstopper (micro strain)			Results obtained with the assimulator							Stresses obtained using elastic constants		Actual vertical stress σ_1 applied by jacks on the coal pillar (lbf/in.^{2})
			Strain readings obtained in the assimulator			Assimulator pressures (lbf/in.^{2})		Principal stresses (lbf/in.^{2})		Principal stresses (lbf/in.^{2})		
e_{90^o}	e_{45^o}	e_{o^o}	e_{90^o}	e_{45^o}	e_{o^o}	90°	0°	σ_1	σ_2	σ_1	σ_2	
+ 485	+ 55	-225	- 485	-155	+225	400	50	358	1.6	250	-36	350
+1,045	+360	-495	-1,045	-200	+495	425	125	372	67.0	535	-78	350
+ 625	+210	-260	- 625	-240	+260	400	25	360	-21.0	324	-25	350
+1,130	+100	-295	-1,130	-120	+300	325	50	290	9.6	495	188	300
+ 805	+390	-140	- 805	-195	+140	350	50	312	7.2	460	83	300
+2,570	+415	-380	-2,570	-400	+380	425	50	380	- 1.0	1,550	268	300
+ 570	+305	- 80	- 570	-250	+130	325	50	290	9.6	338	73	293
+ 465	+300	-110	- 465	-280	+120	350	50	312	7.2	270	23	293
+ 790	+230	-210	- 760	-230	+210	375	50	334	4.4	430	32	293
+1,500	+440	-340	-1,550	-400	+340	575	150	507	74.0	840	103	496

In solid homogeneous rock, consistent and reliable results are easily attainable. Attention, in this connection is drawn to a recent publication [18] in which the results obtained with doorstoppers were compared with those obtained with a borehole deformation gauge. The test showed remarkable agreement in the results and demonstrated that the doorstopper was very much easier to use.

Numerous measurements with doorstoppers throughout the world have confirmed the faith placed in this technique and the doorstopper equipment is now being commercially manufactured.

REFERENCES

1. LEEMAN, E. R. "Rock stress measurements using the trepanning stress-relieving technique". Mine Quarry Eng., Vol. 30, No. 6, June 1964, pp. 250-255.

2. LEEMAN, E. R. "The measurement of stress in rock," Parts I-III, J. S.Afr. Inst. Min. Metall., Vol. 65, September, October, 1964, pp. 45-114, 254-284.

3. LEEMAN, E. R. "Absolute rock stress measurement using a borehole trepanning stress-relieving technique." Proc. Sixth Symp. on Rock Mechanics, Univ. Missouri, October 1964, pp. 407-426.

4. LEEMAN, E. R. "Remote measurement of rock stress under development in South Africa." Eng. Min. J., Vol. 165, No. 9, September 1964, pp. 104-107.

5. HAYES, D. J. "The in situ determination of the complete state of stress in rock: The principles of a proposed technique." Rep. Coun. Scient. Ind. Res. S.Afr., Meg 404, November 1965.

6. LEEMAN, E. R. "The in situ determination of the complete state of stress in rock: Laboratory tests to confirm the validity of a proposed technique." Rep. Coun. Scient. Ind. Res. S.Afr., Meg 463, July 1966.

7. LEEMAN, E. R. "The in situ determination of the complete state of stress in rock: Underground measurements at 64/40 Service Incline, Western Deep Levels." Rep. Coun. Scient. Ind. Res. S. Afr., Meg 512, November 1966.

8. LEEMAN, E. R. and HAYES, D. J. "A technique for determining the complete state of stress in rock using a single borehole." 1st Int. Congr. on Rock Mechanics, Lisbon 1966, Vol. II, pp. 17-24.

9. VAN HEERDEN, W. L. "Measurements of rock stresses at Shabanie Mine, Rhodesia, using the C.S.I.R. Triaxial Strain Cell." Rep. Coun. Scient. Ind. Res. S.Afr., Meg 663, April 1968.

10. BIENAWSKI, Z. T. "Deformational behaviour of fractured rock under multi axial compression." Rep Coun. Scient. Ind. Res. S.Afr., Meg 708, September 1968.

11. BONNECHERE, F. "A comparative study of in situ rock stress measurements." M.S. Thesis, Univ. of Minnesota, February 1967.

12. BONNECHERE, F. and FAIRHURST, C. "Determination of the regional stress field from "doorstopper" measurements." J. S.Afr. Inst. Min. Metall., Vol. 68, No. 12, July 1968, pp. 520-544.

13. VAN HEERDEN, W. L. "The effect of end of borehole configuration and stress level on stress measurements using doorstoppers." Rep. Coun. Scient. Ind. Res. S.Afr., Meg 626, January 1968.

References continued

14. GRAY, W. M. and TOEWS, N. P. "Analysis of accuracy in the determination of the ground stress tensor by means of borehole devices." Proc. 9th Rock Mech. Sym., Golden, Colorado, April 1967.

15. VAN HEERDEN, W. L. "Determination of the accuracy of "doorstopper" stress measurements in coal." Rep. Coun. Scient. Ind. Res. S.Afr., Meg 693, August 1968.

16. HENDROS, G. "The evaluation of Poisson's ratio and the modulus of materials of a low tensile resistance by the Brazilian (indirect tensile) test with particular reference to concrete." Austr. J. of Appl. Science, Vol. 10, No. 3, 1959, pp. 243-268.

17. SALAMON, M. D. G. Private communication.

18. VAN HEERDEN, W. L. and GRANT, F. "A comparison of two methods for measuring stress in rock." Int. J. Rock Mech. Min. Sci., Vol. 4, No. 4, 1967, pp. 367-382.

19. LEEMAN, E. R. "The determination of the complete state of stress in rock in a single borehole - laboratory and underground measurements." Int. J. Rock Mech. Min. Sci., Vol. 5, No. 1, January, 1968, pp. 31-56.

Appendix

THE USE OF A (0^o, 45^o, 90^o) THREE GAUGE ROSETTE TO DETERMINE THE STRESS COMPONENTS AT A POINT

Suppose the strains at any point O on the surface to which the rosette is glued are measured by means of a strain gauge rosette containing three strain gauges G_A, G_B, and G_C oriented relative to two axes X, Y as shown in Fig. A.

By a simple resolution of the strains in Fig. A it can be shown that the relations between the strains e_A, e_B, and e_C measured by the strain gauge G_A, G_B, and G_C and the state of strain at O, are given by:

$$e_A = e_X \cos^2\phi_A + e_Y \sin^2\phi_A + \gamma_{xy} \sin \phi_A \cos \phi_A \qquad (A.1)$$

$$e_B = e_X \cos^2\phi_B + e_Y \sin^2\phi_B + \gamma_{xy} \sin \phi_B \cos \phi_B \qquad (A.2)$$

$$e_C = e_X \cos^2\phi_C + e_Y \sin^2\phi_C + \gamma_{xy} \sin \phi_C \cos \phi_C \qquad (A.3)$$

where e_X and e_Y are the normal strains in the X and Y directions and γ_{xy} the tangential strain at O.

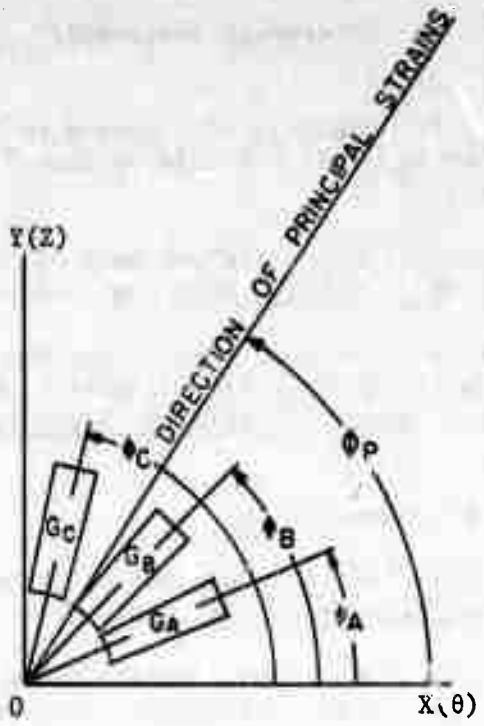
Y(Z)
DIRECTION OF PRINCIPAL STRAINS
ϕ_C
ϕ_P
ϕ_B
ϕ_A
G_C
G_B
G_A
0
X(θ)

Fig. A

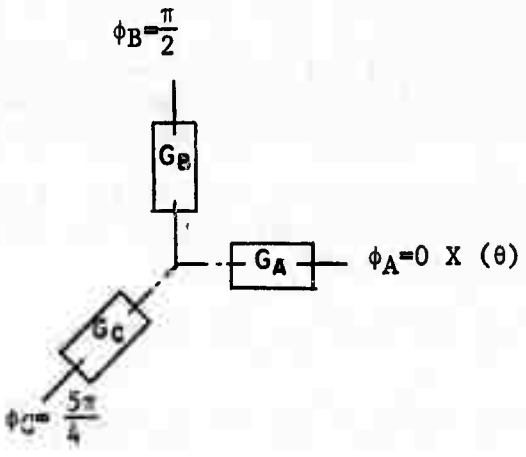
Y(Z)
$\phi_B=\frac{\pi}{2}$
G_B
G_A
$\phi_A=0$ X (θ)
G_C
$\phi_C=\frac{5\pi}{4}$

Fig. B

If now the strain gauges are arranged as shown in Fig. B such that G_A measures in the direction X, G_B in the direction Y and G_C measures at 45° to G_A and G_B then

$$\phi_A = 0, \qquad \phi_B = \frac{\pi}{2} \qquad \phi_C = \frac{5\pi}{4}$$

and substituting in equations (A.1) - (A.3) we obtain.

$$e_A = e_X$$

$$e_B = e_Y$$

$$e_C = e_{45^o} = 1/2 \left\{(e_X + e_Y) + \gamma_{XY}\right\}$$

$$= 1/2 \left\{(e_A + e_B) + \gamma_{AB})\right\}$$

$$\therefore \gamma_{AB} = 2e_C - (e_A + e_B)$$

The magnitudes of the principal strains, e_1 and e_2 may be calculated from the strain gauge readings e_A, e_B, and e_C given by G_A, G_B, and G_C by substitution in the following equation:

$$e_{1,2} = 1/2 \left\{(e_A + e_B) \pm \sqrt{[(e_A - e_B)^2 + \gamma_{AB}{}^2]}\right\}$$

$$= 1/2 \left\{(e_A + e_B) \pm \sqrt{[(e_A - e_B)^2 + \left\{2e_C - (e_A + e_B)\right\}^2]}\right\} \qquad (A.4)$$

Their directions may be calculated from the following expressions:

$$\tan 2\phi_p = \frac{\gamma_{AB}}{e_A - e_B} = \frac{2e_C - (e_A + e_B)}{e_A - e_B}$$

Writing $\sqrt{[(e_A - e_B)^2 + 2e_C - (e_A + e_B)^2]} = \sqrt{X}$

$$\sin 2\phi_p = \frac{e_{AB}}{\sqrt{X}} = \frac{2e_C - (e_A + e_B)}{\sqrt{X}} \qquad (A.5)$$

$$\cos 2\phi_p = \frac{e_A - e_B}{\sqrt{X}} \qquad (A.6)$$

$$\tan \phi_{1,2} = \frac{2(e_{1,2} - e_A)}{2e_C - (e_A + e_B)}$$

Notice, from (A.4) that

$$e_1 + e_2 = e_A + e_B \qquad (A.7)$$

and $$e_1 - e_2 = \sqrt{X} \qquad (A.8)$$

Now if σ_1 and σ_2 are the principal stresses on the surface of the borehole.

$$\sigma_1 = \frac{E}{1-\nu 2} (e_1 + \nu e_2) \tag{A.9}$$

$$\sigma_2 = \frac{E}{1 - \nu 2} (e_2 + \nu e_1) \tag{A.10}$$

where E = Young's modulus of the rock
ν = Poisson's ratio of the rock

The components of the normal stresses σ_A and σ_B in the A and B directions respectively and the tangential stress τ_{AB} are given by:

$$\sigma_A = 1/2 (\sigma_1 + \sigma_2) + 1/2 (\sigma_1 - \sigma_2) \cos 2\phi_p \tag{A.11}$$

$$\sigma_B = 1/2 (\sigma_1 + \sigma_2) - 1/2 (\sigma_1 - \sigma_2) \cos 2\phi_p \tag{A.12}$$

$$\tau_{AB} = 1/2 (\sigma_1 - \sigma_2) \sin 2\phi_p \tag{A.13}$$

In terms of strain, substituting for σ_1 and σ_2 from (A.9) and (A.10) in (A.11) to (A.13)

$$\sigma_A = \frac{E}{2} \left[\frac{e_1 + e_2}{1 - \nu} + \frac{e_1 - e_2}{1 + \nu} \cos 2\phi_p \right] \tag{A.14}$$

$$\sigma_B = \frac{E}{2} \left[\frac{e_1 + e_2}{1 - \nu} - \frac{e_1 - e_2}{1 + \nu} \cos 2\phi_p \right] \tag{A.15}$$

$$\tau_{AB} = \frac{E}{2} \left[\frac{e_1 - e_2}{1 + \nu} \sin 2\phi_p \right] \tag{A.16}$$

and substituting (A.5) to (A.6) in (A.14) to (A.16) we obtain

$$\sigma_A = \frac{E}{2} \left[\frac{e_A + e_B}{1 - \nu} + \frac{e_A - e_B}{1 + \nu} \right]$$

$$\sigma_B = \frac{E}{2} \left[\frac{e_A + e_B}{1 - \nu} - \frac{e_A - e_B}{1 + \nu} \right]$$

$$\tau_{AB} = \frac{E}{2} \left[\frac{2e_C - (e_A + e_B)}{1 + \nu} \right]$$

APPENDIX C

THE PHOTOELASTIC STRESSMETER

This appendix is a reproduction of A Laboratory Study of the Photoelastic Stressmeter, by A. Roberts, I. Hawkes, F. T. Williams, and R. K. Dhir, International Journal of Rock Mechanics and Mining Sciences, Vol. 1, No. 3, 1964. It may not be reproduced, in whole or in part, without the permission of the licensee of the copyright for Pergamon Press Journal back files, namely Microfilms International Marketing Corp. Fairview Park, Elmsford, New York 10523, and payment of the required copyright fee.

A LABORATORY STUDY OF THE PHOTOELASTIC STRESSMETER

A. Roberts, I. Hawkes, F. T. Williams and R. K. Dhir

Postgraduate School in Mining, Sheffield University
(Received 1 December 1963)

Abstract - A glass plug inserted into a borehole in a rock and illuminated by polarised light, acts as a biaxial gauge, the birefringence in the gauge produced by subsequent increase of stress in the rock identifying the ambient stress field in magnitude and direction.

The calibration characteristics of such a gauge are described, in stress fields ranging from uniaxial to hydrostatic, and in various materials of different modulus of elasticity.

INTRODUCTION

During the past few years the needs of mining and civil engineers to measure in-situ rock stresses has lead to the development of a wide range of equipment and techniques. In order to evaluate any particular technique it is necessary to understand the exact nature of the problem. Stresses inside a rock mass or massive structure are always three dimensional and in order to define the state of stress it is necessary to know the magnitude of the three principal stresses, which act at right angles to each other, and their directions in space. Nearly all the meters developed for measurement of in-situ stresses are uniaxial, so that from a single instrument only one randomly orientated stress component can be obtained. The complete evaluation of the stress system thus requires the measurement of independent stress components from six individual meters orientated in a fixed manner[1].

Theoretically it is impossible to measure stress directly. A known stress can be applied to a body provided only that the loads, cross-sectional areas and geometric concentration effects are taken into consideration, but the stresses produced by an unknown load can only be calculated from the resultant strains and a knowledge of the elastic moduli of the body. This gives rise to difficulties, particularly in the case of rocks, as the relationship between stress and strain is seldom uniform and depends, amongst other factors, on whether the rock is being loaded or unloaded, the direction of loading and the nature and past history of the rock.

It is with all these problems in mind that the photoelastic stressmeter has been developed in its present form.

THE PHOTOELASTIC STRESSMETER

The photoelastic stressmeter has been described in several recent publications [2, 3]. It is illustrated in Fig. 1 and consists essentially of a plug of optical glass in the form of a cylinder containing an axial hole, together with a light source and filters producing circularly polarized light. In use, the meter is bonded around its peripheral surface into a borehole in such a manner that the face of the plug remote from the light source can be viewed by an observer looking down the borehole. If the meter is than subjected to stress the nature of the resultant strain can be made apparent by using the birefringent property of the glass material. The full theory of birefringence can be found in any standard text book on photoelasticity, but as applied to

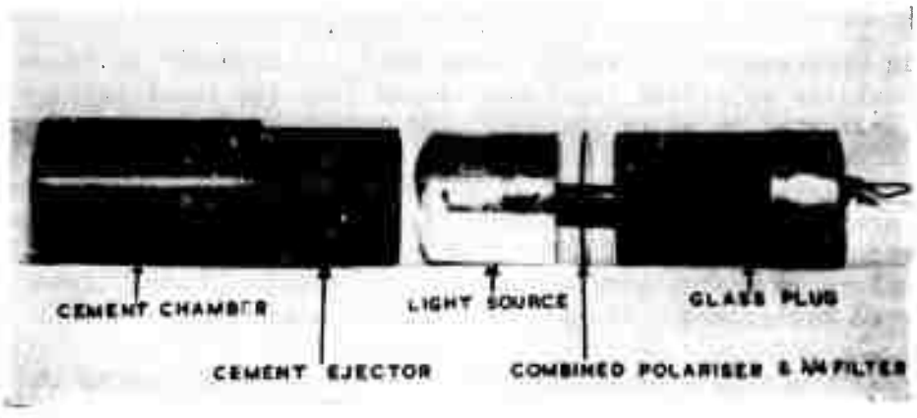

FIG. 1. The Photoelastic Stressmeter.

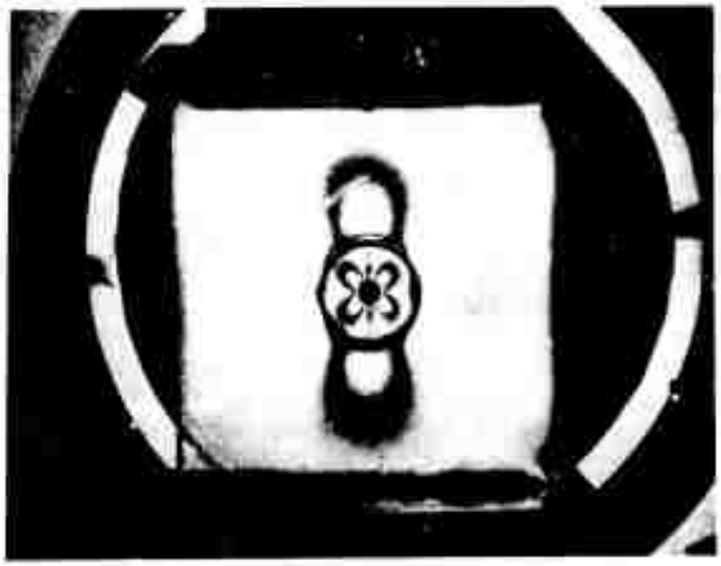

FIG. 3. Fringe pattern observed in a photoelastic stressmeter set in an acrylic resin slab, under uniaxial compression.

the photoelastic stressmeter, it simply means that if the meter is illuminated from behind with circularly polarized light and viewed from the front through a combination of two filters, referred to as an analyser, the shear strain in the glass cylinder will be revealed as a coloured pattern. In this pattern there are zones of very distinct changes of colour between blue and red or green and red areas. These are very easily identified and are called 'tints of passage' as they mark the boundaries between fringe orders in a birefringent pattern. If a coloured filter is incorporated in the analyser the coloured pattern is replaced by a pattern consisting of black lines seen against a uniformly coloured background. The black lines or zones are referred to as 'fringes'.

In both cases the number of fringes is directly proportional to the shear strain in the glass. By means of the process of goniometric (Tardy) compensation in which the plane polarising filter in the analysing viewer is rotated relative to the quarter wave plate, the observed fringe pattern can be optically advanced or retarded to obtain values of fractional fringe orders.

The object of the present paper is to describe the results of a laboratory investigation of the optical characteristics of the stressmeter. In this investigation certain relationships of an empirical nature have been deduced which, together with accepted theory, enable the stress field in a body within which the meter has been inserted to be defined in terms of the number, shape, and orientation if the interference fringes observed.

THEORETICAL CONSIDERATIONS

Three dimensional or triaxial stress field analyses are very complicated and in order to make a theoretical study of the behaviour of the photoelastic stressmeter, the analysis must be limited to the biaxial case. This is quite justified as the photoelastic stressmeter acts as a biaxial gauge in that the shear strains observed as interference patterns are those produced by the stress components acting in the plane perpendicular to the axis of the meter, and the remaining stress component acting along the axis of the meter does not effect these shear strains. Theoretically, therefore, the meter can be considered as a circular inclusion in a body subjected to a biaxial stress field. The relationship between the stress induced in a rigid inclusion, and the stress in the surrounding material has been studied by Sezawa and Nishinuira [5], Coutinho [6] and Wilson [7]. Using their results the shear stress induced in a rigid inclusion is given by:

$$S = \frac{\sigma_1 - \sigma_2}{K - k} \tag{1}$$

Where σ_1 and σ_2 are the principal stresses in the surrounding materials and K and k are two constants dependent on the elastic properties of the surrounding material and inclusion. K and k have been defined by Wilson in the form:

$$K = \frac{(1 + \mu_B)\ (3 - 4\mu_B)}{8(1-\mu_A)\ (1 + \mu_A)} \times \frac{E_A}{E_B} + \frac{5 - 4\mu_A}{8(1-\mu_A)}, \tag{2}$$

$$k = \frac{(1 + \mu_B)\ (1 - 4\mu_A)}{8(1-\mu_A)\ (1 + \mu_A)} \times \frac{E_A}{E_B} + \frac{4\mu_A - 1}{8(1-\mu_A)}. \tag{3}$$

Where E_A and E_B are the modulii of elasticity of the surrounding material and inclusion respectively and μ_A and μ_B are the relevant Poisson's ratios.

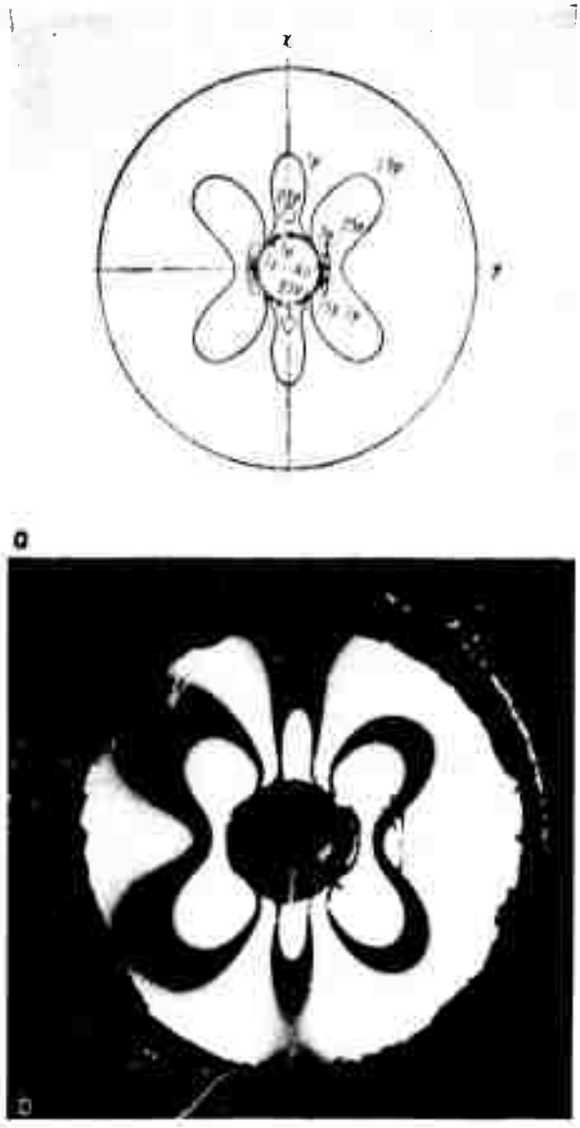

FIG. 2. Theoretical and observed fringe patterns in a phoyoelastic stress-meter.

(a). Theoretical isochromatics in a uniaxial stress field (Hiramatsu et al).
(b). Observed isochromatics in a uniaxial field.

Coutinho plotted values of K and k against the ratio E_B/E_A for various values of E_B/E_A and showed that for ratios of E_B/E_A greater than 2 the values of K and k remain sensibly unaltered. The elastic modulus of the glass used in the photoelastic stressmeter is approximately 10×10^6 psi and this very important theoretical conclusion indicates that if the meter is used in a material having a maximum elastic modulus below 5×10^6 psi any non-linearity of the stress-strain relationship will not influence the stress induced in the meter. In all materials having a modulus less than 5×10^6 psi the shear stress induced in the meter is also independent of the modulus and proportional only to the stresses in the surrounding material. Since the glass used in the meter is elastic, the fringe patterns generated are directly proportional to the stress in the glass and therefore directly proportional to the stresses in the surrounding material.

The stresses induced in a solid circular inclusion however are theoretically uniform throughout the inclusion. In order to produce the differential stresses necessary for interference fringe patterns it is essential to disrupt this uniform shear stress in the meter. This is best achieved by providing the meter with an axial hole. Hiramatsu, Niwa, and Oka [8] have carried out a detailed mathematical analysis of the shear stress pattern induced in such an inclusion. Their results are best illustrated in graphical form and Fig. 2 (a) which shows the shear stress in a meter set in a body under uniaxial compression was calculated by their method. Figure 2 (b) is a photograph of a fringe pattern taken by the authors from a photoelastic stressmeter inserted in a block of rock (Darley Dale sandstone) under uniaxial stress. It will be noted that the shape and symmetry of the fringe patterns coincides closely with the theoretical form.

The theoretical conclusions which can be drawn from the studies of Coutinho and Hiramatsu et al. may be summarised as follows:

1. The orientation of the two principal stresses in the plane of the meter are given by the two axes of symmetry, i.e. in Figs. 2 (a and b) these are vertical and horizontal.

2. The major and minor axes are identified by the distribution of the fringes in the two axes of symmetry. For example it will be noted that in Fig. 2 the distribution of fringes in the upper and lower halves of the meter is quite different from the distribution in the two horizontally adjacent halves. It is not immediately obvious from Fig. 2 which is the major and which the minor axis. The technique for determining these will be discussed later.

3. The magnitude of the principal stresses in the material surrounding the meter is proportional to the number of fringes in the meter. If the meter is inserted into a body with an elastic modulus below 5×10^6 psi the modulus of the material will not effect the sensitivity of the meter. For example the fringe/stress relationship with the meter inserted into sandstone should be equal to that for coal or any other material with a low modulus.

4. The relationship between the principal stresses in the surrounding material will be identified by the shape of the fringe pattern in the meter.

All the theoretical treatment of the photoelastic stressmeter is based on the assumption that the meter is perfectly elastic, and that it is in perfect contact with the surrounding material, which is also completely elastic. All of these conditions are rarely obtained in practice.

The problems which have to be resolved in order to fully evaluate the photoelastic stressmeter can be considered to fall into the following groups:

(a) Transmission of stress from the body to the stressmeter. The main problem here is the influence of the nature and thickness of the cement bond on the fringe patterns in the meter.

(b) The design criteria of the stressmeter. The problems in this category are concerned with the ratio of the outside diameter of the plug in relation to its internal diameter and the overall dimensions of the meter as they effect the sensitivity and ease of reading.

(c) Fringe pattern interpretation. The problems associated with the interpretation of the pattern fall into the following subgroups:

  (1) Identification of the directions of principal stresses.
  (2) Identification of the major and minor axes.
  (3) Identification of the magnitude of the individual principal stresses.

(d) The effects on the stressmeter of creep and of non-linear stress/strain characteristics of the surrounding material.

(e) The effect on the stressmeter produced by non uniform stress fields and the influence of the meter on the stress distribution in the surrounding material.

Many of these problems are, of course, interelated and the object of the experimental investigation was not necessarily to isolate one particular problem, this frequently being impossible, but to examine the behaviour of the stressmeter in a range of different materials under various loading conditions.

EXPERIMENTAL PROCEDURE

In order to examine the behaviour of the meter when inserted into various materials subjected to stress it is essential that the stress field within the test piece is fully understood.

There are two problems in this respect; the first is to ensure that the influence of the inclusion or meter on the stress field does not reach the free surfaces of the test piece; and secondly that the stress field in the area of influence of the meter is uniform and predictable. There is considerable literature on the theoretical stress distribution around a hole in a uniform stress field, the major part of which has been fully confirmed by photoelastic model studies. From this work, which has been summarized by Savin [9], it can be concluded that the influence of the hole does not significantly effect the stress field in the surrounding material for a distance greater than 2d (where d is the diameter of the hole) from the edge of the hole. When the hole is filled by an inclusion having the same modulus as the surrounding material the inclusion has no effect on the stress field which remains completely uniform. Work carried out by Stephen and Pirtz [10] indicates that when the inclusion has a modulus of around 4 times that of the surrounding material the area of influence of the inclusion is roughly one diameter from the edge of the hole.

Tests carried out by the writers have confirmed these general conclusions.

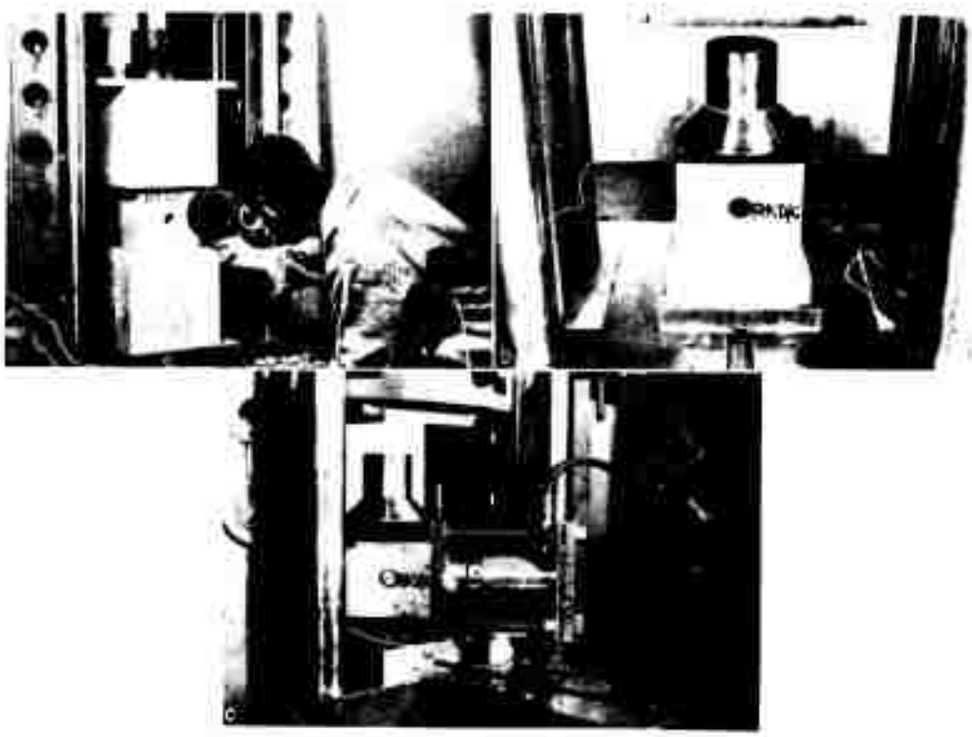

FIG. 4. Arrangement for calibration of stressmeter.

(a). Meter inserted in a cube of rock, set between rock platens.
(b). Meter inserted in a slab of rock.
(c). Biaxial calibration of stressmeter.

CALIBRATION IN TEST SLABS

The system of testing the stressmeter in cubes of material is not a practical one for biaxial stress fields and it was decided to investigate the calibration of the meters in slabs of material having a thickness equal to the stressmeter length. To compare the results obtained in the slabs with those obtained in the cubes and also to check on the required size of the slab relative to the stressmeter diameter, a series of experiments was carried out as follows:

A 1 1/4 in. diameter stressmeter of 1 1/2 in. length was set in an 8 in. cube of Darley Dale Sandstone and calibrated uniaxially, the cube being placed between 12 in. cube platens of the same material. The test cube was then systematically reduced in size by slicing it in a direction normal to the meter until a slab 1 1/2 in. thick was obtained, the meter than occupying the full thickness of the slab. In this form the calibration was repeated between the rock platens and then between steel platens as illustrated in Fig. 4(b). The results are given in Fig. 5 as graphs A, C, and D. The slight difference between the three calibrations is sufficiently small to be neglected. It can be concluded, therefore, that meters calibrated in slabs between steel platens are in a uniform and predictable stress field.

The required size of slab relative to that of the stressmeter was checked by setting a meter in a slab of acrylic resin 10 in. square and 1 1/2 in. thick. The meter was calibrated repeatedly as the slab was progressively reduced in sizes in stages of 1 in. until a 5 in. slab remained. No significant change in the stress/fringe order sensitivity was observed.

A wide range of slab sizes were subsequently tested with various sizes of stress-meter. In all cases the length of the slab side was not reduced below $2 \cdot 5\,d$ where d was the diameter of the stressmeter.

Figure 4 (c) illustrates the biaxial loading system used by the authors. In this case the meter is shown set in a slab of Darley Dale Sandstone.

CALIBRATION PROCEDURE

All the calibration experiments were made with the meter illuminated by transmitted light. The procedure for calibration consisted of setting the test tube or slab, with meter installed, between the appropriate loading platens, taking care to obtain uniform loading. The load was then increased in stages, the fringe pattern being read at each increment of load by viewing the meter through a Precision Hand Viewer illustrated in Fig. 4(a). When loading slabs biaxially the loads along both axes were increased simultaneously, keeping the ratio between the major and minor load directions constant. The fractional fringe orders at each increment were measured by goniometric compensation in the manner which will be described in a subsequent section of the paper.

INTERPRETATION OF FRINGE PATTERNS

The results given in the following sections are related to the use of white light or sodium light, both of which give the same fringe sensitivity. The effects of using coloured filters are discussed in a later section.

Figure 3 illustrates a stress meter set in a slab of birefringent acrylic resin under uniaxial compression. It will be noted that the stress concentration in the material surrounding the meter extends for approximately one diameter above and below the meter. Under biaxial loads a stress concentration would also be produced at the sides of the meter. From these studies it was concluded that the minimum distance from the edge of the hole to the sides of the test specimens should not be less than twice the diameter of the meter.

The design of the loading system required to produce uniform and predictable stress fields has been studied in detail by several workers. Chakravarty [11] carried out such a study using the photoelastic coating technique and he showed that uniform stress fields are produced in the centre third of a specimen having a height to diameter ratio of 3:1. This work formed the basis of the cube calibration technique.

CALIBRATION IN TEST CUBES

In order to obtain uniform uniaxial compressive stresses, test cubes of Darley Dale Sandstone were placed between larger cubes of the same material and loaded in a 100 ton testing machine. Figure 4 (a) illustrates this rock platen loading system. Figure 5 shows the calibration obtained with this system (graph A) as compared with that obtained with steel platens (graph B). It will be seen that the error in calibration when it is assumed that the steel platens give a uniform stress field is of the order of 50 percent. This error is not due to uneven contact but to the frictional effects between the steel and rock and the different Poisson's ratios of these materials. In all the test work very great care was taken to ensure that the loading surfaces of the test specimens were flat, smooth, and parallel. The surfaces of the cubes were cut in one pass by a 2 ft. diameter diamond saw and the resulting face was surface ground and then finally tested, observing the amount of light passing between the rock and a straight edge laid on the rock surface. Spherical seating washers were also employed to ensure axial loading of the specimens.

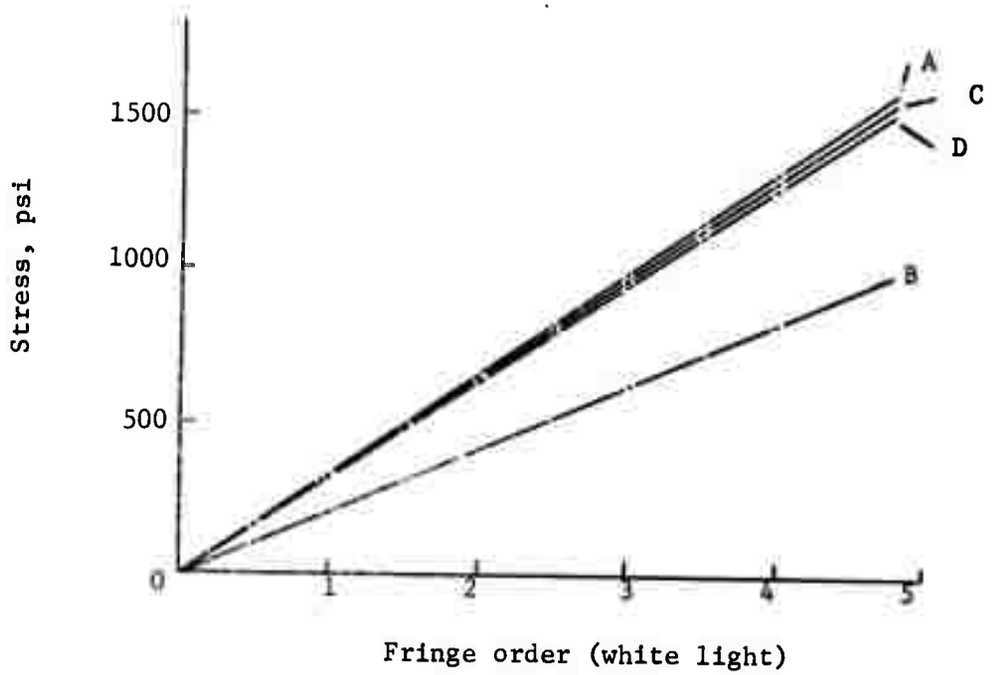

Fig. 5 Calibration characteristics of a photoelastic stressmeter (length 1 1/2 in.) under uniaxial compression, using the 45° compensation points.

A meter set in a cube, between rock platens,
B meter set in a cube, between steel platens,
C meter set in a slab, between rock platens,
D meter set in a slab, between steel platens.

All the experimental work has so far been carried out with the meter subjected only to compressive stress. The transmission of tensile stresses to the meter is a separate problem which is not within the scope of the present paper.

PRINCIPAL STRESS DIRECTIONS

In all the tests carried out, the axes of symmetry of the fringe pattern in the meters were found always to be in the directions of the applied principal stresses. An example of this is shown in Fig. 3 where the direction of loading and pattern symmetry are clearly visible. As the meter is illuminated by circularly polarised light, the axis of orientation of the fringe pattern is dependent only on the stresses applied to the meter from the surrounding material. The accuracy with which the directions of the principal stresses can be interpreted depends entirely on the method of transferring the orientation to some independent datum. For example, by aligning the crosshairs of a telescope with the axis of the pattern, the orientation can be measured with precision.

The next stage of the observation is to establish which is the major principal stress direction. Figures 6 and 7 illustrate a range of typical patterns in which the major stress direction is vertical, i.e. from the top to the bottom of the page. Figure 7 (e) is a special case of hydrostatic uniform loading in which there is no direction of principal stress. Figures 6 (a), (b), (c), and (d) are fringe patterns photographed from a meter under gradually increasing uniaxial compression. It will be noted that the fringes are generated about the minor axis subsequently moving outwards and around towards the major axis. Figure 7 which shows five biaxial patterns at an exact fringe order of 3 shows a similar effect. It is thus possible to establish readily which is the major axis by the symmetry of the observed pattern. A check can be made by observing the movement of the fringes in the process of goniometric compensation. The handle of the Precision Hand Viewer is first aligned with the assumed major stress direction. If the alignment is correct, rotation of the analyser in a clockwise direction from its zero position will retard the pattern, i.e. the fringes crossing the minor axis will shrink towards the central hole of the meter. Holding the meter at 90° to this position with the handle aligned on the minor stress axis will produce the reverse effect, the fringes expanding outwards along the minor stress axis.

COUNTING THE FRINGES

The fringes, which are generated at the inner surface of the central hole in the meter about the minor stress axis, are not uniformly distributed throughout the meter but tend to pack very closely together near the periphery of the hole. This effect can be seen clearly in Fig. 8(a) which illustrates a meter under a biaxial stress field of 1 : 1/2. This concentration of fringes near the hole makes a precise fringe count very difficult at high loads. In order to overcome this difficulty it was decided to blank off the area of the meter immediately around the centre hole by fitting an opaque collar.

Figure 8 (b) illustrates the same meter as in Fig. 8 (a) under the same load but with the collar inserted. In Fig. 8 (b), three full fringes can easily be seen and counted. With this arrangement the fractional fringe order is measured by compensation, i.e. rotating the analysing polaroid, until the fringe nearest the collar is brought back to its edge on the minor axis as shown in Fig. 8 (c). The fractional

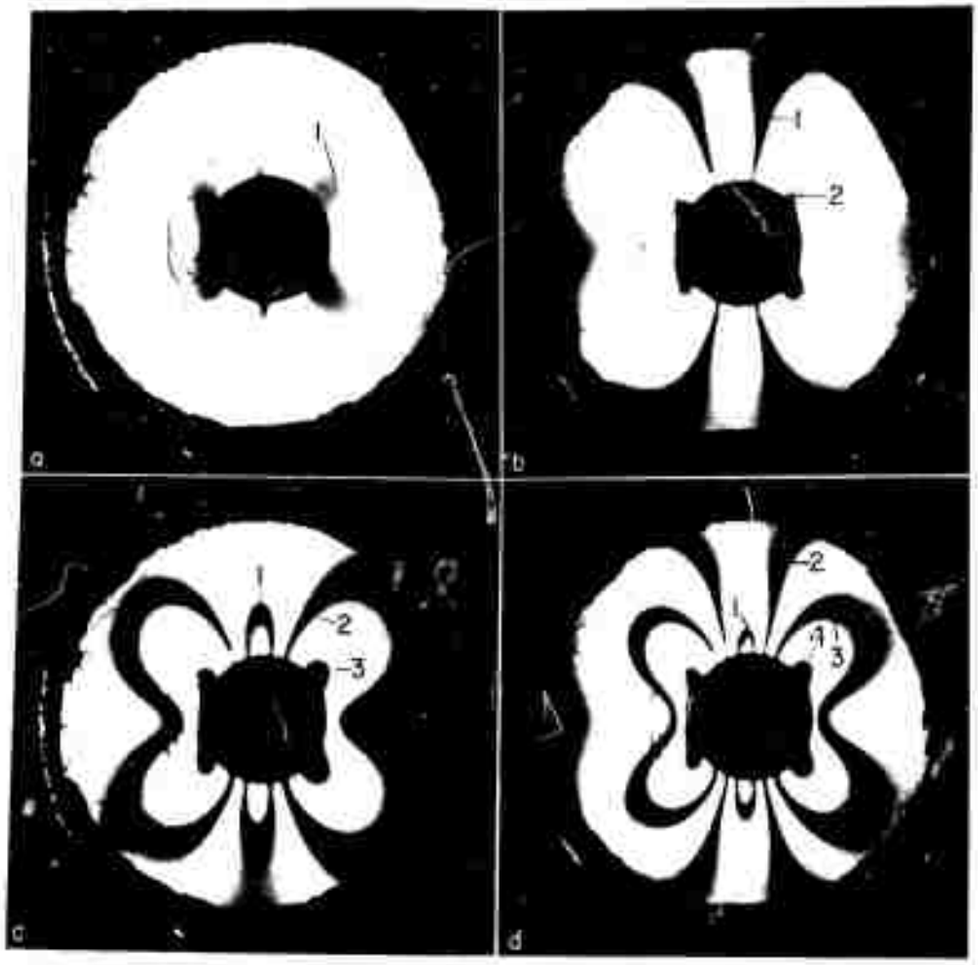

FIG. 6. Uniaxial fringe patterns.

(a). 1 fringe.
(b). 2 fringes.
(c). 3 fringes.
(d). 4 fringes.

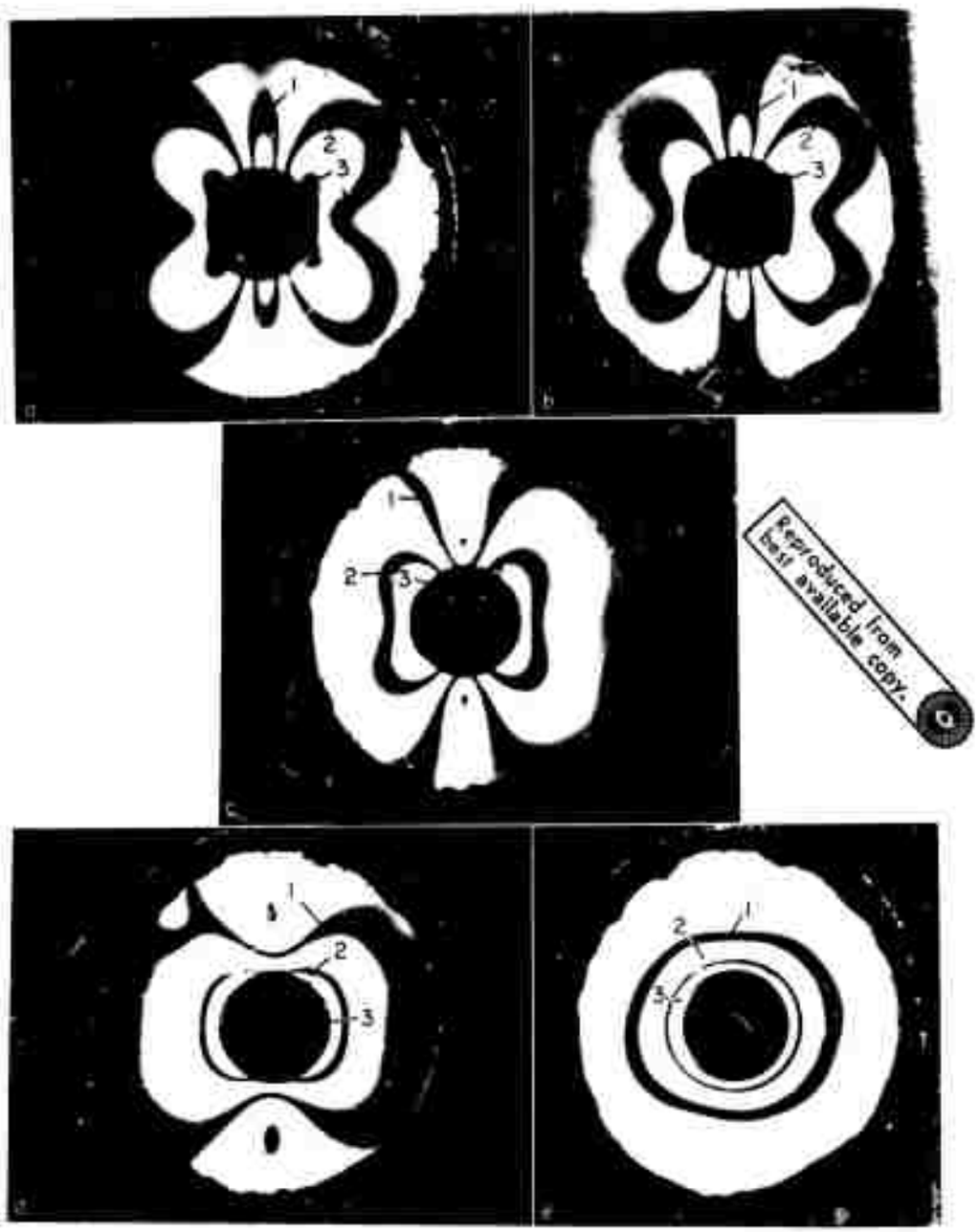

FIG. 7. Biaxial patterns (all at three fringes).

(a). Ratio of principal stresses 1 : 0.
(b). Ratio of principal stresses 1 : 1/4.
(c). Ratio of principal stresses 1 : 1/2.
(d). Ratio of principal stresses 1 : 3/4.
(e). Ratio of principal stresses 1 : 1.

fringe order is then read off the scale of the viewer and then added to the whole fringe count. In the example shown in Fig. 8 the final reading is 3 · 50 fringes. This technique of compensation to bring the last fringe to the collar edge is used for all fringe orders and principal stress ratios. The points to which the last fringe must be compensated are also clearly seen in Fig. 7 in which all the meters read 3 fringes.

UNIAXIAL STRESSES

The fringe pattern in a uniaxial stress field may be considered as a special case in that there are four very distinct points on the pattern at any of which the fringes can be counted and to which they may be compensated. Figure 9 shows two fringe patterns taken from a meter (without the centre collar) set in a sandstone slab under uniaxial compression. Figure 9 (a) shows the meter under a particular stress, and Fig. 9 (b) shows the finges compensated to four points marked 'X' which lie on lines passing through the meter centre at 45° to the principal stress directions. At those four points the fringes develop quite suddenly and very distinctly as the stress increases. Because of the ease at which the fringes can be recognised and compensated at these points they may be used in preference to the technique of compensating to the collar edge if desired. Figure 6 previously referred to show these 45° goniometric compensation points for a range of one to four fringes.

ACCURACY OF READING FRINGE ORDERS

The accuracy with which the fringe orders can be read is dependent on the judgment of the observer in retarding a given fringe pattern to an exact point. A trained observer can compensate a fringe to a predetermined point with an accuracy of ± 0.01 fringes. To check the performance of an average observer, ten laboratory technicians, who previously had never used the equipment were asked to measure a series of fringes in uniaxial compression, compensating the fringes back to the collar edge. Where the fringes were not absolutely symmetrical the fringes were compensated to each side of the collar and the average taken. The results are given in Table 1. It will be noted that even in the case of these untrained observers the deviation amongst them is small.

Table 1. Fringe Orders Read From a Photoelastic Stressmeter Set Under Two Levels of Uniaxial Stress

Observer	Stress level A	Stress level B
1	2·41	1·71
2	2·43	1·69
3	2·41	1·70
4	2·44	1·72
5	2·41	1·69
6	2·40	1·72
7	2·40	1·71
8	2·42	1·75
9	2·43	1·72
10	2·42	1·72

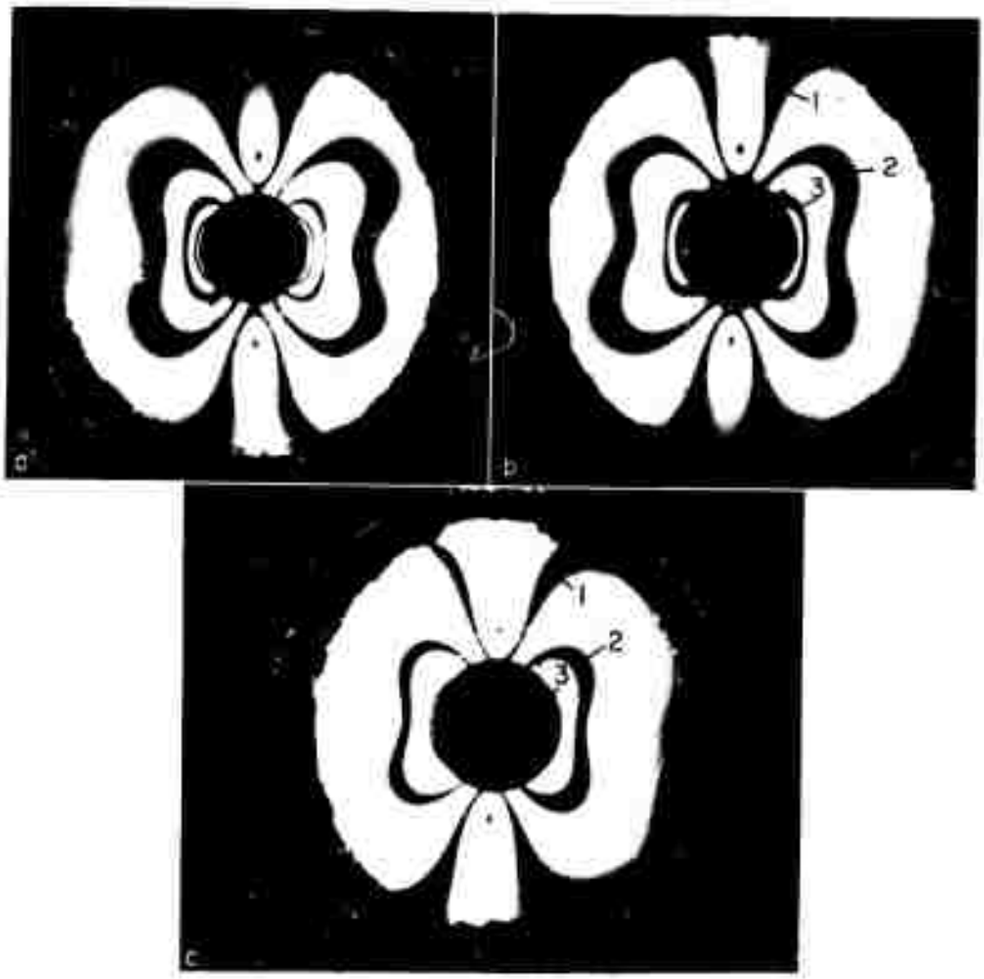

FIG. 8. Stressmeter in a biaxial field (ratio of principal stresses 1 : 1/2),

(a). Appearance of meter without axial collar.
(b). Appearance of meter when fitted with axial collar.
(c). Appearance of meter when fringe pattern is compensated to the collar edge on the minor stress axis.

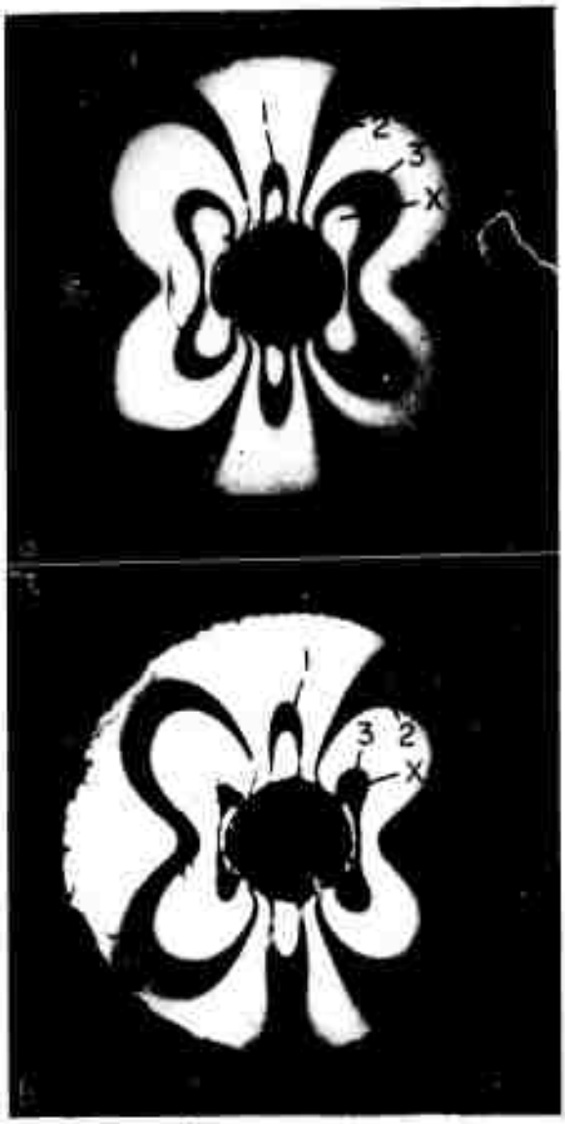

FIG.9.Stressmeter in a uniaxial field.

(a). Appearance of meter as observed before compensation.
(b). Fringe pattern compensated to four reading points (x) at 45° to axes of symmetry.

EVALUATION OF THE MAJOR PRINCIPAL STRESS

The biaxial stress field existing in the plane of measurement of the meter may range from uniaxial, i.e. only one principal stress to 'hydrostatic' in which both stresses have equal magnitude. It is convenient to interpret the fringe pattern in terms of the major stress, as this is likely to be the more important one, and then to evaluate the proportional value of the minor stress.

LINEARITY OF THE FRINGE ORDER-MAJOR STRESS RELATIONSHIP

Figure 10 shows the relationship between applied uniaxial stress and fringe order for three different materials, brass, Cornish granite and Darley Dale sandstone. These may be considered as typical for metal, igneous rock and sedimentary rock respectively. The Young's moduli for these materials are:

Brass 14×10^6 psi
Granite 8.5×10^6 psi
Sandstone 2.4×10^6 psi

When the meter is set in brass and granite slabs the calibration is completely linear with no evidence of hysteresis between loading and unloading cycles. The results shown are averages of several loading and unloading cycles. The scatter of the results, which is relatively small, is indicated on the graphs.

When the meter is set in Darley Dale sandstone however, there is evidence of a certain amound of non linearity and hysteresis between the first and second loading cycle. The results given in Fig. 10 relate to a slab of rock not previously loaded and after the first loading cycle the meter response followed the second cycle pattern of reading shown.

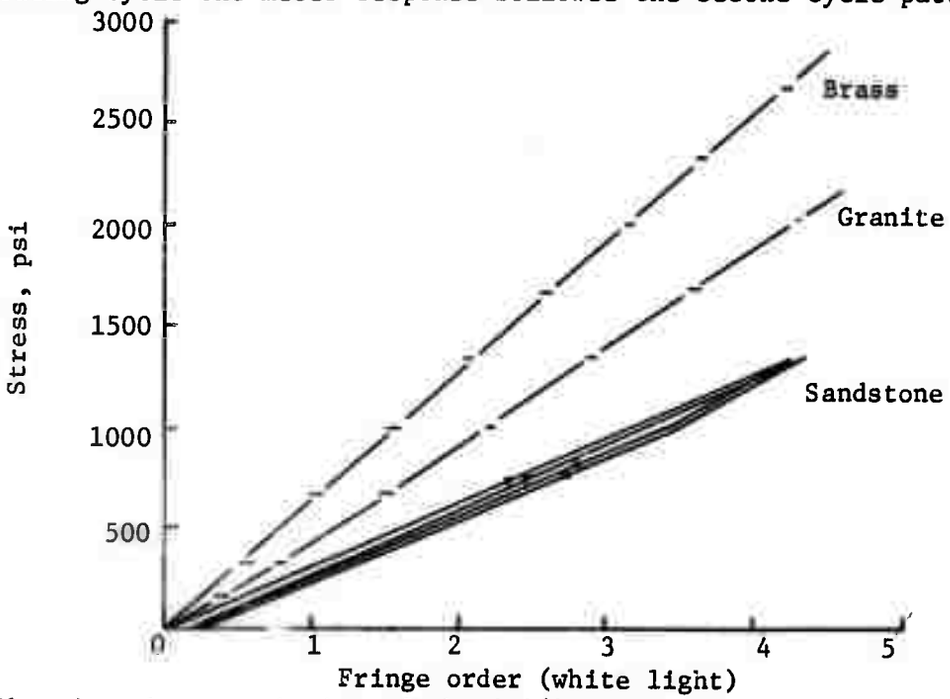

Fig. 10 Calibration characteristics of the 1 1/2 in long stressmeter in three materials (Uniaxial stress field).

It is interesting to note that the inclination of the loading portion of the graphs are parallel and linear for the two cycles, and that the unloading cycles after changes in direction at near maximum stresses are also nearly parallel to the loading cycle graph.

In all, 15 different materials were used in calibration tests of the stressmeter and in all cases linearity in its response to stress was observed. Several of the sedimentary rocks exhibited the hysteresis phenomenon. The results are given in Table 2. Several slabs of material were calibrated under biaxial loading conditions. Figure 11 shows the calibration of Darley Dale sandstone under a range of biaxial loading conditions. The response of the meter in terms of stress increment per fringe varies in the different stress fields but for any particular ratio of principal stresses the relationship is constant. In other words, in any stress field, if the ratio of stresses remains constant, the response of the meter is linear.

EFFECT OF THE CEMENT LAYER

The cement used to bond the meter into the surrounding materials is a cold setting epoxy resin containing a finely ground hard filler. Experiments were made with three different cements and varying quantities of fillers with meters set in acrylic resin slabs. No appreciable changes were observed in the calibration figures obtained.

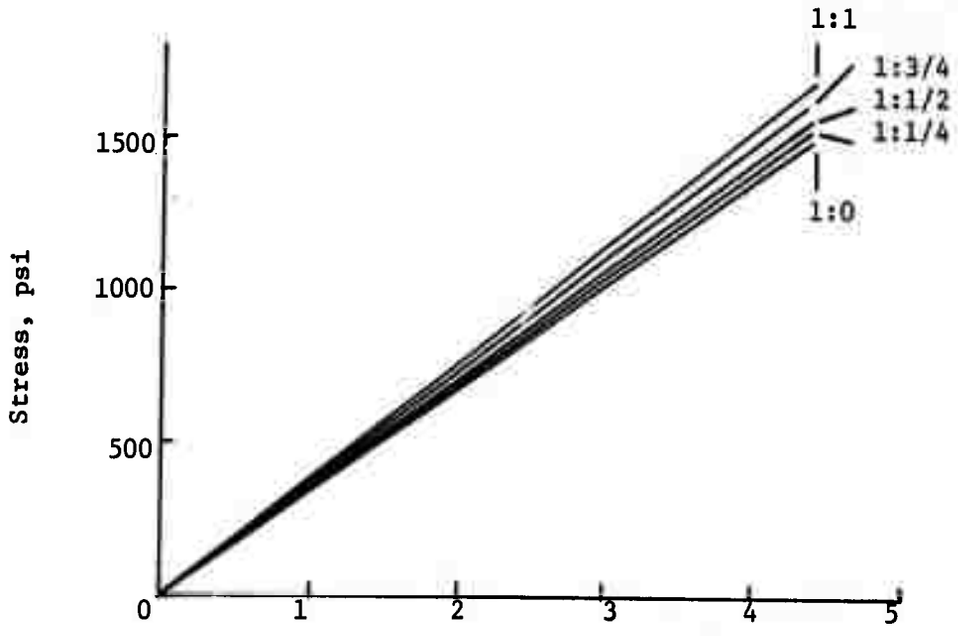

Fig. 11 Calibration characteristics of 1 1/2 in. long stressmeter in sandstone, under various biaxial stress fields (Ratios of principal stresses indicated)

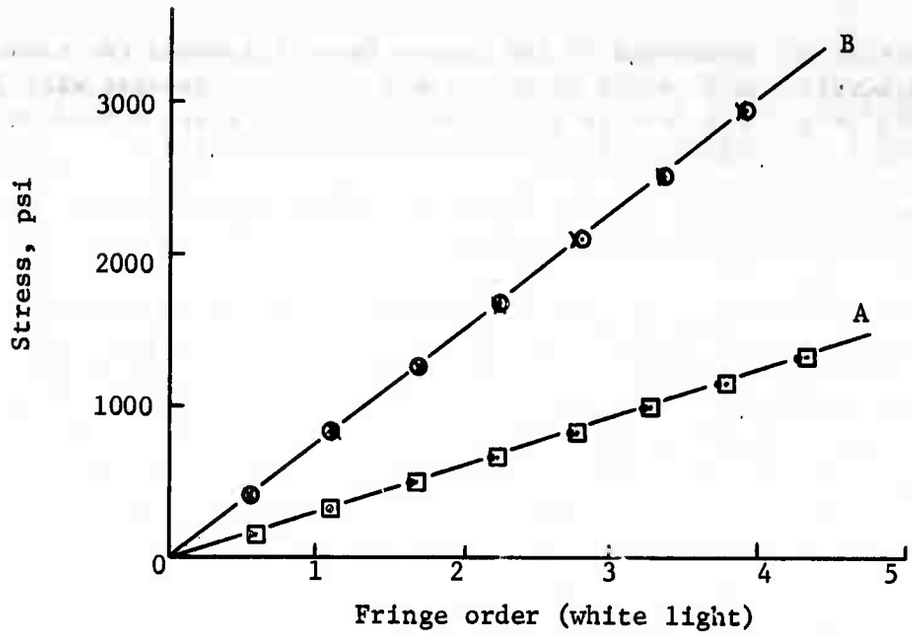

Fig. 12 Calibration characteristics of stressmeters in different materials & cements.

A Meter set in 'perspex' slabs 1 1/2 in. thick.
⊡with 1/32 in. cement layer.
•with 1/16 in. cement layer.

B Meter set in glass slab 1 in. thick.
⊙with no cement.
xwith 1/32 in. cement layer.

Table 2. Effect of Young's Modulus of Test Piece Upon Fringe Sensitivity of the Meter

Material	Young's modulus E psi	Meter sensitivity psi/fringe
Perspex	4×10^5	317
Coal	5×10^5	320
Brick	2.0×10^6	306
Red Sandstone	2.0×10^6	304
Fossiliferous Limestone	2.4×10^6	318
Darley Dale Sandstone	2.4×10^6	316
Portland Limestone	3.6×10^6	297
Coarse Ground Sandstone	3.8×10^6	299
Concrete	4.2×10^6	320
Marble	6.1×10^6	430
Granite	8.5×10^6	470
Glass	10.0×10^6	504
Brass	14.0×10^6	635
Steel	30.0×10^6	1270

To test the effect of variations in the cement layer thickness two identical meters were set in acrylic resin slabs having cement layer thicknesses of 1/16 in. and 1/32 in. respectively. The results are shown in Fig. 12 graph A from which no significant difference is apparent between the two sets of results.

A further investigation into the effect of the cement layer between the meter and surrounding material was carried out as follows:

A 1 in. thick slab of glass was very accurately ground into a rectangle 9.2 x 8 in. and a 1/4 in. hole was drilled through the centre. The slab was then loaded and the fringe orders were read around this central hole using the special uniaxial compensation technique previously described. The hole in the glass was then overcored using a diamond drill 1 1/4 in. internal diameter and wall thickness 1/32 in. The resulting cylinder which is, of course, in the form of a stressmeter, was then cemented back into the hole in the glass slab, and the fringe pattern in it again calibrated against applied stress.

The results of the two calibrations, with and without the cement band are given in Fig. 12, graph B. No significant influence due to the cement was observed. In view of the linearity of the results of other materials it is a reasonable assumption that in so far as stress transmission to the meter is concerned the effect of the cement can be neglected within the range tested. Theoretical work on the transmission of stress to a high modulus inclusion by Wilson [7] supports this general conclusion.

EFFECT OF VARIATION IN DIMENSIONS OF THE STRESSMETER

Theoretically, as has been mentioned earlier, the area of influence of a hole in an elastic body subjected to stress extends to a diameter of approximately 5 d, where d is the diameter of the hole. It would therefore be expected that, in a stressmeter of diameter D, variations in diameter of the central hole below D/5 would have no effect on the sensitivity of the meter. Figure 13 illustrates the results of tests made to substantiate this point. It will be noted that as the ratio OD/ID decreases the sensitivity of the meter increases. It was decided however to standardise on a ratio OD/ID ratio of 5 : 1 as with lower ratios the 1st and 2nd fringes tend to be lost from the field of meters in which the OD/ID ratio is 5 : 1 except where otherwise stated.

From Fig. 13 it will also be noted that there is no scale effect, i.e. the 3 in. dia. meter with a 1/2 in. dia. central hole gives exactly the same reading as a 1 1/4 in. meter with a 1/4 in. hole.

Theoretically the sensitivity of the meter is directly proportional to the length of the light path, i.e. the length of the meter. Tests made with meters ranging from 6 in. down to 1 in. length, illuminated by transmitted light, have completely substantiated this fact.

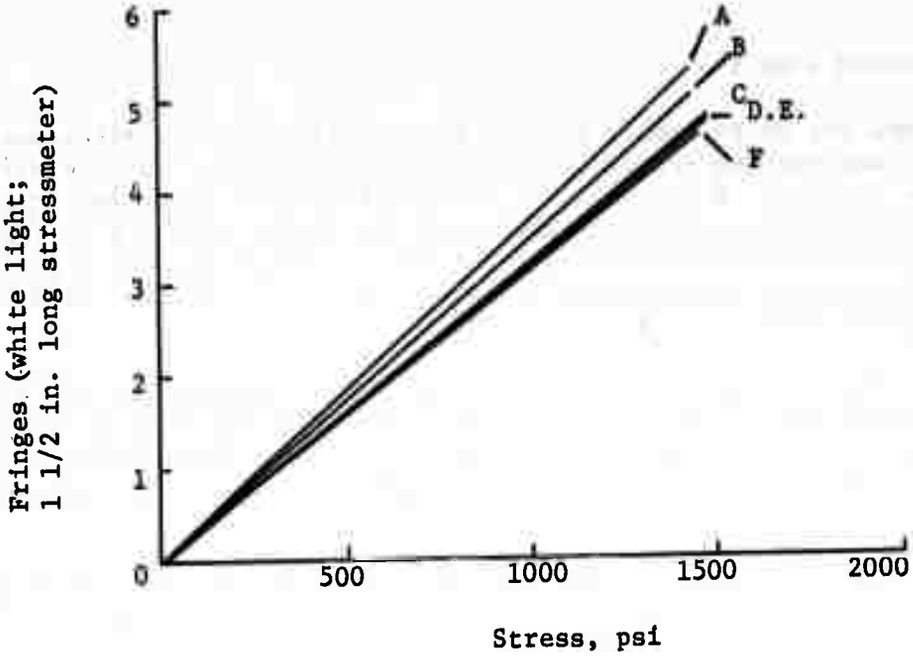

Fig. 13 Calibration characteristics of 1 1/2 in. long stressmeters with various ratios of external to internal diameter in white light (Uniaxial stress field).

stressmeter A ratio 3.2 : 1.
stressmeter B ratio 3.33 : 1.
stressmeter C ratio 5 : 1.
stressmeter D ratio 6 : 1 (1.5 : 0.25).
stressmeter E ratio 6 : 1 (3.0 : 0.5).
stressmeter F ratio 6.66 : 1.

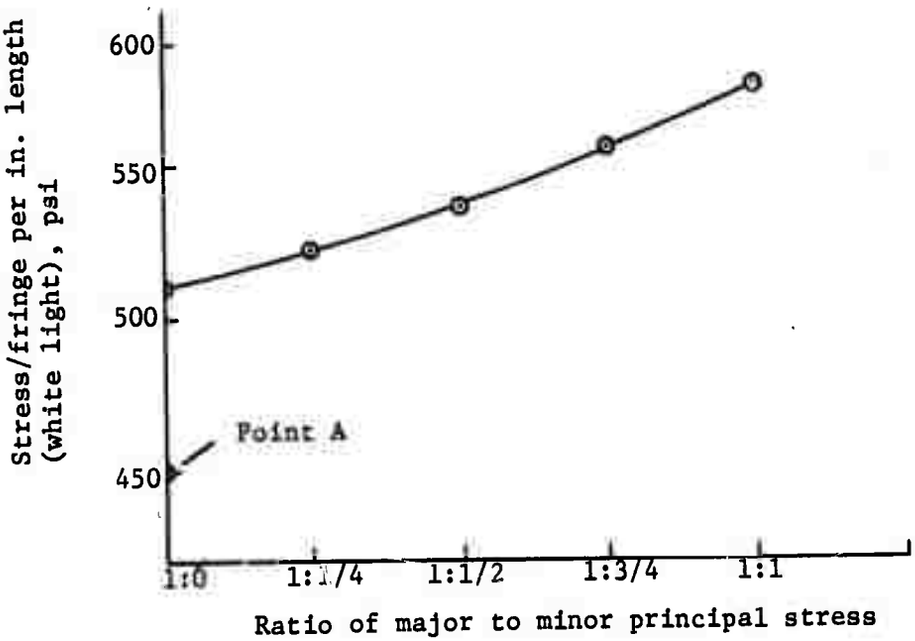

Fig. 14 Variation of stress/fringe characteristic for different ratios of major to minor principal stress.

INFLUENCE OF THE MINOR STRESS

Figure 14 shows the relationship between the sensitivity of a stressmeter for a given major stress and various ratios of major to minor stress. This relationship is dependent upon the position of the point to which the optical patterns are compensated and it is therefore determined by the diameter of the collar relative to that of the meter. The variation in response for a meter 1 in. in length is from 510 to 575 psi per fringe which represents a divergence of approximately $\pm$ 5 percent from the mean value of 543 psi per fringe.

Point A represents the sensitivity of the meter under uniaxial compression using the special 45° compensation points. The sensitivity with this system is higher than when compensating to the collar with the diameter chosen but this is purely incidental and in fact the reverse could be the case if the collar diameter were reduced.

INFLUENCE OF THE YOUNG'S MODULUS OF THE SURROUNDING MATERIAL ON THE STRESS/FRINGE RELATIONSHIP

Fifteen different materials ranging from steel with a modulus of 30 X 10^6 psi to Acrylic resin with a modulus of 4 X 10^5 psi were tested in the form of slabs, uniaxially stressed under identical conditions, and with similar stressmeters cut from the same slab of optical glass.

The results are given in condensed form in Table 2.

The E values of the materials tested were obtained by the authors, loading uniaxially 1 in. dia. X 3 in. long cylindrical specimens and measuring the strain in the centre third of the specimen using a special detachable linear transformer gauge originally developed by Murrell [12] and subsequently modified by Ramez [13]. The determination of stress/strain relationships for rocks of many types has been the subject of much study in the Mining Department at Sheffield University. Based upon the experience gained, the modulus measurements made for the purposes of this paper were obtained from the portion of the stress/strain curves over the range 1000-4000 psi. This avoids the effect of porosity etc. observed at low stress values.

The stress/fringe values, which are those for a 1 1/2 in. long stressmeter compensated to the 45° compensation point, are shown graphically against E values in Fig. 15 graph A. Also in Fig. 15 is the uniaxial (45° compensation point) fringe order per in. stressmeter (graph B) and the average fringe order for the biaxial stress field per in. length of stressmeter (graph C).

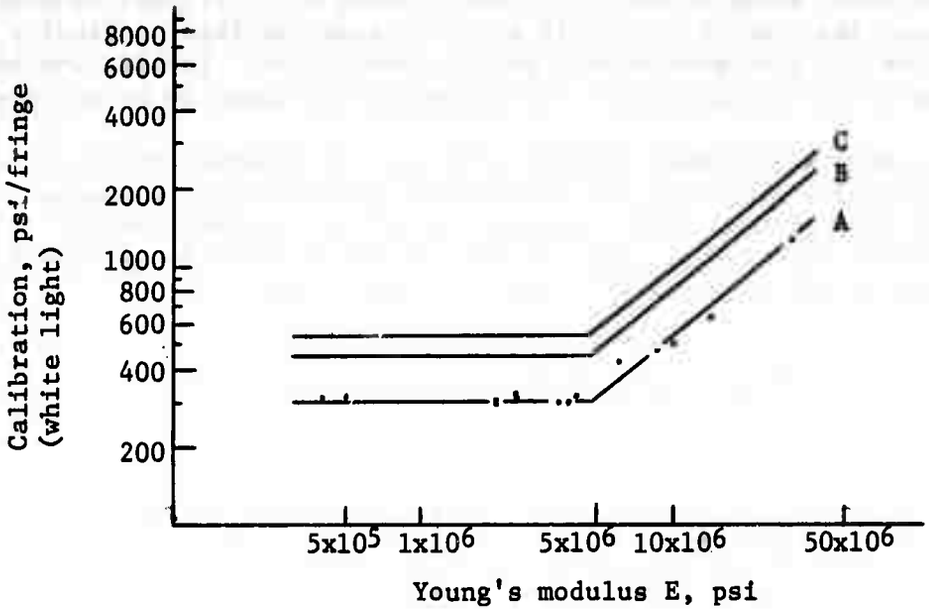

Fig. 15 The effect of the Modulus of elasticity of the surrounding material upon the calibration characteristics of the stressmeter.

A 1 1/2 in. long stressmeter in white light, read at the 45° compensation points. Uniaxial stress field.

B 1 in. long stressmeter in white light, read at the 45° compensation points. Uniaxial stress field.

C 1 in. long stressmeter in white light, biaxial stress field (ratio of principal stresses 1 : 1/2) compensated to collar edge on minor stress axis.

From Fig. 15 (c) it will be noted that when the E value of the surrounding material is below 5 X 10^6 psi the fringe sensitivity of the meter is quite independent of the modulus of the surrounding material at a figure of 540 psi/fringe/in. length of meter. In the special uniaxial case with 45° point compensation the more sensitive figure of 450 psi/fringe/in. length of meter is applicable. Above 5 X 10^6 psi the sensitivity decreases to a figure of 2300 psi/fringe/in. length of meter at an E value of 30X10^6 psi.

THE USE OF COLOUR FILTERS

At high fringe orders, using white light, the fringes are difficult to distinguish due to the colours becoming 'washed out'. In order to overcome this difficulty it is then preferable to view the stressmeter through a colour filter. In this way meters can be easily read up to six fringes above which the pattern tends to be confused.

When the fringe pattern is viewed through a filter the observed fringe count differs from that with white light and the sensitivity of the meter is changed to an extent depending upon the colour. Table 3 gives the extinction wave lengths of three filters employed in these experiments together with those of white and sodium light. The fringe sensitivity of the stressmeter is given in each case.

Table 3. Use of Colour Filters

Colour	Wavelength of fringes	Fringe sensitivity per in. meter psi	
		Biaxial	Uniaxial 45° point
White	$2{\cdot}27 \times 10^{-5}$ in.	540	450
Sodium	$2{\cdot}27 \times 10^{-5}$ in.	540	450
Red	$2{\cdot}48 \times 10^{-5}$ in.	590	490
Blue	$1{\cdot}87 \times 10^{-5}$ in.	445	370

DETERMINATION OF THE MINOR PRINCIPAL STRESS

Theoretically the ratio of major to minor principal stress can be obtained by measuring the fringe order at two points equidistant from the centre of the meter and at specific angles relative to the axes of symmetry of the pattern. The technique requires special instrumentation to establish the necessary orientation for the compensation points and this has proved unsuitable for practical purposes. Two alternative techniques can therefore be considered i.e. a pattern identification system and a model comparator technique. The pattern identification technique consists of the following:

The observed fringe pattern is compensated to an exact fringe order. The pattern is then compared with photographs of the type shown in Fig. 7 which are standard ratios of 1 : 0, 1 : 1/2, 1 : 3/4 and 1 : 1, and the nearest ratio taken. It was expected that this system would allow the minor stress to be obtained within ± 12 1/2 percent of the major stress. In practice, however, the figure has proved to be near ± 15 percent.

A comparator is being developed to determine the ratio of principal stresses more accurately where this is required. It consists of a portable biaxial loading frame on which any biaxial pattern can be set up in an optical gauge by the application of known loads. The observed pattern in a stressmeter can then be matched on the comparator and the principal stress ratio determined directly.

SECONDARY PROBLEMS IN INTERPRETATION

The field application of stressmeters is frequently very different from laboratory testing conditions and various problems arise which affect the confidence with which the results can be interpreted.

NON-UNIFORM FRINGE PATTERNS

The appearance of an irregular fringe pattern in a meter might result either from incorrect setting of the meter or from a non-uniform stress field in the material surrounding it. Should the cement bond be incomplete or the cement incorrectly disturbed around the meter this is made obvious by the appearance of fringes generated in the region of the faulty bond as well as at the periphery of the axial hole. This is due to the fact that at such places there is a region of the meter free from stress, adjacent to a stressed area. In this respect the meter is self checking and meters having irregular patterns can be ignored.

The effect of a non-uniform stress field is to cause the pattern in one portion of the meter to develop more rapidly than others. This is especially liable to happen where a meter is set in reinforced concrete close to a reinforcing rod. In this case the various parts of the meter are read separately and a mean result obtained.

LONG TERM STABILITY

The problem of long tern stability can be considered from two aspects, the stability and creep properties of the meter itself and the creep properties of the material surrounding the meter. Glass is probably the most stable birefringent material that could be used for this technique. Observations made on the glass used by the authors over a 1 year period have shown no significant evidence of creep at normal ambient temperatures likely to be encountered in the field.

Where the meter operates as a high modulus inclusion, that is, when it is set in low modulus materials a concentration of stress appears around it. Stephen and Pirtz [10] have shown that under uniaxial conditions of loading and for a ratio of meter modulus to material modulus of 4 : 1 the stress was increased above and below by some 25 percent (see also Fig. 3). These higher stresses could under certain circumstances produce localised creep of the material or of the cement around the meter. The passage of time would then result in a decrease in fringe order in the meter. It is however very difficult to separate this from general creep in the material. Creep is essentially a stress relieving phenomenon. If a material under load creeps then the stress distribution in the material must change, and it must be expected that the fringe pattern in a meter set in such a body would alter accordingly. This has been observed in laboratory tests, and is the subject of further study at the present time.

CONCLUSIONS

This paper describes a stressmeter of essentially simple construction, the working part of which is a glass cylinder having an axial hole. A necessary addition to this is a light source and circular polarising filter. Observations of stress magnitude and directions are obtained by means of a simple viewing device consisting of a quarter wave plate and a linear polarising filter, the latter being allowed to rotate with respect to the quarter wave plate, with means of measuring the rotation. This combination of stressmeter and viewer forms a biaxial stress measuring system which enables the directions of principal stress in a plane perpendicular to the meter axis to be determined with accuracy, and by further interpretation of the fringe pattern the values of the individual stresses can be obtained.

It is the experience of the authors that compensation of the fringe pattern to obtain fractional fringe orders, recognition of fringe directions and estimation of the ratio of major to minor stress ratios is not difficult, the technique being mastered by most people after only a few days training.

Deep insertion of the stressmeter below the surface of the body under investigation results in no difficulty in reading, a telescope fitted with an analysing device being used in this case. Further, the use of a borehole camera enables permanent records of the state of stress to be made.

In field investigations the chief advantages of the device lie in its simplicity with consequent low cost, and the large amount of information obtainable from a single meter. A consequence of the radial symmetry and biaxial nature of the meter is that no previous knowledge of stress directions in a plane perpendicular to the meter axis is required before the meter is set, and further, that no difficulties arise when during a series of observations the stress directions change with time. The advantages of using a meter which consists of a hard inclusion in the body under stress are, of course, well known.

Briefly stated, they are firstly, that no accurate knowledge of the value of Young's Modulus is required and secondly, that changes in modulus during an investigation are of no importance provided that the modulus does not exceed 5×10^6 psi in the case of the glass stressmeter. In materials of higher modulus an appropriate calibration must be determined in a test piece of the material, or alternatively if the modulus is known the calibration may be obtained from the graphs of Fig. 15.

In many circumstances the design of a structure to be examined is such that certain stressmeters can only be subjected to uniaxial load. Such meters are best read making use of the special calibration system employing the 45° compensation points in order to gain maximum sensitivity from the observations. Where biaxial loading is expected it is recommended that the 'biaxial system' of fringe counting be employed. That is, the points chosen for compensation should be on the minor stress axis at the edge of the collar fitted into the stressmeter. The calibration factor for the two systems are different, and for highest accuracy of stress determination in the latter case the calibration factor may be chosen according to the ratio between the major and minor principal stresses (Fig. 14).

Acknowledgements - The work reported in this paper forms part of the rock mechanics research programme currently in progress at the Postgraduate School in Mining at the University of Sheffield. Acknowledgement is made to Messrs Horstman Ltd. for a grant in aid of the research by Mr. R. K. Dhir.

REFERENCES

1. Baker W. E. and Dove R. C. 'Construction and evaluation of a three dimensional strain rosette'. S.E.S.A. Experimental Mechanics. No. 3 (1963).

2. Roberts A, and Hawkes I. The application of photoelastic devices for measuring strata pressures and support loads, Mine and Quarry Eng. 29, 298-308 (1963).

3. Roberts A, Hawkes I. and Gill V. L. Optical control methods applied to prestressing, Civil Eng. 58, Sept. (1963).

4. Roberts A. and Hawkes I. The determination of in-situ stress and strain using photoelastic techniques. 14th Colloquium Int. Soc. Rock Mechanics, Salzburg (1963).

5. Sezawa K. and Nishinwra G. The stress under tension in a plate with a heterogeneous insertion, Rep. aero Res. Inst. Tokyo. 6 No. 68 (1963).

6. Coutinho A. Theory of an experimental method for determining stresses not requiring an accurate knowledge of the elasticity modulus, Int. Ass. Bridge and Structural Eng. Congress. 83, No. 9. Paris (1949).

7. Wilson A. H. A laboratory investigation of a high modulus borehole plug gauge for the measurement of rock stress, 4th Symposium on Rock Mechanics. Penn. State Univ. 185-195 (1961).

8. Hiramatsu Y., Niwa Y. and Oka Y. Measurement of stress in field by application of photoelasticity, Tech. Rep. Kyoto University, No. 37 (1957).

9. Savin G. N. Stress concentration around holes, Pergamon Press 1961).

10. Stephen R. M. and Pirtz D. Application of birefringent coating to the study of strains around circular inclusions in mortar prisms, S.E.S.A. Experimental mechanics, 3, No. 4, 91-97 (1963).

11. Chakravarty P. K. Application of the photoelastic technique to the problems of rock mechanics. Ph.D. Thesis, Sheffield University (1963).

12. Murrell, S. A. F. The effect of triaxial stress systems on the strength of brittle materials, with particular reference to rocks. Ph.D. Thesis, Sheffield University (1963).

13. Ramez M. H. The structural behaviour of shock and triaxially deformed rocks. Ph.D. Thesis, Sheffield University (1964).

APPENDIX D

THE GOODMAN JACK

This appendix is abstracted from:

(i) The Goodman Jack Instruction Manual, issued by the Slope Indicator Co. , 3668 Albion Place North, Seattle Washington 98103

(ii) The Measurement of Rock Deformability in Bore Holes, by Richard E. Goodman, Tran K. Van and Francois E. Heuze. This paper was originally presented at the 10th Symposium on Rock Mechanics, May 1968, at the University of Texas, Austin, Texas,

THE GOODMAN JACK

Part 1

1. Introduction

The Goodman Jack is a borehole probe with movable rigid bearing-plates for the measurement of wall deformation as a function of applied load. Data obtained from the load-deformation measurements give the elastic modulous of rock directly. The probe is designed to be used in an NX borehole. Hydaulic pressure is transmitted to the rock through the movable plates. Two LVDT displacement transducers are mounted within the jack at each end of the movable plates. The system also includes a portable solid-state indicator for measuring displacement, hydraulic pump, pressure gauge, hydraulic hose and electrical cable. This Jack is shown in figure 1.

2. Specifications

Borehole Size. The jack has been disigned to be used in NX boreholes which have a nominal diameter of three inches.

Effective Jack Force. The area of the operating pistons in the jack is such that the maximum hydraulic pressure, 10,000 psi, produces the following forces unidirectionally against the rock:

	Bearing Plate Pressure (psi)	Total Force Against Rock (lb)
Model 52101 (12 pistons)	9,300	158,000
Model 52102 (3 pistons)	5,544	94,248

LVDT's. The two linear variable differential transformer displacement transducers are mounted within the jack. These are Schaevitz type E-100D which have a linear range of $\pm$0.1 inches. The linearity over this range is within $\pm$1% of the full scale linear range. Linearity beyond this displacement is approximately 8% of the total jack expansion.

Displacement Indicator. The LVDT transducer readout is a portable Schaevitz Tr-100 solid-state instrument. The displacements are indicated on an illuminated projected scale 8 inches in length. Five displacement ranges or scale factors are selectable on the front panel. These set full scale on the indicator equal to jack displacements as shown on the calibration curves.

Displacement Ranges. The system is calibrated so that the linear range of the LVDT's ($\pm$.1 inch) is displayed on the scale which reads 100 - 0 - 100. The scale has 20 major divisions and 100 minor divisions which makes each minor division equal to 0.002 inch. Interpolation to 0.001 inch is easily read. This provides precision measurements from a jack diameter of 2.9 to 3.1 inches.

With the range selector set to different scale factors, the displacement of the jack can be indicated from the fully closed position to the fully upon

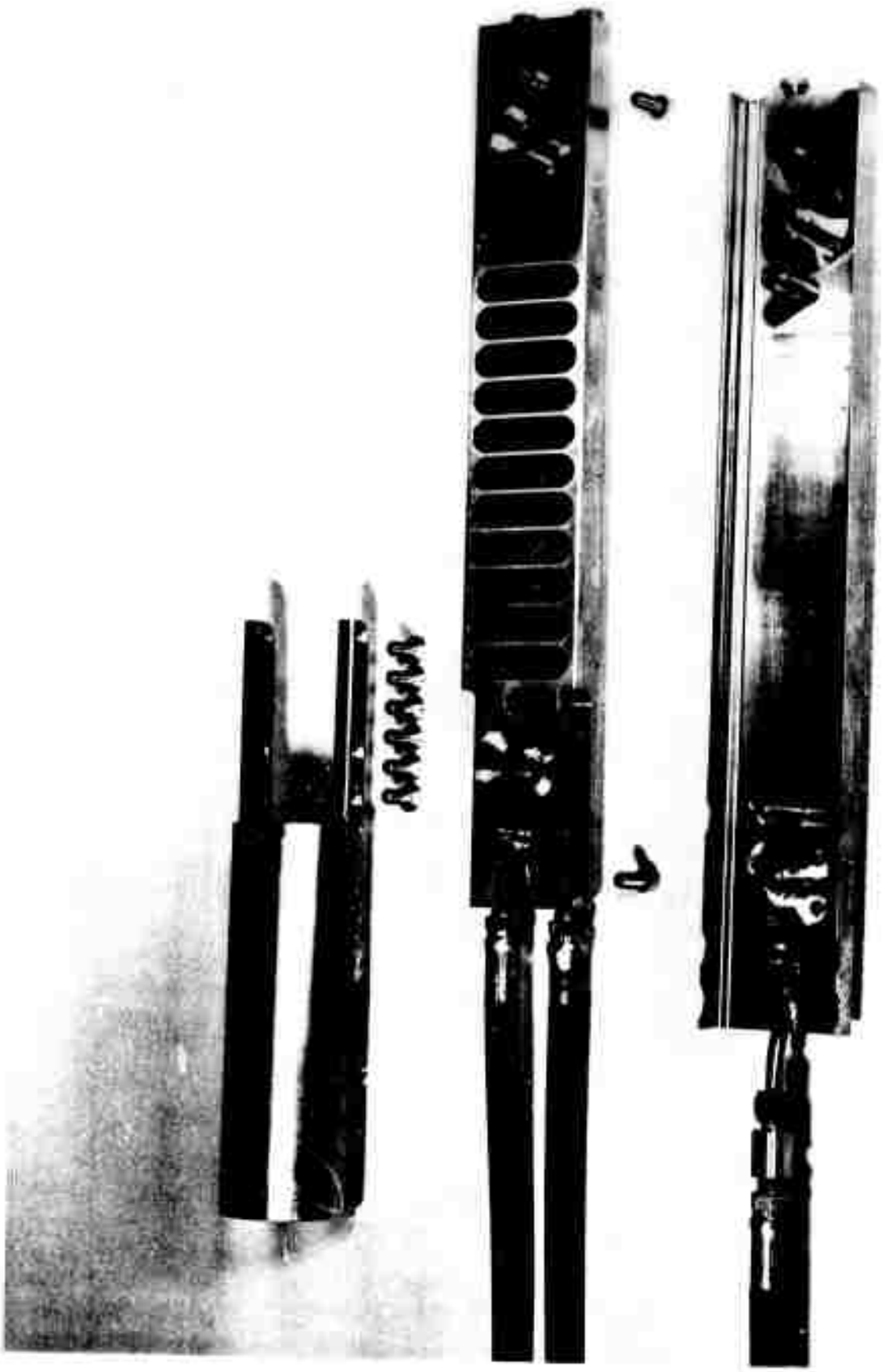

FIGURE 1 The Goodman Jack.

position but with a reduced linear relationship. A calibration curve of displacement versus scale factor is provided.

Operating Point. Adjustments can be made within the jack to shift the operating point of the LVDTs. This allows precision measurements at greater or less expansion of the jack whenever borehole size variations or elastic modulous values necessitate shifting the operating range. For example, in softer rock, the LVDT operating point can be shifted to set the indicator scale to display jack diameter from 3.0 to 3.2 inches or any other suitable range.

Jack Extension Range. The total displacement or extension of the jack is 0.50 inches. When the jack is fully closed, the diametrical distance between the outside surfaces of the two pressure plates is 2.75 inches. When the jack is fully open the diametrical distance is 3.25 inches.

Pressure Range. The jack and the hydraulic components are designed for a 10,000 psi maximum working pressure. The hydraulic pump (Enerpac P-84) produces a maximum output pressure of 10,000 psi.

Pressure Gauge. The pressure gauge, Marsh Type 200, has a bourdon tube sensing element. The accuracy of this gauge is $\pm$.25% of full scale. The full scale pressure is 10,000 psi. The smallest division of the scale is equal to 50 psi. Other gauges with different ranges can be easily adapted when necessary.

AC Voltage Source. The Schaevitz TR-100 Indicator operates from any standard 60 cps power source, 105 to 130 volts, single phase, at 8 watts.

Operating Temperature

LVDT	-65F to +180F
TR-100 Indicator	0F to +130F
Hydraulic Oil	-50F (pour point)

Dimensions.

Jack	Length 48 inches	
	Diameter (Closed)	2.75
Pump	27 x 7 x 6 inches	
Indicator	4 x 9 x 6 inches	

Weights.

Jack	33 pounds
Pump	33 pounds
Indicator	6 pounds
Twin Hose and Electrical Cable	76 lb/100 ft.

Part 2

Bore Hole Jack Data

Quantitative interpretation of measurements made with bore hole jacks involves a more difficult formula because the loading is not continuous over the circumference of the bore hole wall. Further, except in the case of Jaeger and Cook's Quadrantal curved jacks[15], the force is directed at an inclination to the normal to the bore hole wall at all points except the line of symmetry. The boundary condition to be satisfied is one of constant displacement rather than constant pressure. The steel plates are much stiffer than the rock and will be driven out with very little bending. The boundary pressure will not be uniform and pressure readings will represent an average value over the steel-rock boundary. However, as will be shown, constant displacement solutions are very little different from constant pressure solutions in this class of problems if the average pressure and average displacement over the plate - rock contact area are used in computations.

(a) Radial Pressure Over Diametrically Opposed Sectors of the Bore Hole Wall

The solution to this problem was obtained by Jaeger and Cook[15] using the complex variable method. The complete derivation is given in the Appendix. The radial displacement (u_r) at an angular distance θ from the center line of the plate, where the plate extends from $+\beta$ to $-\beta$ (figure 3a) is given by

$$\frac{\pi E}{(1+\nu)} \frac{u_r}{a Q} = -2\beta - \sum_{n=1}^{\infty} \frac{1}{n} \left(\frac{3-4\nu}{2n-1} + \frac{1}{2n+1} \right) \cos 2n\theta \sin 2n\beta \qquad (2)$$

The average displacement of plates of given angle 2β may be obtained by integration. The resulting formula for E would only apply in the case of jacks with radial applied pressure; as yet there are none. This formula should not be used to interpret uniaxially acting bore hole jacks.

(b) Unidirectional Pressure Over Diametrically Opposed Sectors of the Bore Hole Wall

This is theoretically the problem posed by the use of uniaxially acting bore hole jacks. A unidirectional constant pressure boundary condition from $-\beta$ to $+\beta$ may be resolved into a constant radial boundary pressure over the bore hole section of width 2β, and shear and radial pressures distributed sinusoidally over the width 2β as depicted in the Appendix. In the course of this investigation, a solution was obtained for the sinusoidally varying shear and normal force on the wall (Appendix). Superposition with Jaeger's solution (Eq. 2) yields the following formula for the radial displacement of a point on the wall at θ from the line of symmetry.

$$\frac{\pi E}{1+\nu}\,\frac{u_r}{a\,Q} = 2\beta\,[1 + (3 - 4\nu)\cos 2\theta] + \sum_{m=1}^{\infty}\frac{1}{m}\sin 2m\beta$$

$$\left[\frac{(3 - 4\nu}{2m + 1}\cos 2(m + 1)\,\theta + \frac{(3 - 4\nu)}{2m - 1}\cos 2\,m\,\theta\right.$$

$$\left. + \frac{1}{2\,n + 1}\cos 2\,m\,\theta + \frac{1}{2m - 1}\cos 2(m - 1)\,\theta\right] \qquad (3)$$

The average displacement is found by integrating the horizontal displacement over the vertical component of each arc segment in contact with the plate, i.e. from $-\beta$ to $+\beta$. The result, shown fully in Eq. 31, Appendix, may be written

$$E = \frac{\Delta Q}{\Delta \bar{u}_d/d}\,K\,(\nu,\beta) \qquad (4)$$

where $\Delta\bar{u}_d$ is the average diametral displacement for a given increment of pressure ΔQ and d is the bore hole diameter. Values of $K(\nu,\beta)$ are given in Table 2.

BORE HOLE JACK TEST - DISCUSSION OF DATA INTERPRETATION

Influence of Plate Width

Figure 2a, plotted from Table 2, shows the variation of K with change in β, the angle subtended by half the plate width of arc. The quantity K, according to Eq. 4, is the slope of the line relating E to the ratio of the measured quantities ΔQ and $\Delta u_d/d$. The variation of K with β thus affords a comparison of the sensitivity of jacks designed for different plate widths. The maximum sensitivity -- the highest value of K -- occurs at values of β about 45° (figure 2a), the width selected in designing the NX plate bearing test device. It should be noted here that for small values of β, corresponding to narrow plates, a punching failure of the rock might take place. However, this would hardly be the case when β is as large as 45°.

TABLE 2

Values of K (ν,β) for Use in Equation 4 -- Analytical Solution

β	ν: 0	0.05	0.10	0.15	0.20	0.25	0.30	0.35	0.40	0.45	0.50
5.0	0.434	0.433	0.430	0.424	0.417	0.407	0.396	0.382	0.366	0.348	0.327
10.0	0.704	0.703	0.698	0.690	0.678	0.663	0.645	0.622	0.597	0.568	0.536
15.0	0.904	0.903	0.897	0.887	0.873	0.854	0.831	0.803	0.772	0.735	0.694
20.0	1.052	1.051	1.046	1.035	1.019	0.998	0.973	0.942	0.906	0.864	0.818
25.0	1.159	1.159	1.154	1.143	1.127	1.105	1.078	1.045	1.007	0.963	0.914
30.0	1.230	1.231	1.227	1.217	1.201	1.179	1.152	1.119	1.080	1.035	0.985
35.0	1.271	1.274	1.271	1.262	1.247	1.226	1.200	1.168	1.129	1.086	1.036
40.0	1.287	1.291	1.290	1.282	1.269	1.250	1.225	1.195	1.159	1.117	1.069
45.0	1.282	1.288	1.288	1.282	1.271	1.254	1.232	1.204	1.170	1.131	1.087
50.0	1.261	1.268	1.270	1.266	1.257	1.243	1.224	1.199	1.169	1.133	1.092
55.0	1.227	1.236	1.240	1.238	1.232	1.221	1.204	1.183	1.156	1.125	1.088
60.0	1.186	1.197	1.202	1.203	1.199	1.190	1.177	1.160	1.137	1.109	1.077
65.0	1.142	1.154	1.161	1.164	1.162	1.156	1.146	1.132	1.113	1 089	1.062
70.0	1.098	1.111	1.120	1.124	1.125	1.122	1.114	1.103	1.088	1.068	1.045
75.0	1.059	1.073	1.083	1.089	1.091	1.090	1.085	1.076	1.064	1.048	1.028
80.0	1.028	1.042	1.053	1.061	1.064	1.065	1.061	1.055	1.044	1.031	1.013
85.0	1.007	1.022	1.034	1.042	1.046	1.048	1.046	1.040	1.031	1.019	1.004
90.0	1.000	1.015	1.027	1.035	1.040	1.042	1.040	1.035	1.027	1.015	1.000

Effect of Poisson's Ratio

Figure 2b shows that for a given ΔQ and $\Delta u_d/d$, the interpretation of E is fairly insensitive to Poisson's ratio (ν), except at high values of ν. A 50% overestimation in ν, from 0.2 to 0.3, would lead to a 3.25% underestimate of E. If ν were taken as 0.4 rather than the assumed true value of 0.2, and error of 100%, the value assigned for E would be underestimated by 8.50%. As opposed to E, ν is not subject to large discrepancies between field and laboratory values. Thus simple testing on cores retrieved from the bore hole would give a value representative enough to preclude such large errors on the Poisson's ratio, hence reducing the error on E to a negligible amount.

Effect on Non Linear Rock Properties

Qualitative interpretation of bore hole jack or dilatometer data in rock exhibiting non linear stress - strain behavior is entirely appropriate and meaningful. However, as the entire analytical discussion assumes linear elastic relations, quantitative interpretation using these results, even in incremental form, may be erroneous.

Effect of Steel Plate

The mathematical solution to the bore hole jack problem was derived for a condition of constant horizontal pressure on the inner boundary. In actual fact the boundary condition on the loaded border of the bore hole is complex and unknown owing to the unknown coupling between the steel plates and the rock surface. Figure 3a presents a reasonable characterization of the actual boundary condition in the bore hole plate bearing device. A uniform hydraulic pressure bears against the inner sides of the plates. Except in very hard rock, the plates are so much stiffer than the rock as to be driven outward with little bending. The result is a nearly constant horizontal displacement of the rock border; other components of displacement may be considered to exist and be unequal according to the friction and Poisson's ratio contrast between the steel and the rock.

To assess the significance of this departure from the assumed boundary condition, constant displacement and constant pressure solutions were compared for $\nu = 0.25$ using the method of finite element analysis in plane strain. A fine mesh was used with 775 nodal points and 720 elements. The pressure distribution and displacement vectors along the wall of the bore hole are compared for the constant pressure and constant displacement solutions, in figures 3b, c and 3d, e, respectively.

The procedure consists of inputing a constant pressure (or constant X displacement) along the boundary jack-bore hole, computing the average X displacement (or pressure) from the output, and using the average value obtained in Eq. 1. For $\beta = 45°$ and $\nu = 0.25$, one obtains $K = 1.250$ for the constant X displacement case and $K = 1.235$ for the constant pressure case as compared to $K = 1.254$ for the exact analytical solutions. The constant X displacement case is believed to be the more representative of actual field behavior and its simu-

FIGURE 2A Variation of K (ν,β) with respect to β

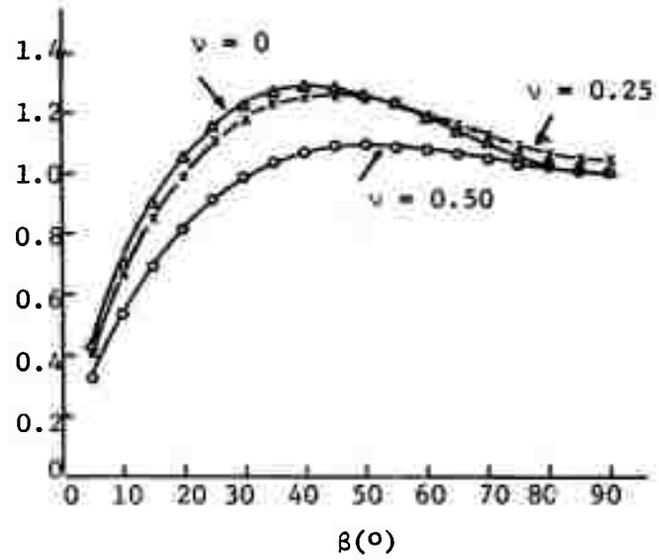

FIGURE 2B Variation of K (ν,β) with respect to Poisson's Ratio (ν)

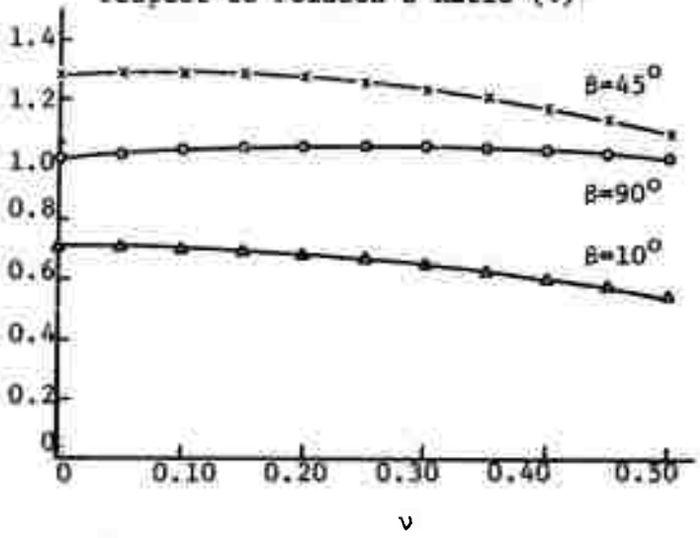

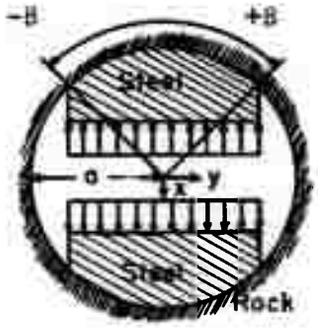

ACTUAL LOADING

3a ACTUAL BOUNDARY CONDITION

3b CONSTANT PRESSURE= 10,000 psi

3d CONTACT PRESSURE RESULTING FROM 3c

CONTACT PRESSURE

3c CONTACT DISPLACEMENT RESULTING FROM 3b

3e CONSTANT DISPLACEMENT U_x=0.01a

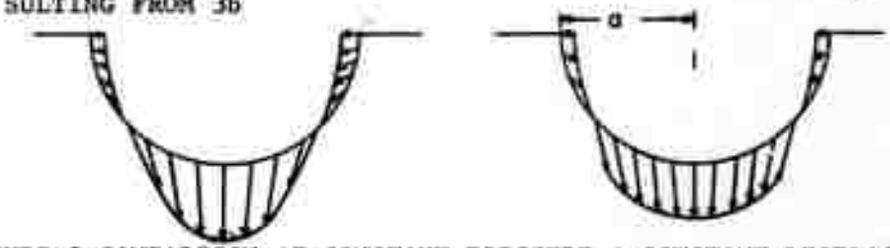

BOUNDARY DISPLACEMENT

FIGURE 3 COMPARISON OF CONSTANT PRESSURE & CONSTANT DISPLACEMENT SOLUTIONS WITH PLANE STRAIN REP. OF JACK PROBLEM

E = 1.0 x 10^6 psi
ν = 0.25

SCALE OF DISPLACEMENT

o ⟵ 10^{-2}a

SCALE OF PRESSURE

o ⟵ 5000 psi

lation by finite element analysis gave the closest result to exact solutions (K = 1.250 versus K = 1.254). This is the extent of the finite element approximation.

Effect of Finite Test Length

The plane strain solution assumes an infinite test length. In actual fact the NX bore hole plate bearing device has a length to diameter ratio of 8"/3". To calculate the effect of the finite plate is a difficult three dimensional problem in prismatic space which could not be solved in closed form.* However, an estimate of the end effect was obtained by performing a three dimensional finite element analysis using a new computer program developed by Professor E. L. Wilson[26]. In this approach, a load of finite length is applied to a portion of a longer space whose cross section is constant. The variation of load along the length of the space is achieved by Fourier expansion making repeated cumulative passes through the problem.

Figure 4 gives the variation of displacement at the border of the bore hole over the width and length subjected to uniform pressure ($\nu = 0.25$). The value of K corresponding to the average displacement under the loaded area is 1.06. The corresponding value from finite element analysis of the plane strain approximation is 1.23. Thus the finite length may be taken into account by reducing by 14% values of E derived from Eq. 4 and Table 2, i.e.

$$E = 0.86\ K\ (\nu)\ \frac{\Delta\ Q}{\Delta u_d/d} \tag{5}$$

In the NX bore hole plate bearing device, d = 3 inches, and Q is 93% of the hydraulic pressure Q_h. Putting these values in Eq. 5 yields the following equation for interpretation of field data in tests with this instrument.

$$E = 2.40\ K\ (\nu)\ \frac{\Delta Q_h}{\Delta u_d} \tag{6}$$

*The related three dimensional problem of a hydrostatic pressure of finite length 2 c in a circular hole of radius a was solved by Tranter in 1946 (Qtly of Applied Mathematics, vol. 4, p. 298). The three dimensional effect was 37% for c/a = 0.5 and was decreasing rapidly with increased load length. In the NX plate bearing test, c/a = 2.67.

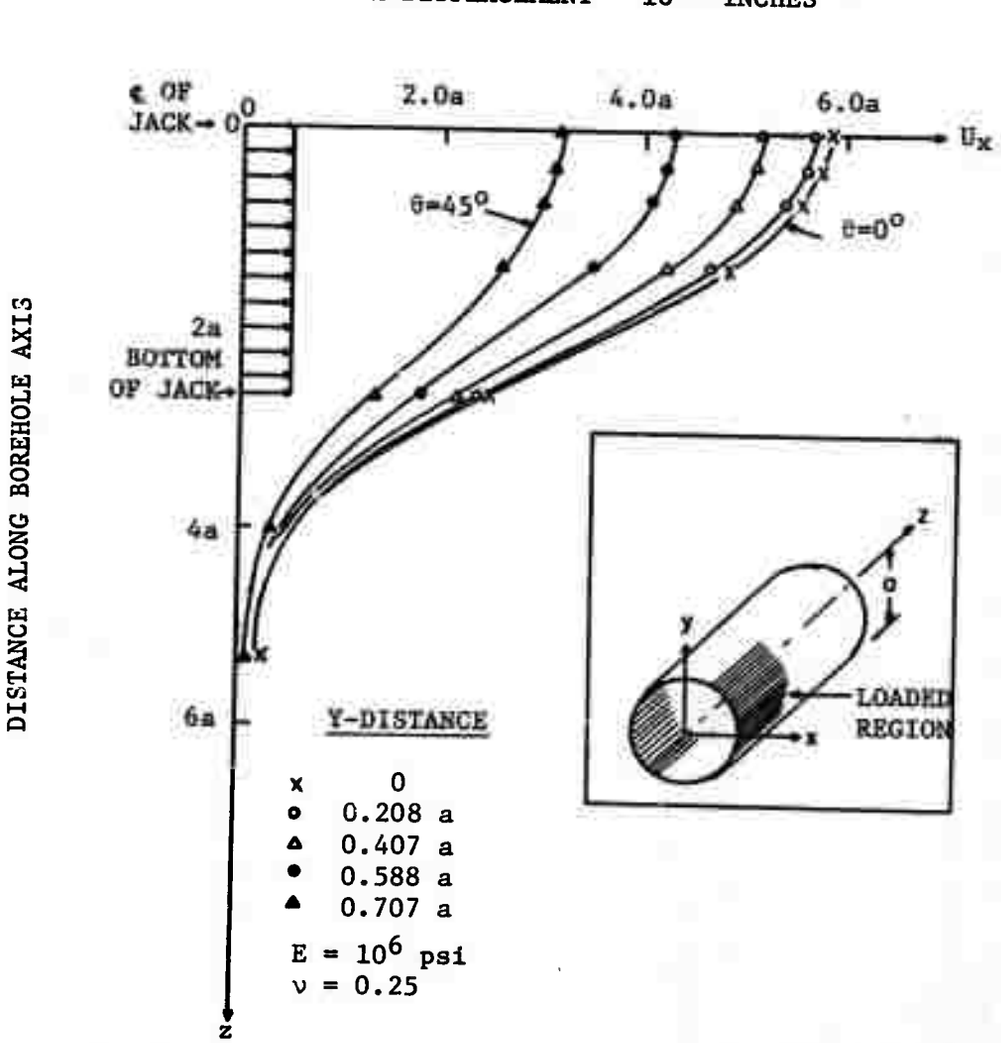

FIGURE 4 VARIATION OF X-DISPLACEMENT ALONG THE BOREHOLE (z DIRECTION) AT DIFFERENT POINTS AROUND THE WALL OF THE BOREHOLE.
PRISMATIC-SPACE-CONSTANT PRESSURE = 375 PSI

TABLE 3

Values of Constants in Equation 6

ν	0	0.05	0.10	0.15	0.20	0.25	0.30	0.35	0.40	0.45	0.50
K (ν)	1.38	1.29	1.29	1.28	1.27	1.25	1.23	1.20	1.17	1.13	1.09
2.40 K (ν)	3.07	3.10	3.10	3.07	3.05	3.00	2.95	2.88	2.81	2.71	2.62

Rock Stress with the Bore Hole Jack

The complex variable method leads to series formulas for the stress components in the rock, as presented in the Appendix. The thrusting apart of the bore hole by the action of the jack leads to a tangential tension on the wall of the bore hole at $\theta = 90°$,

$$\sigma_\theta = - 4 \beta \frac{Q}{\pi}$$

For the NX bore hole plate bearing device, $\beta = \pi/4$ giving a tangential stress concentration at $\theta=90°$ of -1.0. The onset of tensile cracking at this point could be used as a measure of the tensile strength of the rock if a bore hole camera is used concurrently. From Eq. 32, one also obtains at $\theta = 0°$, $\sigma_\theta = 0.8/5$ Q (compressive).

The stresses around the bore hole expressed as a concentration of the jack pressure are presented in figures 5a, b, and c.

Influence of Possible Crack Formation

In all that precedes, the rock has been assumed to be homogeneous, isotropic and linearly elastic. Moreover, no failure criterion has been considered around the bore hole. However, owing to the magnitude of stresses which the jack can induce, superimposed onto the in situ stress concentrations, it is not unlikely that cracking might develop around the bore hole particularly in soft or weak rocks. Cracks could be originated and propagated primarily in those regions where high tensile stresses are found to develop; the critical ones will be the tangential stresses. Then, upon data analysis, corrections shall be introduced to take care of the apparent reduction in the computed modulus of elasticity to obtain the true value for intact rock. Both concepts presented above are now discussed.

The complete tangential stress field at selected points (on the walls of the bore hole and in the planes of principal stresses) around the bore hole can be readily obtained by superposition of the effects of in situ biaxial stress field (S, T) and of jacking (Q). Figure 6a gives the tangential stress concen-

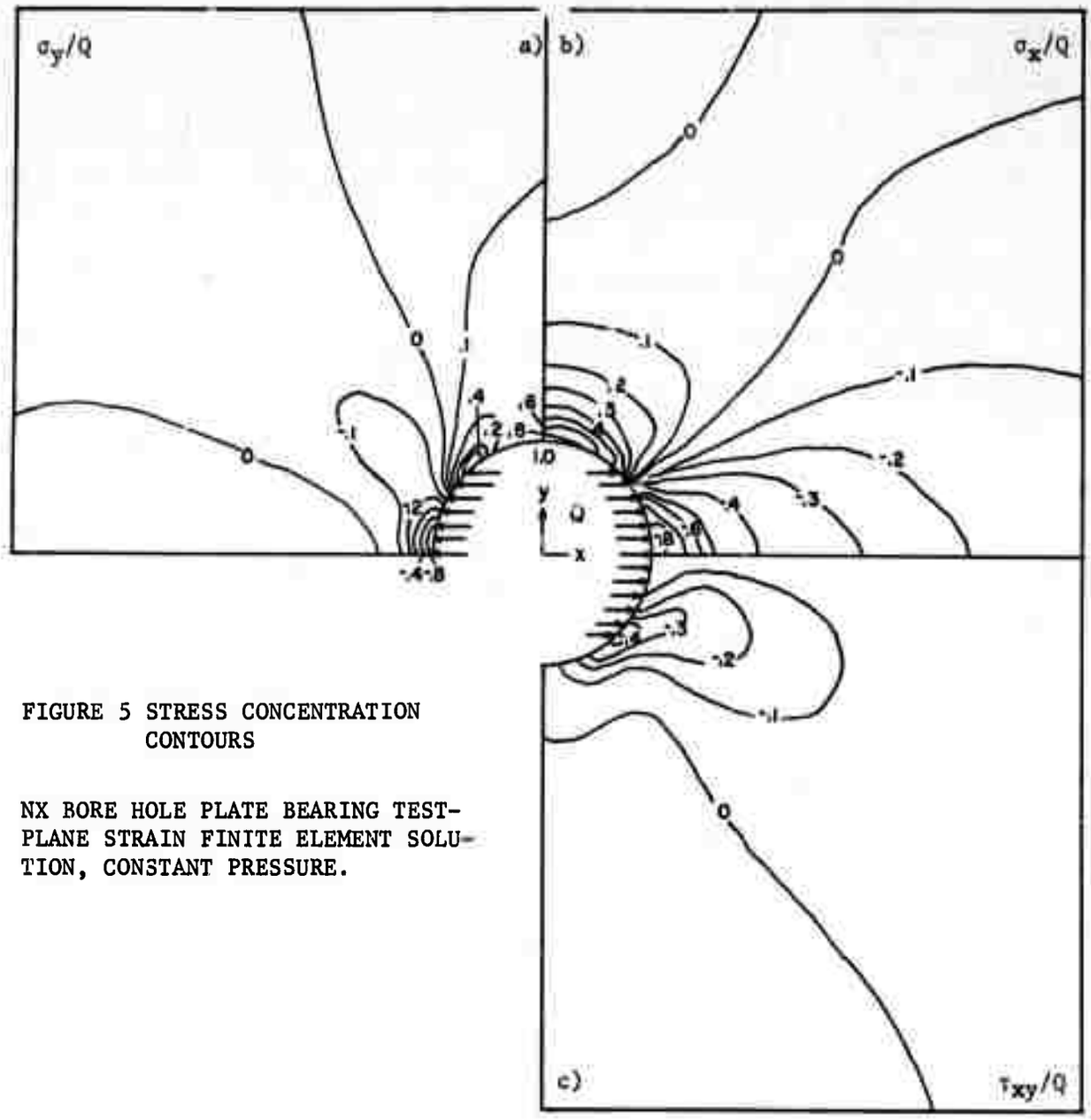

FIGURE 5 STRESS CONCENTRATION CONTOURS

NX BORE HOLE PLATE BEARING TEST-PLANE STRAIN FINITE ELEMENT SOLUTION, CONSTANT PRESSURE.

tration factors. Depending upon the ratio S/T, the stress pattern before jack pressurization can take different forms. They are shown on Figure 6b assuming that $S/T = N = \nu / (1 - \nu)$ (lateral constraint). If S and T have been actually measured, the proper value will then be used. Upon application of a jack pressure Q, the additional tangential stress induced is for $\beta = 45°$ at $\theta = 90°$, $\sigma_\theta = -Q$ and at $\theta = 0°$, $\sigma_\theta = 0.875\ Q$. Accordingly, the complete tangential stress pattern at the selected points is shown on Figures 6c and 6d when jacking takes place in the direction of either principal stress. These are the two extreme cases in terms of tangential stress magnitude. It can be seen that the most unfavorable situation is when jacking takes place in the direction of the minor principal stress. High tensile tangential stresses will then be induced in the plane perpendicular to the direction of jacking and the lower the Poisson's ratio of the rock, the higher their magnitude.

In the eventuality of crack formation in a plane perpendicular to the direction of jacking, the observed displacement of the jack plates will be greater than the one taking place in an intact body. Thus, the modulus of elasticity computed from load - deformation curves will be lower than if no crack is initiated. Evaluation of the required correction on E was attempted by simulation technique. The constant X displacement finite element model was used according to previous conclusions. Cracking was simulated by allowing no tensile strength for a certain distance d from the bore hole along the plane perpendicular to the direction of jacking. Three cases were considered:

$d = a/2$ (crack extending to a half radius distance)

$d = a$ (crack extending to a one radius distance)

$d = 5a$ (simulates a half infinite medium for all practical purposes)

The results are compared in Table 4 with the case of no cracking.

TABLE 4

Influence of Possible Crack Formation

Length of Crack	K	Variation in K	Apparent Decrease in E
0	1.250	+ 0	---
a/2	1.410	+ 13%	- 13%
a	1.553	+ 24%	- 24%
5 a	1.614	+ 29%	- 29%

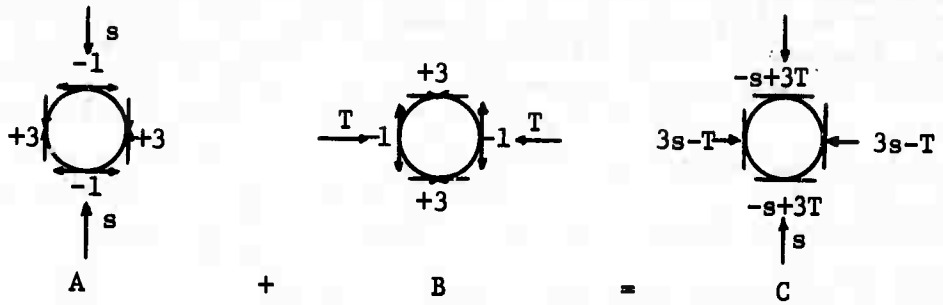

a) TANGENTIAL STRESS CONCENTRATION FACTORS AROUND A BOREHOLE IN A BIAXIAL STRESS FIELD.

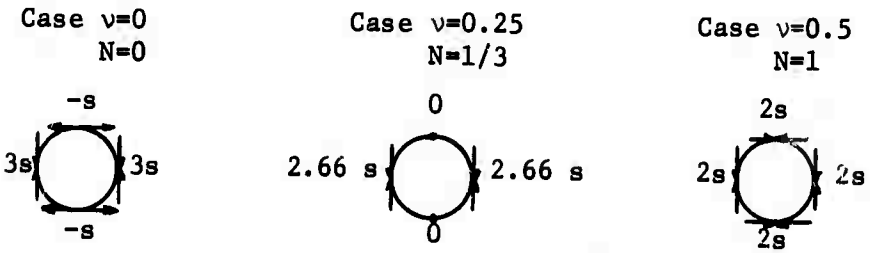

b) TANGENTIAL STRESSES AROUND BOREHOLE - NO JACKING.

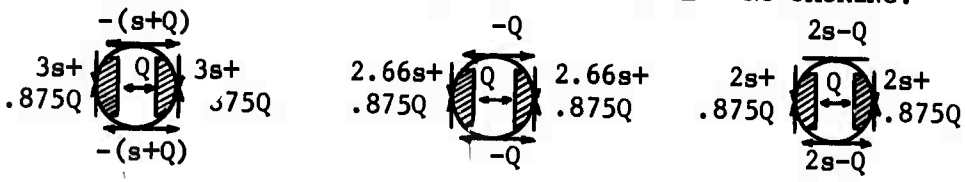

c) JACKING IN DIRECTION OF MINOR PRINCIPAL STRESS.

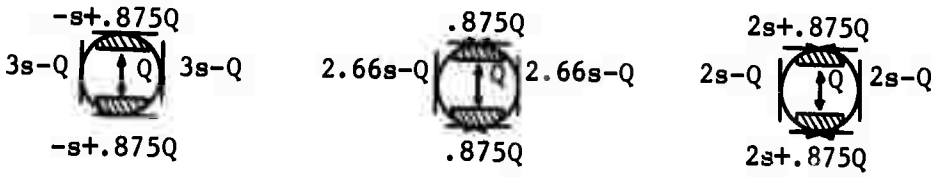

d) JACKING IN DIRECTION OF MAJOR PRINCIPAL STRESS.

s=Major principal stress (positive in compression)
T=Minor principal stress (positive in compression)
Q=Jack pressure (positive)

FIGURE 6

Unless indicated by a break, or yield point, in the load deformation curve, cracking a depth in a borehole would be monitored by means of bore hole camera, but its extent from the wall inside would be extremely difficult to measure. However, from figure 5b, one can see that at a distance, d = 1 radius, the maximum tensile tangential stress induced by jacking has decreased to 0.1 Q (maximum value = 930 psi). Moreover, within a short distance from the bore hole, the in situ stress field is again compressive. Thus it is very unlikely that a crack could propagate beyond between 1/2 and 1 radius from the bore hole even in the weakest rock. Accordingly, the corresponding maximum correction to be introduced in the computed modulus of elasticity will probably never exceed 15%. This is well within the limits of accuracy required for engineering purposes knowing that usually results of any test are checked against results obtained by other methods. In case of jacking across a joint intersecting the borehole, the required correction could reach close to 30% and it is suggested that a close examination of jacking explacements be made before actual testing in order to avoid the influence of major discontinities in the rock mass.

Influence of Wall Roughness and Roundness

Other investigators [30, 31] have analyzed the influence of borehole wall roughness and roundness on the accuracy of stress determinations from borehole deformations. They conclude that with modern diamond drilling equipment and honing devices the morphology of the bore holes enable accurate measurements. In the case of jack testing, crushing of asperities might take place at the beginning of loading but the modulus of deformation is obtained from the linear portion of the load deformation curve which corresponds to a uniform loading. After Suzuki[30], roughness can be limited to about 10^{-3} inches, whereas, plate displacement is of the order of several 10^{-2} inches, so that for practical purposes, no correction will have to be introduced.

The Size of Bore Hole Jack Tests

A bore hole jack produces non homogeneous stress and displacement fields in the rock around the bore hole. Figures 5a, b, and c give the rate at which the applied pressure decays with depth, and figure 7 presents the decay of displacement with depth. The size of the test can be expressed by the volume of rock significantly stressed, say to a minimum of 1,000 psi, and within which most, ca. 90% of the displacement has occurred. At a plate pressure of 9,000 psi this volume extends about 4.5 inches deep from the wall of the NX bore hole. Thus, the test may be considered as operating on an irregularly shaped rock domain roughly one foot in maximum extent. It is much larger than laboratory tests, and somewhat smaller than conventional plate bearing tests conducted in adits.

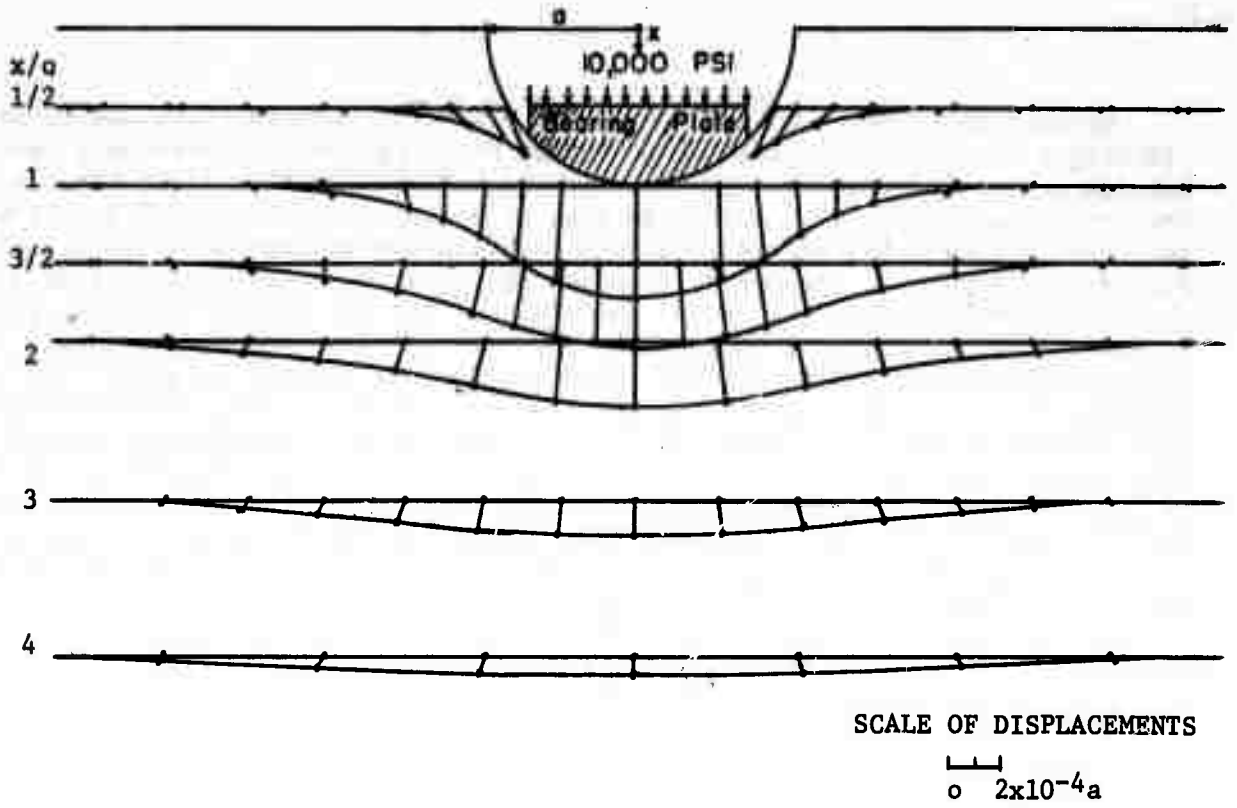

Fig. 7 DISPLACEMENTS OF ROCK UNDER 10,000 PSI LOAD BY BORE HOLE JACK. ELASTIC MODULUS OF ROCK = 1.0×10^6 PSI.

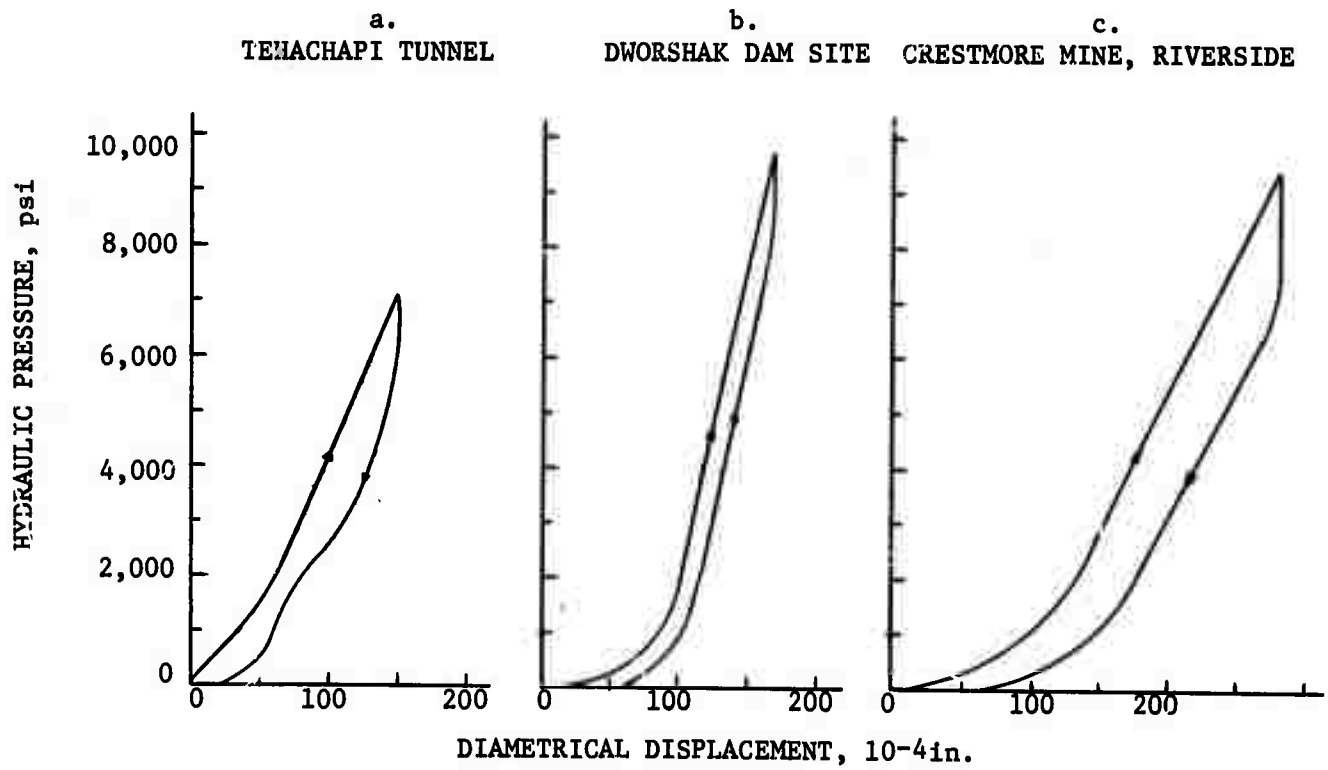

Fig. 9 PRESSURE DEFORMATION CURVES FOR FIELD TESTS WITH Nx PLATE BEARING DEVICE.

COMPARISON OF BORE HOLE JACK AND OTHER IN SITU TESTS

NX bore hole plate bearing tests were conducted in three underground test chambers where extensive in situ testing programs had been completed or were in progress. These were at the Tehachapi tunnel near Bakersfield (California Department of Water Resources); Dworshak dam near Orofino, Idaho (Walla Walla District, U. S. Corps of Engineers); and the Crestmore mine near Riverside, California (American Cement Co.). The equipment used in these tests included the NX bore hole plate bearing device, two Schaevitz servo indicators, a double acting 10,000 psi hand pump, and Bourdon pressure gages.

At the test gallery of the Tehachapi project an adit to the discharge tunnel, the rock is a closely fractured diorite gneiss with seams of clay derived from the rock by hydrothermal alteration. Several hard, fresh pieces of core were obtained in drilling the NX holes for the bore hole plate bearing tests but the overall recovery was only fair. Four bore hole jack tests were conducted in two horizontal holes.

In situ tests included stress measurements, seismic measurements, and plate bearing tests. Four plate bearing tests were performed; and analyses were made of the data assuming both uniform and rotational deflections, as discussed by Kruse, et al.[27], for similar tests at Orville. Figure 9a presents a typical pressure versus diametral displacement curve for the bore hole jack tests at this location. The average value of E from plate bearing tests was 700,000 psi; the average value of E from bore hole jack tests was 840,000 psi in the same pressure range.

The Dworshak dam tests were conducted in a test gallery employed previously by Shannon and Wilson[28] for a comprehensive program of in situ rock tests. The rock at this site is a massive to moderately jointed epidote quartz-diorite gneiss. The in situ tests included plate bearing test, a chamber test, and seismic measurements.

There was great scatter in the results of plate bearing tests; the mean modulus of elasticity in plate bearing was 3.4 million psi with individual results ranging from 500,000 psi to 5 million psi. Fourteen bore hole jack tests were conducted in eight bore holes, three of which were water filled. The average modulus from these tests was 2.1 million psi, with little scatter. A typical curve of pressure versus displacement for bore hole jack tests is shown in figure 9b.

An extensive program of in situ tests were completed by Heuze' and Goodman[29] at Crestmore mine, an underground room and pillar mine in massive, coarse, crystalline marble. In situ tests included flat jack measurements, plate bearing tests, and field seismic measurements. Bore hole jack tests were conducted in two horizontal bore holes at the site of the flat jack emplacements. The modulus of elasticity values computed from the load deformation curves on pressuring the flat jacks averaged 1.8 million psi. The bore hole jacks gave an average value of 1.5 million psi for E. A typical curve of plate pressure versus diametral displacement for the bore hole tests is given in figure 9c.

Table 5 is a summary and comparison of test results from the three areas.

At each of the sites, E was measured, additionally, in unconfined compression tests on NX core specimens in the laboratory. These values were, in all cases, considerably higher than the results of static tests in situ -- by a factor of 3 or more. This discrepancy between field and laboratory values is a common one in rock testing. Laboratory testing is usually conducted on sound samples which are not fully representative of the rock mass with its defects. The results of the bore hole jack tests were comparable to those of other in situ tests.

CONCLUSION

Bore hole jack tests are well suited to measurements of rock deformability at engineering sites. The tests are easier and less costly to conduct than plate bearing, flat jack, and other in situ techniques; thus many more measurements can be made. Furthermore, being conducted in drill holes, rock volumes remote from the surface can be tested. These facts allow one to establish the attributes of the rock mass quantitatively and qualitatively in every rock member reached by a work. The values obtained from these tests in three cases discussed herein were comparable to values obtained by other more costly in situ techniques.

ACKNOWLEDGEMENTS

The authors wish to thank the engineering agencies and personnel who generously offered their sites for field testing and furnished data from their own laboratory and in situ tests. We are particularly indebted to George Kruse and A. O'Neill of the California Department of Water Resources; Charles Monahan of Walla Walla Distric, U. S. Army Corps of Engineers; and Frank Foster of American Cement Company. We also acknowledge the help of Ann Finucane and Gloria Pelatowski. The NX bore hole plate bearing device was partially developed with the aid of a grant from the Pacific Gas and Electric Company. Studies at the Crestmore mine were supported by a grant from American Cement Company. This research was also partially supported by NASA Contract NSR 05-003-189. The authors are very grateful to Edward Wilson, Assistant Professor of Structural Engineering at the University of California, Berkeley, for allowing us to use his new prismatic space program.

TABLE 5

SUMMARY OF TEST RESULTS

Comparison of In Situ, Core, and Bore Hole Jack Tests

Site	Rock Type	Poisson's Ratio	Young's Modulus, 10^6 psi: Unconfined Compression (Laboratory (Average)	Plate Bearing* (In Situ)	Flat Jack* (In Situ)	Bore Hole Jack* (In Situ)
Tehachapi Tunnel	diorite gneiss; fractured and seamy	0.35	11.3	0.53 to 0.83		0.61 to 1.03
Dworshak Dam	granite gneiss; massive to moderately jointed	0.20	7.5	0.5 to 5.0		1.54 to 2.70
Crestmore Mine	marble; massive	0.25	6.9	1.74 to 2.72	1.79 to 2.98	1.35 to 1.70

*in the same pressure range 0-3,000 psi

REFERENCES

15. Jaeger, J. C. and Cook, N. G. W., "Theory and Application of Curved Jacks for Measurement of Stresses," International Conference on State of Stress in Earth's Crust, Santa Monica, California, May 1963, Elsevier Press (ed. Judd), pp. 12-1.

16. Stears, J. H., "Evaluation of Penetrometer for Estimating Roof Bolt Anchorage," USBM Report of Investigation 6646, U. S. Bureau of Mines, 1965.

17. Hult, J., "On the Measurement of Stresses in Solids," Transactions of Chalmers University of Technology, Gothenburg, Sweeden, No. 280, 1963.

18. Dryselius, G., "Konstricktion au Matcel for Beigtrychsstudier" (Design of a Measuring Cell for the Study of Rock Pressure), IVA Ingeniorsvetenskapsakademiens Meddelande, 142 Stockholm, 1965, pp. 135-144.

19. Goodman, R. E., "Research In Geological Engineering at the University of California, Berkeley," Proceedings of 4th Annual Symposium on Engineering Geology and Soils Engineering, Moscow, Idaho, Idaho Department of Highways, 1966, pp. 155-165.

20. Absi, E. and Seguin, M., "Le Nouveau Géoextensomètre," Supplement to Annales de L'Institut Technique du Batiment et des Travaux Publics. No. 235-236, July-August 1967, pp. 1151-1158.

21. Ladanyi, B., "Evaluation of Pressuremeter Tests in Granular Soils," Proceedings of 2nd Panamerican Conference on Soil Mechanics and Foundation Engineering, Vol. 1, 1963, pp. 1-20.

22. Ladanyi, B., "Etude Théoretique et Expérimantaic de L'Expansion dans un Sol Pulvérulent d'une Cavité Présentant une Symétrie Sphérique on Cylindrique, Annales des Travaux Publics de Belgique, Bruxelles, Vol. 2 and 4, 1961.

23. Gibson, R. E. and Anderson, W. F., "In-situ Measurement of Soil Properties with the Pressuremeter," Civil Engineering and Public Works Review, London, May 1961.

24. Group de Travail du Comité National Francais, "Mesure des Modules de Deformation des Massifs Rocheux Dans les Sondages," Proceedings 8th Congress on Large Dams, R. 16, Q. 28, May 1964, pp. 320-323.

25. Jaeger, J. C., Elasticity, Fracture and Flow, Methuen and Co., London, 2nd ed., 1962.

26. Wilson, E. L., "Stress Analysis of Prismatic Solids," SESM Report, Dept. Civil Engineering, University of California, Berkeley (in press) 1967.

27. Stropponi, E. W. and Kruse, G. H., "Discussion of 'Foundation Modulus Tests for Karadj Arch Dam'" by Waldorf, et al., Journal Soil Mechanics and Foundation Division, Proceedings, ASCE, Vol. 90, N. SM 2, March 1964, pp 191-205.

28. Shannon and Wilson, Inc., "In Situ Rock Tests for Dworshak Dam Site," January 25, 1965.

29. Heuzé, F. E. and Goodman, R. E., "Mechanical Properties and In Situ Behavior of the Chino Limestone, Crestmore Mine, Riverside, California." Proceedings 9th Symposium on Rock Mechanics, AIME, April 1967 (in press).

30. Suzuki, K., "Fundamental study of rock stress measurements by borehole deformation method," Proceedings 1st Congress of Int'l Soc. Rock Mechanics, Vol. II, pp. 35-39.

31. Agarrval, R., "Sensitivity analysis of borehole deformation measurements of in situ stress determination when affected by borehole excentricity." Proceedings 9th Symposium on Rock Mechanics, Golden, Colorado, April 1967.

APPENDIX

SOLUTION OF UNIAXIAL STRESS PROBLEM

BY COMPLEX VARIABLE METHOD

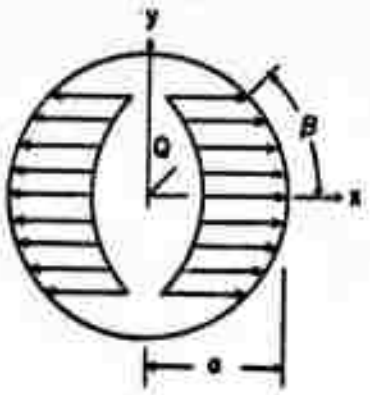

Boundary condition at $r = a$, $\sigma_y = 0$, and $\tau_{xy} = 0$

$$\sigma_x \quad \begin{cases} Q & -\beta < \theta < \beta \ , \qquad \pi - \beta < \theta < \beta + \pi \\ 0 & \beta < \theta < \pi - \beta \ , \qquad \pi + \beta < \theta < 2\pi - \beta \end{cases} \tag{1}$$

At θ from x - axis ($Q = 2p$):

$$\begin{aligned} \sigma_r &= p + p \cos 2\theta \\ \sigma_\theta &= p - p \cos 2\theta \\ \tau_{r\theta} &= -p \sin 2\theta \end{aligned} \tag{2}$$

The problem can be conveniently decomposed into two more simple problems, A and B. Eash problem will be solved separately, and the results are added. The displacement relations and the stress relations are expressed in complex forms.

A. UNIFORM STRESS OVER TWO SYMMETRICAL PORTIONS OF THE CIRCULAR BOREHOLE*

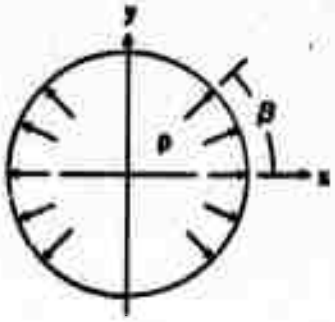

Boundary conditions at r = a

$$\tau_{r\theta} = 0 \tag{3}$$

$$\sigma_r = \begin{cases} p & -\beta < \theta < \beta \quad \pi - \beta < \theta < \pi + \beta \\ 0 & \beta < \theta < \pi - \beta \quad \pi + \beta < \theta < 2\pi - \beta \end{cases} \tag{4}$$

$$\sigma_r - i\,\tau_{r\theta} = \sum_{n=-\infty}^{\infty} An\ e^{in\theta} \tag{5}$$

where

$$An = \frac{1}{2\pi} \int_0^{2\pi} (\sigma_r - i\,\tau_{r\theta})\ e^{-in\theta} d\,\theta \tag{6}$$

$$\sigma_r - i\,\tau_{r\theta} = \phi'(z) + \overline{\phi'(z)} - [\,z\,\phi''(z) + X''(z)\,]\,e^{2i\theta} \tag{7}$$

*This problem was first solved by Jaeger and Cook in State of Stress in the Earth's Crust (W. R. Judd, ed.), Elsevier, 1964, p. 381-396.

$$\phi'(z) = \sum_{n=0}^{\infty} a_n z^{-n}$$

$$X''(z) = \sum_{n=0}^{\infty} b_n z^{-n} \qquad (8)$$

$$a_0 = b_0 = 0$$

$$\xi a_1 + \overline{b_1} = 0 \qquad (9)$$

Solve for a_n and b_n:

$$\phi'(z) = \sum_{n=0}^{\infty} a_n z^{-n} = \sum_{m=1}^{\infty} \frac{p a^{2m}}{m \pi} \sin 2m\beta \; z^{-2m} \qquad (10)$$

$$X''(z) = \sum_{n=0}^{\infty} b_n z^{-n} = -\frac{2\beta p}{\pi} a^2 z^{-2} + \sum_{m=1}^{\infty} \frac{2 p a^{2(m+1)}}{\pi} \sin 2m\beta \; z^{-2(m+1)} \qquad (11$$

Determination of Displacement:

$$2G(U_r + i u_\theta) = [\xi \phi(z) - z \overline{\phi'(z)} - \overline{X(z)}] e^{-i\theta} \qquad (12)$$

$$2G u_r = \text{Real (R.H.S.)} = -\frac{2\beta p p a}{\pi} + \sum_{m=1}^{\infty} \frac{\xi p \rho^{(2m-1)}}{m(1-2m)} a \sin 2m\beta \cos 2m\theta$$

$$- \sum_{m=1}^{\infty} \frac{p\rho^{(2m-1)}}{m\pi} a \sin 2m\beta \cos 2m\theta$$

$$+ 2 \sum_{m=1}^{\infty} \frac{p \rho^{2(m+1)}}{\pi (2m+1)} a \sin 2m\beta \cos 2m\theta \qquad (13)$$

$$\rho = 1 = \frac{r}{a}$$

$$2\,Gu_r \frac{\pi}{p\,a} = -\,2\,\beta - \sum_{m=1}^{\infty} \frac{1}{m} \left[\frac{\xi}{2\,m-1} + \frac{1}{2\,m+1} \right] \sin 2m\beta \cos 2m\theta \qquad (14)$$

Stress Determination:

$$\sigma_\theta + \sigma_r = 4\ \text{Real}\ [\ \phi'(Z)\ ] \qquad (15)$$

$$\sigma_\theta - \sigma_r + 2i\tau_{r\theta} = 2\,[\ \bar{z}\,\phi''(z) + X''(z)\ ]\,e^{2i\theta} \qquad (16)$$

$$\sigma_\theta \frac{\pi}{p} = -\,2\beta\rho^2 + 2 \sum_{m=1}^{\infty} \frac{1}{m}\,\rho^{2m}\,(m\,\rho^2 - m + 1) \sin 2m\beta \cos 2m\theta \qquad (17)$$

$$\sigma_r \frac{\pi}{p} = 2\beta\rho^2 + 2 \sum_{m=1}^{\infty} \frac{1}{m}\,\rho^{2m}\,(m + 1 - m\,\rho^2) \sin 2m\beta \cos 2m\theta \qquad (18)$$

$$\tau_{r\theta} \frac{\pi}{p} = 2(1 - \rho^2) \sum_{m=1}^{\infty} \rho^{2m} \sin 2m\theta \sin 2m\beta \qquad (19)$$

B. THE EXPONENTIAL BOUNDARY CONDITION PROBLEM: $\sigma_r - i\,\tau_{r\theta} = p\,e^{2i\theta}$*

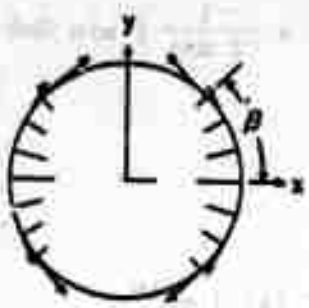

Boundary Condition at $r = a$

$$\sigma_r = \begin{cases} p\cos 2\theta & -\beta < \theta < \beta \\ \tau_{r\theta} = -p\sin 2\theta & \pi-\beta < \theta < \pi+\beta \end{cases}$$

$$\sigma_r = \begin{cases} 0 & \beta < \theta < \pi-\beta \\ \tau_{r\theta} = 0 & \pi+\beta < \theta < 2\pi-\beta \end{cases} \qquad (20)$$

With boundary conditions (5) and (7) where An is defined by (6), the Fourier series representacion of boundary conditions:

$$\sigma_r - i\tau_{r\theta} = \begin{cases} p\,(\cos 2\theta + i\sin 2\theta) = p\,e^{2i\theta}, & -\beta < \theta < \beta,\ \pi-\beta < \theta < \pi+\beta \\ 0, & \beta < \theta < \pi-\beta,\ \pi+\beta < \theta < 2\pi-\beta \end{cases} \qquad (21)$$

*To the authors' knowledge this problem has not been solved before.

Using (9) and computing for a_n and b_n:

$$\phi'(z) = \sum_{n=0}^{\infty} a_n z^{-n} = \frac{2 p \beta}{\pi} a^2 z^{-2} + \sum_{m=2}^{\infty} \frac{p a^{2m}}{\pi(m-1)} \sin 2(m-1) \beta \, z^{-2m} \qquad (22)$$

$$x''(z) = \sum_{n=0}^{\infty} b_n z^{-n} = - \frac{p a^2}{\pi} \sin 2 \beta \, z^{-2} - \frac{p a^4}{2\pi} \sin 4 \beta \, z^{-4} + \frac{6 p \beta}{\pi} a^4 z^{-4}$$

$$+ \sum_{m=2}^{\infty} \frac{(2m + i)}{\pi(m-1)} p a^{2(m+1)} \sin 2 (m-1) \beta \, z^{-2(m+1)}$$

$$- \sum_{m=2}^{\infty} \frac{p a^{2(m+1)}}{\pi(m + 1)} \sin 2 (m + 1) \beta \, z^{-2(m+1)} \qquad (23)$$

Calculation of Displacements:

Using (12) at $\rho = 1$

$$2 G u_r \frac{\pi}{pa} = - 2 \xi \beta \cos 2 \theta - \sum_{m=1}^{\infty} \frac{1}{m} \left[\frac{\xi}{2m + 1} \cos 2(m+1) \theta \right.$$

$$\left. + \frac{1}{2m-1} \cos 2(m-1) \theta \right] \sin 2 m \beta \qquad (24)$$

Calculation of Stresses:

Using (15) and (16)

$$\sigma_\theta \frac{\pi}{p} = 6\,\beta\,\rho^4 \cos 2\theta - \sum_{m=2}^{\infty} \frac{2\,\rho^{2m}}{m-1} [\,2m-2-(2m+1)\,\rho^2] \sin 2(m-1)\,\beta \cos 2m\theta$$

$$- \sum_{m=0}^{\infty} \frac{\rho^{2(m+1)}}{m+1} \sin 2(m+1)\,\beta \cos 2m\theta \qquad (25)$$

$$\sigma_r \frac{\pi}{p} = 8\,\beta\,\rho^2 \cos 2\theta + \sum_{m=2}^{\infty} \frac{\rho^{2m}}{(m-1)} [2+2m-(2m+1)\,\rho^2] \sin 2(m-1)\,\beta \cos 2m\theta$$

$$+ \sum_{m=0}^{\infty} \frac{\rho^{2(m+1)}}{(m+1)} \sin 2(m+1)\,\beta \cos 2m\theta \qquad (26)$$

$$\tau_{r\theta} \frac{\pi}{p} = 2\,\rho^2 (2-3\,\rho^2) \sin 2\theta$$

$$+ \sum_{m=2}^{\infty} \frac{\rho^{2m}}{(m-1)} [\,2m - (2m+1)\,\rho^2\,] \sin 2(m-1)\,\beta \sin 2m\theta$$

$$+ \sum_{m=0}^{\infty} \frac{\rho^{2(m+1)}}{(m+1)} \sin 2(m+1)\,\beta \sin 2m\theta \qquad (27)$$

C. NET RESULTS -- Obtained by Summing Solutions of A and B.

Net Radial Displacement

Add (14) and (24) to obtain the net radial displacement relation:

$$2 G u_r \frac{\pi}{pa} = -2\beta(1+\xi\cos 2\theta) - \sum_{m=1}^{\infty} \frac{1}{m} \sin 2m\beta \left[\frac{\xi}{2m+1} \cos 2(m+1)\theta + \left(\frac{\xi}{2m-1} + \frac{1}{2m+1} \right) \cos 2m\theta + \frac{1}{2m-1} \cos 2(m-1)\theta \right] \quad (28)$$

At $\theta = 0$, radial displacements is maximum.

$$2 G u_{rmax} \frac{\pi}{p a} = -2\beta(1+\xi) - \sum_{m=1}^{\infty} \frac{4(\xi+1)}{(2m+1)(2m-1)} \sin 2m\beta \quad (29)$$

For the application of the results to the calculation of modulus of deformability, it is necessary to obtain a relation containing the integrated value of displacement.

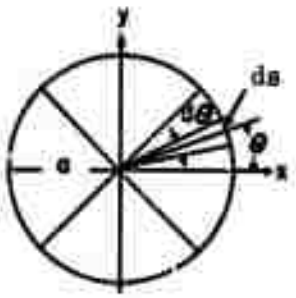

$$dy = ds \cos\theta = a \cos\theta \, d\theta$$

$$\left[2 G \bar{u}_r \frac{\pi}{p a} \right] a \sin\beta = \int_0^{\beta} [\text{R.H.S. (28)}] \, a \cos\theta \, d\theta \quad (30)$$

Replacing $\xi = 3-4\nu$ in the result gives:

$$\left[2 G \bar{u}_r \frac{\pi}{p a} \right] \sin \beta = -2 \beta \left[\frac{5-4\nu}{2} \sin \beta + \frac{3-4\nu}{6} \sin 3\beta\right]$$

$$- \sum_{m=1}^{\infty} \frac{1}{2m} \sin 2m\beta \left[\frac{3-4\nu}{2m+1} \left[\frac{\sin (2m+1)\beta}{2m+1} + \frac{\sin (2m+3)\beta}{2m+3} \right]\right.$$

$$+ \left[\frac{3-4\nu}{2m-1} + \frac{1}{2m+1} \right] \left[\frac{\sin (2m-1)\beta}{2m-1} + \frac{\sin (2m+1)\beta}{2m+1} \right]$$

$$\left. + \frac{1}{2m-1} \left[\frac{\sin (2m-3)\beta}{2m-3} + \frac{\sin (2m-1)\beta}{2m-1} \right]\right] \qquad (31)$$

Net σ_θ

Add (17) and (25) and rearrange the terms.

$$\sigma_\theta \frac{\pi}{p} = -2\beta\rho^2 + 6\beta\rho^4 \cos 2\theta + \sum_{m=0}^{\infty} \frac{\rho^{2(m+1)}}{m+1} \sin 2(m+1)\beta$$

$$\left[\cos 2m\theta + [(m+1)\rho^2 - m] \cos 2(m+1)\theta \right.$$
$$\left. + [(2m+3)\rho^2 - 2m - 2] \cos 2(m+2)\theta\right] \qquad (32)$$

At $\theta = \pi/2$, $\rho = 1$ σ_θ is maximum. Replacing

$$\cos 2m\theta = \begin{cases} +1 & m = 0, 2, 4, \ldots \\ -1 & m = 1, 3, 5, \ldots \end{cases}$$

into (32)

$$\sigma_\theta \pi/p = -8\beta \qquad (33)$$

For $\beta = \pi/4$ $(Q = 2p)$, $\sigma_\theta = -Q$ (34)

This result checks with finite element analysis.

At $\theta = 0$, $\rho = 1$.

$$\sigma_\theta \frac{\pi}{p} = 4\beta + \sum_{m=0}^{\infty} \frac{3}{m+1} \sin (m+1)\, 2\, \beta$$

For $\beta = \frac{\pi}{4}$

$$\sigma_\theta \frac{\pi}{p} = \pi + 3 \text{ Arc tan } 1 = \pi + \frac{3\pi}{4} \quad \text{then } \sigma_\theta = 1.75\, p \approx 0.875\, Q$$

Net σ_r

Add (18) and (26) and rearrange the terms.

$$\sigma_r \frac{\pi}{p} = 2\beta\rho^2 [1+(4-3\rho^2) \cos 2\theta] + \sum_{m=0}^{\infty} \frac{\rho^{2(m+1)}}{m+1} \sin 2(m+1)\beta$$

$$\left[\cos 2m\theta + [m+2-(m+1)\rho^2] \cos 2(m+1)\theta + [2m+4-(2m+3)\rho^2] \cos 2(m+2)\theta\right] \qquad (35)$$

Net $\tau_{r\theta}$

Add (19) and (27) and rearrange the terms.

$$\tau_{r\theta} \frac{\pi}{p} = 2\beta\rho^2 (2-3\rho^2) \sin 2\theta + \sum_{m=0}^{\infty} \rho^{2(m+1)} \sin 2(m+1)\beta$$

$$\left[\frac{1}{m+1} \sin 2m\theta + 2(1-\rho^2) \sin 2(m+1)\theta + \frac{1}{m+1} [2m+4-(2m+5)\rho^2] \sin 2(m+2)\theta\right] \qquad (36)$$

Equation (31) is used in the calculation of the modulus of deformation in terms of applied pressures and corresponding deformations. Using $Q = 2p$, $\bar{u}_d = 2\bar{u}_r$, $d = 2a$, and $G = E/(2(1+\nu))$, (31) can be rewritten as:

$$E = \frac{1}{\sin \beta} \frac{(1+\nu)\, d}{2\pi} \frac{Q}{\bar{u}_d} \left[\text{R. H. S.}\right]$$

$$E = K(\nu,\beta) \frac{Q\, d}{\bar{u}_d} \qquad (37)$$

Values of $K(\nu,\beta)$ are expressed in Table 2 for different values of ν and β. Q is the pressure actually applied to the rock (see 37). The variation of K (ν,β) with respect to β is shown in Figure 2 for values of $\nu = 0.25$, 0.40, and 0.10. It is observed that K has a maximum value at $\beta = 45^{\circ}$, the case of the NX bore hole uniaxial jack.

NOTE: R. H. S. signifies the terms to the right of the equal sign in Equation (31).

APPENDIX E

THE USBM CYLINDRICAL PRESSURE CELL

This appendix is a reproduction of Determination of the Modulus of Rigidity of Rock by Expanding a Cylindrical Pressure Cell in a Drill Hole, by Louis A. Panek, Edward E. Hornsey, and Robert L. Lappi. This paper was originally presented at the 6th Symposium on Rock Mechanics, University of Missouri at Rolla, 1964.

DETERMINATION OF THE MODULUS OF RIGIDITY OF ROCK BY EXPANDING A CYLINDRICAL PRESSURE CELL IN A DRILLHOLE

by

Louis A. Panek[1], Edward E. Hornsey[2], and Robert L. Lappi[3].

ABSTRACT

The modulus of rigidity of rock can be determined by a fairly simple procedure in which a cylindrical pressure cell is first calibrated by expanding it inside two metal test cylinders and then is expanded inside a drillhole in rock. The two test cylinders have different expansion characteristics (different material and/or different wall thickness), which make possible the determination of two calibration constants. Change of diameter of the pressure cell is determined from the volume of fluid pumped into it. The essential apparatus consists of a cylindrical pressure cell, a Bourdon pressure gage, a volume-metering fluid pump, and two test cylinders. Some advantages of the method are that a rock sample is not required, a diamond drill is not required, and the rock is tested in place.

---

[1]Supervisory Physical Research Scientist, Bureau of Mines, College Park, Maryland.

[2]Formerly Mining Research Engineer, Bureau of Mines, College Park, Maryland.

[3]Mining Engineer, Bureau of Mines, College Park, Maryland.

Work on manuscript completed June 1964

INTRODUCTION

The cylindrical pressure cell (CPC) is a device for determining the modulus of rigidity G of rock by direct measurement from an in situ test inside a small drillhole by pumping fluid into it at pressures up to 10,000 psi. Most tests to date have been made in 1.5-inch diameter drillholes using 8-inch-long pressure cells. This report deals only with the 1.5-inch CPC, although the principles are the same for any size cell.

Change of volume of the drillhole per increment of applied hydrostatic pressure was measured during the test. The results were interpreted by means of the classical thick-wall cylinder equations for an elastic body. The objective was to develop a convenient apparatus and a technique for making routine field determinations of G in mine and tunnel rocks. The method has the usual advantages of an in situ test, namely that no test specimen need be drilled out, transported to the laboratory, prepared (shaped, gages applied), and tested. Laboratory tests are time consuming and are open to the objections that the rock properties may be affected by exposure to the atmosphere, and the test specimen necessarily does not include major defects.

The ratio $E/(1+\nu)$ appears frequently in equations involving the convergence of an opening in a strained medium, the design or a tunnel lining, and the like (1, 4, 8)[4]. This method yields the value of $G = E/2(1+\nu)$ from a single test in rock, as compared to conventional testing in which the modulus of elasticity E and Poisson's ratio ν must be separately determined. Because E can be calculated from G and $(1+\nu)$, and $(1+\nu)$ typically has a value of about 1.3, a large error in ν has relatively little effect on $(1+\nu)$, which means that E can be calculated with relatively little error by using only a rough estimate of ν. In this sense the method is a practical one for determining E as well as G. Of course if the value of ν is known, the method determines E as accurately as G.

[4]Underlined numbers in parentheses refer to items in the list of references at the end of this report.

EQUIPMENT AND PROCEDURES

The equipment is simple, lightweight, and rugged. As shown in figure 1, the CPC (cylindrical pressure cell) consists of a 1-piece steel core to which is silver-brazed a copper shell and a connecting tube (1/4-inch diameter steel tubing). The steel core prevents extension of the CPC during test and provides a strong thread, which is needed to withstand repeated extraction operations. When the copper shell fails or is damaged, it is removed and a new one is brazed to the steel core. In use, the tube is connected by means of cone-type high-pressure fittings to a valve-gage unit (Bourdon pressure gage brazed onto a high-pressure stainless-steel needle valve.) Glycerin is pumped into the CPC by means of the Bureau of Mines pressure control mechanism (PCM), figure 2[5] which serves also to meter to within 0.0002 cubic inch the volume of fluid that is injected.

Change of diameter of the borehole is proportional to the volume of fluid injected into the CPC. To accurately determine the volume change of the drillhole and the hydrostatic pressure applied to the wall of the drillhole, some account must be taken of such factors as the fluid pressure that is required to expand the copper shell, the "end effects" of the CPC, the compression of the fluid and the expansion of the "plumbing". This is accomplished by performing two calibration tests, expanding the CPC inside two metal tubes, to determine the values of two constants. The calibration tests are performed at the test site immediately preceding the test in rock, to eliminate the need for a temperature correction.

The usual test procedure to determine G is as follows. After fabrication, the CPC and valve-gage unit are vacuum-filled with glycerin. The CPC is placed inside a steel cylinder (6-inch. o. d. 1.445-inch i. d.) and proof-tested to about 10,000 psi, to preclude failure in the field. For a series of field tests, all CPC's to be used, as well as the two calibration cylinders, are taken into the mine several hours before the tests are to be performed (usually the day preceding the tests), to reach equilibrium with the ambient temperature. A CPC is connected to a valve-gage unit and pressure control mechanism (PCM), figure 2; the CPC is coated with a thin film of oil (to facilitate extraction) and is inserted in the first calibration cylinder. The fluid pressure is raised by the PCM to about 7,500 psi, decreased to about 500 psi, then raised to about 7,000 psi, and decreased to zero; fluid is injected at the rate of 1/4 turn per minute of the PCM piston (1turn = 0.0192 cubic inch); which corresponds to a diameter expansion of about 0.0003 inch per minute; the fluid pressure is recorded at each multiple of 1/4 turn. The CPC is extracted from the first calibration cylinder (figure 3), inserted in the second calibration cylinder (figure 4), and the pressure-volume cycling repeated. The CPC is finally inserted in the drillhole in rock, the pressure-volume cycling is repeated, and the CPC extracted from the drillhole (figure 5). The effective or active length L of the CPC is measured to within

---

[5]U.S. Patent No. 3,108,716, granted October 29, 1963 to L. A. Panek and J. A. Stock, and licensed for public use by the Department of Interior.

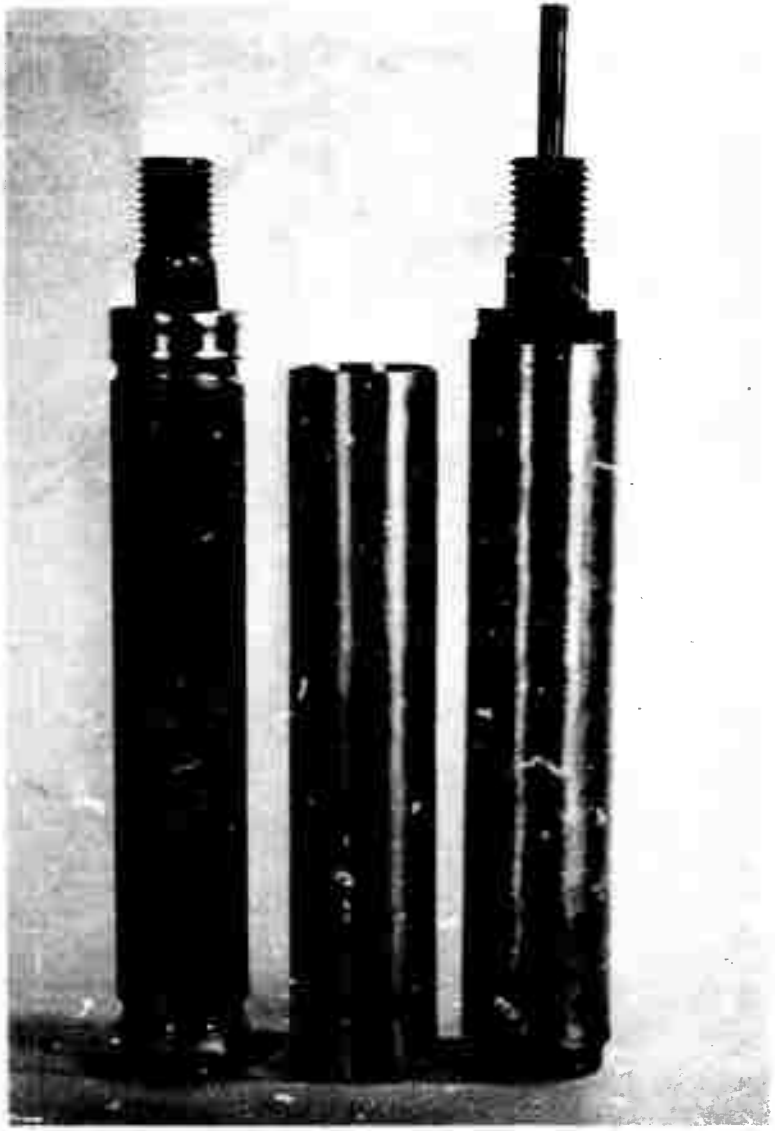

FIG. 1. Cylindrical pressure cell, showing core, 1.5-inch shett, and brazed assembly.

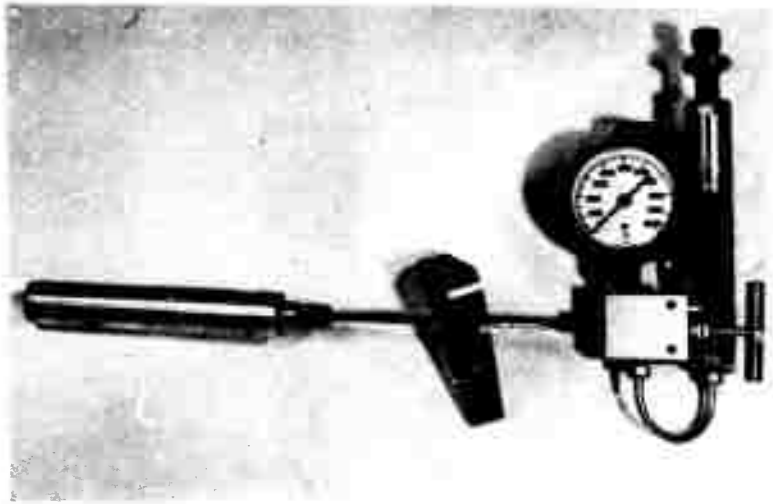

FIG. 2. Cylindrical pressure cell connected to valvegage unit and pressure control mechanism, ready for test.

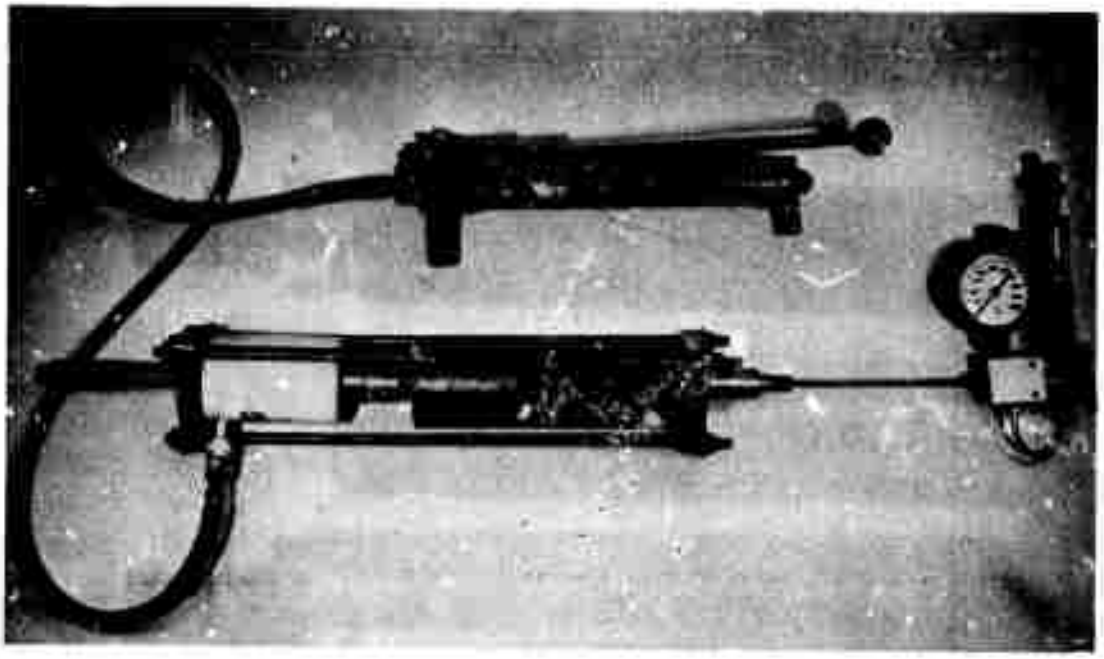

FIG. 3. CPC being pushed out of a calibration cylinder by use of a hydraulic ram.

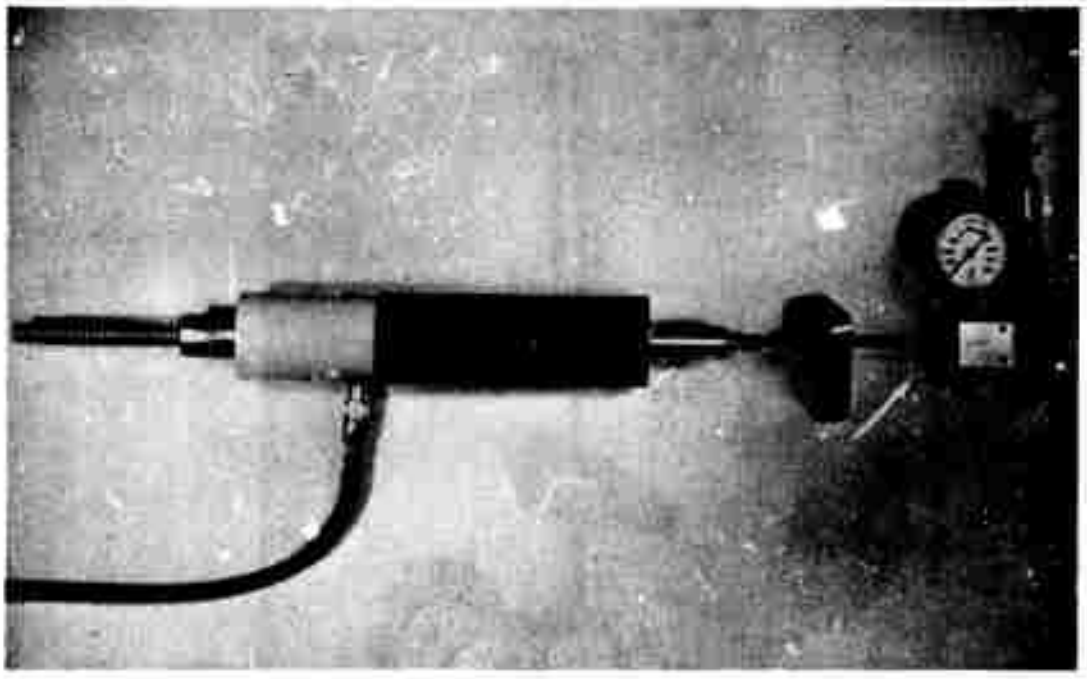

FIG. 4. CPC being pushed into a calibration cylinder by use of a hydraulic ram (the pulling bar is threaded into the end of the CPC).

FIG. 5. CPC being withdrawn from a drillhole by use of a hydraulic ram.

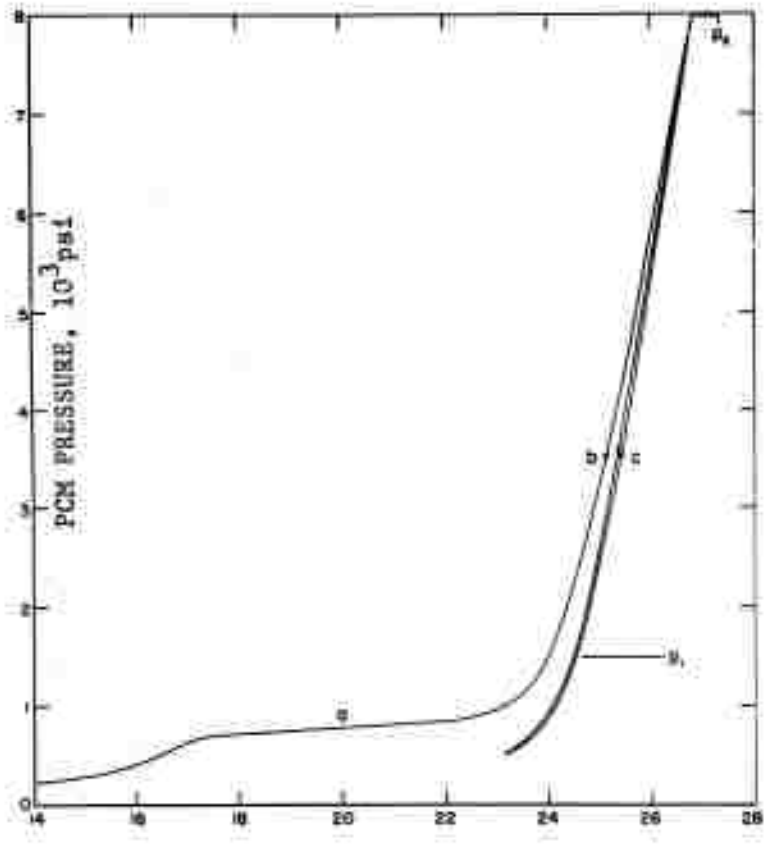

FIG. 6. Pressure-volume relationship obtained by expanding a 1.5-inch diameter CPC inside a 6-inch diameter steel cylinder.

1/25-inch and recorded; visual inspection clearly reveals the raised portion of the copper shell that was in contact with the wall of the drillhole. Unless the measurement indicates a large deviation, the value L = 6.9-inches (an average based on experience) is used for data reduction.

The general form of the pressure-volume graph for a CPC in a cylinder or a drillhole is shown in figure 6. Along path a the copper shell is being expanded (plastic flow) to meet the wall of the hole. Along b the cylinder or drillhole is being dilated, and thus the slope is much steeper than along a because of the additional pressure that must be supplied to achieve each increment of dilation. Pressure decrease occurs along c; the slope is steeper than along b because both the cylinder and the copper shell recover only elastic strain. Subsequent pressuring cycles tend to follow path c if $p_1 < p < p2$.

In routine testing, two pressuring cycles are performed, data being recorded only for the second cycle. The essential piece of information derived from a dilation test is the slope of the graph along path c, $\Delta p/\Delta T$, expressed in the units psi/turn of the PCM piston. As the slope varies with the total fluid volume contained in the system (approximately 2 cu. in.), the latter must be kept constant (no fluid bled off or added) during the calibration test and subsequent rock tests.

QUANTITATIVE INTERPRETATION OF DILATION TEST

The measurement of $\Delta p/\Delta T$ that is obtained at the PCM must be related quantitatively to the dilation of the cylinder or drillhole. We therefore proceed to find expressions for the dilation predicted by elastic theory and for the dilation indicated by the PCM piston displacement. The radial displacement u_r of a point in a thick-wall circular cylinder is given by Love (3), and may be presented in the form

$$u_r = \frac{(1+\nu)(1-2\nu)}{E}\frac{(p_i r_i^2 - p_o r_o^2)}{(r_o^2 - r_i^2)} r - \nu r \varepsilon_z + \frac{(1+\nu)(p_i - p_o) r_o^2 r_i^2}{rE (r_o^2 - r_i^2)} \qquad (1)$$

where r = radial distance to a given point, inches, from the cylinder axis,

r_i = inner radius of the cylinder, inches,

r_o = outer radius of the cylinder, inches,

P_i = hydrostatic pressure, psi, against the inner wall of the cylinder,

P = hydrostatic pressure, psi, against the outer wall of the cylinder

ε_z = uniform longitudinal strain, inches/inch,

E = modulus of elasticity, psi,

ν = Poisson's ratio.

Equation (1) is a plane strain solution that incorporates a uniform strain in the longitudinal direction. For the tests discussed in this report, there is exerted an internal

pressure p_i but no external pressure p_o. Setting $p_o = 0$ and $r = r_i$ in equation (1) we obtain the following expression for the displacement of a point on the inner wall of a cylinder with respect to the cylinder axis, that is, the change of internal radius u_i due to p_i:

$$u_i = \frac{(1+\nu)(1-2\nu)p_i r_i^3}{E(r_o^2 - r_i^2)} - \nu r_i \varepsilon_z + \frac{(1+\nu)p_i r_o^2 r_i}{E(r_o^2 - r_i^2)} \tag{2}$$

$$= \frac{P_i}{E/R} \tag{3}$$

$$\text{where } R = r_i \left[\frac{1+r_i^2/r_o^2}{1-r_i^2/r_o^2} + \nu - \frac{2\nu^2}{r_o^2/r_i^2 - 1} - \frac{\nu E \varepsilon_z}{P_i} \right] \tag{4}$$

Analysis of test data shows that the measured longitudinal strain ε_z of a calibration cylinder being dilated by a CPC is neither zero, as in the usual definition of plane strain, nor does it correspond to the plane stress condition, defined by $\sigma_z = 0$. Equation (2) takes account of this longitudinal strain, and therefore is sufficiently general to be applied to a calibration cylinder.

Equation (2) applies also to a dilation test in a drillhole. The rock surrounding the drillhole is a thick-wall cylinder for which r_o approaches infinity. Because of the superposition principle of the theory of elasticity, the change of internal radius u_i of a drillhole is not affected by the stress system that ordinarily is present in the rock before or during a dilation test. For the test in a drillhole, ε_z is assumed to be zero, owing to the confinement of the rock (the test is performed several feet from the collar of the drillhole). Substituting these values of r_o and ε_z in equation (4):

$$R_{\text{drillhole}} = r_i(1+\nu). \tag{5}$$

From equations (3) and (5), we find for the dilation test in a drillhole that

$$\frac{P_i}{u_i} = \frac{E}{R} = \frac{E}{r_i(1+\nu)} = \frac{2G}{r_i} \tag{6}$$

because $G = E/2(1+\nu)$. The dilation test is therefore a direct method for determining the modulus of rigidity G of the rock.

Physically, however, the pressure is not applied directly to the wall of the drillhole but to the inside of the copper shell, which transmits pressure to the rock. Moreover, u_i is not determined by measuring the change of drillhole diameter, but by measuring the change of the volume contained inside the copper shell. Since there is negligible change of volume of the copper itself (u_i/r_i is very small), the change of volume inside the copper shell equals the change of volume inside the drillhole, and thus

$$\Delta V_i = \pi(r_{i2}^2 - r_{i1}^2)\, L \tag{7}$$

where

ΔV_i = change of drillhole volume, cubic inches,

r_{i1}, r_{i2} = inner radius of drillhole, inches, at any two internal pressures P_{i1} and P_{i2},

L = active length of the cylindrical pressure cell, inches (length of actual contact with the wall of the drillhole).

Since u_i/r_i is very small, and $r_{12} - r_1 = u_1$, we may substitute

$$r_{i2}^2 - r_{i1}^2 = 2\, r_i u_i \tag{8}$$

in eq. (7), which becomes

$$\Delta V_i = 2\pi r_i\, L u_i. \tag{9}$$

Dividing both sides of eq. (9) by p_i,

$$\frac{\Delta V_i}{P_i} = \frac{2\pi r_i L}{P_i/u_i}. \tag{10}$$

Substituting the relationship $p_i/u_i = E/R$, from equation (3)

$$\frac{\Delta V_i}{P_i} = \frac{2\pi r_i L}{E/R}. \tag{11}$$

The relationships (10) and (11) apply to the inner wall of a cylinder or drillhole.

As stated earlier, expanding the CPC against the wall of a calibration cylinder or drillhole yields a value of $\Delta V/\Delta p$, where ΔV is measured in terms of the PCM piston displacement and Δp is the corresponding change of fluid pressure. We may logically expect to find a consistent relation between the latter and the $\Delta V_i/p_i$ at the inner wall of a calibration cylinder or drillhole. Consider the implications if this relationship is of the form

$$\left[\frac{\Delta V_i}{p_i}\right]_{\substack{\text{Cylinder or}\\ \text{drillhole}}} = A + B \left[\frac{\Delta V}{\Delta p}\right]_{PCM} \tag{12}$$

The calibration constants A and B are in effect correction factors. A, which has dimensions cubic inches/psi, corrects primarily for apparent change of fluid volume that is not due to change of hole diameter, such as compression of fluid in the system (in the tubing and the PCM as well as in the shell), and expansion of the auxiliary apparatus and connecting tube. B corrects mainly for the fact that a given increase of fluid pressure is not transmitted undiminished to the wall of the cylinder or drillhole, because a small portion is used in expanding the copper shell. The form (12) is therefore a logical one; equation (12) is also a useful form because it automatically corrects for both constant and proportional effects, whether or not they are known. A series of tests was conducted to verify that equation (12) is in fact adequate to describe the relationship between $\Delta V_i/p_i$ at the inner wall of a cylinder or drillhole and the $\Delta V/\Delta p$ observed at the PCM.

Finally, equation 13 is derived by substituting the expression given by equation (11) for the left side of equation (12) and dividing by ΔT in the numerator and denominator on the right side:

$$\left[\frac{2\pi r_i L}{E/R}\right]_{\substack{\text{Cylinder}\\ \text{or drillhole}}} = A + B \left[\frac{\Delta V / \Delta T}{\Delta p / \Delta T}\right]_{PCM} \tag{13}$$

Equation (13) is the basic equation of the CPC. $\Delta V / \Delta T$, 0.0192 cubic inch displacement per turn of the PCM piston, is a constant for the PCM. The primary purpose of every CPC expansion test, whether in a calibration cylinder or in a drillhole, is to determine $m=\Delta p/\Delta T$, the slope of the pressure-volume graph, which depends on the ratio E/R and on the calibration constants A and B. In the calibration tests the E/R ratios are known; equation (13) is solved for A and B. When the CPC is subsequently expanded in a drillhole, A, and B are known; equation (13) in effect is solved for the ratio E/R of the rock, which equals 2 G/r, as shown by equation (6). By substituting the latter relationship into equation (13), we obtain the following equation for G:

$$\left[\frac{\pi r_i^2 L}{G}\right]_{\text{Drillhole}} = A + B \left[\frac{\Delta V / \Delta T}{\Delta p/\Delta T}\right]_{PCM} \tag{14}$$

The fundamental interpretation of equation (14) becomes evident upon substituting

$$[\,V_i\,]_{\text{Drillhole}} = \pi r_i^2 L \tag{15}$$

in the left side of equation (14), and equation (12) for the right side of (14):

$$\frac{[V_i]_{\text{Drillhole}}}{G_{\text{Rock}}} = \left[\frac{\Delta V_i}{p_i}\right]_{\text{Drillhole}} \tag{16}$$

from which

$$G_{\text{Rock}} = \left[\frac{p_i}{\Delta V_i / V_i}\right]_{\text{Drillhole}} \tag{17}$$

That is, the rock G equals the ratio of the hydrostatic pressure, applied to the wall of the drillhole, to the fractional change of drillhole volume. Measuring the change of volume of a drillhole as it is dilated is therefore a direct method for determining G.

REDUCTION OF DATA

Based on the foregoing principles, calculation of the calibration constants A and B from two calibration tests and calculation of the modulus of rigidity is done as follows:

Let $\frac{2\pi r_i}{E/R} = C$, a constant for any calibration cylinder;

$\frac{\Delta V}{\Delta T} = K$, volume displaced per turn of the piston, a constant for any PCM;

$\frac{\Delta p}{\Delta T} = m$, the slope of the pressure-volume graph that is obtained by dilating (with CPC) a calibration cylinder or drillhole.

Substituting C, K, and m into equation (13), the two calibration tests (subscripts 1, 2) yield the following two equations:

$$C_1 L = A + BK/m_1 \tag{18}$$

$$C_2 L = A + BK/m_2$$

from which

$$B = \frac{(C_1 - C_2)\,L}{K}\,\frac{m_1 m_2}{m_2 - m_1} \tag{19}$$

$$A = C_1 L - BK/m_1 \quad . \tag{20}$$

Expanding the CPC in a drillhole (or another cylinder) yields the new value m_3, which, with the A and B obtained from the calibration tests is substituted in equation (14) to obtain the modulus of rigidity:

$$G = \frac{\pi r_3^2 L}{A + BK/m_3} , \tag{21}$$

where the subscript 3 refers to the test in the drillhole.

The numerator of equation (21) is the volume of the part of the drillhole that is dilated, which is determined from the pressure-volume test data as follows. The difference in PCM piston displacement as between the CPC in a calibration cylinder and in the drillhole at the same pressure, say 1,000 psi, equals the difference in volume between the calibration cylinder and the drillhole. That is, for example,

$$K (T_3 - T_1) = V_3 - V_1 . \tag{22}$$

Substituting the relation

$$V_3 - V_1 = \pi L(r_3^2 - r_1^2) \tag{23}$$

in equation (22), we obtain

$$\frac{K (T_3 - T_1)}{\pi L} + r_1^2 = r_3^2 . \tag{24}$$

Each of the two calibration cylinders (1, 2) yields a value of r_3^2; the average of these two values is used for r_3^2 in equation (21).

In summary, it may be observed that the cylinder constants C_1, C_2, r_1, r_2, the PCM constant K, and the effective length L are known before the tests are made. The two calibration tests and the drillhole test yield m_1, m_2, m_3, and an average r_3^2 (from $T_3 - T_1$ and $T_3 - T_2$), which suffice to calculate the calibration constants A, B, and the modulus of rigidity G.

VERIFICATION OF THE BASIC CPC EQUATION

The linearity of equation (13) was demonstrated by a number of tests of CPCs in metal cylinders that had E/R ratios ranging from 2.91 to 14.25 x 10^6 psi/inch, table 1.

Table 1 - Specifications of calibration cylinders

Cylinder	Material	E 10^6 psi	Outer diam., inches	Inner diam., inches	Avg. ε_z/p $\mu\varepsilon/10^3$ psi	ν	E/R, 10^6 lb/in^3
A	Steel	30.57	2.124	1.455	-5	.253	14.25
B	Aluminum	11.00	4.984	"	-1	.297	10.29
C	"	11.00	2.999	"	-7	"	8.03
D	"	11.00	2.251	"	-12	"	5.72
E	"	11.00	2.001	"	-14	"	4.45
F	"	11.00	1.874	"	-18	.287	3.66
L	Steel	30.57	2.124	1.490	-8	.253	13.10
M	Aluminum	11.00	2.251	"	-14	.297	5.34
N	"	11.00	1.874	"	-13	.287	3.30
P	Steel	30.57	2.124	1.525	-4	.253	12.24
Q	Aluminum	11.00	2.251	"	-16	.297	4.98
R	"	11.00	1.874	"	-22	.287	2.91

These tests simulated the behavior of rocks with E values ranging from about 2 to 11 x 10^6 psi (assuming $\nu = 0.25$), because from equation (3), $E/R = p_i/u_i$, and therefore all cylinders that have the same E/R ratio (a calibration cylinder or the rock around a drillhole) will experience the same change of internal radius u_i in response to a given internal pressure p_i, irrespective of the dimensions of the cylinder or the elastic constants of the cylinder material. As can be seen in table 1, the E/R ratio for a cylinder of given inside diameter depends primarily on its outer diameter and the E of the cylinder material. E and ν were determined by compressing each cylinder axially in a press and measuring the resulting strains with two-element resistance strain gages bonded to the outer surface. The same strain gages provided values of ε_z/p_i for each cylinder from several calibration tests, the average value of which is used in eq. (4) to calculate R.

Figure 7 shows the results for tests of four CPCs in metal cylinders; the linearity of the relation (12) or (13) is apparent. CPCs of 1.5 inch nominal diameter were tested in cylinders of three different internal diameters: 1.455 inch diameter, which was the standard size of cylinder for calibrating a CPC before testing it in a 1.5 inch drillhole; 1.490 inch diameter, an intermediate size; and 1.525 inch diameter, an arbitrarily chosen upper limit that was considered to provide a range of expansion sufficient for drillhole tests. The tests show that the calibration constants were unaffected by the amount of CPC expansion (plastic deformation); therefore the values of A and B determined from a calibration test in 1.455 inch internal diameter cylinders will be the same for a test at a larger diameter inside a drillhole.

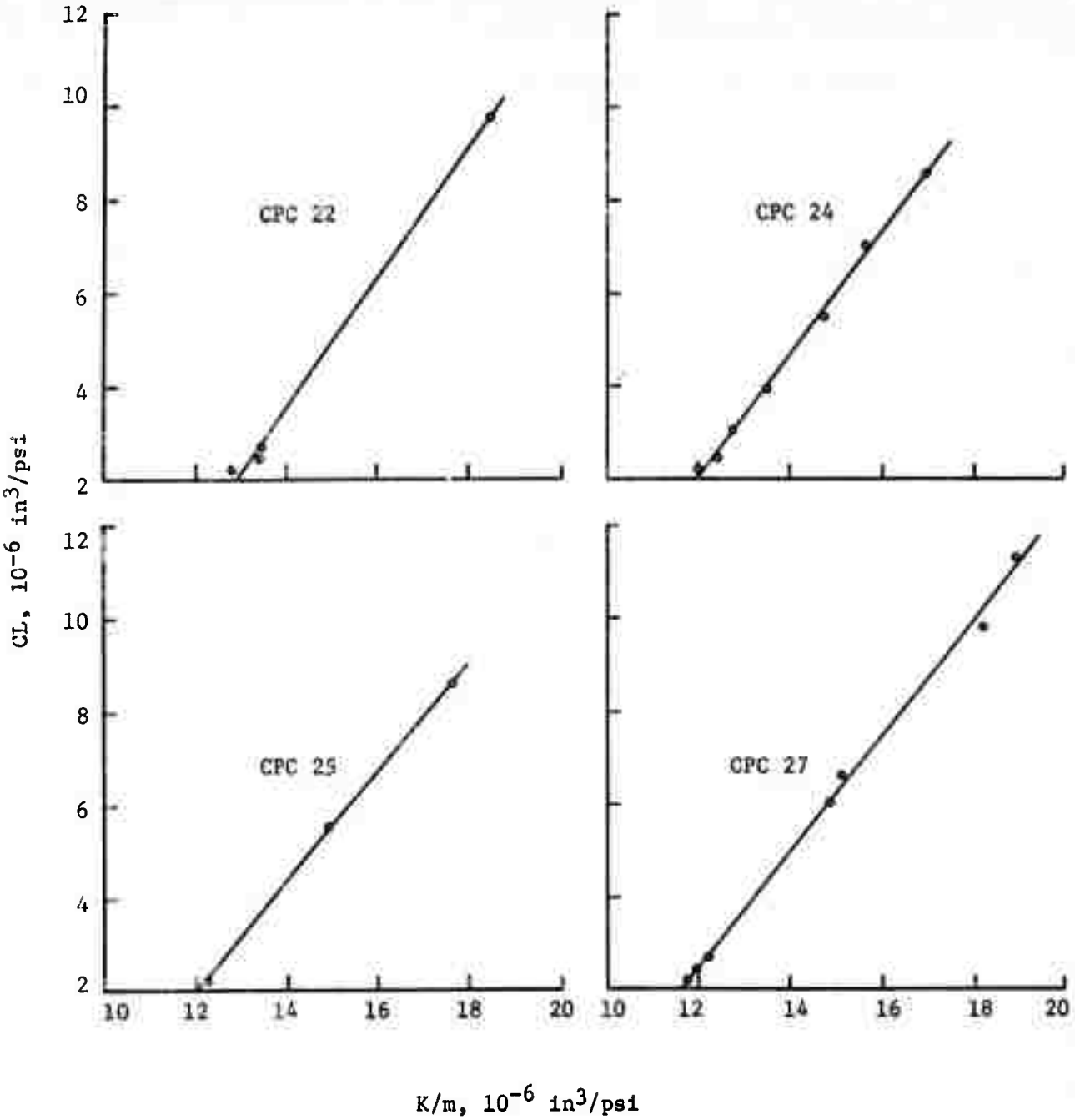

Figure 7. Tests of CPC's in metal cylinders, showing the linear relationship between CL[$\Delta V_i/p_i$] cylinder or drillhole and K/m=[Δ V/Δ p] PCM.

TESTS IN DRILLHOLES

The tests in metal cylinders having shown that the pressure-volume relationship for a CPC is described by equation (12) and that it does not change as the CPC is expanded (within limits), the final step was to perform tests in drillholes to show that the value of G as determined by this method is in fact "correct". Results obtained by testing 11 CPCs are summarized in table 2.

Table 2 - Modulus of rigidity G of cylinder B and of limestone, determined from CPC tests.

CPC No.	Calibration constants[1] A	B	Cylinder B G 10^6 psi	Drillhole No.	Limestone K/m3, 10^{-6} in^3/psi	G, 10^6 psi
29	-13.47	1.34	-	2	12.51	3.7
31	-13.64	1.34	-	1	12.63	3.7
35	-11.06	1.15	-	1	12.54	3.6
38	- 7.77	1.21	-	1	9.47	3.3
40	- 9.03	1.37	3.8	1	8.99	3.7
41	-13.82	1.41	4.6	2	12.14	3.6
43	-10.77	1.33	4.2	2	10.45	3.8
46	- 8.80	1.14	4.3	2	10.49	3.7
47	-10.35	1.29	4.3	2	10.38	3.9
48	- 8.59	1.23	4.2	2	9.62	3.6
49	-10.29	1.19	3.8	2	11.70	3.3
Avg.		1.27	4.2			3.6

[1]From tests in calibration cylinders A and D.

As verification of the method was the prime objective, a rock with uniform properties was desirable for test purposes. The tests were therefore performed in the hanging-wall limestone of No. 4 mine, Bethlehem Cornwall Corp., Cornwall, Pennsylvania, which had exhibited desirable characteristics in earlier test work (7). All tests were performed in two drillholes, 3.5 feet from the collar, over a three-month period. The two drillholes, designated 1 and 2, were only a few inches away from the 6 inch overcoring holes "E" and "F", respectively, which are nearly opposite each other on the two sides of the drift (7). Cores from five holes in this drift were tested by other methods to determine the elastic constants, thus making possible a comparison of results. Each CPC was used for

only one test in rock, in order to obtain information as to the variation in CPC characteristics. Since the rock E was known to be of the order of 10 x 10^6 psi, calibration cylinders A and D were selected so that the drillhole dilation would be intermediate between those of the two calibration cylinders. Figure 8, a typical example of the test data, shows the second-cycle graphs for tests of CPC 31 in the calibration cylinders and in the drillhole, from which m_1, m_2, and m_3 were determined graphically.

Six of the CPCs were calibrated in three cylinders, instead of only two as in the standard procedure, for purposes of checking the calibration. The third calibration test could be averaged with the other two to obtain a more accurate estimate (in the statistical sense) of the calibration constants A and B. However, it is instructive to look upon the test in the third cylinder (cylinder B) as simulating a test in a drillhole and to compare the average G obtained by the CPC test procedure, 4.2 x 10^6 psi, with the G obtained by the uniaxial compressive test, which is also 4.2 x 10^6 psi (= 11.00 x 10^6/ 2(1+0.297), values from table 1). In view of the close agreement, there is little likelihood that the standard test procedure will yield an inaccurate value of G in a drillhole in rock because the thick-wall cylinder equations are equally valid whether the outer diameter of the cylinder is finite or infinite.

The average G of the limestone was found to be 3.6 x 10^6 psi, with a range of ± 10 pct. The relatively large variation in calibration constant A is due to deliberate changes in the total fluid volume of the system, as different plumbing arrangements were tried. The greater the total fluid volume, the greater the numerical value of A and the greater the value of K/m_3 (the "softer" the system).

ELASTIC CONSTANTS BY OTHER METHODS

Elastic constants of the limestone at the test site, determined by other methods, are given in Tables 3 and 4, for comparison.

In the first group of tests, cores of 5.62 inch outer diameter and 1.5 inch inner diameter, drilled out at intervals along the drift in a previous investigation (7), were tested in the Bureau's biaxial loading apparatus (2), yielding an average E = 9.2 x 10^6 psi as shown in table 3. In this test, a length of core is subjected to hydrostatic pressure on its cylindrical outer surface, while the corresponding change of diameter of the internal 1.5 inch hole is measured with the Bureau's borehole deformation gage (6). These tests were performed underground at the test site within a day or two after drilling out the core.

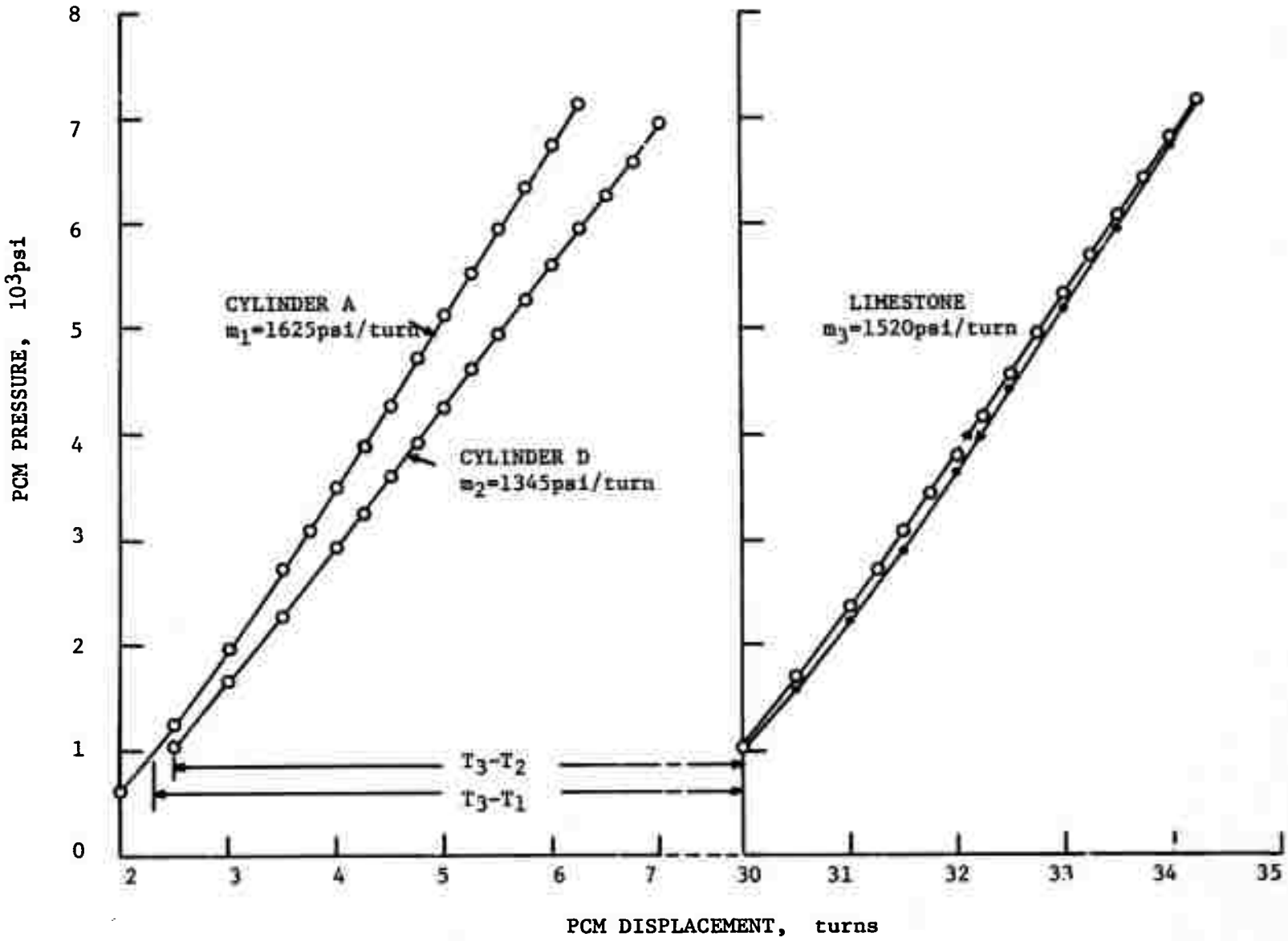

Figure 8. Tests of CPC 31 in calibration cylinders and in limestone drillhole.

Table 3 - Modulus of elasticity E determined under biaxial load, 10^6 psi.

Specimen from hole--	Direction of Measurement		
	60° c.c.w.[1]	Vertical	60° c.w.[2]
A	9.2	8.4	10.3
B	9.6	10.5	10.8
C	7.6	7.8	7.3
D	8.6	9.9	8.9
F	11.0	8.7	9.0

Average E = 9.2×10^6 psi

Corresponding G = 3.3×10^6 psi (taking $\nu = 0.41$, table 4)

[1]Angle measured counterclockwise from the vertical direction.

[2]Angle measured clockwise from the vertical direction.

Some of these 5.62 inch cores were taken to the laboratory and stored for future testing. About 1 year later two 10 inch long sections were cut from these cores for the second group of tests. The ends of the core sections were ground flat, and two element resistance strain gages were cemented to the outer cylindrical surfaces. Each core was placed in the Bureau's triaxial loading apparatus (5). Results are shown, table 4 (a) for loading in which the radial pressure was varied, similar to the loading used in the second group of tests except that a constant longitudinal load of 1,200 psi was maintained during the test, and (b) for triaxial loading, in which the ratio of the longitudinal stress to the radial pressure was maintained at one half while both loads were varied. For both loading methods the change of internal diameter of the core was measured with the borehole deformation gage, and the tangential and axial strains were measured by the resistance strain gages, thus permitting the values of E and ν to be calculated both from the borehole deformation gage measurements and from the tangential strain measurements.

Table 4 - Elastic constants determined under triaxial load

Core Specimen	Measurement	Constant longitudinal stress			Variable longitudinal stress		
		E, 10^6 psi	ν	G^1 10^6 psi	E 10^6 psi	ν	G^1 10^6 psi
1	SG[2]	10.0	0.40	3.6	9.5	0.42	3.3
	BDG[3]	11.6	.41	4.1	10.8	.47	3.7
2	SG[2]	10.0	.39	3.6	9.1	.40	3.3
	BDG[3]	11.0	.40	3.9	10.8	.41	3.8
Average		10.6	.40	3.8	10.0	.42	3.5

[1]Calculated from $E/2(1+\nu)$ [2]Strain gage [3]Borehole deformation gage

CONCLUSIONS

The average modulus of rigidity determined by the 11 CPC tests in drillholes, 3.6×10^6 psi, is in reasonable agreement with the results obtained by the other methods, 3.3, 3.8, and 3.5×10^6 psi, to the extent that realistic comparisons can be made, considering that there is no accepted method of determining the absolute value. The state of stress in the rock for the CPC tests in drillholes was quite similar to that in the other tests, and hence agreement was to be expected, confirming the outcome of the CPC tests that correctly determined the G of a third cylinder. However, the authors believe that CPC test results must be considered superior to those obtained from testing rock cores because in the CPC tests the rock is virtually in an undisturbed condition.

It has been demonstrated that the cylindrical pressure cell, auxiliary equipment, and test procedure provide a simple and convenient method for determining the modulus of rigidity of elastic rock in situ. Since the test is made in a drillhole, the result is free from surface effects such as blasting-induced fractures. Although the calculations involve the fractional change of volume of the dilated drillhole, it is unnecessary in this procedure to caliper the drillhole or to measure the total quantity of fluid in the system. All the information required for calculating the modulus of rigidity of the rock is obtained from pressure-volume measurements, using an ordinary Bourdon pressure gage and a pressure control mechanism.

This technique is now being used (1) to make routine determinations of the modulus of rigidity, (2) to study the influence on G of the volume of rock that is strained during the test (effect of cracks and other nonhomogeneities), and (3) to study the stress-strain behavior of inelastic rock materials.

REFERENCES

1. Bleifuss, D. J. Theory for the Design of Underground Pressure Conduits. Proc. ASCE, July 1955, vol 81, paper 741, 10 pp.

2. Fitzpatrick, John. Biaxial Device for Determining the Modulus of Elasticity of Stress-Relief Cores. BuMines Rept. of Inv. 6128, 1962, 13 pp.

3. Love, A. E. H. Theory of Elasticity, 4th ed., reprinted by Dover Publications, 1944, p. 144 eqs. (55) and (57).

4. Moody, W. T. Importance of Geological Information as a Factor in Tunnel-lining Design. Engineering Geology Case Histories No. 3, Geological Society of America, New York, May 1959, pp 48-51.

5. Obert, L. An Inexpensive Triaxial Apparatus for Testing Mine Rock. BuMines Rept. of Inv. 6332, 1963, 10 pp.

6. Obert, L., R.H. Merrill, and T.A. Morgan. Borehole Deformation Gage for Determining the Stress in Mine Rock. BuMines Rept. of Inv. 5978, 1962, 11 pp.

7. Panek, L. A. and J. A. Stock. Development of a Rock Stress Monitoring Station Based on the Flat Slot Method of Measuring Existing Rock Stress. BuMines Rept. of Inv. 6537, 1964, 61 pp.

8. Timoshenko, S., and J. N. Goodier. Theory of Elasticity. McGraw - Hill Book Co., Inc., New York, 1951, p. 188.

APPENDIX F

THE MENARD PRESSUREMETER

This appendix has been abstracted, in part, from The Geocel Pressuremeter. Interpretation of Pressuremeter Tests, issued by Geocel Inc., 11680 West 44 Avenue, P. O. Box 316, Wheat Ridge, Colorado 80033 with the permission of the Company.

THE MENARD PRESSUREMETER

DESCRIPTION

The Pressuremeter is a borehole radial expansion device designed to measure soil and rock properties including E, the deformation modulus. The main components are (see Figures 1 and 2).

A pressure-volumemeter cylinder
A probe
A length of coaxial tubing

It is operated by the gas pressure from a cylinder of carbon dioxide or nitrogen.

The pressure-volumemeter consists of a cylinder containing antifreeze to which a scale is attached to measure volume changes, and a pressure gage. The gas cylinder is attached to the pressure-volumemeter and to the coaxial tubing, and pressure-volumemeter is also attached to the coaxial tubing, both through a series of valves. This allows gas to be released directly into the tubing as well as to be used to force liquid into the tubing.

The other end of the coaxial tubing is connected to the probe. The gas and liquid are under very nearly the same pressure, so that the gas in the annulus of the tubing tends to restrict the expansion of the liquid tubing, and thus "harden" the instrument.

The probe is a cylindrical metal assembly securing rubber membranes arranged to form three independent cells connected to the coaxial tubing. The central measuring cell contains antifreeze under gas (and hydrostatic) pressure, so that the increase in the volume of this cell is measured by the fall in liquid in the volumemeter at the surface. The upper and lower cells, known as guard cells, expand under equal gas pressure from the surface and thus avoid end effects in the central measuring cell. Pressure and volume changes are read to a timed program, and the preliminary results of the test are available at once.

CALIBRATION

The instrument is calibrated in two tests, the Compressibility Test and the Inertia test.

The Compressibility Test is designed to determine the volume of liquid required to compress the instrument at various pressure levels. The probe is placed in a rigid steel tube (2 3/4" ID), and the pressure is increased in 5 kg/cm^2 steps from 5 to 60 kg/cm^2, with volume readings being taken at 15, 30, and 60 second intervals. The pressure is then reduced to atmospheric in 5 kg/cm^2 steps, with volume readings being taken at 15 second intervals only. Compressibility of the unloading phase should be about 80% of the compressibility of the loading phase. The compressibility volume over a given pressure range is subtracted from the field test volume variation prior to computing the deformation modulus E.

The Inertia Test is designed to determine the pressure required to deform the instrument to various sizes. The probe is placed in an upright position with the sheath completely unrestricted. A pressure of 1 kg/cm^2 is applied, and the volume

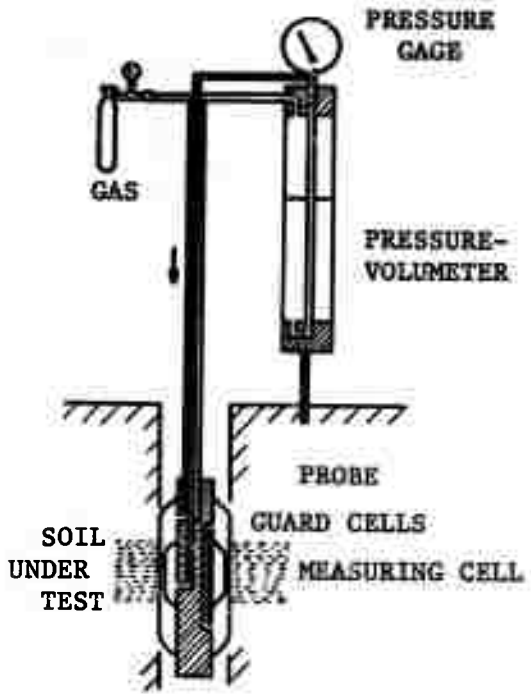

Fig. 1. Schematic drawing illustrating the principle of the Pressure Meter and its operation.

Fig. 2. The Menard Pressureplate.

at 15, 30 and 60 second intervals. The pressure is then increased in 0.5 kg/cm^2 steps, with the volumes being read, until the total volume is 800 cm^3. The pressure is then released, with no unloading figures being taken. The total inertia should not exceed 5 kg/cm^2. The pressure required to expand the probe to any given volume is deducted from the pressure gage reading in a field test at that volume.

COMPUTATION OF THE STANDARD MODULUS OF DEFORMATION

For an increase in pressure dp, the wall of the boring hole increases in radius by dU and they are related by the equation:

$$dU = \frac{1 + \sigma}{E} (r_o + U)\, dp \qquad \text{(equ. 42)}$$

(see equation 6, Appendix E. This implies plane strain. Author's note)

in which σ is the Poison's ratio, r_o the radius of the hole at the beginning of the test, U the increase in radius due to the increase in pressure to the pressure p_m at which is measured the standard Modulus of Deformation E.

E corresponds to the pseudo-elastic phase of the test; p_m can range from po to pf

E is defined by:

$$E = (1 + \sigma)\, (r_o + U)\, \frac{dp}{dU}$$

RELATION BETWEEN RADIUS AND VOLUME

As we measure volumes with the pressuremeter, we have to express E in terms of pressure and volume changes.

Volume of measuring cell:

$$V = v'o + vm - va = \pi\, (r_o + U)^2\, L$$

where v'o = volume of the empty measuring cell, vm = volume reading

L = length of measuring cell, va = volume compensation for plastic tubes

We have $dV = 2\, \pi\, L\, (r_o + U)\, dU$

then: $$E = 2\, \pi\, L\, (r_o + U)^2\, (1 + \sigma)\, \frac{dp}{dv}$$

$$E = 2\, V\, (1 + \sigma)\, \frac{dp}{dv}$$

We can define a coefficient of compression K (v) variable with the volume of the measuring cell and characteristic of a probe:

$$K\,(v) = 2\, V\, (1 + \sigma) = 2\, (v'o + vm - va)\, (1 + \sigma) \qquad \text{equation 45}$$

then: $E = K(v) \frac{dp}{dv}$

The modulus E is inversely proportional to the slope of the curve V = f (p) of the pressuremeter test in the pseudo-elastic phase.

In this area the curve is generally a straight line and E is defined as an average on the whole pseudo-elastic phase taking into account the average value of K.

In some materials (over consolidated clays, some sands, etc...) the slope of the curve can step up to 20% within the pseudo-elastic phase: in these cases different values of E must be computed for different ranges of pressure.

COMPUTATION OF K (V)

As va is much smaller than v'o + vm (va < 3% of v'o + vm), it is usual to express K (v) as so: K (v) = 2 (v'o + vm) (1 + σ).

The EX (32 mm O.D., L = 630 mm), AX (44 mm O.D., L = 370 mm) and BX (60 mm O.D., L = 210 mm) probes have been designed to have a same value of K - for increasing values of diameter, they have decreasing lengths. The NX (70 mm O.D., L = 210 mm) has different values of K.

For σ = 0,33 and for vm varying from 0 to 800 cm3 the values of K (v) are as follows:

TABLE II - 2

VALUES OF COEFFICIENT OF COMPRESSION OF THE PROBES K (V)

	K (v) (cm3) for the probes	
Vm cm3	EX, AX and BX	NX
0	1,420	2,100
50	1,560	2,200
100	1,690	2,350
150	1,820	2,500
200	1,960	2,600
250	2,090	
300	2,220	2,800
350	2,350	
400	2,490	3,050
450	2,620	
500	2,750	3,300
550	2,890	
600	3,020	3,500
650	3,150	
700	3,290	3,750
750	3,420	
800	3,550	4,000

These values can be computed for different values of σ.

The Standard Modulus of Deformation takes into account some rheological factors due to the behavior of the soil during the test.

COMPENSATIONS ON E

A rough value E_1 is given by the diagram for the values of vm and pm read on the pressuremeter:

$$E_1 = K \frac{dpm}{dvm}$$

But as between vm and vm + dvm, the value of q_i (v) has varied by dq_i (v) and va by dva = a . dp, the right value of E is given by:

$$E = K \frac{dp - dq_i\ (v)}{dv - a\ .\ dp}$$

Some transformations can be made:

$$E = K \frac{dp}{dv} \frac{1 - \frac{dq_i(v)}{dp}}{1 - \frac{adp}{dv}}$$

$$E = E_1 \frac{1 - \frac{dq_i(v)}{dp}}{1 - \frac{adp}{dv}}$$

1°) <u>E is small (E < 100 kg/cm2)</u> : weak soils

The contribution $\frac{adp}{dv}$ can be neglected.

$$E = E_1\ (1 - (1 - \frac{dq_i(v)}{dp}\ ))$$

$$= E_1\ (1 - \frac{dq_i(v)}{dv}\ \frac{dv}{dp}\ )$$

$$= E_1\ (1 - \frac{dq_i(v)}{dv}\ \frac{K\ (v)}{E_1}$$

$$E = E_1 - K(v) \frac{dq_1(v)}{dv}$$

The correction is substractive and depends only on the volume..

A table of the correction to be substracted is given for the different probes:

Vm (cm3)	$K(v) \frac{dq_1(v)}{dv}$			
	AX Nude	AX with split tube	BX Nude	NX Nude
100	6	10	10	15
200	3	5	6	9
300	2	4	4	6
400	2	3	2	5
500	2	3	2	4
600	1,5	3	1,5	3
700	1,5	3	1	2

If this correction is neglected above 300 cm3, the relative error does not exceed 5% for non-compressible soils ($E \geq 100$ kg/cm2) and it can be neglected.

On the contrary, for very compressible soils, this correction is very important.

2° E is high ($E > 1000$ kg/cm2) : rock and rock masses

The contribution $\frac{dq_1(v)}{dp}$ can be negledted and

$$E = E_1 \frac{1}{1 - a \frac{dp}{dv}} = E_1 \frac{1}{1 - a \frac{E_1}{K(v)}}$$

This correction is additive and depends slightly on the volume and especially on the value of E_1 itself.

The value of a , for coaxial rilsan tubing is very small and depends mainly on the compressibility of the rubber membrane and of eventual air bubbles in the water circuit.

When the filling of the pressurementer has been done roughly (which is usually the case in the field), a = 0,1 cm3/Kg/cm2.

For the measurement of high modulus in rock masses, a cautious filling has to be performed and a check on the actual values of a as described later is recommended just before testing and after testing.

In these conditions for the ϕ 60 mm probe and with the current rubber membranes, a realistic value of a is:

a = 0,03 cm3/Kg/cm2.

Charts can be made up for different probes, different volumes and different values of a.

As a reference the following tables give the corrected values of E versus the rough value E_1 for the NX probe ϕ = 70 mm, for a volume vm = 400 cm3 and for two values of a:

a = 0,1 cm3/Kg/cm2

a = 0,03 cm3/Kg/cm2

E_1 Kg/cm2	E (Kg/cm2) a = 0,1	a = 0,03
1000	1040	1010
2000	2140	2040
5000	6000	5250
10,000	15,000	11,100
20,000	60,000	25,000
50,000		100,000
75,000		300,000

The measurable values of E are limited by the equipment and especially by the probe. To be able to measure accurately high values of E, the value of K should be increased and the value of a should be decreased.

GAUGING THE APPARATUS FOR THE DETERMINATION OF a:

The probe to be used is inserted in a tube which must be very rigid with respect to the apparatus and of the same inside diameter as the boring hole.

The stiffness of the tube can be given by a very thick walled steel tube or by two coaxial thin steel tubes welded together at their extremity and between which the same pressure is applied as in the probe.

A test following the normal procedure is done, the pressure steps being of the same scale as for the investigation in rock.

For very accurate studies, such a gauging should be performed in the field right before and after testing.

APPENDIX G

THE BOREHOLE DILATOMETER

This appendix is abstracted from

(i) T. E. 9 BHD-Borehole Dilatometer, Tests and Equipment, by M. Rocha. Laboratorio Nacional de Engenharia Civil, Lisboa, Portugal

(ii) Memoria No. 339, Determination of the Deformability of Rock Masses Along Boreholes, by Manuel Rocha, Antonio da Silveira, Nuno Grossmann, and Emilio de Oliveira, Ministerio Das Obras Publicas, Laboratorio Nacional da Engenharia Civil, Lisboa, 1969

THE BOREHOLE DILATOMETER

GENERAL DESCRIPTION

The Lnec dilatometer meets the following requirements: (i) is suitable for test diameters from 74 to 82 mm and for vertical depths down to 200m, and is still operative in boreholes holding water; (ii) applies radial pressures up to 200 kg/sq.cm; and (iii) measures the radial displacement of borehole wall to within μm, along four diameters 45° apart. The BHD can be used in holes drilled in any direction, the maximum allowable depth being less, the closer to the horizontal the hole.

Fig. 1 is a diagrammatic drawing of the BHD longitudinal section. The external diameter of the apparatus is 70 mm in the zone that applies the pressure. This corresponds to a 6 mm clearance in relation to the most frequent (NX) borehole diameter, viz 76 mm. By pumping water between the rubber jacket and the steel body, the wall of the hole is made to withstand a uniform radial pressure, over a length of more than seven times its diameter. Upon conclusion of each test, a realief valve, operated by the water pump, drains the water previously fed to the jacket, thus allowing the BHD to be moved into another test position.

Eight feelers to follow the radial displacement of the borehole wall are bound to the jacket on generatrices at 45° intervals. The two opposite feelers moving along each direction are centred on cross sections 15 mm apart; the corresponding distance is 40 mm, for two feelers 45° apart. Each feeler is attached to the magnetic core of a displacement transducer with a 5 mm stroke and the accuracy 1 μm. Once connected to its reading unit the BHD has the overall sensitivity 2 dial divisions per micron.

The different parts of the apparatus are displayed in Fig. 2.

Fig. 3 shows the BHD testing equipment, complete except for the steel positioning rods which install the apparatus inside the borehole, and define both its depth and azimuth at the test point. While Fig. 4 shows the calibration setup, as used to determine the sensitivity of each transducer, prior to carrying out a test program.

Typical BHD loading diagrams are presented in Fig. 5, where the ordinates are pressures applied by the dilatometer, and the abscissae the corresponding radial deformations along each direction of measurement. Assuming the tested rock mass to be homogeneous, isotropic and elastic, the plotted diagrams yield the moduli of deformability

$$E = (1 + \nu)\, d\, e$$

where ν is Poisson's ratio of the rock mass, d is the diameter of the test borehole, and e stands for deformation under the applied pressure, to be read on every diagram, for the pressure interval selected.

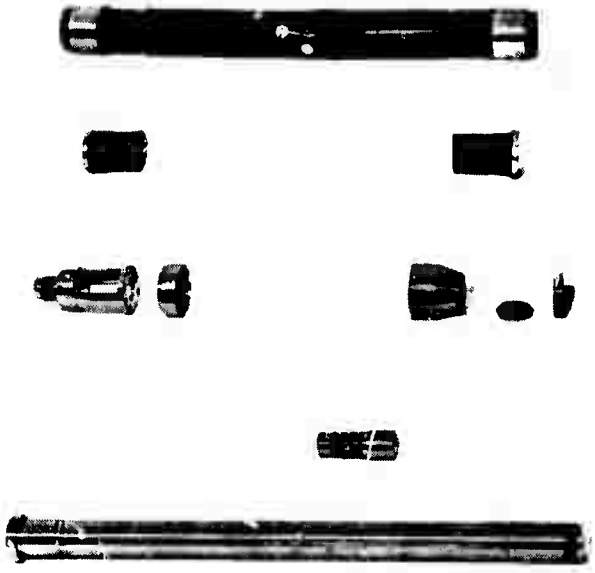

FIG. 2

FIG. 4

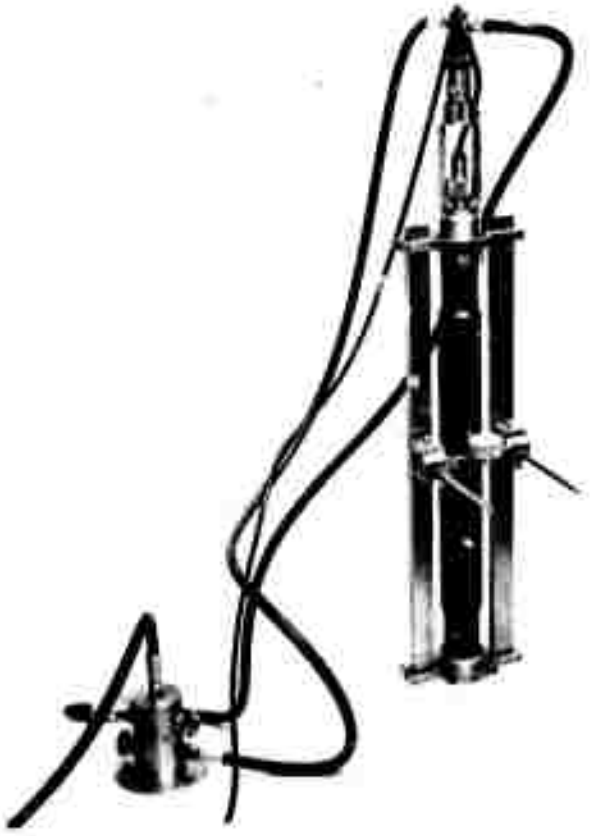

FIG. 3

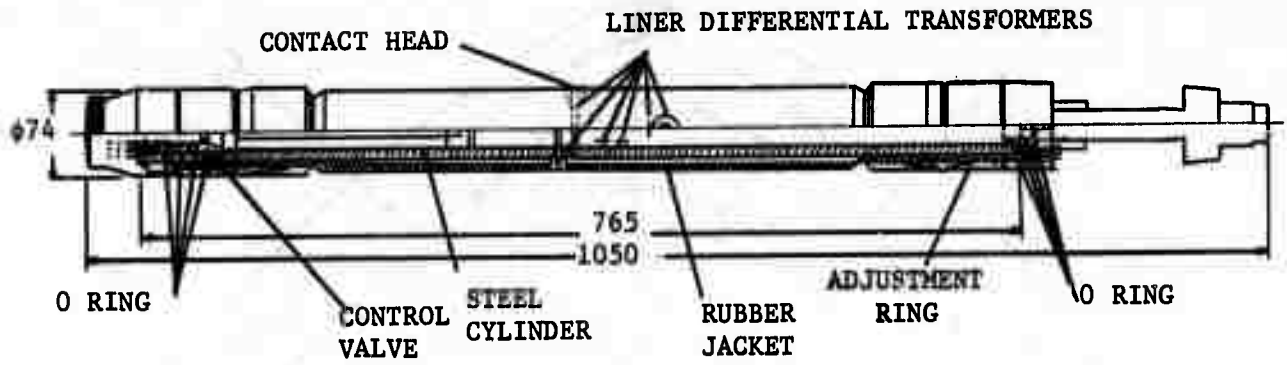
CONTACT HEAD
LINER DIFFERENTIAL TRANSFORMERS
φ74
765
1050
0 RING
CONTROL VALVE
STEEL CYLINDER
RUBBER JACKET
ADJUSTMENT RING
0 RING

FIG. 1

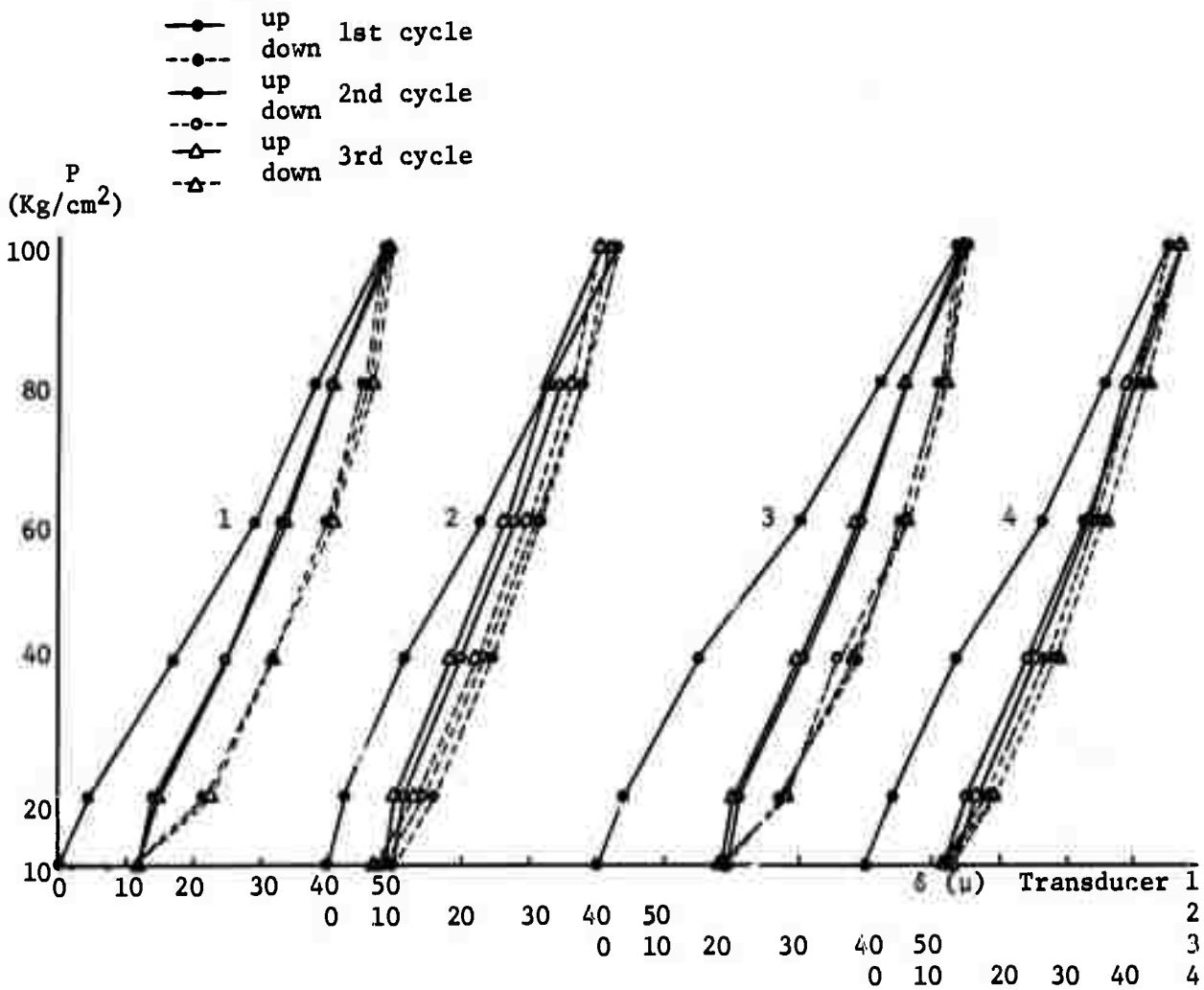
up
down
1st cycle
up
down
2nd cycle
up
down
3rd cycle
P
(Kg/cm2)
100
80
60
40
20
10
1
2
3
4
0 10 20 30 40 50
δ (μ)
Transducer 1
2
3
4

FIG. 5

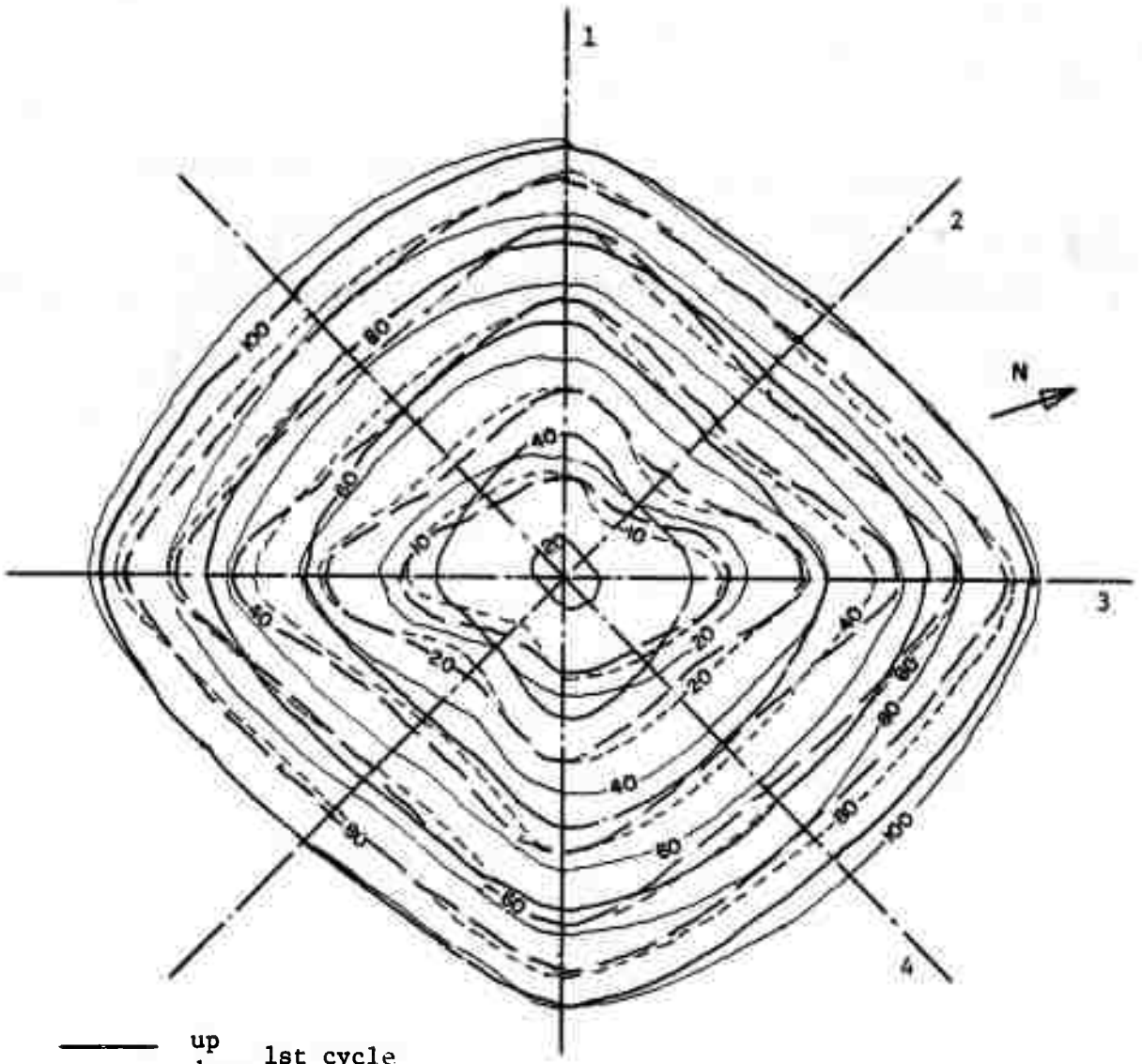

FIG. 6

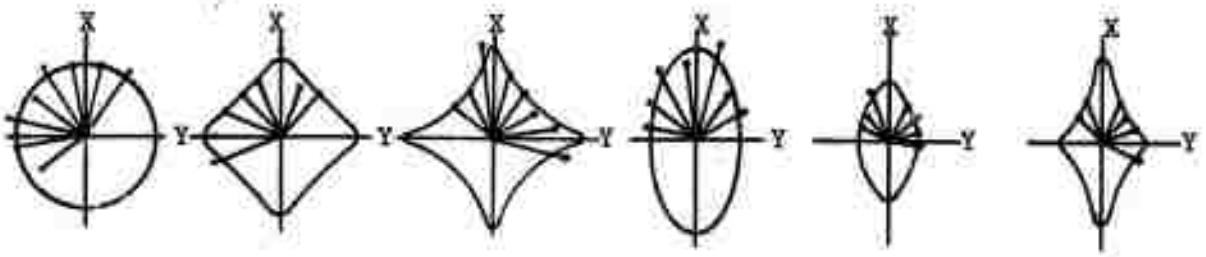

FIG. 7

Sometimes, polar diagrams are also drawn to outline the building up and subsiding of all measured deformations while the cyclic pressure is applied. Such diagrams are similar to the one depicted as Fig. 6, where diametral deformations for two load cycles were plotted for the applied pressure inserted in each curve.

When the envisaged approach calls for measurements along more than four diametral directions, it is quite feasible to double-test each point in a borehole, i.e., to test each point twice while installing the BHD at azimuthal angles 22.5° apart. This technique provides anisotropy figures such as are shown in Fig. 7, in connection with which a few anisotropy ratios may be defined.

GENERAL TECHNICAL DATA (*)

Dilatometer Weight: about 12 kg.

Dilatometer body supports the rubber jacket, and houses the displacement transducers and their electronic circuits. High-strength stainless steel. Overall dimensions: 800 mm x Ø 64 mm.

Rubber jacket applies the test pressure, and holds the eight feelers. Neoprene with suitable hardness, resilience, and fatigue strength. Tops prevented from extruding by special sleeves.

Relief valve sealed by O-rings on the dilatometer body, closes and opens the water system, at the far end of the body. Water-pressure operated. Stainless steel.

Displacement transducers follow the radial displacement of the feelers against the borehole wall. LVDT type. Range: 5mm.

Electronic circuits feed the transducer primary coils, under 8 kHz, and rectify and filter the displacement signals. Inside a water-tight compartment. Input: 18 volts DC. Sensitivity: 1 volt/mm.

Water pump via a 2-way valve, supplies either the test pressure to the rubber jacket or the operating pressure to the relief valve. Manual, with two pistons for facility of operation. Stainless steel and bronze. Two Bourdon manometers, with the ranges 50 kg/ sq.cm and 300 kg/sq.cm, respectively, and 1% F.S. accuracy.

Reading unit selects the transducers, and measures the displacement of each core relative to its coil assembly. Reads by the potentiometric compensation method, either every transducer or the sums for both transducers belonging to each direction of measurement. Fed by a 24-volt battery. Sensitivity: adjusted to 2 div./μm. Accuracy: readings up to 50 μm; 0.5 μm; above 50 μm, 2% of the reading.

Electrical cable connects the dilatometer to its reading unit. PVC-sheathed cable: 9 flexible conductors, 0.3 mm^2 in section + 1 shielded conductor, 0.5 mm^2.

(*) All specifications are subject to change without notice.

Positioning rods convey the water to the installed dilatometer, besides transferring and controlling its azimuth. Tubular steel with screwed connections. House two water-tight tubes, one for the water which supplies the applied pressure, the other for the water that operates the relief valve.

Winch supported drum to coil the steel cable which carries the dilatometer down the hole to the test point. Overall weight: 60 kg. Cable diameter: 6mm. Maximum load: 1000 kg.

REFERENCES

ROCHA, M.; SILVEIRA, A.; GROSSMAN, N.; OLIVEIRA, E. -- Determination of the deformability of rock masses along boreholes. Proc. 1st Congr. Int. Soc. Rock Mech., 1, p. 697. Lisbon, 1966.

ROCHA, M.; SILVEIRA, A. ; RODRIGUES, F. P. ; SILVERIO, A. ; FERREIRA, A. -- Characteriaztion of the deformability of rock masses by dilatometer tests. Proc. 2nd Congr. Int. Soc. Rock Mech., 1,2-32. Belgrade, 1970.

CALCULATION OF THE MODULUS OF ELASTICITY OF THE ROCK MASS. INFLUENCE OF FISSURATION

Suppose that the rock mass can be assumed to be homogeneous, isotropic and elastic and that the ratio of the length of the hole under the pressure applied by the dilatometer to the diameter of the hole is sufficiently great for the middle zone of the tested volume to be considered in plane equilibrium. The state of stress in this zone is the same that is induced in an infinite plate with a hole by a pressure p (fig. 3):

$$\sigma_r = p \frac{a^2}{r^2} \quad \text{(compression)}$$

$$\sigma_\theta = - p \frac{a^2}{r^2} \quad \text{(tension)}$$

Since $\sigma_r + \sigma_\theta = 0$, stresses are zero in the elements of area normal to the axis of the borehole in plane equilibrium.

As σ_r and σ_θ decrease very rapidly with the distance to the axis of the borehole and the ratio of the length of the borehole under pressure to the diameter of the hole is $\frac{540}{76} = 7.2$, the preceding expressions are assumed to apply to the dilatometer developed.

The deformation of the diameter of the hole is given by the expression

$$\Delta = 2 \frac{1 + \nu}{E} a p \qquad (1)$$

where E and ν are the modulus of elasticity and the Poisson's ratio of the rock mass. The modulus of elasticity can therefore be obtained from the measured value of Δ by means of the expression

$$E = 2 \frac{1+\nu}{\Delta} a p$$

The application of the dilatometer giving rise to tensile stresses σ_θ which equal the pressure exerted on the side walls of the borehole, a question to be investigated is the influence of possible fissures on the value obtained for the deformation of the diameter of the hole and consequently for the modulus of elasticity determined. Let us assume that the pressure applied by the dilatometer gives rise to radial fissures which extend to a distance b from the axis of the hole and make angles α with one another (fig. 4). Assuming that fissures start from the two points A, they will hardly affect the tensile stresses σ_θ at points B, so that it is to be expected that a slight increase of the pressure p will give rise to two other fissures approximately perpendicular to the first ones. As pressure increases, other fissures will successively occur.

In order to calculate the deformation of the diameter of the hole, it is assumed that the state of stress in the wedge LM L'M' (fig. 5) at a point at a distance r from the axis of the hole is

$$\sigma_r = \frac{ap}{r} \qquad \sigma_\theta = \tau_{r\theta} = 0$$

and also that the distribution of stresses beyond a cylinder of radius b is the same that arises in an indefinite solid with a hole of radius b subjected to a uniform pressure

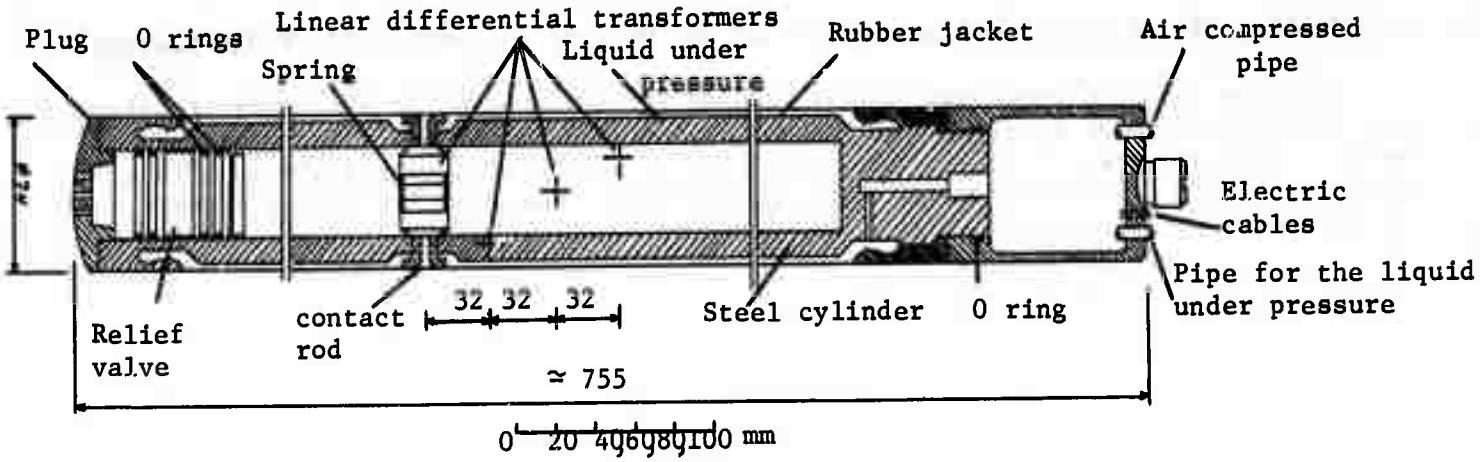

FIG. 2

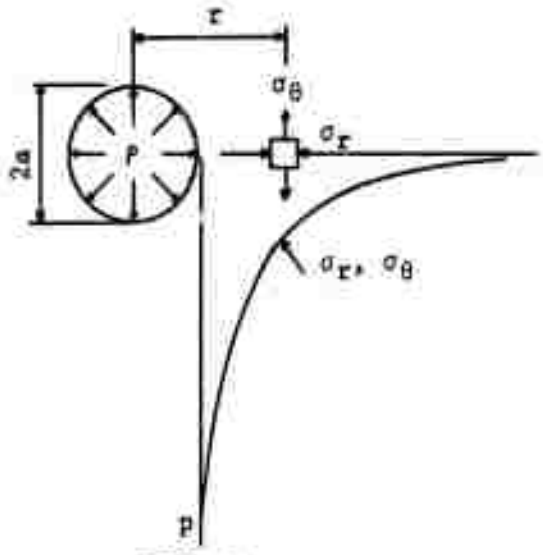

FIG. 3

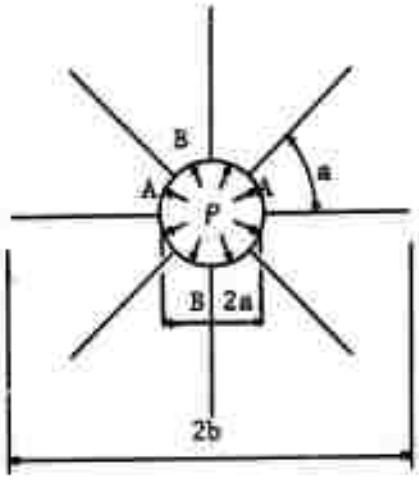

FIG. 4

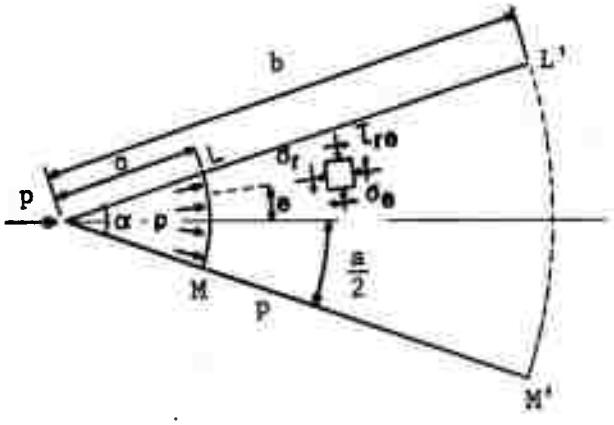

FIG. 5

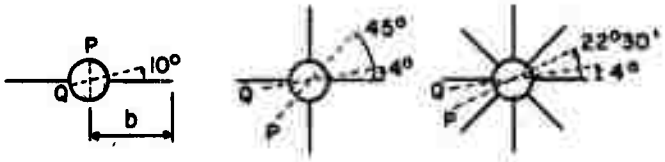

FIG. 6

$p' = p \frac{a}{b}$. The deformation of the wedge in a radial direction is

$$\int_a^b \frac{\sigma_r}{E} dr = \frac{ap}{E} \log \frac{b}{a}$$

and the deformation of the hole considered is given by expression (1), i. e. it has the value

$$\frac{bp'}{E} (1+\nu) = \frac{ap}{E} (1+\nu)$$

Therefore the deformation of the diameter of the hole in a fissured rock mass equals twice the sum of the preceding deformations

$$\Delta' = 2 \frac{ap}{E} \left(\log \frac{b}{a} + 1 + \nu \right) \qquad (2)$$

From the preceding assumptions on the distribution of stresses in a fissured solid, a value of Δ' independent of the angle α, i. e. of the number of fissures, and of the azimuth θ was derived. Therefore expression (2) is not correct but, as we are going to see, its error is not considerable.

For that puspose the state of stress and the state of strain in the diameter of a fissured plate with a hole were calculated by an integral numeric method recently developed at the LNEC [7] for solving plane equilibria whatsoever. Consider the case of a hole with a diameter 2a = 7.6 cm under a pressure p = 100 kgf/cm^2 and with 2, 4, and 8 fissures with depths such that $\frac{b}{a}$ amounts to 2, 4, and 8 (fig. 6). It is also assumed that E = 100,000 kgf/cm^2 and ν = 0.2. The values of the deformation Δ' of the diameter, computed on basis of expression (2), and of the deformation of the diameter at points P and Q of fig. 6, designated by Δ'_P and Δ'_Q respectively, computed by that numeric method, are presented in the following table; the values of the deformation of the diameter in a solid without fissures are also indicated in the table in order to assess the accuracy of the numeric method used.

Table I

Conditions	$\frac{b}{a}$	Δ' (μ)	Δ'_P (μ)	Δ'_Q (μ)	$\frac{\Delta'_P - \Delta'_Q}{2}$ (μ)
2 fissures	2	142	130	82	106
	4	194	192	86	139
	8	246	254	94	174
4 fissures	2	142	132	101	117
	4	194	182	134	158
	8	246	246	200	223
8 fissures	2	142	142	140	141
	4	194	194	214	204
	8	246	236	242	239
No fissures	0	90	90	90	90

As seen, in the absence of fissures the deformation of the diameter as determined by the numerical method coincide with the value derived from the Theory of Elasticity. The table shows an excellent agreement between the values of Δ' and Δ' p, which correspond to the points farthest removed from the fissures. Therefore in the particular case in which the location of the fissures is known, very satisfactory results can be obtained from expression (2), if measurements are taken at points P. On the other hand, considerable differences are observed between Δ' and Δ'_Q , except in the case of 8 fissures. Taking the mean of $\Delta'p$ and $\Delta'Q$, this value is seen to differ by less than 20% from Δ', save in the case of two fissures. As the instrument developed measures deformations along four diameters, it makes possible to determine a mean deformation, which, as we have just seen, fairly approaches Δ', all the more so as the case of two fissures rapidly turns into the case of four fissures. It follows that, the values of b and E being known, expression (2) yields a satisfactory value for the mean deformation of the diameter of the hole and parameters α and θ need no longer be taken into account.

As seen, in a solid with a hole stresses are zero in the surface elements normal to the axis of the hole. Yet when fissures occur, the state of stress in the wedges thus formed becomes $\sigma_r = \frac{ap}{2}$, giving rise to a compressive stress amounting to $\sigma_z = \nu\sigma_r$ parallel to the axis of the borehole, as the equilibrium is assumed to be plane. Therefore the radial deformation at each point becomes $\frac{\sigma_r}{E} - \nu \frac{\sigma_z}{E} = \frac{\sigma_r}{E}(1-\nu^2)$.

For the current values of ν, ν^2 can be neglected, i. e. the influence of σ_z need not be considered in the calculation of the deformation Δ' of the diameter of the hole.

Let us see now the influence of the fissures on the value of the deformation of the diameter of the hole. The unit increase of the deformation of the diameter due to the occurrence of fissures is given by

$$\frac{\Delta' - \Delta}{\Delta} = \frac{1}{1+\nu} \log \frac{b}{a} = \frac{2.3}{1+\nu} \log_{10} \frac{b}{a}$$

The values of $\frac{\Delta' - \Delta}{\Delta}$ in percentage for different values of $\frac{b}{a}$ and assuming $\nu=0.2$ are presented below:

b/a	1	2	4	6
$\frac{\Delta' - \Delta}{\Delta}$ (%)	0	58	115	150

Therefore the influence of fissuring on the deformation of the diameter proves to be very important. Notice however that, given the limited length of the borehole subjected to pressure p, the value of $\frac{b}{a}$ cannot be very large.

σ being the tensile strength of the rock and fissures being assumed to extend down to a depth such that $\sigma_\theta = \sigma$, it follows that

$$\sigma = \left[\frac{p\,\frac{a}{b}\cdot b^2}{r^2}\right]_{r=b} = p \cdot \frac{a}{b}$$ and therefore the depth reached by the fissure is $b = a\,\frac{p}{\sigma}$

Consequently the deformation of the diameter is given by the expressions

$$\Delta = 2\,\frac{ap}{E}\,(1+\nu) \qquad \text{for } p < \sigma$$

$$\Delta' = \frac{ap}{E}\left(\log\,\frac{p}{\sigma} + 1 + \nu\right) \qquad \text{for } p > \sigma$$

The curve representing the evolution of the deformation of the diameter in a test during which fissuring occurs in the rock mass is presented in fig. 7.

The modulus of elasticity can be calculated from the linear stretch by means of the expression

$$E = 2\,\frac{ap}{\Delta}\,(1+\nu)$$

Since for $p > \sigma$, the calculation of E requires ascribing to the tensile strength of the rock a value which as a rule is not reliable, it is very advisable to begin measuring Δ at very small pressures in order to observe the linear stretch.

If the diagram obtained in a test does not begin with a well-marked linear stretch, the modulus of elasticity has to be calculated by the expression

$$E = 2\,\frac{ap}{\Delta'}\left(\log\,\frac{p}{\sigma} + 1 + \nu\right)$$

where Δ' is the average of the values observed for the deformation of the four diameters. As for the uncertainty of the value of σ, notice that E changes very slowly with σ.

If the rock mass behaves elastically and if failure obeys the theory assumed for deriving the expression (2), the value of σ can even be determined from the experimentally determined curve of Δ' in function of p. In fact let us ascribe to the tensile strength in the expression of E not its true value σ but $n\,\sigma$. The following expression is then obtained in function of p:

$$f(p) = 2\,\frac{ap}{\Delta'}\left(\log\,\frac{p}{n\sigma} + 1 + \nu\right)$$

hence

$$f(p) = \frac{2p}{\Delta'}\left(\log\,\frac{p}{\sigma} + 1 + \nu\right) + 2\frac{ap}{\Delta'}\,\log\,\frac{1}{n}$$

$$f(p) = E + 2\,\frac{ap}{\Delta'}\,\log\,\frac{1}{n}$$

This means that by ascribing successive values to a σ and computing f(p) from experimental values of p and Δ', a family of straight lines should be obtained and the true tensile strength is the value of σ for which f(p) is constant. The existance of such a value of σ will confirm the reliability of the expression determined for Δ'.

When stresses are present in the rock mass, their influence has to be taken into account in the problem of the occurrence and propagation of fissures. Thus let us consider in the plane perpendicular to the borehole a state of compression with the two principal stresses with the same value σ_1. A concentration of stresses thus arises in the neighborhood of the hole with its maximum $\sigma_\theta = 2\ \sigma_1$ at the side walls, and consequently $\sigma + 2\ \sigma_1$ must replace σ in the expression of Δ'.

When the two principal stresses are very different in magnitude, σ_θ will markedly change with θ and fissuring will occur preferably in the plane of the maximum principal stress. It is then advisable to measure the deformation of the hole approximately in the direction of the maximum principal stress, i. e. about the plane of the two first possible fissures, because this deformation, as seen in Table I, is little influenced by fissures, and the modulus of elasticity can be determined from the expression of Δ, i. e. independently of σ. In the case of rock masses anisotropic with respect to tensile strength, it will also be advisable to take measurements perpendicularly to the direction of the minimum tensile strength.

After the maximum test pressure has been attained, decompression proceeds along the straight line AO (fig. 7) provided it is assumed that tensile fissuration does not give rise to important permanent deformations. When pressure is applied again, the load diagram follows the straight line OA; if the applied pressure exceeds the maximum of the preceding cycle, the diagram will bend beyond A resuming its logarithmic shape. If the rock mass is subjected to a hydrostatic compression σ_1, the diagram of decompression will be AO', with an ordinate $2\ \sigma_1$ at point O'.

LABORATORY AND IN SITU DILATOMETER TESTS

In order to investigate the performance of the dilatometer developed and the accuracy of the measurements, the instrument was tested inside a steel pipe. Accuracy was assessed by comparing the values of the deformations of diameters of the pipe, as measured by the dilatometer in the internal face and by mechanical 0.001 mm deflectometers in the external face.

An overall view of the setup used is presented in fig. 8. It shows the leads and the air and water pipes of the dilatometer connected through the top of the steel pipe, the measuring instruments, the water pump that applies the pressure with the corresponding pressure gauges, and the mechanical deflectometers that measured the diametral deformation along the external face of the pipe. Due to the high sensitivity of the strain measuring instruments used, the tests were performed in a conditioned room. In order to determine more accurately the pressure applied by the dilatometer, several pressure gauges with different maximum pressures were successively used.

The transducers of the dilatometer were previously calibrated, the calibration diagrams obtained (fig. 9) being perfectly linear.

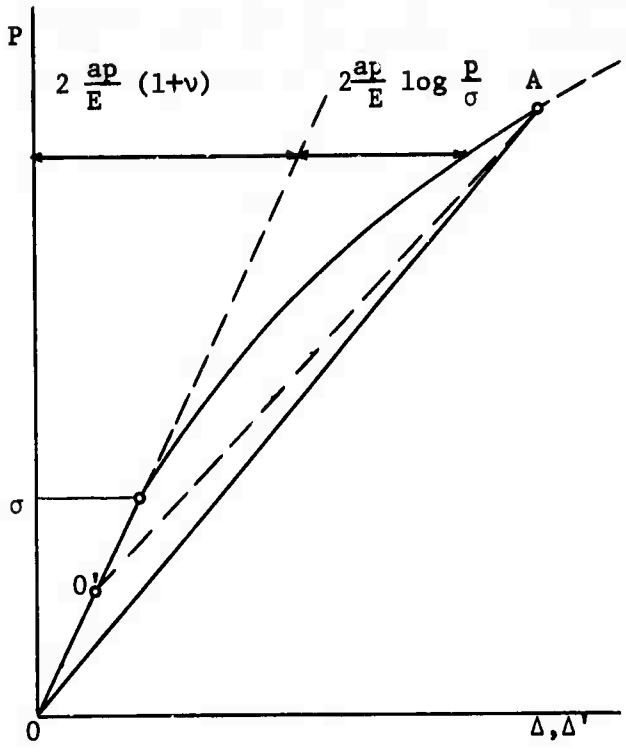

FIG. 7

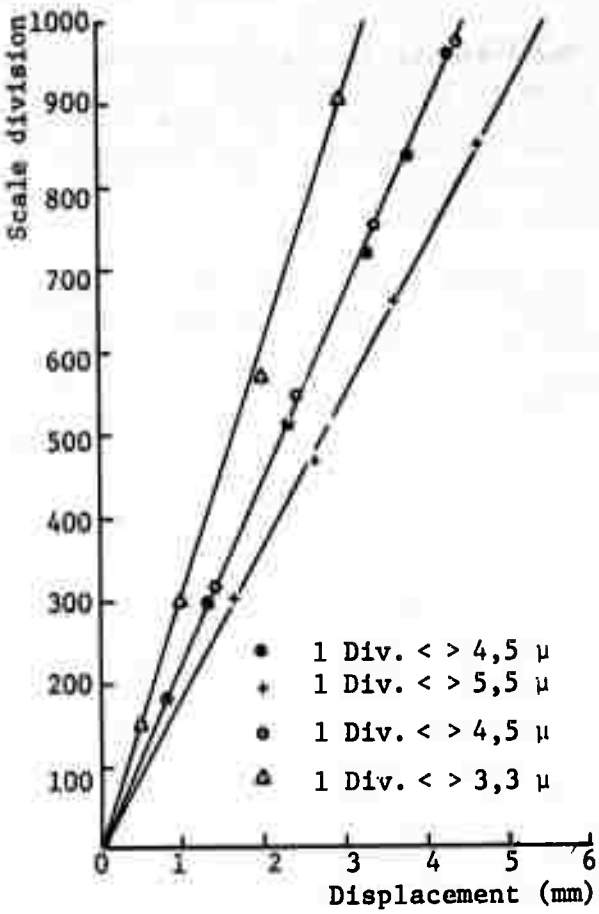

FIG. 9

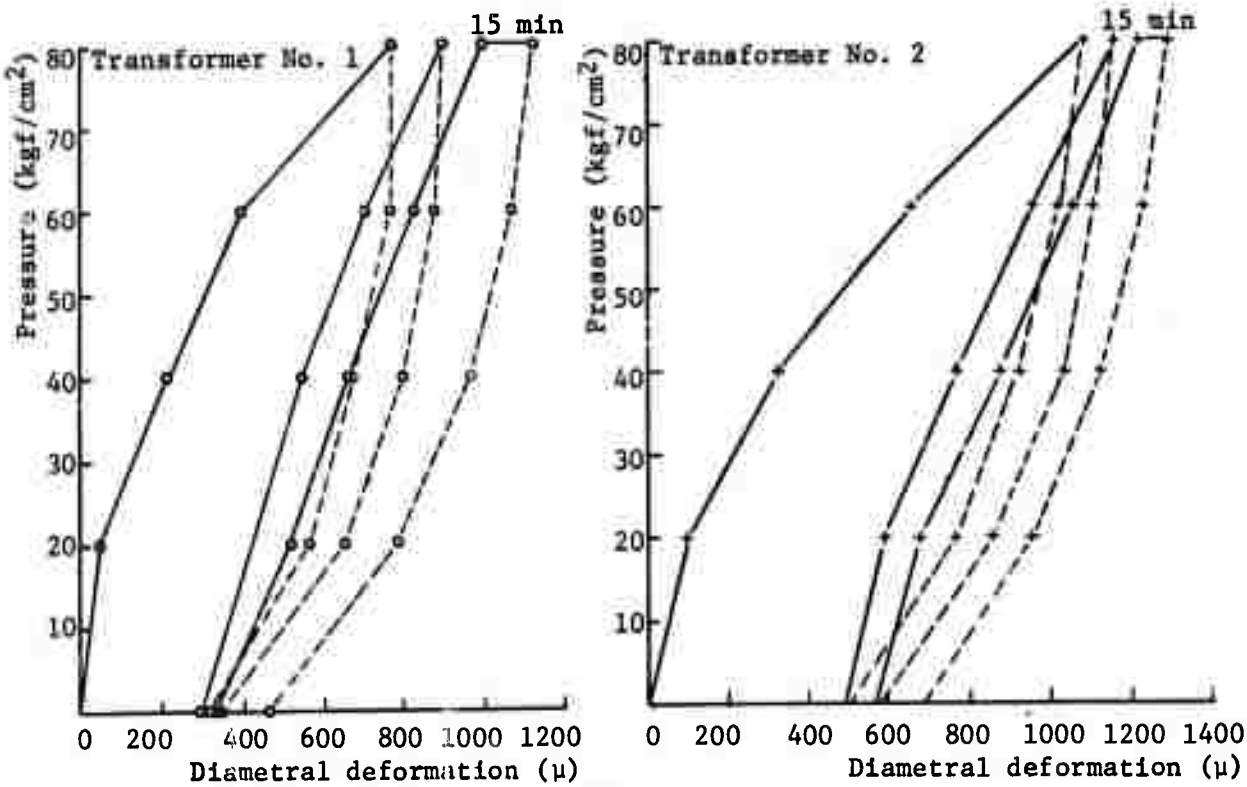

FIG. 10

The test inside the pipe showed that the different parts of the dilatometer were operating in good conditions. Thus, pressure is radial and is applied throughout the surface of contact with the pipe; the air pressure system operating the transducer rods, which are sucked in when the instrument is applied in a pipe or a borehole, and the command of the water relief valve located at the base of the dilatometer were also operating as planned.

The comparison of the values measured in the inside and the outside faces of the pipe confirmed that the instrument is entirely reliable and accurate. Thus, under a pressure $p = 80$ kgf/cm^2, the average strain in the diameter of the pipe was 39.5μ as measured by the four transducers of the dilatometer, 39.0μ as measured by the external deflectometer and 40μ as calculated according to the Theory of Elasticity.

The dilatometer was tested in the field inside a borehole with a diameter $2a = 7.6$cm drilled in a very altered granite. The diagrams of the strains in two diameters at 45° with one another in function of pressure are presented in fig. 10. The other two measuring units of the dilatometer yielded anomalous values, because, as seen later, their rods were applied over fissures of the rock mass.

As for the diagrams of fig. 10 it is noteworthy that they are very similar and regular for both the diameters observed, which is a proof of the accuracy of the measurements. As seen, the diagrams obtained under the first application of pressure are markedly curved with the concavity directed towards the decreasing pressure. This curvature, we believe, is caused by a progressive fissuration of the rock mass, which is to be expected due to the high pressure applied and the reduced strength of the rock. As shown, fissuration bends the diagram towards decreasing pressure (fig. 7) whereas the reverse is true in current load tests, in which, due to the progressive consolidation of the rock mass, the force-strain diagrams are bent in the reverse direction. The fact that roughly straight diagrams were obtained in the second and third loading shows that, after the initial fissuration and a possible consolidation, the behavior of the rock mass is roughly elastic. It is worth noting that the unloading diagrams are very similar to the current loading diagrams.

The permanent set in the first loading being very considerable, it did not seem legitimate to consider the diagram of the first loading as corresponding to the logarithmic curve of fig. 7. It was preferred to determine the modulus of elasticity from the diagram of the second loading. As the linear diagram corresponds to a medium already fissured, E should be calculated by the expression

$$E = \frac{2\,ap}{\Delta}\left(\log\frac{p}{\sigma} + 1 + \nu\right) .$$

Taking, in the left-side diagram of fig. 10, the strain $\Delta' = 605\mu = 0.0605$ cm which corresponds to $p = 80$ kgf/cm^2, adopting $\nu = 0.2$ and for the tensile strength a value $\sigma = 5$ kgf/cm^2 and bearing in mind that, due to the nature of material and to the small depth of the tested zone, stresses in the rock mass should not be high, it is

$$E = \frac{7.6 \times 80}{0.0605}\left(\log\frac{80}{5} + 1 + 0.2\right)$$

$$E = 10{,}049\ (2.3 \log_{10} 16 + 1.2)$$

$$E = 39{,}600 \text{ kgf/cm}^2$$

Notice that, for σ = 10 kgf/cm^2, the change of E is small with respect to the accuracy of practical interest, becoming 32,960 kgf/cm^2.

For the right-side diagram of fig. 10 a value E = 39,890 kgf/cm^2 is obtained likewise for σ = 5 kgf/cm^2.

CONCLUSION

The tests carried out with the dilatometer developed, although very few, proved satisfactory.

The instrument seems to be of much practical interest, as it enables tests to be carried out in current boreholes for soil exploration. As the tests are very quick, deformability can be determined continuously along the borehole and can be considered as a quality index of the rock formations.

ACKNOWLEDGEMENTS

The authors are much grateful to Mr. Ravara, engineer of the Department of Bridges and Buildings for his help in connexion with the numerical calculation of deformations in the fissured media, to Mr. Tavares Cardoso, Engineer of the Division of Instrument Design and Construction, who supervised the electrical units of the dilatometer, to Mr. Barroso, engineer of the Department of Dams, and to Mr. Americo Almeida, general forman of the mechanics workshop for his co-operation in the construction of the dilatometer..

REFERENCE

[7] OLIVEIRA, E. R. A. -- A utilizacao dos metodos numericos integrais na resolucao de problemas de elasticidade plana, Internal Report, LNEC, April 1955. Lisbon.